
BINDING SERVICES
Tel +44 (0)29 2087 4949
Fax +44 (0)29 20371921
e-mail bindery@cardiff.ac.uk

# Gene delivery to human skin using microneedle arrays

*Sion Andrew Coulman*

A thesis submitted to Cardiff University in accordance with the requirements for the degree of

DOCTOR OF PHILOSOPHY

Drug Delivery Department
Welsh School of Pharmacy
Cardiff University

May 2006





ProQuest LLC
789 East Eisenhower Parkway
P.O. Box 1346
Ann Arbor, MI 48106-1346

## Acknowledgements

I must give greatest thanks to my supervisors, Dr James Birchall and Dr Chris Allender, for their continued guidance, advice and also friendship during my research studies.

I must also thank our collaborators, Professor David Barrow at Cardiff School of Engineering, Helen Sweetland at Llandough NHS Trust, Chris Gateley and Alexander Anstey at the Royal Gwent Hospital. Extended gratitude must go to Dr Anthony Morrissey and Nicole Wilke at Tyndall National Institute (TNI), the 'microneedle makers', for their skills, hard work and enthusiasm.

I would also like to thank Dr Antoine Hann and Mike Turner for their assistance in electron microscopy studies.

I must also thank the numerous people in the department who have helped me and have made the last few years so enjoyable (relatively) including Dr Keith Brain, Dr Darren Green, Dr Mark Gumbleton and the PCB boys, Dr Allan Cosslett, Dai John, Marc, everyone that I have worked with in the lab, all of the technical staff and last but not least the coffee crew!

I must also acknowledge the Royal Pharmaceutical Society of Great Britain for the studentship.

Finally thank you to my family for their encouragement and continued support in everything that I do.

| | |
|---|---|
| Ag | Antigen |
| APC | Antigen presenting cell |
| ATP | Adenosine triphosphate |
| BCA | Bichichonic acid |
| BMZ | Basement membrane zone |
| BSA | Bovine serum albumin |
| CSE | Cardiff School of Engineering |
| Da | Daltons |
| DC | Dendritic cell |
| DDC | Dermal dendritic cells |
| DNA | Deoxyribonucleic acid |
| DOTAP | 1,2-dioleoyl-3-triammonium-tropane |
| EB | Epidermolysis bullosa |
| EDTA | Ethylenediaminetetraacetic acid |
| EPU | Epidermal proliferation units |
| FACS | Fluorescence activated cell sorting |
| GFP | Green fluorescent protein |
| H&E | Haematoxylin and eosin |
| HCl | Hydrochloride |
| hr | Hour |
| ISF | Interstital fluid |
| KOH | Potassium Hydroxide |
| LB | Lamellar bodies |
| LC | Langerhans cell |
| LCN | Lipid-coated nanosphere |
| LPD | Liposome-polycation-pDNA |
| MEA | Microenhancer Array |
| MHC II | Major Histocompatibility class II complex |
| min | Minute |
| MTT | [3-(4,5-dimethylthiazol-2-yl)-2,5-diphenyltetrazolium bromide] |
| MW | Molecular weight |
| N | Newtons |

| | |
|---|---|
| $NBDC_{12}$-HPC | 2-(12-(7nitrobenz-2-oxa-1,3-diazol-4-yl)amino)dodecanoyl-1-hexadecanoyl-sn-glycero-3-phosphocholine |
| NFR | Nuclear fast red |
| NLS | Nuclear localisation signal |
| OCT | Optimal cutting temperature |
| PBS | Phosphate buffered saline |
| PCS | Photon Correlation Spectroscopy |
| pDNA | Plasmid DNA |
| RF | Radiofrequency |
| RLU | Relative light units |
| SC | Stratum corneum |
| sd | Standard deviation |
| SDP | Size distribution processor |
| SEM | Scanning electron microscopy |
| Sec | Second |
| TA | Transit amplifying cells |
| TBE | Tris-borate EDTA |
| TE | Tris-EDTA |
| TEM | Transmission electron microscopy |
| TNI | Tyndall National Institute |
| UK | United Kingdom |
| USA | United States of America |
| UV | Ultraviolet |
| X-gal | 4-bromom-5-chloro-3-indoyl-β-D-galactopyrosanide |
| XP | Xeroderma pigmentosum |

## Summary

Cutaneous delivery of macromolecules is significantly impeded by the inherent barrier properties of the stratum corneum (SC). Within the last decade sophisticated engineering techniques have enabled the manufacture of microneedle arrays. These are innovative devices consisting of micron-sized needles which when inserted into the skin create physical conduits across the SC but do not impinge upon underlying nerve fibres or blood vessels. This study assessed the ability of microfabricated silicon microneedle arrays to penetrate the SC of *ex vivo* human skin for the localised delivery and subsequent expression of non-viral gene therapy formulations. Cutaneous gene therapy may represent a new method for the treatment of, or vaccination against, a range of candidate diseases.

Microneedle arrays of variant geometries and morphologies, created using dry- and wet-etch microfabrication methods, were characterised by scanning electron microscopy. The potential of these devices for the cutaneous delivery of gene therapy formulations was initially demonstrated by permeation of a size and surface representative fluorescent nanoparticle across microneedle treated human epidermal membrane and observation of these nanoparticles in micron-sized conduits created in excised human skin. The ability to express exogenous genes within *ex vivo* human skin was subsequently proven by intradermal injection of the pCMVβ reporter plasmid. However, a non-viral gene therapy vector failed to enhance cutaneous transfection. Cutaneous plasmid DNA delivery using the microneedle device facilitated effective, if somewhat limited and irreproducible, transfection of epidermal cells proximal to microchannels created in the skin.

These investigations confirmed the ability of a silicon microneedle device to deliver macromolecular formulations, including plasmid DNA, to the viable epidermis and have demonstrated exogenous gene expression within human skin. However, limited and unpredictable gene expression following microneedle mediated delivery indicate that further studies to optimise the microneedle array morphology, its method of application and the plasmid DNA formulation are warranted.

# CHAPTER 1

# Introduction

## 1.1. GENERAL INTRODUCTION

Localised delivery and the subsequent expression of nucleic acid formulations within the skin may be used to treat inheritable skin disorders (genodermatoses), to advance wound healing strategies or for the development of a genetic vaccination. However the outermost layer of skin, the epidermis, presents a formidable physical and immunological barrier to the ingress of exogenous material. To enable cutaneous delivery of hydrophilic, high molecular weight (MW) structures such as gene-based therapies, more radical methods of delivery must be employed.

The aim of this study was to determine the ability of microfabricated microneedle devices to facilitate localised delivery and subsequent expression of exogenous genes within the viable epidermis of human skin. This introductory chapter considers the structure of human skin, the fundamental principles of gene therapy and the skin as an attractive target for such therapeutic strategies. Within these topics, the barrier properties of the skin tissue, the target cells of the viable epidermis and the novel methods of cutaneous delivery that have been employed to promote localised nucleic acid delivery are scrutinised, with a particular focus upon the progression of the microneedle array device to the present date.

## 1.2. THE SKIN BARRIER: Structure and Function

As the primary interface between a living creature and the environment within which it resides, skin plays a significant role in protection of an organism and its ability to successfully interact with the external environment. Human skin is the largest and arguably most complex organ of the body responsible for, and contributing to, a range of functionalities (Menon, 2002). For pharmaceutical scientists, its direct accessibility and large surface area make skin an attractive portal for the delivery of therapeutic entities. However, its primary role is to protect the body from possible insult by chemicals, invading pathogens, physical trauma or UV radiation (Menon and Elias, 2001, Williams, 2003). The formidable physical, biological and immunological barrier properties of skin have therefore restricted successful trans/intradermal delivery systems to a limited number of therapeutic candidates (Roberts and Walters, 1998).

### 1.2.1. Skin Anatomy

The skin is essentially a bilayer consisting of (i) the dermis; a connective tissue layer comprising the major proportion of the skin thickness and (ii) the epidermis; a cellular region overlying the dermis that is in contact with the external environment (Fig 1.1). Sub-cutaneous fat is an insulating layer located beneath the dermis that provides mechanical protection to underlying tissues and organs of the human body.

The epidermis can itself be considered as a two layered structure. The outermost layer, the stratum corneum (SC), consists of flattened terminally differentiated cells and it is the passage of therapeutic compounds through this layer that is considered to be the primary hurdle to successful transdermal drug delivery (Scheulplein and Blank, 1971). For macromolecules such as nucleic acid therapies this barrier is formidable and penetration therefore requires radical transdermal delivery methods. Below the SC lies the viable epidermis, so termed as it contains nucleated cells and the proliferative cells that are responsible for regeneration and renewal of epidermal tissue (Lajtha, 1979) (Fig 1.2).

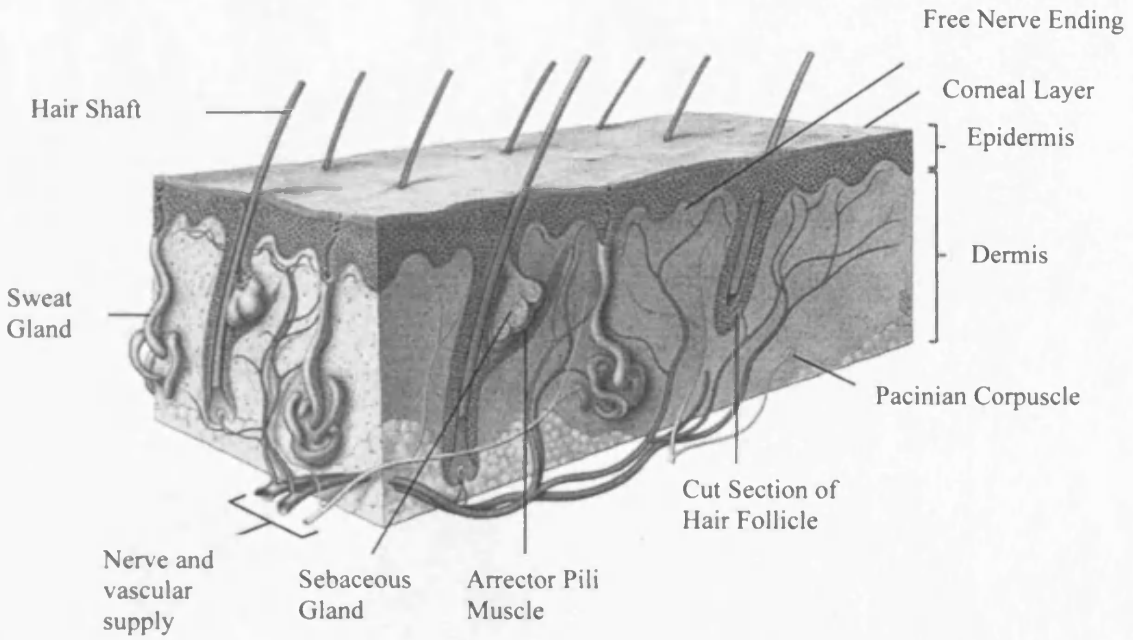


*Figure 1.1.* An illustration of the gross anatomy of full thickness human skin.

*(Adapted from http://www.homestead.com/doctorderm/skinanatomy.html accessed 24.05.2006)*

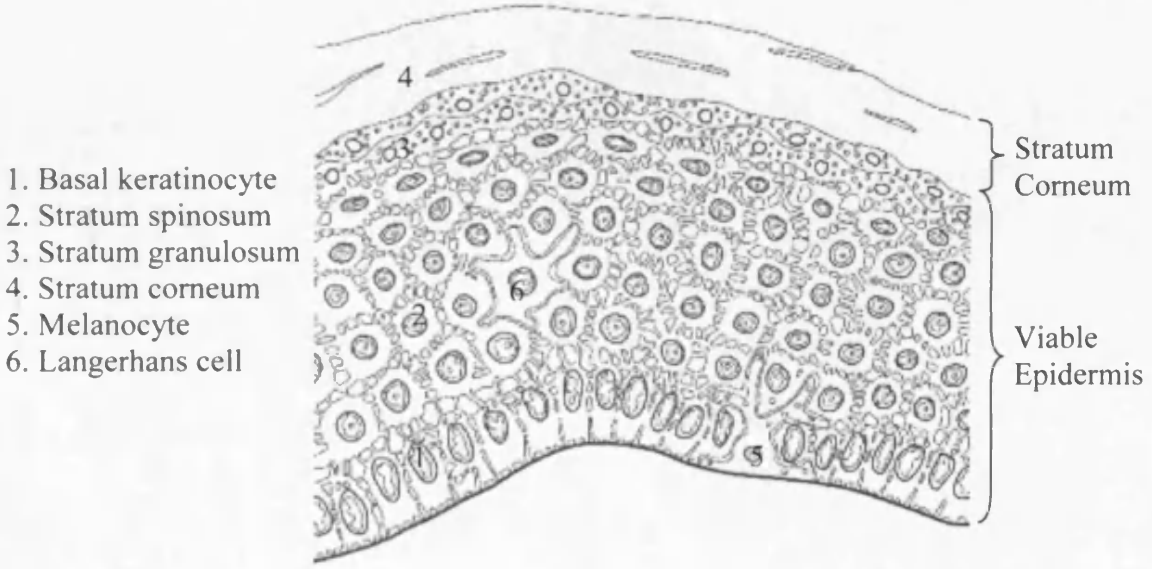


*Figure 1.2.* An illustration of the viable epidermis, highlighting the cellular organisation of the tissue.

*(Adapted from http://upload.wikimedia.org/wikipedia/nl/e/e8/Epidermis.jpg accessed 13.10.2005)*

#### *1.2.2.1. The Dermis*

The dermis is a connective tissue matrix consisting of, (i) collagen; which provides the skin with tensile strength and elasticity and (ii) elastic fibres; which resist deformation of the skin following the application of mechanical forces (Haake et al., 2001). The primary function of the dermis is to provide the skin barrier with an ability to resist mechanical injury. However, the dermis is also home to nerve fibres and the cutaneous vasculature and therefore has important roles in sensation, the transport of nutrients, thermal regulation and the movement of cells and biological mediators between the local and systemic environments (Haake et al., 2001, Williams, 2003). The upper region of the dermis, the papillary dermis, also contains a number of cells including fibroblasts, macrophages and dermal dendritic cells (DDC). The former of these cell types is responsible for maintenance of the connective tissue structures, whilst the latter two cell types are involved in the cutaneous immune system (Haake et al., 2001).

#### *1.2.2.2. The Viable Epidermis*

The viable epidermis is a complex cellular region in which the primary cell type, the keratinocyte, undergoes progressive differentiation from its origins in the basal epidermis to its destination within the SC, where it completes its life as a non-nucleated corneocyte. This differentiation process within the viable epidermis occurs over approximately 21 days (Roberts and Walters, 1998) with the resulting corneocyte then remaining in the SC for a further 14 days (Montagna and Parakkal, 1974) before it is eventually shed in the desquamation process. Other cell types within this layer include Langerhans cells, Merkel cells and melanocytes.

##### *1.2.2.2.1. Stratum Basale (Basal Layer)*

The region of columnar shaped keratinocytes located above the epidermal-dermal junction is often referred to as the basement membrane zone (BMZ). Basal keratinocytes are tightly bound to the underlying dermis by proteinaceous anchoring filaments called hemidesmosomes. Cytoskeletons of the cells consist of the keratin filaments, K5 and K14 (Menon, 2002). These are indicative keratins that are specific to cells located within this region. Loss of keratin or hemidesmosome functionality results

in mechanical disruption of the BMZ as can be seen in blistering conditions such as the inheritable genetic disease, epidermolysis bullosa (Jonkman, 1999).

Continual loss of skin cells from the SC necessitates renewal of the underlying layers to maintain skin homeostasis. This regeneration is ultimately controlled by proliferative cells located within the basal layer of the viable epidermis. Division of these cells, their release from the basal layer and subsequent migration toward the SC is a tightly controlled mechanism that ensures maintenance of the skin barrier function (Fuchs, 1990, Kaur and Li, 2000). Proliferative cells within the basal layer include both stem cells (Section 1.2.3.) and transit amplifying cells (TA), actively proliferating keratinocytes which after a number of divisions will eventually differentiate themselves. Therefore it is only within the basal layer of the skin epidermis that cells are actively dividing.

*1.2.2.2.2. Stratum Spinosum*

Migration of cells from the basal layer to the stratum spinosum is accompanied by morphological and biochemical changes. Keratinocytes become more polyhedral in shape and develop large bundles of intracellular keratin filaments that merge into cellular extensions. These terminate with desmosomes that bind the cells together in a tight cohesive unit (Fuchs, 1990). Lamellar bodies (LB), containing stacks of lipid enriched disks, are also evident in the cytoplasm of cells in this layer, particularly at the interface between the stratum spinosum and the overlying cells of the stratum granulosum (Odland, 1960).

*1.2.2.2.3. Stratum Granulosum*

Cells continue to flatten on their transition through the stratum granulosum and begin to develop characteristic granules which contain a high density of keratin filaments (Haake et al., 2001). Increasing levels of protein synthesis is accompanied by lipogenesis and a resultant increase in the membrane bound lipid rich LB. Within the upper layers of the stratum granulosum LBs fuse with the cell membrane, resulting in release of their lipid contents into the extracellular space. Remodelling of the lipid within this environment by co-secreted enzymes converts the lipid into a continuous intercellular lamellar structure. These are the beginnings of the characteristic extracellular lipid bilayers that

are present in the SC. Within the stratum granulosum, intracellular enzymes also begin to degrade the cell organelles, thus decreasing cell viability.

*1.2.2.2.4. Langerhans Cells*

The skin is equipped with specialised antigen presenting cells (APC), called Langerhans cells (LC), that can respond to the invasion of pathogens into the skin (Fig 1.3). These cells, identified by Paul Langerhans in 1868 (Wolff, 1991), exist in the suprabasal area of the viable epidermis and although they only account for 2-8% (Larregina and Falo, 2005) of the epidermal cell population, their finger like projections form a network that covers over 25% of the total skin surface area (Schuler and Steinman, 1985, Yu et al., 1994). Immunohistochemical *en face* images reveal a 'spiderlike' network of APC (Romani et al., 2003) within the epidermal layer whilst light and electron microscopy studies (Oota, 1999, Stoitzner et al., 2002) highlight the characteristic 'veiled' morphology of individual LCs (Fig 1.3). Their position and role in the viable epidermis will be discussed in greater detail during consideration of the cutaneous immune system (Section 1.2.4.). Antigen presentation is currently acknowledged as the primary role of the LC however it is unlikely to be the sole function (Larregina and Falo, 2005).

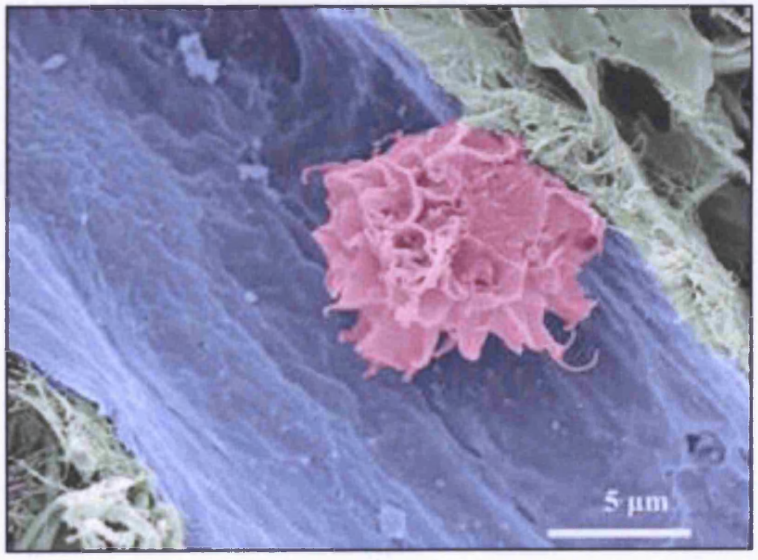


*Figure 1.3.* A scanning electron micrograph of a dendritic Langerhans cell reveals the 'veiled' morphology of the cell.

*(Adapted from http://www.nature.com/ncb/journal/v5/n10/full/ncb1003-867.html accessed 16.10.2005)*

### *1.2.2.3. The Stratum Corneum*

The barrier function of the skin is imparted by the outermost layer of the epidermis, the 10-20μm thick SC layer (Scheulplein and Blank, 1971). This competent physical barrier has frustrated attempts to deliver numerous therapeutic compounds across the skin, resulting in the clinical use of relatively few therapeutic products. The aim of this investigation is to physically bypass the SC using a microneedle device.

The SC consists of tightly packed, flattened corneocytes, 20-40 μm in diameter, surrounded by a lipid matrix. This is often compared to a 'brick and mortar' structure, the bricks being the corneocytes and the mortar being the intercellular multi lamellar lipid sheets that surround them (Elias, 1983). These sheets consist primarily of three lipid types, ceramides, cholesterol derivatives and fatty acids. The corneocytes are densely packed with insoluble intracellular keratin filaments and although they contain active enzymes, their inability to regenerate and the absence of functional cellular organelles suggests that these cells are essentially non-viable (Madison, 2003).

Recently, it has been suggested that the 'brick and mortar' model of the SC should be extended to include the presence of desmosomes (Cork, 2004), protein rivets that are responsible for the cohesion of cells within the layers of the SC. These desmosomes might be considered to be steel reinforcing rods that span the SC layer, holding the tight cohesive unit in place and maintaining cell shape and cell to cell adhesion (Wertz and van den Bergh, 1998). In the outer layers of the SC proteases are released from cells. These degrade desmosomes, which therefore permits controlled corneocyte release from the skin surface (Sondell et al., 1995). The SC is therefore in a dynamic state, with continuous renewal and modification of the extracellular barrier lipids by a host of different enzymes and the controlled desquamation of corneocytes from the skin surface. Therefore, although the SC is considered a non-viable tissue, regulation of the desquamation process, the continuous differentiation of corneocytes and the ability of the layer to respond to insult has lead to its description as 'intelligent' ((Menon and Elias, 2001), see (Elias, 2005)for a recent review).

### 1.2.2. Cutaneous Innervation and Vasculature

The structure of the cutaneous vasculature is well documented (Singh and Swerlick, 2001) (Fig 1.4). Capillaries from a deep plexus located at the base of the dermis extend upward to the dermal papillary areas between the epidermal projections/ridges, to form dermal papillary loops. It is at these loops that oxygen and nutrient transfer with viable epidermal cells takes place. Networks of nerve fibre bundles responsible for sensory perception (including pain) are found alongside capillaries and lymphatic vessels, in the papillary dermis. Therefore, despite the suggested presence of intraepidermal nerve endings over the past few decades (Hilliges et al., 1995, Vaalasti et al., 1988), restricting the penetration of a microneedle array to the epidermis reduces/prevents pain and bleeding during insertion.

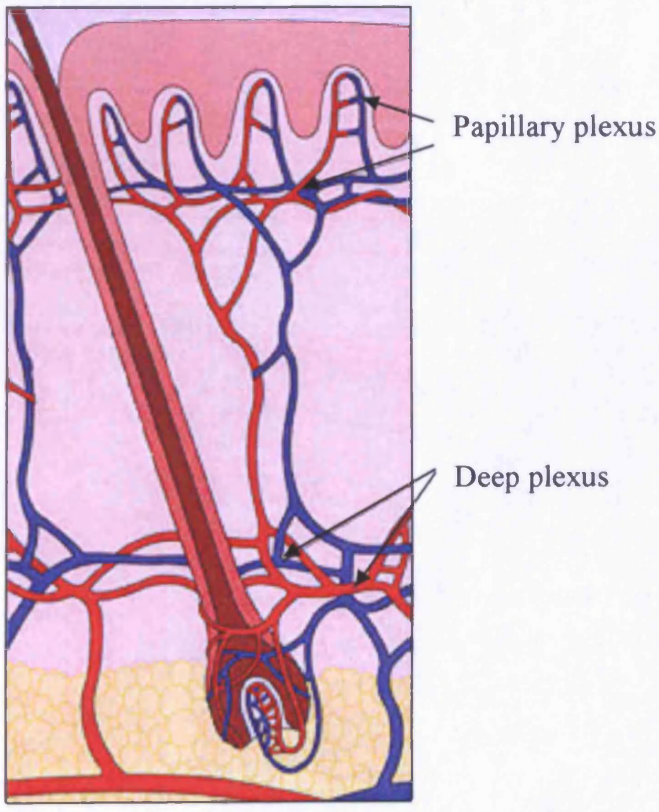


*Figure 1.4.* The vasculature structure within human skin.
*(Adapted from http://cai.md.chula.ac.th/lesson/lesson4410/data/image_s17.jpg accessed 25.10.2005)*

### 1.2.3. Stem Cells

The ability to transfect stem cells within any tissue is a highly attractive proposition for those working within the field of gene therapy as it presents an opportunity for stable i.e. 'lifelong', correction of genetic defects. Within the skin, genetic modification of stem cells may permit treatment of patients who suffer from currently untreatable inheritable skin disorders. However, there are a number of challenges to this therapeutic proposal, most notably an inherent difficulty in identifying keratinocyte stem cells (Potten and Booth, 2002).

A reservoir of multipotent stem cells within the hair follicle bulge has been identified (Alonso and Fuchs, 2003a, Alonso and Fuchs, 2003b, Gambardella and Barrandon, 2003, Potten and Booth, 2002, Spradling et al., 2001). However, it is stem cells in the interfollicular epidermis that are responsible for continuous renewal of the skin barrier (Alonso and Fuchs, 2003b).

Investigations using murine skin indicate that keratinocytes are organised into epidermal proliferating units (EPU), where a single stem cell in the basal layer gives rise to a column of cells that extends towards the skin surface (Alonso and Fuchs, 2003b, Potten and Booth, 2002). These columns are approximately 10 basal cells wide. However unlike human skin, the basal layer of the mouse epidermis is relatively flat and therefore these observations cannot be directly extrapolated to the human setting (Jones et al., 1995).

Taichman and co-workers have recently elucidated the location of EPUs within human skin and suggest that the distribution of basal stem cells is in fact non-uniform (Ghazizadeh and Taichman, 2005) (Fig 1.5). In this study, labelled stem cells were present along the length of the basal layer and from these stem cells narrow EPUs extended toward the skin surface. Three major observations were made in this study:-

1. The EPU has no preferred site of origin i.e. 44% were located in the flat regions, 17% were on the side of rete ridges, 22% were at the base of rete ridges and 17% were on the tip of dermal papillae.

2. EPUs varied in width from one to ten cells, with the widest EPUs originating from the side of the rete ridge and the narrowest from the base of the rete ridge.
3. Migration from the basal compartment is perpendicular to the skin surface.

Stable expression of an exogenous gene within the skin requires transfection of stem cells. Targeting these cells with a nucleic acid therapeutic therefore requires a device that can deliver the formulation to the basal region of the epidermis and a specific cellular marker that can promote stem cell transfection.

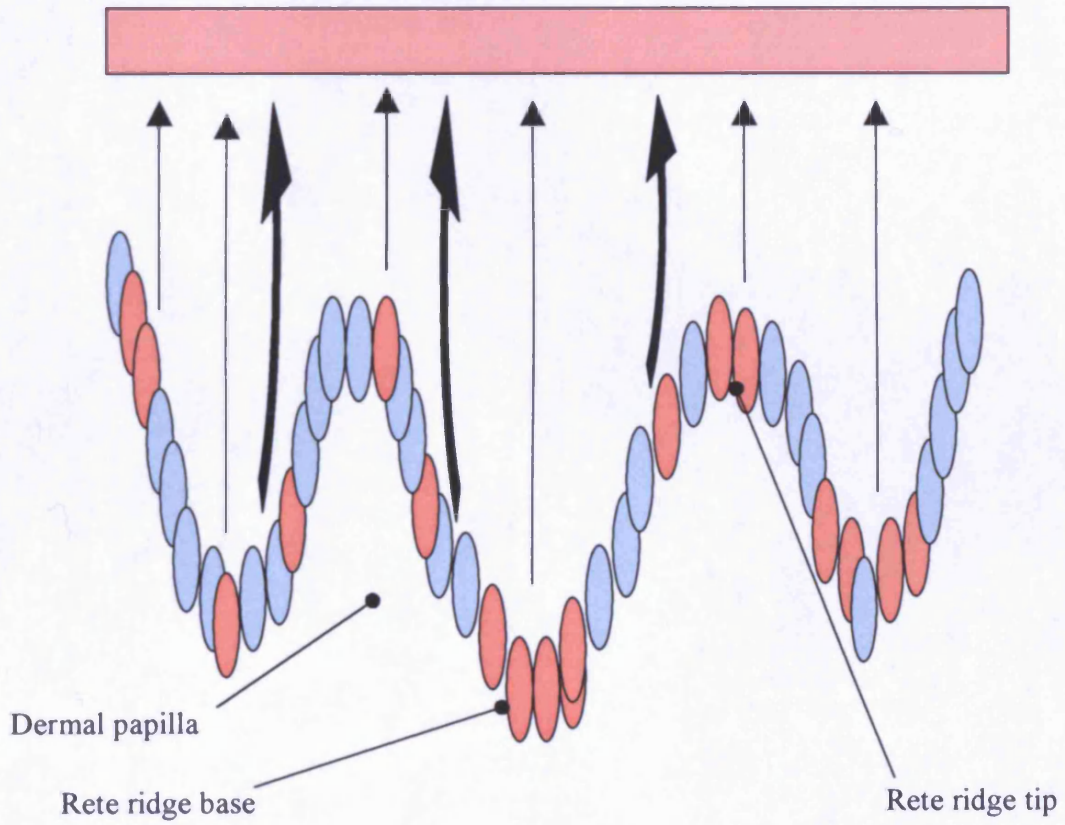


*Figure 1.5.* The distribution of stem cells (red) within epidermal proliferation units found within the viable epidermis of human skin.

*The image is adapted from (Ghazizadeh and Taichman, 2005).*

### 1.2.4. Cutaneous Immunity

The physical barrier afforded to the skin by the SC retains external micro-organisms on the skin surface. Disruption or breach of this barrier however can facilitate cutaneous invasion of pathogens and subsequent localised or systemic infection. The skin has therefore been equipped with a highly competent immune surveillance system that ensures protection from such microbial insult.

The immunocompetence of the skin is highlighted by the primary cell type, the keratinocyte. This cell can release over 20 different cytokines that signal to other cells of the immune system and maintain the immunological balance of the microenvironment (Williams and Kupper, 1996). Keratinocytes within the epidermis therefore assist in the maturation and migration of immature resident APCs and are also responsible for maintaining cells of the immune system at the site of infection through the expression of surface adhesion molecules.

Immature LCs (Section 1.2.2.2.4) are a type of dendritic cell (DC), possessing 'finger-like' protrusions that forge a network of cellular extensions within the suprabasal keratinocyte layer (Fig 1.2). This mesh facilitates their sentinel role within the skin by ensuring a large area for antigenic capture. DCs, such as LCs, are now recognised as powerful primary initiators (Schuler and Steinman, 1985) and modulators of the immune response (see (Banchereau and Steinman, 1998, Larregina and Falo, 2005, Romani et al., 2003) for comprehensive reviews). Antigens (Ag) that penetrate across the SC barrier are therefore captured by the LC network and engulfed by phagocytosis, macropinocytosis or receptor mediated endocytosis. Only picomolar levels of Ag are required for some of these uptake mechanisms to successfully stimulate an immune response (Banchereau and Steinman, 1998). Once the immature LC has engulfed and processed the Ag into immunogenic peptides, a large quantity of major histocompatibility class II complexes (MHC II) are released from vacuoles within the cell. These bind to the Ag fragments and the resulting complexes migrate towards the cell surface. Concurrently, the maturing LC is released from its sentinel position within the viable epidermis, possibly by a decrease in adhesion to surrounding keratinocytes (Williams and Kupper, 1996). Downward migration of a LC through the basement

membrane and their subsequent translocation into the draining lymph node, located in the dermal tissue, results in interaction with and subsequent activation of naive T cells.

Presentation of an exogenous Ag by the MHC II complex stimulates CD4+ (T helper) cells. However, LCs may also process endogenous Ags i.e. those Ags synthesised within the cell. Endogenous Ags presented by MHC class I molecules activate CD8+ (T cytotoxic) cells and therefore stimulate a different immune response. Vaccinologists have proposed that direct transfection of both LCs and keratinocytes within the viable epidermis will promote a sustained, balanced immune response and therefore an enhanced immune protection against disease (Howarth and Elliott, 2004, Kutzler and Weiner, 2004, Larregina et al., 2001, Morel et al., 2004, Pardoll and Beckerleg, 1995).

## 1.3. GENE THERAPY AND THE SKIN

### 1.3.1. Gene Therapy

Conceptually human gene therapy is simple; 'the introduction of an exogenous gene into a host cell to achieve a therapeutic benefit' (Morgan and Anderson, 1993). Conventional gene therapy aims to identify the defective gene(s) associated with a disease state and introduce to those affected cells a functional copy of the mutant gene. Cell functionality is consequently restored and the pathogenesis is therefore reversed. Such an elegant yet simple concept stimulated rapid and significant interest in the technology and during the 1990's the scientific and public domains became increasingly enthusiastic toward gene therapy as a revolutionary new medicine. This was mirrored by a rapid increase in the number of human gene therapy trials from the first, conducted in 1989 by Rosenberg and colleagues (Rosenberg et al., 1990) to a peak of 117 trials worldwide in 1999 (http://www.wiley.co.uk/genmed/clinical/, 2006). However the death of Jesse Gelsinger in 1999 (caused by an inflammatory response to the adenovirus vector), combined with the hindered development of therapeutically useful gene therapy technologies, contributed to a significant reduction in this growth, with just 27 trials in progress during 2005 (http://www.wiley.co.uk/genmed/clinical/, 2006).

Nonetheless, the scientific understanding of gene therapy has progressed considerably since the late 1980's and based upon information collated from over 1000 human gene therapy trials over the past 15 years the technology is now developing at a more sustainable rate. Increasing therapeutic proposals for gene therapy mean that it is not regarded now as simply the corrective treatment of inherited disease states but a method of introducing exogenous nucleic acids into cells to produce a therapeutic effect.

### 1.3.2. Gene Therapy Vectors

The successful expression of therapeutic genes within a target cell is highly dependent on effective formulation of the nucleic acid within a vector formulation that promotes nuclear delivery and translation of the genetic sequence into a therapeutic protein (Piskin et al., 2004). The inherent ability of a virus to infect and introduce foreign nucleic acid into the nucleus of a host cell has resulted in significant clinical

investigation into viral vectors as a method to deliver gene therapies (http://www.wiley.co.uk/genmed/clinical/, 2006). However, the high transfection efficiencies are undermined by safety concerns, including reversion to wild-type, adverse immunogenic response and random host integration of the exogenous nucleic acid. The 'ideal' viral vector therefore remains elusive. As a corollary to the inherent safety concerns of viral gene transfer vectors, non-viral vectors have been developed as an alternative approach. Synthetic delivery systems, including naked DNA or DNA condensed within a lipid or polymer vector system can be 'tailor made' using well characterised materials and are therefore associated with significantly reduced safety concerns.

Lipid-based plasmid DNA (pDNA) complexes are well characterised non-viral vectors used within gene therapy studies to promote cell transfection (Pedroso de Lima et al., 2001). The lipid component of these complexes is often a cationic liposome that interacts spontaneously upon combination with pDNA, resulting in condensation of the nucleic acid. These complexes, termed lipoplexes, offer significant advantages over naked DNA during extra- and intra-cellular delivery, improving interaction with the target cell and protecting the nucleic acid from enzymatic degradation (Lian and Ho, 2003, Lleres et al., 2004). Advances in the understanding of non-viral vector technology has led to the inclusion of polycations, such as protamine (Park et al., 2003), within non-viral formulations in order to improve the condensation of particles, their stability in the extracellular environment and their resulting transfection efficiencies (Faneca et al., 2004, Gao and Huang, 1996, Lleres et al., 2004). These cationic liposome-polycation-DNA complexes, termed LPDs, exist in a colloidal suspension and have been used for both systemic (Zhang et al., 2003) and local gene transfer (Birchall et al., 2000).

However the application of non-viral vectors, such as the LPD, is severely limited by poor transfection efficiencies, attributable to the hostile extracellular environment and the poorly understood mechanisms of intracellular delivery and trafficking (Belting et al., 2005, Lechardeur et al., 2005, Nishikawa and Huang, 2001, Ruponen et al., 2003). A number of key hurdles have been identified in the transition of the non-viral gene therapy from the extracellular space to the nucleus of the cell (Fig 1.6).

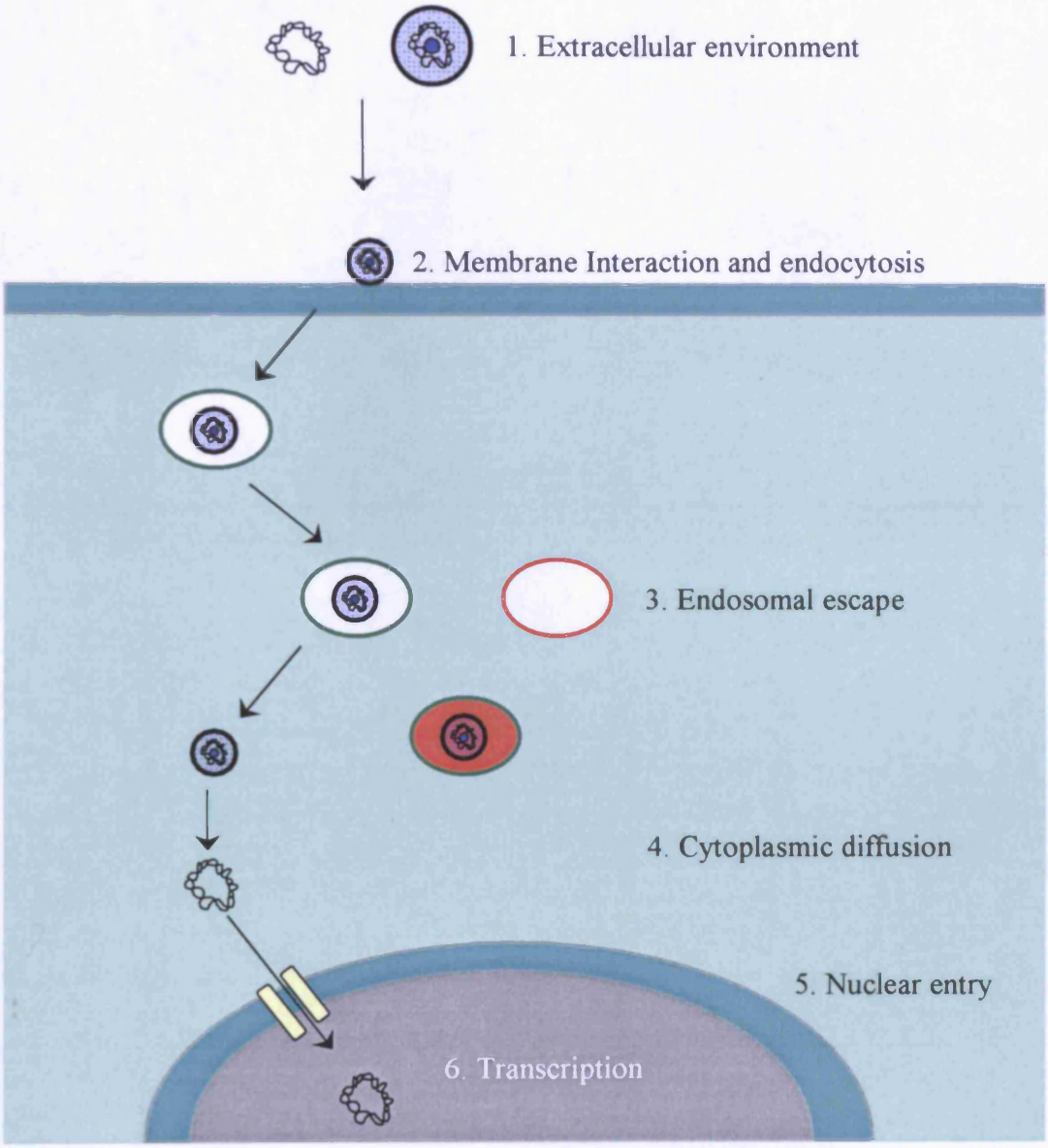


*Figure 1.6.* A schematic diagram highlighting the extra- and intra- cellular barriers to successful gene delivery.

### *1. The Extracellular Environment*

Interaction of pDNA and cationic delivery systems with components of the extracellular environment is a significant obstacle to effective gene therapy within localised tissues such as the skin (Ruponen et al., 2003). Barry and colleagues suggest that 99% of cutaneously delivered naked nucleic acid will be destroyed by extracellular endonucleases in just 90 minutes (Barry et al., 1999). Interestingly there is no correlation between the level of endonuclease activity within the skin tissue and the transfection efficiencies. The author attributes this observation to the variability associated with delivery by intradermal injection and the specific keratinocyte cell population located at the point of injection (Barry et al., 1999).

### *2. Membrane Interaction and Endocytosis*

Cationic non-viral gene delivery systems interact non-specifically with the cell surface by electrostatic interaction (Gao and Huang, 1995). The phospholipid barrier that surrounds cells prevents the passage of hydrophilic macromolecules by simple diffusion (Belting et al., 2005) and therefore endocytotic mechanisms are required for passage of DNA therapeutics across the plasma membrane. Studies suggest that for cationic gene therapy complexes, such as lipid and polymer based non-viral vectors, clathrin-dependent endocytosis is the responsible mechanism (Lechardeur et al., 2005), although a number of alternative mechanisms have also been implicated (Belting et al., 2005, Wiethoff and Middaugh, 2003).

### *3. Endosomal Escape*

Endocytic vesicles fuse with lysosomes resulting in exposure, and subsequent degradation of, nucleic acids by acidic hydrolases and endonucleases (Howell et al., 2003). It is therefore essential for a nucleic acid to escape the endosome soon after its entrance into the cell. Cationic lipids are thought to facilitate this process by destabilising the endosomal membrane (Lechardeur et al., 2005, Wattiaux et al., 2000), thereby releasing their pDNA into the cytoplasm.

*4. Cytoplasmic Diffusion*

Once released from the endosome, pDNA must migrate, through the cytoplasm, to the nucleus. However, the cytoplasm consists of a network of filaments, submerged in a 'soup' of macromolecules and cellular organelles (Lechardeur et al., 2005). Therefore although the cytosol possesses a viscosity comparable to water, for a high MW structure such as pDNA, molecular crowding and physical obstacles within the cytoplasm dramatically reduces the mobility of the nucleic acid. Hampered lateral diffusion (Dowty et al., 1995) and the activity of cytosolic nucleases (Lechardeur et al., 1999) have resulted in the identification of cytoplasmic permeation as a significant hurdle to successful transfection. This factor may be considerable in keratin and lipid packed keratinocytes located within the epidermis (Section 1.2.2.2).

*5. Nuclear Entry*

The transfer of macromolecules between the cytoplasm and the nucleus is fundamental to the functioning of a eukaryotic cell and is controlled by nuclear membrane pores termed nuclear pore complexes (Sebestyen et al., 1998). These 50nm diameter pores allow the passive diffusion of molecules that are approximately 9nm in diameter (Wiethoff and Middaugh, 2003). Activation of the pore by a nuclear localisation signal (NLS) though facilitates passage of larger molecules, potentially pDNA (Collas and Alestrom, 1997, Munkonge et al., 2003).

However, the more established mechanism of pDNA nuclear entry is more opportunistic. During mitosis i.e. when the cell is dividing, the nuclear envelope disintegrates thereby allowing the plasmid freedom to access the nucleus. Transfection may therefore be highly influenced by the rate of cell division. This stage of the transfection process is generally regarded as the rate limiting step (Dean et al., 2005a) and therefore within the skin, where the majority of cells are terminally differentiated, this is likely to be a considerable obstacle.

*6. Transcription*

Once the pDNA has reached the nucleus it remains distinct from the host cells genome (episomal) and utilises the host cell's machinery for transcription. However when those transfected cells divide, pDNA is degraded or diluted (Hengge et al., 2001). Within the skin, it is important to remember that progressive differentiation of cells and the desquamation process will therefore ultimately lead to plasmid loss from the tissue.

### 1.3.3. Cutaneous Gene Therapy

During the infancy of gene therapy in the early 1990's, the epidermis was recognised as an 'attractive target tissue for gene therapy' (Greenhalgh et al., 1994). Some of the reasons for such optimism in cutaneous gene therapy remain true today:-

1. The tissue is readily accessible for manipulation.
2. Treated areas of skin can be visually monitored and removed surgically if an adverse event to treatment is detected.
3. Integration of an exogenous gene within proliferative stem cells located in the basal layer of the epidermis can potentially facilitate stable integration of the gene and the correction of a genetic defect
4. The biology of the epidermis and the cells contained within this stratified tissue are well understood.
5. Primary human keratinocytes can be maintained *in vitro* thereby allowing *ex vivo* treatment of skin disorders before reintroduction of treated cells to the patient.
6. The epidermis may be used as a bioreactor to synthesise therapeutic proteins for systemic therapeutic activity.

However just five years later negative publicity and restricted scientific progress prompted the question, 'how realistic is cutaneous gene therapy' (Hengge et al., 1999). At this stage, the principles of gene therapy were proven but a number of limitations prevented progression to the clinic. These included tissue targeting, stable gene expression, the control of immune responses, correction of all defective cells in the organ, the creation of an acceptable topical gene formulation and safety concerns. Since then, cutaneous gene therapy has been developing at a steady rate. In 2005, Hengge

reflected upon developments over the previous decade and was encouraged by progression but mindful of the scientific advances required for successful translation of therapeutics to the clinic (Hengge, 2005).

For cutaneous gene therapy target cells are located in the viable epidermis, a narrow region of cells, sandwiched between the outermost SC barrier and the underlying dermal connective tissue. Accessibility to the target region is therefore restricted. The second major difficulty is obtaining efficient, reproducible and sustained transfection of cells within a tissue that is in the continuous process of cell renewal and differentiation. Numerous therapeutic applications have been proposed for cutaneous gene therapy, including the treatment of cutaneous malignancies (Green and Khavari, 2004, Kitagawa et al., 2003, Merdan et al., 2002, Rakhmilevich et al., 1996, Sotomayor et al., 2002) and the promotion of wound healing (Andree et al., 1994, Jeschke, 2003, Yang et al., 1990, Yao and Eriksson, 2000). However, the majority of published work investigates its potential within the treatment of genodermatoses or the development of a genetic vaccine.

#### *1.3.3.1. Genodermatoses*

Improvements in gene sequencing technologies during the 1990's and the human genome project have led to the identification of the defective genes responsible for numerous inherited disease states (Irvine and McLean, 2003, van Ruissen et al., 2002). Defects in a single gene may be responsible for a disease phenotype and therefore correction of the identified defective sequence may enable cure of the inherited skin disorder (genodermatosis). By the year 2000, 80 genes associated with inherited skin diseases had been identified (Uitto and Pulkkinen, 2000) and just three years later this had increased to 139 genes (Irvine and McLean, 2003). However the increased molecular and genetic understanding of genodermatoses has not been mirrored by advances in the treatment of patients.

Two of the most studied inherited disease states include epidermolysis bullosa (EB) (Jonkman, 1999) and xeroderma pigmentosum (XP) (Magnaldo and Sarasin, 2004). Our understanding of these diseases has increased exponentially over recent years, aided by the development of representative animal models (Arin and Roop, 2004, Jiang and

Uitto, 2005). However treatment remains symptomatic. EB is a blistering condition, associated with the dysfunction of hemidesmosomes (Jonkman, 1999), which may be debilitating, disfiguring and in the more serious cases life threatening for patients. Corrective gene therapy would offer these patients a curative treatment. Progress within this field has led to recent initiation of an *ex vivo* clinical trial (Dellambra et al., 2000, Ferrari et al., 2005), the results of which are eagerly anticipated by the cutaneous gene therapy community.

*Ex vivo* delivery of the therapeutic transgene to diseased skin involves removal of a skin biopsy, propagation of skin cells *ex vivo*, transfection of those cells with the selected genetic sequence and the subsequent grafting of cells back to the patient. This is a time consuming and practically difficult process that may result in the scarring of patients due to the surgical procedures involved. However, to date it has been preferred to *in vivo* delivery primarily because *ex vivo* skin may be enriched for those transfected cells and also expanded to regenerate large skin areas. This is a vital consideration in the treatment of EB, where extensive areas often require graft treatment (Lombry et al., 2000). *In vivo* delivery of a therapeutic to treat genodermatoses would be a less complicated and more patient acceptable method of treatment (Chaote and Khavari, 1997) but its application may be restricted to cutaneous disorders with a phenotype that is limited to isolated skin areas. The simplicity of *in vivo* delivery and the progressive development of novel cutaneous delivery methods will continue to stimulate the attention of those in the field of genodermatoses (Woodley et al., 2004).

#### *1.3.3.2. Genetic Cutaneous Immunisation*

As discussed previously (Section 1.2.4), the skin is a highly immunocompetent organ (Banchereau and Steinman, 1998, Larregina and Falo, 2005, Williams and Kupper, 1996). It is therefore unsurprising that vaccinologists and immunologists now consider the skin, and more correctly the viable epidermis, to be a potential target for localised vaccine delivery (Babiuk et al., 2000, Glenn et al., 2003, Partidos et al., 2003, Partidos and Muller, 2005). Intradermal delivery aims to provide safer and more comprehensive vaccination regimens (Babiuk et al., 2000, Mikszta et al., 2005).

Established immunisation schemes rely primarily on the delivery of vaccines by intramuscular or subcutaneous injection. Therefore acknowledgment of the skin as a competent immunological organ has directed vaccinologists toward the development of safer and less invasive methods of vaccination (Partidos et al., 2003). Studies by Glenn and co-workers suggest that topical application of antigenic peptide vaccines to hydrated skin can induce levels of systemic immunological protection (Glenn et al., 1998a, Glenn et al., 1998b). However the SC barrier restricts vaccine candidates to small peptide Ags (Partidos et al., 2002, Partidos et al., 2003) which themselves only elicit limited immune responses (Glenn et al., 1998a, Glenn et al., 1998b). More recent studies by Glenn and colleagues have therefore used tape-stripping techniques and emery paper to disrupt the outer layers of the skin prior to topical Ag application (Glenn et al., 2003).

The poor permeability of the SC to vaccines has stimulated the development of alternative vaccine delivery strategies (reviewed in (O'Hagan and Rappuoli, 2004, Partidos, 2003)). Needle-free vaccine technologies include the helium driven Powderject™ device (Chen et al., 2004, Chen et al., 2000) and the more recently developed microneedle array (Mikszta et al., 2002, Mikszta et al., 2005, Widera et al., 2006). Microneedle facilitated localised delivery of both model (Widera et al., 2006) and therapeutic Ags (hepatitis B (Mikszta et al., 2002) and anthrax (Mikszta et al., 2005)) have been shown to produce equivalent or even greater immune responses than injected delivery techniques. Cutaneous delivery of a vaccine can potentially target key mediators of the immune system, the LCs, and therefore in doing so aims to improve immune responses and reduce systemic adverse effects.

The potential of cutaneous immunisation using a DNA vaccine was realised over a decade ago (Tang et al., 1992) and has since progressed towards the treatment of candidate diseases including hepatitis B (Kwissa et al., 2000, Osorio et al., 2003, Roberts et al., 2005, Tacket et al., 1999, Xiao-wen et al., 2005), human immunodeficiency virus (HIV) (Giri et al., 2004, Lisziewicz et al., 2006, Lisziewicz et al., 2005, Liu et al., 2001) and influenza (Chen et al., 2000, Dean and Chen, 2004, La Montagne and Fauci, 2004, Van Kampen et al., 2005, Watabe et al., 2001). The concept is simple; an antigen-encoding plasmid is introduced into the skin tissue, resulting in

expression of the antigenic protein *in vivo* and the subsequent induction of an immune response. Current established vaccination strategies utilise killed or live attenuated vaccines, which although successful in certain cases, have a number of drawbacks. These may be addressed by DNA vaccination. Creation of an Ag *in situ* mimics infection by viral pathogens and therefore, unlike killed vaccines, DNA vaccination may stimulate a more balanced immune response (Babiuk et al., 2000). DNA vaccination is also free from the safety concerns that surround the reversion of live attenuated vaccines to the wild type. Practical benefits of pDNA include the ability to rapidly construct pDNA for a named Ag, the rapid synthesis and purification of large pDNA stocks, improved stability (Babiuk et al., 2000, Walther et al., 2003) possibly removing the requirement of cold chain storage and low manufacturing costs (Babiuk et al., 2000). Such benefits would permit rapid production and distribution of immunisations and therefore DNA vaccines have become a particularly attractive proposition to those working in the field of biodefence (Dean et al., 2005b, Garmory et al., 2005) and for the treatment of pandemic diseases, such as influenza (Kaiser, 2004).

Significant interest in genetic immunisation, since its conception in 1992 (Tang et al., 1992), resulted in the publication of over one thousand articles by the millennium (Shedlock and Weiner, 2000) and the notion of pDNA as the 'third generation of vaccine' (Alarcon et al., 1999). However although interest continues to expand, the technology has not advanced to clinical use (Restifo et al., 2000). The primary hurdles to successful cutaneous genetic immunisation are consistent with those that exist within other areas of gene therapy i.e. inefficient transfection and poor localised delivery of the formulation. However, more encouragingly, the immunocompetence of skin means that only small quantities of the Ag are required for an effective immune response (Banchereau and Steinman, 1998) and therefore, the transfection efficiencies are likely to be less than that required in the treatment of genodermatoses (Pertmer et al., 1995) or cancers (Sotomayor et al., 2002). It should also be noted that in order to stimulate a systemic immune response it may only be necessary to deliver the vaccine to a small area of skin. For these reasons cutaneous genetic immunisation is considered to be the most realistic therapeutic application of microneedle mediated gene delivery to the skin.

## 1.4. TRADITIONAL AND NOVEL TRANSDERMAL DELIVERY

### 1.4.1. Traditional Transdermal Delivery

The skin is a lucrative interface for systemic and localised drug delivery, possessing numerous advantages including its direct accessibility, the avoidance of first pass metabolism, an opportunity for controlled release products, the ability to monitor the therapeutic system and the potential to produce a simplistic 'patient friendly' drug delivery system. However the skin, and in particular the SC, presents a formidable barrier to the penetration of therapeutic compounds. Diffusion of compounds through the cutaneous 'brick and mortar' structure is primarily by the intercellular route (Potts and Francoeur, 1991). To enhance transdermal penetration of small therapeutic molecules, a number of elegant formulation strategies have been employed. This has lead to the successful development of transdermal patches, which attract annual worldwide revenue of over 2 billion pounds (Barry, 2001).

However, after decades of research only a handful of clinically useful compounds are delivered successfully via the transdermal route (Mitragotri, 2004). Therapeutic candidates are restricted primarily to potent molecules with a MW of less than 500Daltons (Da) (Bos and Meinardi, 2000) and high lipophilicity (Prausnitz et al., 2004). Therefore, nucleic acids such as pDNA, a hydrophilic macromolecule of up to 10MDa, are poor candidates for conventional methods of cutaneous delivery.

### 1.4.2. Novel Transdermal Delivery

The emergence of macromolecular therapeutics, spawned from advances in the biotechnology industry, has stimulated interest in alternative transdermal delivery strategies. Cutaneous gene therapy relies on localised delivery of macromolecular and nanoparticulate formulations that are often greater than 1MDa and/or 100nm in diameter. Novel transdermal delivery techniques have therefore been investigated for delivery of such macromolecules. Techniques can be grossly divided into those that disrupt the skin barrier and those that completely bypass the SC.

### 1.4.3. Disrupting the Skin Barrier

#### *1.4.3.1. Electrical Methods*

Electroporation is an electrically assisted method of transdermal delivery involving the application of short high-voltage (>50Volts) pulses across the skin. The mechanism of permeation enhancement has not been conclusively proven however it is believed that electrical stimulation opens up transient aqueous pores in the skin (Banga and Prausnitz, 1998). Electroporation has been shown to enhance the delivery of hormones (Medi and Singh, 2003) and model macromolecules up to 40kDa (Lombry et al., 2000). It has also been considered for DNA vaccination approaches (Banga and Prausnitz, 1998). However, failure to deliver 14nm nanoparticles across human SC suggests that there is an upper limit to the size of therapeutics that can be delivered by this method (Chen et al., 1999).

Iontophoresis, a related technique using low voltage electrical currents (<10Volts) facilitates the cutaneous delivery of 'smaller' macromolecules, such as insulin (6kDa) (Kari, 1986), but there is little evidence of its applicability in nucleic acid delivery (Kalia et al., 2004).

#### *1.4.3.2. Sonophoresis*

Sonophoresis involves permeabilisation of the skin by application of low frequency ultrasound, creating disruptions within the SC by cavitation (Wu et al., 1998). This technique has also been linked to vaccination and more significantly facilitation of cutaneous gene therapy applications, including the correction of genodermatoses (Lavon and Kost, 2004). However although the technique has recently demonstrated an adjuvant effect in transcutaneous immunisation with tetanus toxoid (Tezel et al., 2005), the largest transdermally delivered molecule to date is erythropoetin (Wu et al., 1998), a 48kDa macromolecule, which is up to one hundred times smaller than pDNA.

#### *1.4.3.3. Photomechanical Waves*

Pressure waves generated by laser radiation are reported to reversibly permeabilise the SC, creating temporary channels through which drug compounds can diffuse (Doukas and Kollias, 2004). Evidence for successful photomechanical delivery of

macromolecules remains limited, although permeation of nanoparticles up to 20nm in diameter, up to a depth of 5μm, has been reported (Lee et al., 1998).

### 1.4.4. Circumventing the Skin Barrier

#### *1.4.4.1. Intradermal Injection*

The simplest and most commonly used method for the localised introduction of macromolecules, most notably vaccines, into skin has been intradermal injection using a needle and syringe. Although precise volumes can be administered by this method, the depth of needle penetration and therefore the localisation of delivery is highly variable, dictated by the skill of administration and inter- or intra-variability in skin structure. A hypodermic needle, over 300μm in diameter (Zahn et al., 2001), creates 0.41-0.71mm holes within the skin (Baxter and Mitragotri, 2005) and therefore cannot facilitate targeted delivery to those viable keratinocytes and LCs within the epidermis. Injections also suffer from practical difficulties such as needle-stick injury, pain, needlephobia and administration dependent upon trained personnel. However, despite these disadvantages, intradermal injection provides an assured passage across the SC for a range of macromolecular formulations, including pDNA, and therefore maintains its position in the clinical and scientific setting as the 'gold standard' to which other cutaneous delivery techniques must be compared.

#### *1.4.4.2. Follicular Delivery*

Appendageal skin structures such as the hair follicle only contribute to 0.1% of the skin area available for diffusion (Barry, 2001). Although the use of the hair follicle as a portal for localised or systemic delivery is questionable (Meidan et al., 2005), it remains a target for gene therapy (Hoffmann, 2000, Ohyama and Vogel, 2003). Topical application naked DNA (Fan et al., 1999), cationic lipoplexes (Domashenko et al., 2000, Li and Hoffmann, 1995) and viral vectors (Hoffmann, 2003) have been used to facilitate transfection of cells within hair follicles.

#### *1.4.4.3. Ballistic Delivery*

Ballistic devices aim to propel powder and particulate formulations across the SC barrier within a high velocity gas stream (Fynan et al., 1993). The technology has been

used widely in the delivery of genes to the viable epidermis, resulting in a large body of published work (for reviews see (Chen et al., 2002, Dean et al., 2003, Kendall, 2006)). The 'gene gun', has been used extensively for genetic immunisation (Dileo et al., 2003, Fensterle et al., 1999, Fynan et al., 1993, Lin et al., 2000, Pertmer et al., 1995, Wang et al., 2004) against diseases such as hepatitis B (Roberts et al., 2005) and influenza (Dean and Chen, 2004, Dean et al., 2003). Recent publications assess the capabilities and also the current limitations of the Powderject™ system (Kendall et al., 2004, Raju et al., 2006). One of the principal advantages of this technique is that it facilitates direct intracellular delivery of the nucleic acid and therefore eliminates extracellular barriers to successful gene delivery. However, limitations include variable depth of particulate penetration, the unknown fate of the gold carrier particles and a reduction in cell viability within treated areas of skin. The expense and complexity of this technology also restricts distribution and so hampers its employment for mass immunisation schemes.

Jet injection is a related technique in which a high speed stream of liquid is fired at the skin surface from an air or spring driven jet injector. Although the ability to deliver compounds across the SC barrier using this technology has been evident for many years (Hingson et al., 1963, Perkin, 1950), the mechanisms of delivery are only now being elucidated. Studies by Mitragotri and colleagues indicate that the technology creates conduits of similar diameter to the jet stream, approximately 100μm in diameter that extend to depths of over 10mm (Modamio et al., 2000, Schramm-Baxter and Mitragotri, 2004). It is therefore unsurprising that the successful delivery of macromolecules such as insulin (Bremseth and Pass, 2001) has stimulated examination of this technique for cutaneous gene therapy (Aguiar et al., 2001, Cui et al., 2003, Mumper and Cui, 2003, Sawamura et al., 1999).

#### *1.4.3.4. Laser Ablation*

Laser methods including the ruby (Woan-Ruoh et al., 2002), carbon dioxide (Woan-Ruoh et al., 2002) and argon-fluoride (Fujiwara et al., 2005) laser have been used to facilitate transdermal delivery. However the erbium:yttrium-aluminium-garnet (erbium:YAG) laser, used to ablate the SC layer, has been characterised most extensively (Lee et al., 2003, Lee et al., 2002, Nelson et al., 1991, Woan-Ruoh et al.,

2002). Transdermal delivery of small molecules such as vitamin C (Lee et al., 2003) and 5-fluorouracil (Lee et al., 2002) has been followed by the cutaneous delivery of insulin and model macromolecules up to 77kDa (Fang et al., 2004), with minimal levels of skin damage (Lee et al., 2003). The upper size limit for cutaneous delivery using the erbium:YAG laser is yet to be determined and therefore its potential in cutaneous gene delivery remains unknown.

#### *1.4.3.5. Radiofrequency Ablation*

In 2003, Levin and colleagues reported the development of a device capable of creating a uniform pattern of microconduits through the SC using radiofrequency thermal ablation (Sintov et al., 2003). The Via Derm™ generator, developed by TransPharma Medical®, consists of an ordered arrangement of stainless steel electrodes that are positioned on the skin surface and which, on application of a high frequent electric current, ablate the underlying cells to create a visible aqueous pore. These pores, termed radiofrequency (RF) microchannels, are typically 30μm in diameter and 70μm in depth although the dimensions of the conduits can be altered by simple adaptation of the device and its settings. The device has facilitated delivery of small molecules (Sintov et al., 2003) and human growth hormone (22kDa), to produce plasma levels equivalent to that achieved by sub-cutaneous injection (Levin et al., 2005). More recently, studies conducted within our laboratories have provided evidence for successful cutaneous delivery of pDNA through RF microchannels (Birchall et al., 2006) (Appendix III).

#### *1.4.4.6. Thermal Ablation*

Thermal ablation involves the application of focused bursts of thermal energy to create an array of micron sized holes within the skin (Prausnitz, 2001). Development of this technology has been led by Altea Therapeutics® and has resulted in the development of a device that can facilitate the cutaneous delivery of a number of macromolecules including pDNA (http://www.alteatherapeutics.com/, 2005).

#### *1.4.4.7. Microscission*

Recent reports by Weaver and colleagues revealed a new minimally invasive transdermal delivery technique, termed microscission (Bates, 2004, Herndon et al.,

2004). This technology utilises inert sharp sided aluminium crystals within a vertically applied high pressure gas stream to 'scize' the underlying tissue, thus creating substantial disruptions to the skin surface of human subjects. The created microchannels are up to 250μm in diameter and 200μm in depth and therefore, although the clinical usefulness of this technology is yet to be examined, the cutaneous delivery of macromolecules is a realistic proposition.

#### *1.4.4.8. Microneedles*

The microneedle array device is a recent innovation (Henry et al., 1998a), attracting significant interest within academic organisations and industry for the cutaneous delivery of protein and nucleic acid drugs. Its primary advantage over the previously mentioned technologies is that it is a simple mechanical device and therefore is potentially less expensive and more easily distributed. This promotes accessibility of the technology to a wider patient population and will hopefully accelerate its progression to the clinical setting. However, progression from laboratory prototypes to clinically useful devices requires scientists to address a number of challenges regarding the manufacture and therapeutic application of the device.

## 1.5. MICROFABRICATED MICRONEEDLES

### 1.5.1. The Microneedle Concept

The use of a traditional needle and syringe to deliver therapeutic compounds across restrictive biological barriers, as exemplified by the SC, was initiated in the 19$^{th}$ century (McGrew and McGrew, 1985). Surprisingly, over the previous 150 years there has been limited progress in the device technology, with the smallest needles available (30G) possessing a diameter of more than 300μm and a penetration depth that is essentially dependent upon the skill of the administrator (Zahn et al., 2001). Therefore although direct intradermal injection will remain an important delivery strategy for the clinician there is significant interest in the development of less invasive methods of drug administration.

Over the last decade an exciting alternative method for enhancing cutaneous permeation of molecules has been developed, the microneedle array. The concept of this device (Fig 1.7) was described three decades ago (Gerstel and Place, 1976). However it is only through progression of microfabrication techniques, used in the microelectronics industry, that micron-scale devices such as the microneedle array were realised (Henry et al., 1998a). In 1998, Dr Mark Prausnitz and his colleagues at the Georgia Institute of Technology published details of the first microneedle device to be used in transdermal delivery strategies (Henry et al., 1998a). The device consisted of an array of silicon, micron-sized needles, on the surface of a solid support backing, created using well defined silicon etching techniques.

Microneedles arrays are, as the term describes, a group of micron scale needles that when applied to skin penetrate the SC to produce conduits that extend into the underlying tissue layers. This provides a direct route of permeation for therapeutic formulations. The original microneedle concept was to use needles, ~150μm in length, which would not impinge on nerve fibres and blood vessels that reside in the underlying dermis. The microneedle array has therefore provided an interface for macromolecule delivery, that eliminates the pain and bleeding that is associated with a traditional needle and syringe (Henry et al., 1998b). Primary studies revealed, as would be intuitive, that application of a device and its removal prior to application of a topical formulation facilitates significantly greater cutaneous penetration of a topically applied formulation than untreated skin (Fig 1.7) (Henry et al., 1998a, Henry et al., 1998b).

The microneedle device holds benefits for patients, clinicians and the pharmaceutical industry. Advantages include:-

1. The direct and controlled delivery of a therapeutic compound or macromolecule across the SC.
2. A 'patient friendly' method of drug delivery with no pain or bleeding at the application site, potentially useful in the vaccination of children or patients suffering from needlephobia.
3. Topical application of a formulation over a large surface area (dictated by the device dimensions) and accessibility to large numbers of epidermal cells.

4. Combination of a microneedle device with traditional transdermal delivery formulations to promote cutaneous delivery.
5. The ability to tailor the dimensions and geometries of individual microneedles and the spacing and density of microneedles within the array pattern, to suit its therapeutic application.
6. Mass production of the device in a reproducible and cost effective manner.
7. The potential to create a device that does not require a skilled user for application i.e. it may be adapted for self-administration.

Over recent years the microneedle concept has been embraced by a number of research groups in North America, Europe and the Far East. Collaborative efforts between engineers and drug delivery scientists have resulted in the progressive development of the microneedle geometries and morphologies. Optimisation of array characteristics and the integration of pharmaceutical formulations aim to create a delivery system that can progress from the laboratory to clinical practice.

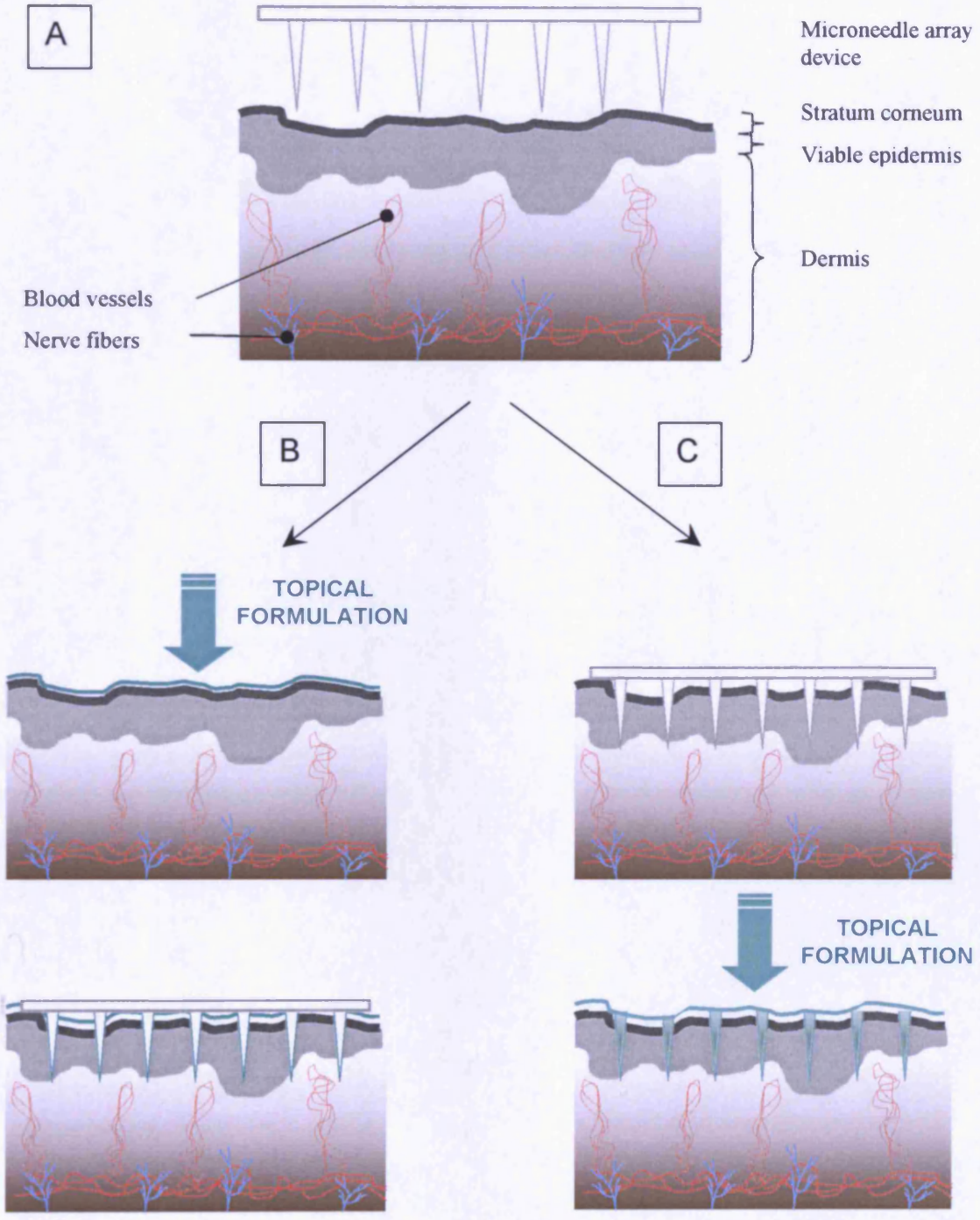


*Figure 1.7.* A schematic representation of the microneedle concept.

A: Microneedles are positioned above the area of skin to be treated.
B: A topical formulation is applied to the skin and microneedles are subsequently inserted using a downward force. The device may remain in place or be removed from the tissue.
C: Microneedles are inserted into the skin and then removed to expose an array of intradermal microchannels. A topical formulation is then applied to the treated area.

### 1.5.2. Silicon Microfabricated Microneedles

The manufacturing methods employed by Prausnitz and co-workers for creation of silicon microneedle arrays (Henry et al., 1998a) have been adopted and adapted by a number of research groups to yield microneedle arrays of varying geometries, dimensions and morphologies (Chabri et al., 2004, Haider et al., date unknown, Luttge et al., 2003, Newton et al., 2003, Sivamani et al., 2005, Teo et al., 2005, Wilke et al., 2005, Xie et al., 2005). The principles of manufacture and the technology required are detailed in the subsequent chapter (Section 2.1.1).

Initial studies by Prausnitz and co-workers demonstrated a 10,000 fold increase in calcein (623Da, 0.6nm radius) permeation through microneedle treated human cadaver skin (Henry et al., 1998a). Subsequent studies used similar devices to promote permeation of bovine serum albumin (BSA) (66kDa, 3.5nm radius), insulin (6kDa) and even nanoparticles (25nm and 50nm diameter) through the epidermal membrane (McAllister et al., 2003).

### 1.5.3. Alternative Microneedle Materials

Microneedle design, manufacture and materials have progressed from the original prototype. Although silicon has established itself as a useful material, the creation of microneedles on a laboratory scale can be expensive, time consuming and their manufacture requires established clean-room facilities. Silicon can also be brittle and has not been proven to be biocompatible. Therefore, glass, metal and polymer microneedles have all been developed and used to deliver a variety of compounds using microneedle heights from 100 to 1000μm (Martanto et al., 2004, McAllister et al., 2003).

The creation of titanium and stainless steel microneedle arrays does not require the complex microfabrication procedures synonymous with their silicon counterparts (Cormier et al., 2004, Lin et al., 2001, Martanto et al., 2004, Matriano et al., 2002). Solid stainless steel microneedles are laser patterned within a sheet of metal and are subsequently manually moved out of the plane of the metal sheet to create the array structure (Martanto et al., 2004). In recent years, Daddona and colleagues at ALZA

Corporation have utilised a titanium microneedle array within a patch system, termed Macroflux™. This technology has been used to deliver ovalbumin (a model antigenic protein) (Matriano et al., 2002), desmopressin (Cormier et al., 2004) and antisense oligonucleotides (Lin et al., 2001) into the skin of hairless guinea pigs. A recent study by Prausnitz and colleagues has also examined insulin delivery into diabetic hairless rats using a steel microneedle array (Martanto et al., 2004). Localised treatment of the skin with the device followed by topical insulin application resulted in a reduction of blood glucose levels in a comparable manner to subcutaneous hypodermic injection (Martanto et al., 2004). Similar studies have also been conducted using bevelled glass microneedles, created using simple drawn-glass micropipette techniques (McAllister et al., 2003, Wang et al., 2005). In the future, microneedle devices may offer a painless method of insulin delivery for diabetic patients.

Polymer microneedles have been created by micromoulding techniques, using a silicon microneedle device as a template (McAllister et al., 2003, Park et al., 2005). A recent study demonstrates the functionality of the polymer microneedle array in facilitating the delivery of a simple chemical dye, calcein and BSA through treated human cadaver skin (Park et al., 2005). Polymer microneedles offer a potentially robust, biocompatible and possibly biodegradable material that can be manipulated to fashion microneedle devices outside of the high cost clean-room facilities required for silicon structures.

### 1.5.4. Hollow Microneedles

The permeation of drug molecules from a topically applied formulation through aqueous microconduits created in the SC by a solid microneedle array relies upon the diffusive properties of the therapeutic. Permeation through such microconduits is influenced by interaction of the therapeutic molecule with components of the surrounding biological environment. Passage through the bore of a hollow microneedle however permits greater control over the properties of the permeation route. More significantly, pressure-driven flow of a formulation through hollow microneedles permits the active cutaneous delivery of specific volumes of a medicament at a controllable rate. This potentially allows complete control over cutaneous delivery profiles. However, we might expect hollow microneedles to be structurally weaker than solid needles. It is therefore important to adapt the shape of microneedles and/or employ

robust materials such as metals and polymers in order to retain sufficient mechanical strength to facilitate successful insertion and removal from human skin tissue. Hollow microneedle arrays have now been manufactured using polymer, glass and silicon, with a range of needle heights and shapes (McAllister et al., 2003).

A number of commercial companies are developing hollow microneedle devices, intended for sustained drug delivery. The Micropyramid™ is a hollow silicon microneedle structure, created by Nanopass Technologies in conjunction with Silex Microsystems, (Gardeniers et al., date unknown, http://www.nanopass.com/, 2005, http://www.silexmicrosystems.com/mems.asp?page=s3, 2006). This array can be inserted repeatedly into the skin with minimal damage to the robust pyramidal structure. The technology is currently being utilised in the development of a sustained delivery device (Nanopump™) and also a bolus injection device (MicronJet™), the latter of which combines the microneedle array with a jet injection mechanism. Other commercial devices include 3M's microstructured transdermal system (MTS™) and BD's Microinfusor™.

Prausnitz and colleagues have prepared straight walled hollow microneedles by electrodeposition of metals such as nickel on to silicon or polymer moulds (McAllister et al., 1999, McAllister et al., 2003). Such microneedles are capable of penetrating the outer layers of human skin without breaking. Upon insertion, tips do not become obstructed with biological debris and therefore permit efficient delivery of liquid formulations (McAllister et al., 1999). A recent *in vivo* study using diabetic hairless rats utilised hollow microneedles for the cutaneous delivery of insulin (Davis et al., 2005).

Hollow microneedles can also extract fluid from skin tissue and may therefore be used for therapeutic monitoring. Initial studies have used single glass bevelled microneedles (not microneedle arrays) to inject and extract fluid from skin tissue (Wang et al., 2002). However, hollow silicon microneedle arrays capable of multiple tissue sampling points have now been described (Mukerjee et al., 2004, Wang et al., 2005). Small arrays of solid glass bevelled microneedles, similar to those previously described to deliver insulin (Wang et al., 2002), have also been used in the collection of interstitial fluid (ISF), for glucose monitoring, both within hairless rats and also human subjects (Wang

et al., 2005). However, although the cutaneous penetration of solid glass microneedles followed by vacuum driven extraction of ISF through the created microchannels has demonstrated a degree of success (collection of 1-10μl ISF), the extraction of ISF through the bores of a hollow microneedle was more problematic.

The difficulties in sampling of interstitial fluid from the skin using a hollow microneedle array may be attributed to a failure to pierce the skin, buckling of the microneedle upon application or blockage of the needle tip on insertion (Mukerjee et al., 2004). However, these problems may be overcome by optimising the height and morphology of microneedles and the location and size of the microneedle bore. Silicon microneedles with 'snake fang' morphology have now proven successful in the sampling of ISF (Mukerjee et al., 2004), using only capillary action as a driving force for fluid withdrawal. The addition of a micropump to hollow microneedle devices has permitted development of an integrated glucose sensing and insulin infusion device where a feedback-controlled system controls the insulin delivery profile in direct response to the patients' blood glucose levels (Zahn et al., 2004, Zahn et al., 2001).

### 1.5.5. Microneedle Structure and Mechanics

The majority of microneedle investigations have focused upon the impact of their design on the delivery of therapeutics. However, it is also important to consider the mechanical strength of the device and its method of application. A balance between miniaturisation and the rigidity needed to resist the forces imposed on needles during insertion is of paramount importance if the device is to be accepted as a reliable and 'safe' drug delivery platform.

It is interesting to note that the length of microneedles used in experimental studies has progressed from 150μm (Henry et al., 1998a) to 1000μm (Martanto et al., 2004, McAllister et al., 2003), with microneedles from 300 to 600μm in length being used routinely by the major research groups (Lin et al., 2001, Matriano et al., 2002, Prausnitz et al., 2003). Evidence of bleeding following application of microneedle devices containing 225μm to 600μm length needles has been shown to be minimal and short lived (less than 24hours) with no evidence of infection or scarring during subsequent days (Widera et al., 2006). The average penetration depth for 50% of microneedles on

an array was recorded at 165μm for the 225μm microneedles and 315μm for the longer microneedles used and all microneedles penetrated further than 90μm below the skin surface.

Application forces for those silicon microneedle arrays created by Prausnitz and co-workers at the end of the last decade were considered to be approximately 10Newtons (N), which was described as 'the force required to push an elevator button' (Henry et al., 1998a, Henry et al., 1998b). This resulted in approximately 95% of microneedles penetrating the skin surface. However, the force required to penetrate the skin is dependent upon the microneedle tip diameter, its sharpness, the needle length and interneedle spacing (Davis et al., 2004, Haider et al., date unknown), not forgetting the elasticity and tension of the tissue into which the array is inserted. These factors were highlighted in a recent publication (Teo et al., 2005) where solid silicon microneedles demonstrated successful, but much reduced, calcein permeation in comparison to those original studies conducted by Prausnitz and co-workers (Henry et al., 1998a). The authors attributed the reduced capabilities of the microneedle array to a combination of the reduced sharpness of individual microneedles, the smaller interneedle spacing and the cushioning effect of the underlying subcutaneous fat.

Theoretical pressures required to puncture human skin have been calculated and used to try and determine the forces required for effective microneedle penetration (Aggarwal and Johnston, 2004). Ultimately, a needle will penetrate the skin at the moment where the pressure at the needle tip exceeds the skins tensile strength. Davis *et al* have addressed such issues comprehensively (Davis et al., 2004). Their findings can be summarised thus:-

1. Insertion force varies linearly with interfacial area of needle tip.
2. Insertion forces required for microneedle penetration vary from 0.1-3.0 N.
3. The force needed to fracture microneedles increases if their walls are made thicker and their angle is increased.

From these findings a margin of safety is determined whereby if the ratio of fracture force to insertion force is greater than one, then microneedles are considered robust enough to insert into the skin.

Applicators onto which microneedles have been mounted are relatively primitive, the most popular devices being metal/wooden rods (Davis et al., 2004, Henry et al., 1998a), syringe barrels (Sivamani et al., 2005, Teo et al., 2005) or even just downward pressure from a fingertip. Descriptions of effective applicator devices for microneedle arrays are limited (Cormier et al., 2004, Martanto et al., 2004, Widera et al., 2006). However, the development of devices by commercial companies such as Nanopass, 3M and BD will be accompanied by advances in the development of a commercially acceptable application device. Interestingly, preliminary experiments have been conducted to investigate the possibility of promoting microneedle insertion using vibratory devices, imparted by a piezoelectric (Newton et al., 2003) or vibratory actuator (Yang and Zahn, 2004), and suggest up to a 70% reduction in the required insertion force.

### 1.5.6. *In vivo* Human Microneedle Studies

The vast majority of microneedle studies have been conducted using animal models (primarily rats and guinea pigs) and/or human cadaver skin. Although both of these are accepted experimental models, there are notable differences in the structure of animal models and cadaver/freeze-thawed human skin to *in vivo* human tissue (Kendall et al., 2004, Panchagnula et al., 1997, Sekkat, 2002). It is therefore important to appreciate those studies that have been conducted in the most representative setting, human subjects. These studies provide a true reflection of the pain of microneedle insertion and the ability of a microneedle array to deliver compounds to/through human skin for future therapeutic application.

Initial studies applied 150μm silicon microneedle arrays to human volunteers who did not report any pain but sometimes describe a mild 'sensation' on application of the device (Henry et al., 1998a). A number of human studies have now been conducted, using a variety of microneedle lengths and all studies report a sensation of pressure but limited or no pain upon insertion of the device (Kaushik et al., 2001, Miyano et al., 2005, Shirkhanzadeh, 2005, Sivamani et al., 2005, Smart and Subramanian, 2000, Wang et al., 2005). Early studies used microfabricated needles that were 2mm in length (not true 'micro'needles) and even application of these structures recorded a score of 'barely noticable' (Smart and Subramanian, 2000). A recent publication by Prausnitz and co-workers also highlights the inability to extract ISF from microchannels created within

human skin after a period of 10 to 20 minutes and attributes this to the possible resealing of microneedle channels (Wang et al., 2005).

Until recently, the penetrative efficiency of microneedles in human volunteers relied upon measures of skin integrity following application (Henry et al., 1998a). However a recent study has employed a hollow silicon microneedle array, mounted on the end of a syringe, to deliver a pharmacologically active molecule, methyl nicotinate (a potent vasodilator) into the arms of eleven human volunteers (Sivamani et al., 2005). This study confirmed the delivery capabilities of microneedle arrays in human subjects. Notably, the lumen position of the hollow microneedles had a significant bearing on the flux values that were obtained, with symmetric microneedles permitting less than half the flux of the pointed microneedles.

### 1.5.7. Microneedles for Macromolecule Delivery

The localised delivery of a macromolecular structure to cells of the viable epidermis is a particularly attractive proposition for scientists within the fields of cutaneous gene therapy and intradermal vaccination. As discussed previously, early studies characterised microneedle facilitated delivery of model macromolecules, such as BSA, and also nanoparticles across the skin. However, the delivery of therapeutically relevant macromolecules and their subsequent biological functionality has received more limited attention.

Desmopressin, a 1.1kDa synthetic peptide used in the treatment of enuresis, has been delivered transdermally using the titanium Macroflux® microneedle technology (Cormier et al., 2004). This macromolecule, normally delivered by injection, was coated onto the microneedle array and then combined with a transdermal patch which held the array in position for a 15 minute treatment interval. Therapeutic levels were achieved and although transdermal delivery showed some variability, peptide plasma levels were maintained within the therapeutic window.

An intradermal biodefensive vaccine using a polymeric microneedle device has been investigated by BD technologies for the treatment of anthrax (Mikszta et al., 2005). The polymeric array consisting of pyramidal microneedle structures was 'scraped' laterally

across the skin surface and the recombinant anthrax Ag was then applied topically to the treated area. Results indicate that although direct intradermal injection produces a more efficient immune response, such a technique has the potential to provide a less invasive vaccination method upon further improvements to the device and the vaccine formulation.

The group at ALZA have also published a detailed study examining the intracutaneous delivery of ovalbumin (45kDa), using the Macroflux® array (Widera et al., 2006). This study, a follow up to previous data (Matriano et al., 2002), characterised the effects of microneedle length, the density of microneedles within an array, the surface area of treatment and the Ag (ovalbumin) dose on the systemic immune response within hairless guinea pigs. The study indicates that the immune response obtained is dictated primarily by the Ag dose, although the surface area exposed to the treatment at high Ag doses (where Ag uptake by LC might be saturated) may also play a role. Due to the solubility of ovalbumin it is able to diffuse within the skin structure and therefore was detected throughout the epidermal layer, regardless of microneedle length and array density. Therefore, for soluble therapeutics, it may only be necessary for microneedles to create aqueous microconduits within the SC barrier, and diffusion may then facilitate contact of the Ag with cells throughout the underlying tissue layers. However, for insoluble proteins or more sterically hindered macromolecules such as nucleic acids, diffusion from the site of deposition may be limited. Observations of oligonucleotide delivery using the Macroflux® array indicates that lateral diffusion of nucleic acids around microchannels is significantly restricted (Lin et al., 2001).

Microneedle mediated nucleic acid delivery to cells within the viable epidermis of skin is currently poorly characterised. Studies using a puncture mediated method (similar to the tattooing process) (Ciernik et al., 1996) and a microseeding method (Eriksson et al., 1998) have been used to transfect skin cells with reporter plasmids. Mikstza and colleagues have also transfected murine keratinocytes using a 'microabrasion' application method (Mikszta et al., 2002). The potential of conventional silicon microneedle devices for the delivery of gene therapy vectors below the skin surface has been recognised (Chabri et al., 2004). However, microneedle mediated transfection of keratinocytes within human skin tissue remains elusive.

### 1.5.8. Novel Microneedle Formulations

Continued optimisation of the microneedle device for clinical application must be accompanied by the development of pharmaceutical formulations that enable cutaneous delivery of a therapeutic entity in a controlled manner. The challenge for the microneedle community is to create a 'one-step' integrated drug delivery system consisting of a microneedle device and therapeutic within a delivery system that promotes efficient cutaneous delivery of the active agent.

Daddona and colleagues have developed a reproducible method of coating titanium microneedle devices using an ovalbumin formulation (Matriano et al., 2002). Modification of the formulation and refinement of the coating method permitted control over coating thickness and restriction of the coating to the tips of individual microneedles (Widera et al., 2006). Application of these devices to the skin surface resulted in relatively efficient deposition (>50%) of the formulation within the viable epidermis. Dry coating a microneedle array not only ensures that the formulation is brought into close contact with cells of the viable epidermis but also offers significant advantages in formulation stability. Unstable formulations, including proteins and nucleic acids may be dry coated on to an array which could then be sealed and stored under nitrogen. This would ensure an extended shelf life of the product, would prevent the requirement for 'cold storage' and therefore allow rapid mass distribution, a particularly important feature in the development of vaccinations for mass immunisation schemes.

Chitosan coated silicon microneedles demonstrated the ability to control the release, and therefore transdermal permeation, of macromolecules from a microneedle array (Xie et al., 2005). The therapeutic is dissolved in the hydrophilic chitosan matrix, which is then cast onto the microneedle surface. By altering the thickness of the chitosan film the release of the therapeutic can be controlled. The authors note the applicability of this process for the controlled release of hydrophilic macromolecules and therefore pDNA may be selected as a future candidate for this approach.

A calcium phosphate formulation capable of delivering a macromolecular therapeutic from a coated microneedle array has also been developed (Shirkhanzadeh, 2005). This

strategy uses porous calcium phosphate, loaded with trehalose, to coat the tips of acupuncture needles. Penetration of needle tips in to the skin resulted in the rapid dissolution of the trehalose reservoir and its diffusion into the local environment. This was followed by the more prolonged dispersion of the calcium phosphate component. Both trehalose and calcium phosphate are recognised by the authors as possible vehicles for the delivery of protein and DNA therapeutics. Altering the components of the coating material to control dissolution kinetics may provide an opportunity for a bolus dose followed by sustained release of such macromolecules from the microneedle array.

A recent innovation has been the development of biodegradable polymer microneedle arrays (Miyano et al., 2005, Park et al., 2005). Prausnitz and colleagues have characterised biodegradable microneedle arrays produced using polylactic acid and polyglycolic acid, well characterised biocompatible materials (Park et al., 2005). Use of such materials improves the safety profile for microneedle devices, those microneedles that break and become deposited within the skin during or following application may degrade safely within the biological environment. Hanada and co-workers have also created biodegradable microneedles within which an active therapeutic material was dispersed (Miyano et al., 2005). In this case application of the microneedle was intended to be followed by breakage and the deposition of microneedles within the upper skin layers. Release of the therapeutic into the local tissue can then be controlled by the dissolution rate of individual microneedles.

Successful progression of a microneedle device to the clinic relies upon coordinated advances in the device structure, optimisation of microneedle mechanics, a reliable method of application and effective formulation of the pharmaceutical product. An integrated microneedle delivery system for the cutaneous delivery of macromolecular therapeutics, such as gene therapies, therefore requires close collaboration between engineers and scientists within the pharmaceutical field.

## 1.6. THESIS AIM AND OBJECTIVES

**Thesis aim**

To assess the potential of silicon microfabricated microneedle arrays for the cutaneous delivery of macromolecular therapeutics and their prospective employment in the delivery and subsequent expression of an exogenous DNA formulation, within human skin.

**Thesis objectives**

- To characterise microneedle devices created by dry- and wet-etch microfabrication procedures.
- To determine the ability of microneedle devices to penetrate the outermost layer of human skin tissue (SC) and to assess the dimensions of conduits created by microneedle devices within human skin.
- To determine the integrity of microneedle devices following their application to human skin.
- To investigate the importance of microchannel dimensions and the zeta potential of nanoparticle formulations, representative of non-viral gene therapy vectors, on permeation through a model microporous membrane.
- To assess the ability of a microneedle array to deliver nanoparticle formulations through heat separated human epidermal membrane.
- To maintain the viability of excised human skin within organ culture.
- To deliver a nanoparticular/macromolecular formulation to the viable epidermis of *ex vivo* human skin, maintained in organ culture.
- To examine the expression of exogenous reporter genes within *ex vivo* viable human skin.
- To transfect keratinocyte cells *in vitro* and *ex vivo* using a reporter plasmid(s).
- To facilitate and investigate epidermal gene expression within human skin using a microfabricated microneedle array.

# CHAPTER 2

# Microneedle array characterisation

## 2.1. INTRODUCTION

The establishment of silicon microfabrication techniques to create microneedle devices (Henry et al., 1998a) and the acknowledged ability of such devices to penetrate the skin barrier (Haider et al., Henry et al., 1998b, Luttge et al., 2003, Newton et al., 2003, Sivamani et al., 2005, Teo et al., 2005, Watkins et al., 2005, Xie et al., 2005) has prompted the selection of silicon as a material from which to create microneedle devices to be used in these studies. However the manufacture of such devices can be a complex and expensive process, requiring experienced engineers working within established clean-room facilities. A multidisciplinary approach to the development of an intra/transdermal delivery device is therefore crucial and so collaborations with engineers at Cardiff School of Engineering (CSE) and, more recently, Tyndall National Institute (TNI), Cork, Ireland has been of paramount importance during the investigations detailed within this report.

### 2.1.1. Microneedle device manufacture

The manufacture of functional microneedle arrays uses fabrication processes that are sensitive to small alterations in manufacturing conditions. The creation of microneedle arrays by collaborative groups in CSE and TNI was a stepwise manufacturing process, the experimental conditions of each 'etch run' being revised to optimise/customise the dimensions and morphology of the microneedles created on each silicon wafer. Microneedle devices used within this study have been fashioned by two manufacturing processes, dry-etch and wet-etch microfabrication. Initial microneedle devices used within the laboratory were created by the group at CSE using dry-etching methods. However recent collaboration with the engineers at TNI has provided microneedles that were created by both dry-etch and wet-etch technologies. This not only provided an alternative manufacturing process but also microneedle devices with different structural properties.

#### *2.1.1.1. Dry-etch manufacture*

Dry-etch fabrication of microneedle devices in silicon wafers uses a lithographically patterned mask and a blend of reactive ion gases (therefore it is also termed reactive ion

etching) to fashion micron-sized needles on the silicon wafer (Fig 2.1). During the creation of microneedle arrays, the photoresist pattern, etching times and etching conditions can be altered to fabricate various array patterns and microneedles with a diverse range of geometries. However, the development of microneedle devices by this manufacturing method can be expensive, time consuming and requires a high level of technical skills and equipment.

#### *2.1.1.2. Wet-etch manufacture*

Wet-etch fabrication takes advantage of the anisotropic behaviour of silicon in a potassium hydroxide (KOH) solution (Wilke et al., 2005a, Wilke et al., 2005b). This technique does not require the complexity of equipment involved in dry-etching procedures and the fabrication process is capable of parallel etching up to 25 wafers. The method is therefore more amenable to the mass production of devices. However control of the manufacturing process is very complex, presenting a number of technical challenges (Reed et al., 1998). Morrissey and colleagues at the TNI have developed reliable and more importantly reproducible methods of wet-etch manufacture to create microneedle arrays that have been employed within studies detailed in this report (Fig 2.2) (Wilke et al., 2005b).

The process relies upon precise alignment of the crystal planes within the silicon structure and the lithographically patterned mask prior to the wafers exposure to KOH solution (Fig 2.3). Very slow etching planes, known as "etch stop" planes, result in a resistance to etching along the edges of the square mask. However, the corners of the square are less resistant and therefore are slowly under-etched to create an octagonal structure. When the convex corners meet the tip of the microneedle is formed and the etching procedure is halted. The major disadvantage of this fabrication process is that it relies upon the etch behaviour of the silicon material (crystal structure) and therefore lacks the 'freedom' to significantly manipulate microneedle geometry and density as is possible with dry-etching methods (Wilke et al., 2005a, Wilke et al., 2005b).

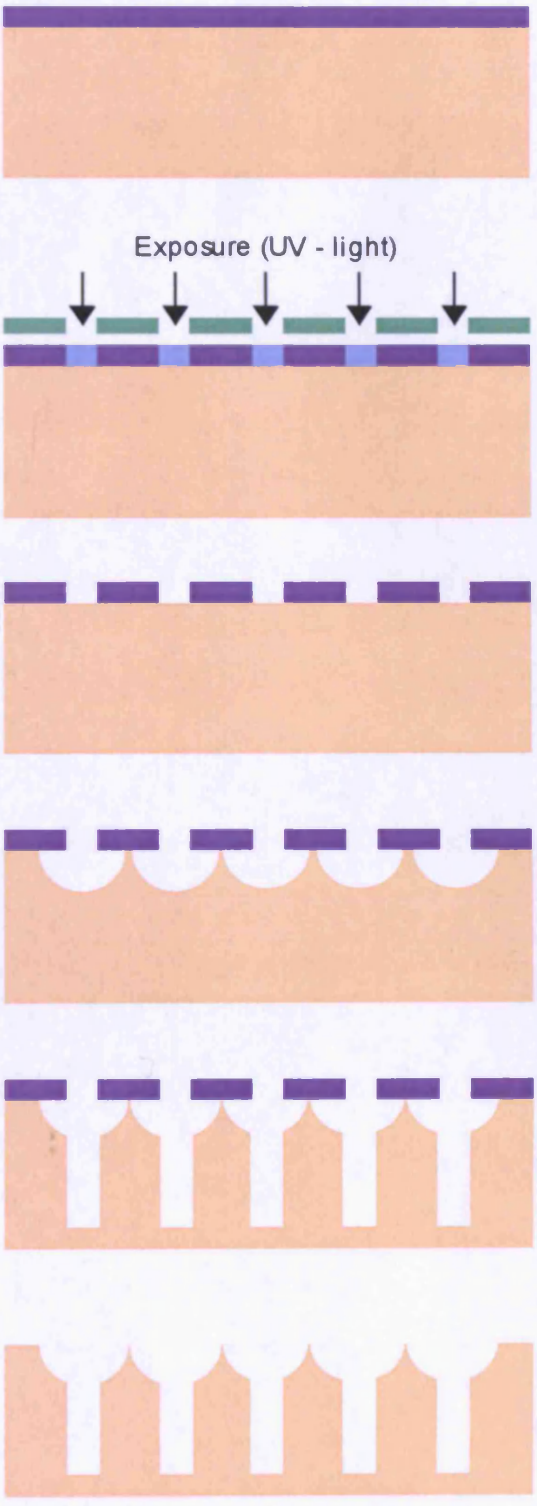


P-type silicon wafer, 10cm in diameter, 525 µm thick; covered with positive-photoresist.

Lithography: Exposure using chromium glass mask with circular patterns (100 µm diameter); cross-linking of exposed resist.

Lithography: Development of exposed areas; circular patterns of chromium mask now replicated into resist layer.

Etch step I: Isotropic silicon etch using $SF_6$; etch depth equal to circle radius.

Etch step II: Deep Reactive Ion Etch (DRIE) using BOSCH process to create cylindrical needle body.

Removing of remaining resist pattern followed by cleaning procedures.

*Figure 2.1.* Process flow chart for dry etching silicon microneedles with isotropically etched needle tip and vertical walls made by DRIE (BOSCH process).

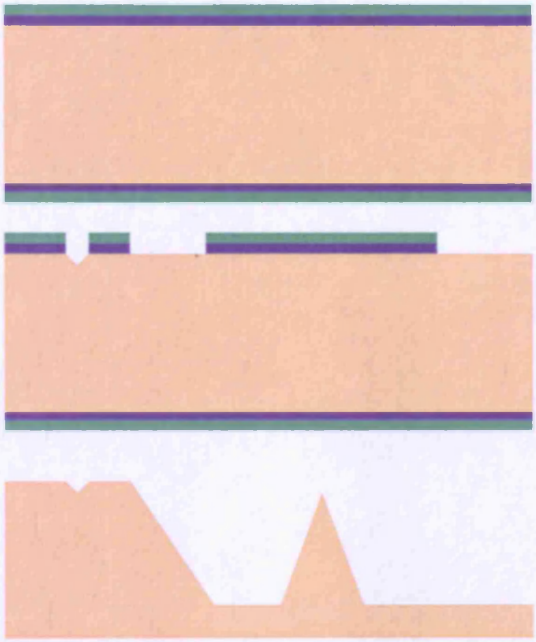

P-type silicon wafer, 10cm in diameter, 525 µm thick.
Low Pressure Vapour Deposition (LPCVD) of oxide and nitride layer as mask material.

After etching crystal alignment marks the lithographic mask for microneedles (square mask shape for each microneedle) was created oxide and nitride patterned by plasma etching of non-protected areas.

Silicon wet etch process in 29% KOH at 79°C.

*Figure 2.2.* Process flow chart for wet etching silicon microneedles at TNI.

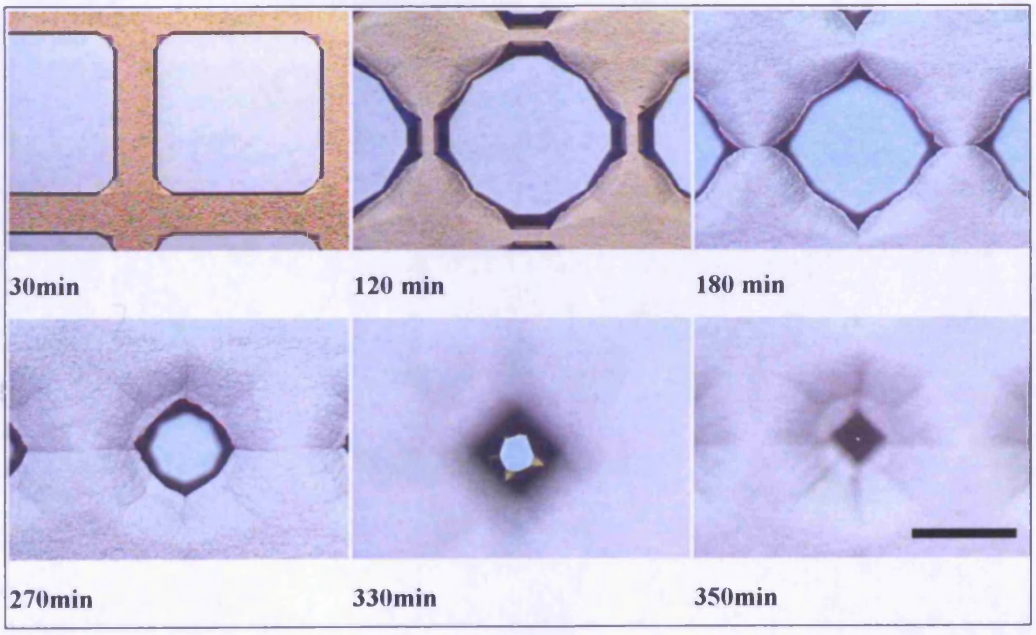


*Figure 2.3. En face* micrographs of the evolution of a wet-etch microneedle through convex corner undercutting. Scale Bar = 500µm. (Figure reproduced with permission of Nicolle Wilke and Anthony Morrisey at TNI, Cork).

## 2.2. AIMS AND OBJECTIVES

### Chapter Aim

The aim of this chapter is to assess the functionality of microneedle devices created by collaborative groups in TNI and CSE. The ability of dry- and wet-etch microneedles to puncture the human skin surface, the dimensions of microconduits created by microneedle devices and their location within the skin will be assessed. The integrity of microneedle devices following their application to human skin will also be considered.

### Chapter Objectives

- To describe the dry-etch and wet-etch microfabrication technologies, used to prepare the microneedle arrays utilised in this investigation.

- To characterise the morphology and dimensions of microneedle devices created by Cardiff School of Engineering and Tyndall National Institute.

- To illustrate the ability of microneedle devices to create micron-sized conduits within *ex vivo* human skin.

- To examine the influence of the array structure and individual microneedle morphology on the dimensions of microchannels created within human skin.

- To evaluate the integrity of microneedle structures following repeated application to human skin.

## 2.3. MATERIALS AND METHODS

### 2.3.1. Materials

All reagents were obtained from Fisher (Loughborough, UK) and were of analytical grade, unless otherwise stated.

Deionised water was obtained from an Elga reservoir (High Wycombe, UK). Glutaraldehyde solution 50% was obtained from Sigma (Gillingham, UK).

All histology materials, including Optimal Cutting Temperature (OCT) embedding media, Histobond® adhesive microscope slide were obtained from RA Lamb Limited (Eastbourne, UK) or in the case of toluidine blue, Harris' haematoxylin, Gurrs' eosin aqueous solution 1%, Histomount®, xylene (low sulphur) from Lab 3 (Bristol, UK).

Equipment:-

Leica CM305S Cryomicrotome (Leica Microsystems (UK) Limited, Milton Keynes, UK)
Disposable microtome blade (Leica Microsystems (UK) Limited, Milton Keynes, UK)
Olympus BX-50 system microscope (Olympus Optical, London,UK)
Olympus DP-10 Camera (Olympus Optical, London,UK)
Olympus TH3 Power unit (Olympus Optical, London,UK)
Schott KL1500 fibre optic light source (Schott UK Limited, Stafford, UK)
Philips XL-20 Scanning Electron Microscope (Philips, Eindhoven, Netherlands)
Bal-Tec CPD030 Critical Pont Drier (Bal-Tec, Balzers, Lichenstein)
Gold sputter coater (EM Scope, Kent, UK)

### 2.3.2. Scanning electron microscopy of microneedle devices

A scanning electron microscope is a complex instrument that can be considered as a column containing a heated tungsten filament within an electron gun at the top and the sample, mounted on an aluminium stub, to be examined at the other end. Samples, contained under high vacuum, are irradiated by a thin beam of electrons resulting in the emission of secondary electrons from the sample surface that are collected by a detector. The beam scans over the sample surface and converts the collected signal to a representative two dimensional image that can be viewed on a visual display unit. This method of microscopy allows visualisation of submicron structures at high resolutions.

Microneedle structures can vary within and between microfabrication runs and therefore the shape and morphology of each device was inspected at high magnification by SEM prior to experimentation. It was not necessary to sputter coat the sample prior to SEM and so following application of a microneedle device to human skin, the device was often re-examined to confirm its structural integrity.

### 2.3.3. Light microscopy of microneedle devices

Gross alterations in the structure of microneedle devices, were analysed by light microscopy. The mounted microneedle array was placed on a glass microscope slide, on the stage of the Olympus BX-50 microscope and was illuminated using a fibre optic light source. The orientation and positioning of the device was systematically adjusted to enable visualisation of each row of the microneedles in turn.

### 2.3.4. Microneedle device applicators

Dry-etch microneedles were mounted, using adhesive tape, upon the aluminium stubs that were normally used to analyse SEM samples. Wet-etch microneedle devices were mounted upon stainless steel rods of various lengths, using epoxy resin.

### 2.3.5. SEM analysis of microneedle treated human epidermal membranes

#### *2.3.5.1. Preparation of human epidermal membrane*

Isolation of the epidermal barrier (SC and viable epidermis) from human skin (Christophers and Kligman, 1963) is an established preparatory method. The resulting membrane has been shown to be a good model of the *in vivo* state when used *in vitro* (Roberts and Walters, 1998). Removal of the dermis also dramatically reduces the volume of the skin tissue, thereby simplifying and improving tissue preparation prior to SEM evaluation, resulting in enhanced *en face* imaging of the skin surface. Epidermal membranes have been used in SEM studies to demonstrate the penetrative capabilities of various microneedle devices.

Human breast skin was obtained from mastectomy or breast reduction procedures with full ethical committee approval and informed patient consent. Tissue from female donors, stored at -20°C for a maximum of 6 months, was allowed to reach room temperature over a period of 1hour (hr). A number of different donors were used (detailed in figure legends). Under containment 2 conditions, full thickness skin was immersed in heated deionised water (60°C) for 60seconds (secs) to enable removal of the epidermal membrane from the underlying dermal tissue, using curved forceps. The transfer of the epidermis to cool deionised water allowed the outstretched membrane to orientate, with the hydrophobic SC facing upward. The epidermis was then collected on aluminium foil and transferred back onto the previously removed dermis, supported by a flat cork board, prior to microneedle treatment. The microneedle array was pressed onto the skin surface at an approximate pressure of $2g/cm^2$ for 10secs. Untreated membranes were not subjected to microneedle application.

#### *2.3.5.2. Human epidermal membrane processing and analysis*

A conductive thin gold coat was used to promote the effective visualisation of non-conductive specimens such as biological samples. Therefore, following removal of the microneedles the membrane was fixed (2.5% glutaraldehyde) and subsequently dehydrated using an ethanol gradient (70%, 90%, 100%). A critical point dryer was used to complete dehydration of the specimen, which was then mounted on an aluminium stub and gold sputter coated prior to SEM analysis.

### 2.3.6. SEM analysis of microneedle penetrated human epidermal membranes

Wet-etch microneedle penetration was also assessed by applying the device to a human epidermal membrane and then mounting the skin, with the inserted microneedles still in place, onto an aluminium stub with the viable epidermis facing upwards. The aim of this procedure was to visualise the microneedles protruding through the viable epidermis.

### 2.3.7. *En face* imaging of stained microneedle treated human skin

Skin tissue, stored at -20°C for a maximum of 6 months, was removed from storage and allowed to equilibrate at room temperature for 1hr before the sub-cutaneous fat was removed by blunt dissection. The skin was then pinned onto a cork support and the microneedle device was applied. The treated area was subsequently covered with a small volume (approximately 100µl) of methylene blue solution (approximately 1%w/v). After 5mins excess methylene blue was removed from the skin surface. The full thickness human skin was subsequently swabbed with ethanol (70%v/v).

On removal from the donor organism, intracellular enzymes and bacteria begin to digest the cellular structure, altering the morphological, biochemical and immunological properties of the tissue (Junqueira and Carneiro, 2005a). Fixatives, such as glutaraldehyde, are used to cross-link proteins and other structural tissue elements. This process preserves the structure of the tissue for histological analysis. Prior to analysis skin tissue was therefore fixed by submersion in 2.5%v/v glutaraldehyde, on ice for 1hr. To ensure effective penetration of the fixative into human skin, it was important that the tissue volume was maintained as a low as possible (Junqueira and Carneiro, 2005a). Finally, the tissue was rinsed in phosphate buffered saline (PBS) for 5mins and visualised *en face* using an Olympus BX-50 microscope and a fibre optic light source. Following *en face* analysis the tissue was embedded in OCT medium on solid carbon dioxide and stored at -86°C prior to cryosectioning using a cryomicrotome.

### 2.3.8. Microneedle application methods

In all cases the tissue was pinned onto a cork support before application of the microneedle device. Dry-etch devices were applied with downward pressure, left in place for 10secs and then removed (Fig 2.4A). Wet-etch microneedles were applied in a rolling motion (Fig 2.4B).

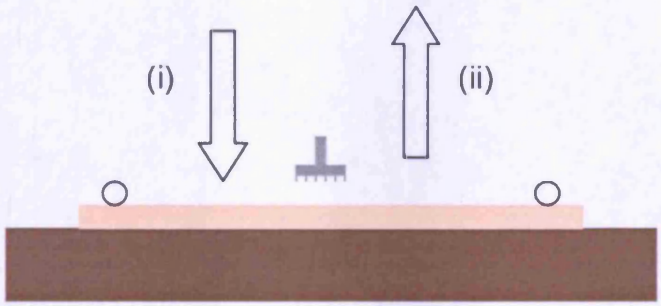


A. Dry-etch microneedles were applied with a downward force (i), left in place for 10secs and then removed (ii).

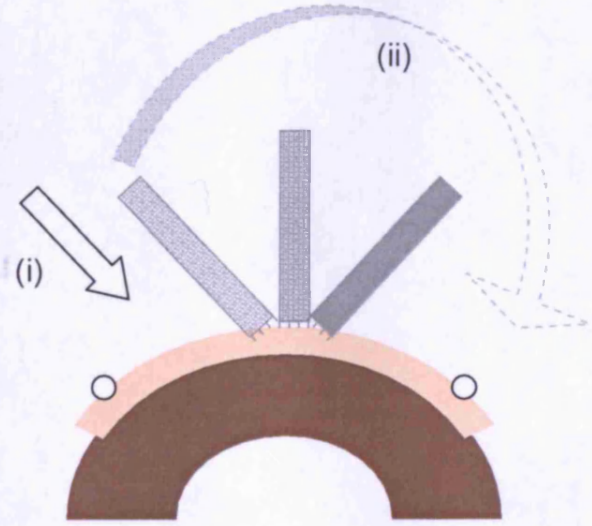


B. Wet-etch microneedles were applied at approximately 90 degrees to the skin surface (i) and the applicator was then rotated slowly through a 90 degree angle (ii).

*Figure 2.4.* A schematic illustration of microneedle application methods for wet-etch and dry-etch arrays.

### 2.3.9. Light microscopy of microneedle treated human skin

During this study, *en face* examination of skin tissue by light microscopy was often followed by histological evaluation of the sample. Sample preparation required fixation, embedding, sectioning, staining and mounting steps to produce histological sections that could be analysed by bright field light microscopy.

#### *2.3.9.1. OCT embedding*

Following fixation of human skin tissue the specimen was positioned in an OCT filled cryomould. OCT gel is an inert matrix, which protects cell integrity and limits desiccation, that hardens upon rapid cooling (Bratthauer, 1999, Webster, 1999). The cryomould was therefore surrounded by solid carbon dioxide and the embedding media was allowed to solidify over a period of 15mins. The embedded tissue was then wrapped in a single layer of aluminium foil, placed in an airtight plastic container (important steps to limit desiccation) and stored at -87°C.

#### *2.3.9.2. Cryosectioning*

The OCT block was mounted within a cryochamber (-21°C), allowed to equilibrate over a period of 30mins and then sectioned using a steel blade to a thickness of 10-12μm (Paulsen, 2000). Individual cryosections were collected on a coated microscope slide (Histobond® or Superfrost Plus® slides) and sections were allowed to dry at room temperature overnight. Cryosections were finally fixed by immersion in acetone (100%) at 4°C for 10mins, and then stained.

#### *2.3.9.3. Histological staining*

***Toluidine Blue*** - Slides were rinsed briefly in tap water and then covered in toluidine blue staining solution for 5mins. Excess stain was removed by rinsing in tap water and slides were allowed to dry at room temperature.

***Eosin*** - Tissue sections were submerged in Gurrs' eosin for 5secs and then rinsed in tap water. The slide was then allowed to dry at room temperature.

***Haematoxylin and Eosin (H&E)*** - Slides were washed briefly in tap water and then immersed in Harris' haematoxylin for 2mins. Excess stain was removed by immersion in tap water before and the slide was subsequently submerged in acid alcohol (1% hydrochloric acid (1M) in 70% ethanol) for 10secs. The slide was then rinsed once more in tap water for a period of 30secs before immersion in Gurrs' eosin for 5secs. Following a final 5min rinse in tap water the slide then allowed to dry at room temperature.

#### *2.3.9.4. Permanent slide mount for analysis*

Slides were dehydrated in an increasing ethanol gradient (50%, 70%, 90%, 100% and 100%v/v) before immersion in xylene. After 10mins slides were removed from the xylene and allowed to dry. A drop of Histomount® and a glass coverslip were used to permanently mount the sections.

## 2.4. RESULTS AND DISCUSSION

During this investigation, the complex manufacturing processes, progressive optimisation of microneedle designs, damage to devices during use and repeated applications have resulted in the examination of a number of microneedle devices, with differing morphologies. A comprehensive catalogue of all microneedle arrays, created by the academic institutions at Cork and Cardiff, up to July 2005, has been included as an appendix (Appendix I). Images selected for this chapter illustrate the development of microneedle devices throughout the course of this investigation. Such developments were dependent upon advances in manufacturing techniques developed by collaborative groups in TNI and CSE and the subsequent assessment of devices following their application to human skin tissue.

### 2.4.1. Dry-etch microneedle array devices

The engineering difficulties associated with creating three dimensional silicon microneedle structures using dry-etch technologies are highlighted in Fig 2.5A. Modification of experimental conditions addressed the problem, resulting in the fabrication of three dimensional cylindrical and cuboidal structures on the silicon wafer surface (Fig 2.5B & 2.5C). However further amendments to the etching conditions were required to produce microneedle arrays that would prove useful in laboratory investigations (Fig 2.6). Microneedles selected for tissue application possessed sharp tips capable of penetrating the skin surface and cylindrical bodies. Individual structures were approximately 150μm in length, 50μm in diameter and adjacent microneedles within the array were 200μm apart (centre to centre spacing ratio). These 20x20 microneedle arrays, mounted on aluminium stubs were designed to overcome the skins dermatoglyphics, penetrate the SC and protrude into the viable epidermis without impinging on nerve fibres located in the underlying layers (Kaushik et al., 2001).

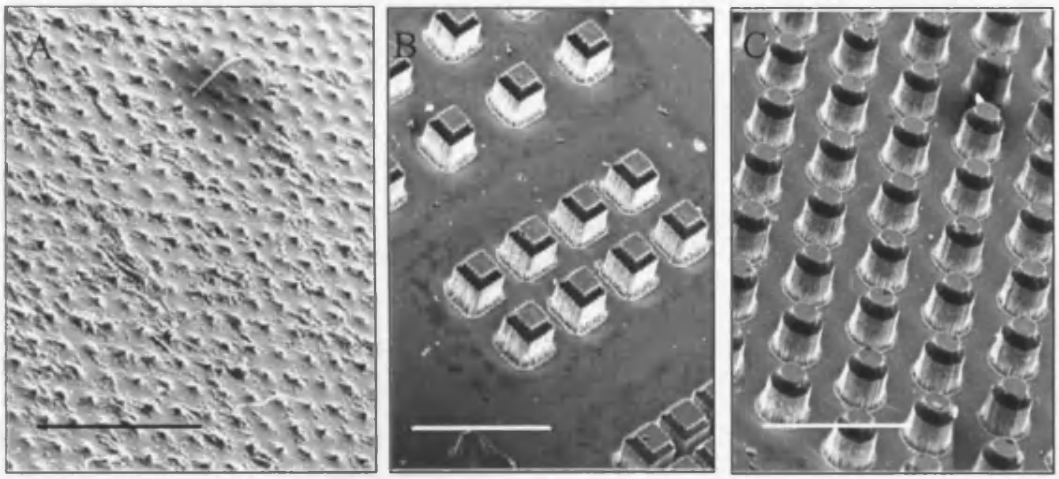


*Figure 2.5.* Scanning electron micrographs of initial attempts, by CSE, to create microneedles using a dry-etch manufacturing procedure. A, B, scale bar = 500μm; C, scale bar = 1000μm.

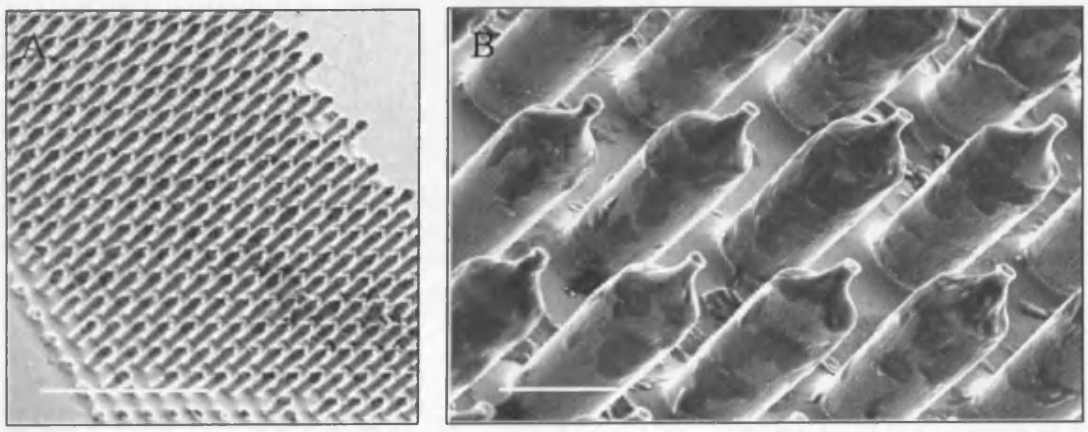


*Figure 2.6.* Scanning electron micrographs of the successful creation of a microneedle array, by CSE, using a dry-etch manufacturing procedure. A, scale bar = 1000μm; B, scale bar = 100μm.

The group at TNI also produced microneedle array structures by dry-etch fabrication methods. Microneedles, within a 15x16 array, possessed heights of 250-280μm and base diameters of 160-170μm (Fig 2.7A). These microneedles were significantly larger than those created by the group at CSE. A platinum coat was also applied to these arrays in order to increase the resistance of individual microneedles to the shear stress imparted on them during application to the skin surface (Fig 2.7B).

An interesting feature of these dry-etch devices was the disfigurement of microneedles located at the perimeter of the array pattern (Fig 2.7C & 2.7D). This resulted in an oval cross section (Fig 2.7C). Microneedle tips, designed to be symmetrical sharp points (Fig 2.7E), were also variable with some microneedles possessing a 'neck' in place of a sharp microneedle tip (Fig 2.7F). These morphological irregularities highlight the technical challenges of creating uniform symmetrical microneedles that can penetrate the skin reproducibly.

### 2.4.2. Wet-etch microneedle array devices

The most noticeable difference between dry-etch and wet-etch devices was the much reduced microneedle density on the wet-etch arrays (Fig 2.8). This is an inherent handicap of the fabrication procedure (Wilke et al., 2005b) and although current studies by TNI aim to address this problem, wet-etch devices have a minimum proximity to adjacent microneedles, thereby limiting the array population (Section 2.1.1.2).

The wet-etch microfabrication method was developed to provide a more cost effective alternative to dry-etch manufacture. However the fabrication process has interestingly yielded microneedles with a pyramidal shape and both pointed (Fig 2.8) and 'frustum' (Fig 2.9) shaped tips.

Pyramidal microneedles were approximately 280μm in length with base diameters of up to 200μm (depending on the batch) (Fig 2.8). The failure force of a microneedle increases with base diameter (Park et al., 2005) and therefore the platinised pyramid shaped microneedles were predicted to withstand much greater sheer forces upon application. The dimensions of microneedles created by wet-etching methods were also

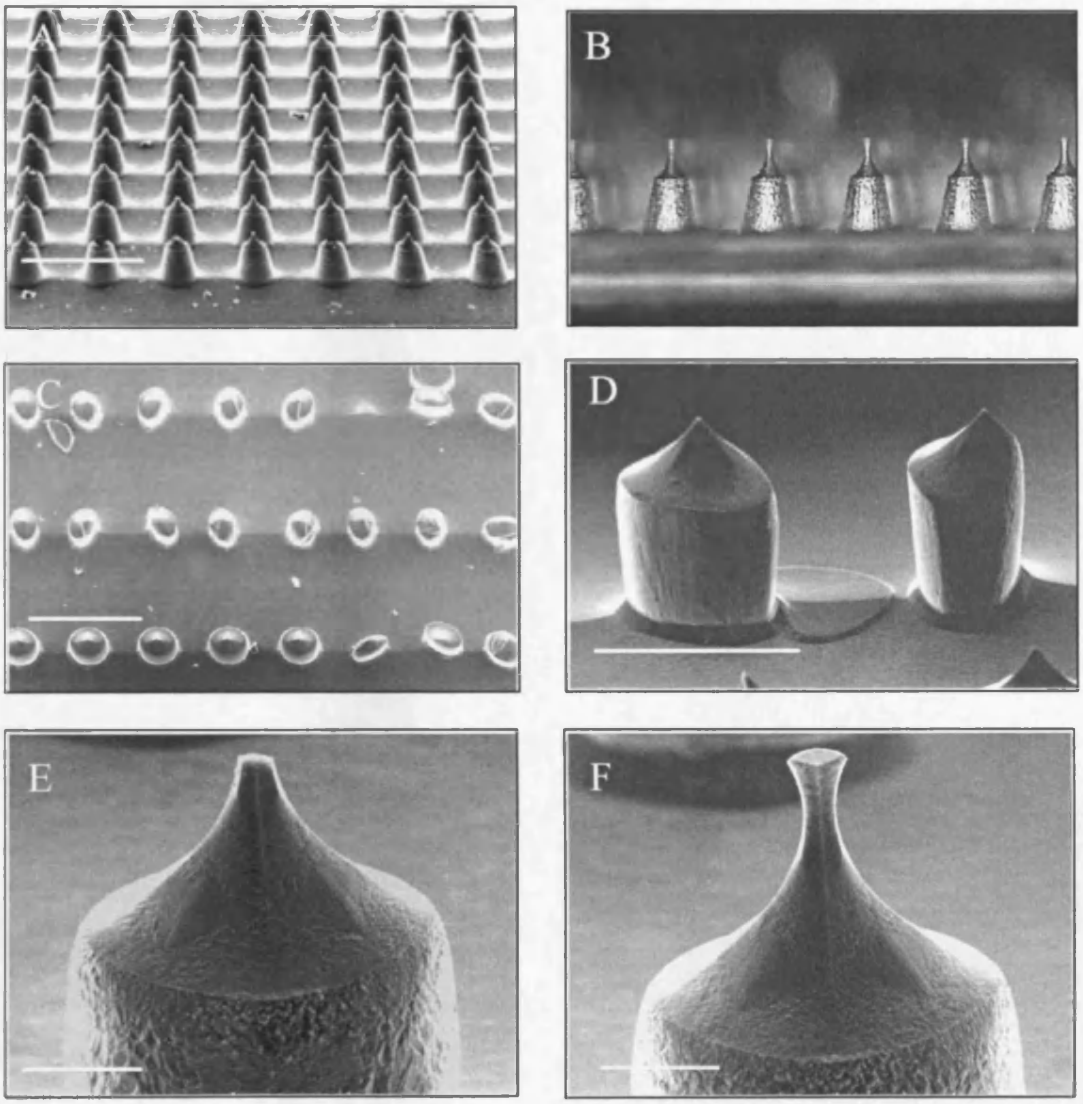


*Figure 2.7.* Scanning electron micrographs of microneedle arrays created in TNI by the dry-etch manufacturing procedure. A, C, scale bar = 500μm; D, scale bar = 200μm; E, F, scale bar = 50μm. Fig B was kindly contributed by Nicolle Wilke from TNI.

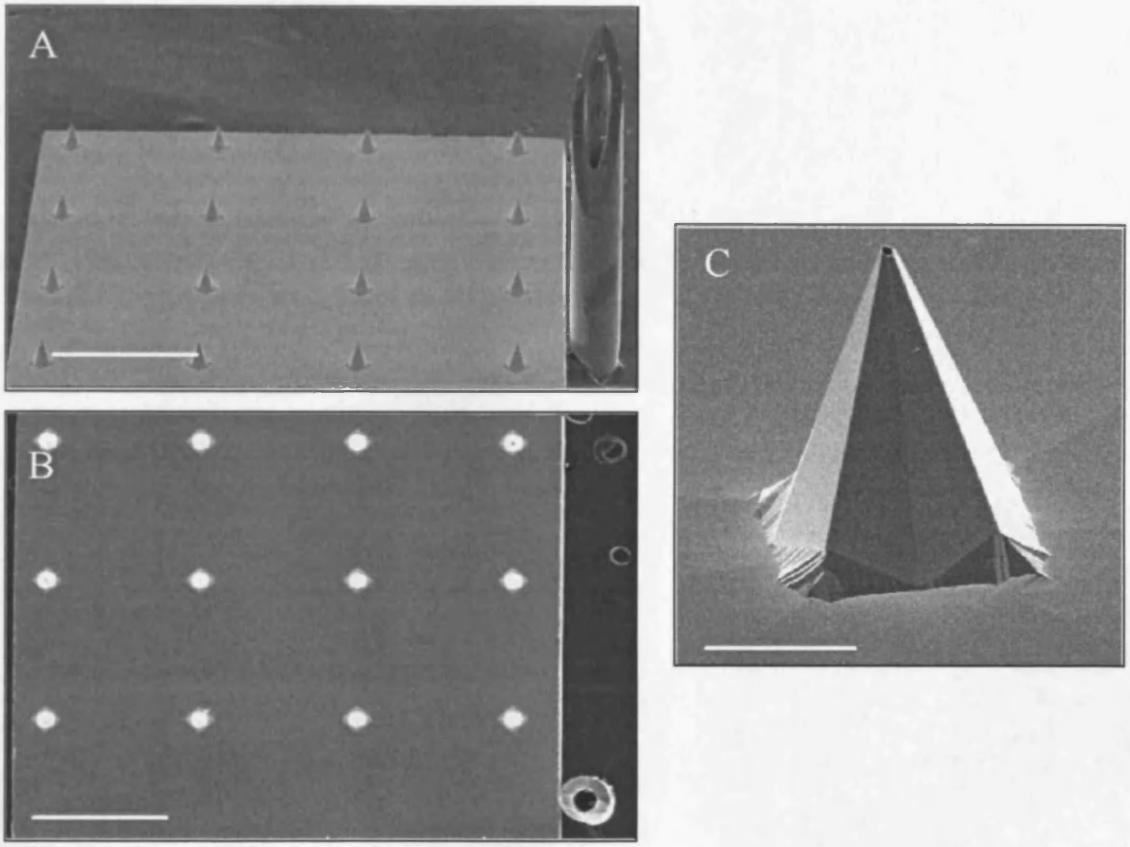


*Figure 2.8.* Scanning electron micrographs of a typical wet-etch microneedle array created by TNI. Individual microneedles have pointed tips and are equally spaced in a 4x4 array pattern. The tip of a hypodermic needle (30G) is included within images A and B as a comparative visual aid. A, B, scale bar = 1000μm; C, scale bar = 100μm.

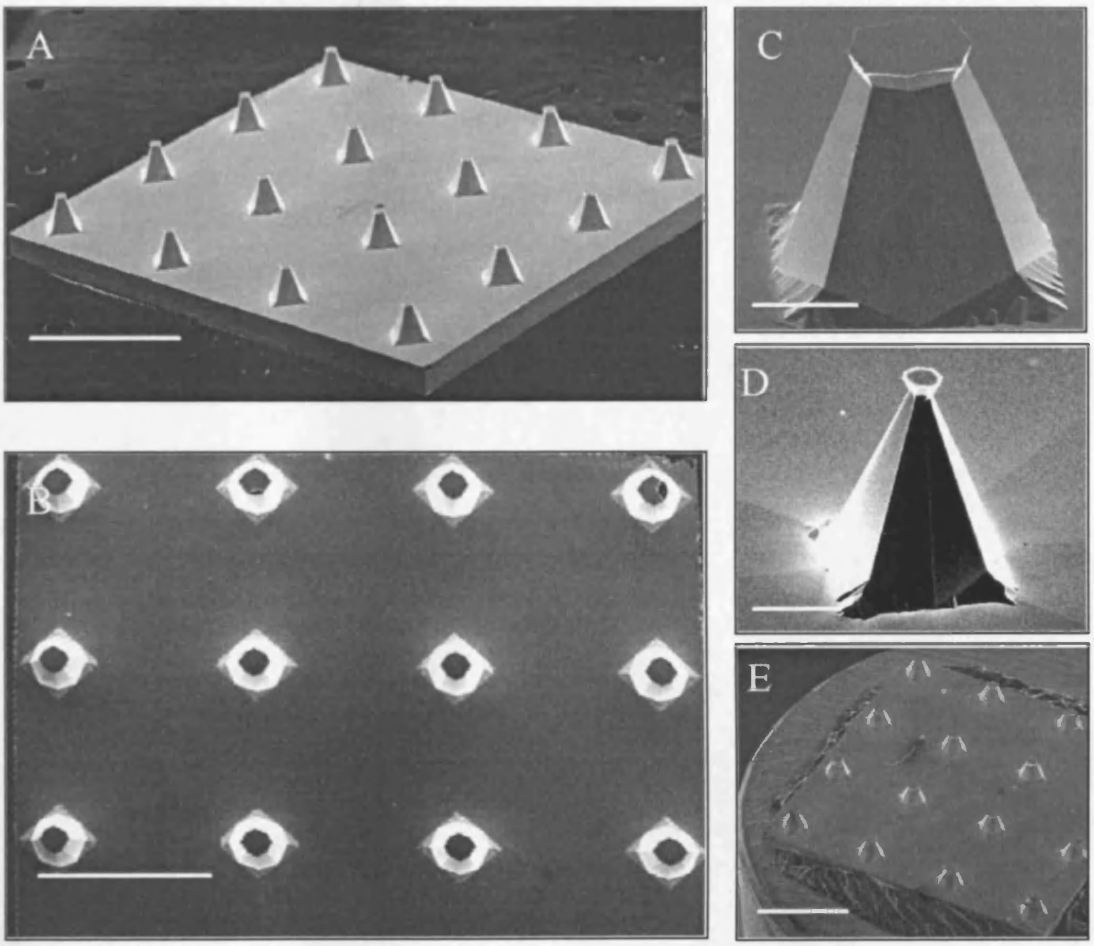


*Figure 2.9.* Scanning electron micrographs of typical wet-etch microneedle arrays created by TNI. Individual microneedles have frustum shaped tips and are equally spaced in a 4x4 array pattern. A, B, E, scale bar = 1000μm; C, D, scale bar = 100μm.

greater than those of the dry-etch microneedles created by CSE. However, the micron scale dimensions of the microneedle protrusions remain significantly smaller than that of a hypodermic needle (Fig 2.8). The bodies of frustum and pointed tipped microneedles were of comparable dimensions. However the tips of the frustum tipped microneedles, created by minor adjustments to the manufacturing process, measured up to 100μm wide (Fig 2.9C & 2.9D). The insertion force for a microneedle is proportional to the microneedle tip area (Davis et al., 2004) and therefore an increased application pressure was predicted to be necessary for successful penetration of these microneedles.

The wet-etch microneedle array devices were created on smaller areas of silicon wafer than dry-etch devices (~0.5cm$^2$). These reduced dimensions permitted adhesion to a steel rod (Fig 2.9E) which enabled much greater control over the array during application to the tissue surface.

### 2.4.3. SEM analysis of microneedle treated human epidermal membranes

Following characterisation of microneedle geometries and morphologies, both types of microneedle device were applied to human epidermal membrane and the skin surface was analysed by electron microscopy. The aim of these initial studies was to determine the ability of microneedle devices to create microdisruptions in the skin surface that could subsequently be characterised.

#### *2.4.3.1 SEM analysis of untreated human epidermal membranes*

Multiple layers of flattened polyhedral shaped corneocytes provide the robust continuous membrane, the SC, which is responsible for the skins significant barrier properties (Fig 2.10A & 2.10B). It is these cell layers that a microneedle device must disrupt to facilitate cutaneous delivery of macromolecules.

Viable keratinocytes of the BMZ can be visualised on the underside of the untreated human epidermal membrane (Fig 2.10C-2.10F). The loose connection between cells and their ~10μm diameter was in stark contrast to the ~40μm diameter of the tightly packed corneocytes (Fig 2.10A). Skin appendages, including sweat ducts (Fig 2.10C) and the hair follicle (Fig 2.10D) (Hoffmann, 2000, Hoffmann, 2003), must also be considered as

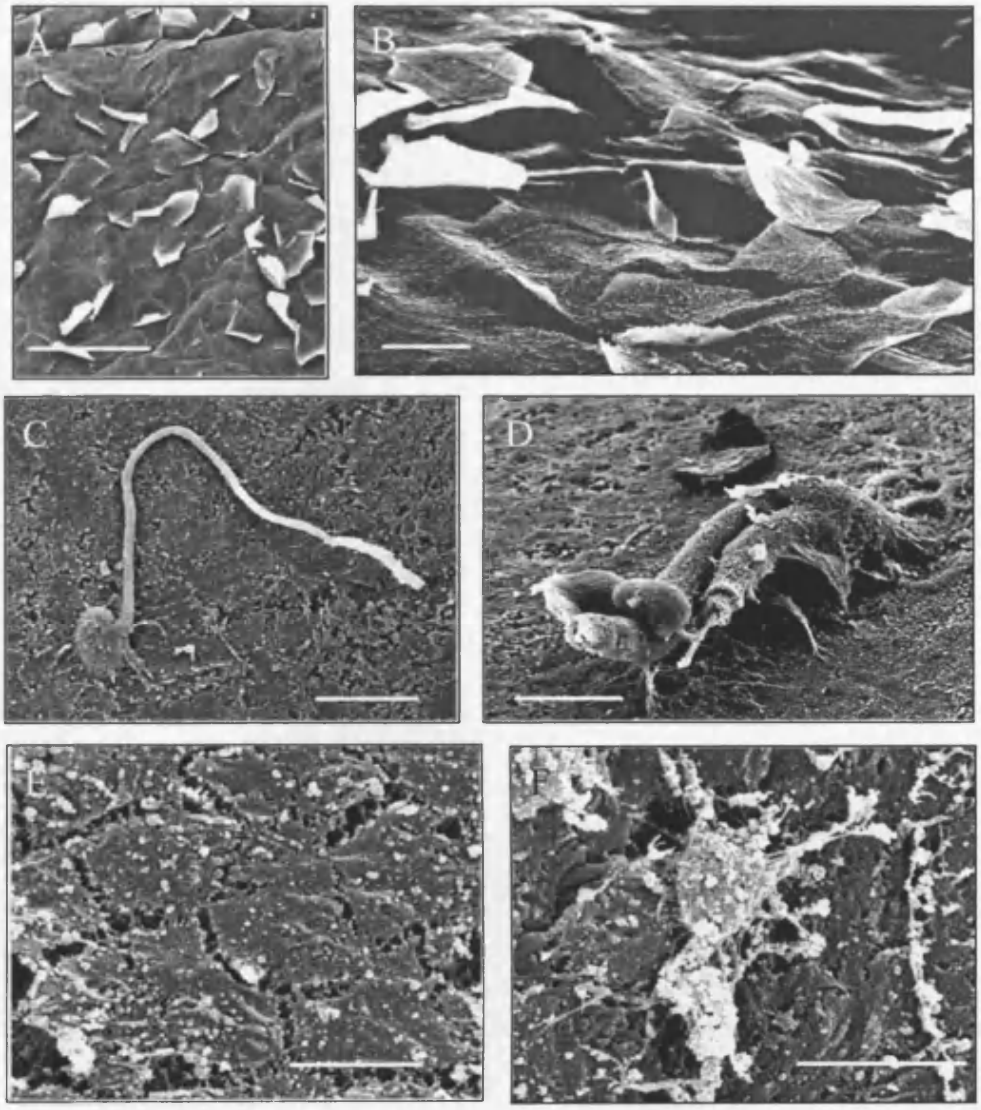


*Figure 2.10.* Scanning electron micrographs of untreated heat separated human epidermal membrane. Images A and B illustrate the untreated stratum corneum surface. Image C-F are pictured from the underside of the heat separated membrane. Image C pictures an eccrine sweat duct extending from the viable epidermis. Image D illustrates a hair shaft. Keratinocytes pictured in image E compose the basal layers of the viable epidermis. The 'finger like' projections extending from the cell pictured in image F are indicative features of a Langerhans cell. A, scale bar = 1000μm; B scale bar = 20μm; C, D, scale bar = 200μm; E, F scale bar = 10μm. Skin donor is a 67 year old female.

possible portals for localised delivery of gene therapeutics. Interestingly, SEM images also revealed a number of structures protruding from the BMZ whose morphology was synonymous with that of a LC (Fig 2.10E) (Stoitzner et al., 2002). It is possible that cells captured within these images have been activated and are migrating from the BMZ and into the underlying dermal tissue. Intradermal immunisation strategies aim to stimulate these specialised APCs to evoke a protective immune response (Section 1.2.4).

#### *2.4.3.2. SEM analysis of dry-etch microneedle treated human epidermal membrane*

Downward application of the dry-etch microneedle array onto the skin surface produced a uniform pattern of microdisruptions that was consistent with the pattern of microneedles on the device (Fig 2.11). The hair follicle pictured on the top right of the micrograph provides a reference to the scale of the microchannels created by this device. Images suggested that microchannels were 30-40 μm in diameter at their opening on the skin surface. This is slightly smaller than the diameter of the individual microneedles but may be explained by retraction of the elastic skin tissue following removal of the microneedle device. Tissue constriction is also an established artefact of tissue preparation for SEM analysis (Junqueira and Carneiro, 2005a) and therefore these images may have underestimated the microchannel diameter.

#### *2.4.3.3. SEM analysis of wet-etch microneedle treated human epidermal membrane*

The most noticeable feature of skin membranes that were treated with wet-etch microneedles was the failure to detect a uniform pattern of microchannels (data not shown). This might have been attributable to the significantly reduced microneedle populations and the restricted density within a single array. However the inability to visualise a true array pattern was more likely a consequence of the failure of some microneedles to penetrate the skin membrane effectively.

The microdisruptions that were attributed to effective penetration of the microneedle device vary in both morphology and geometry. Frustum tipped arrays appeared to produce both cylindrical channels and 'tares' in the membrane (Fig 2.12A & 2.12B).

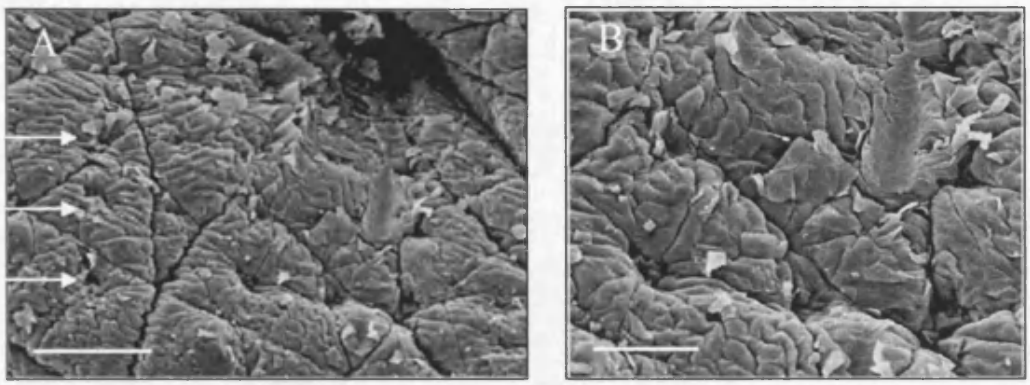


*Figure 2.11.* Scanning electron micrographs of human epidermal membrane that has been treated with a dry-etch microneedle array (Fig 2.6). A uniform pattern of microdisruptions within the skin surface was observed (indicated by arrows). A, scale bar = 200μm; B, scale bar = 100μm. Skin was obtained from a 66 year old female.

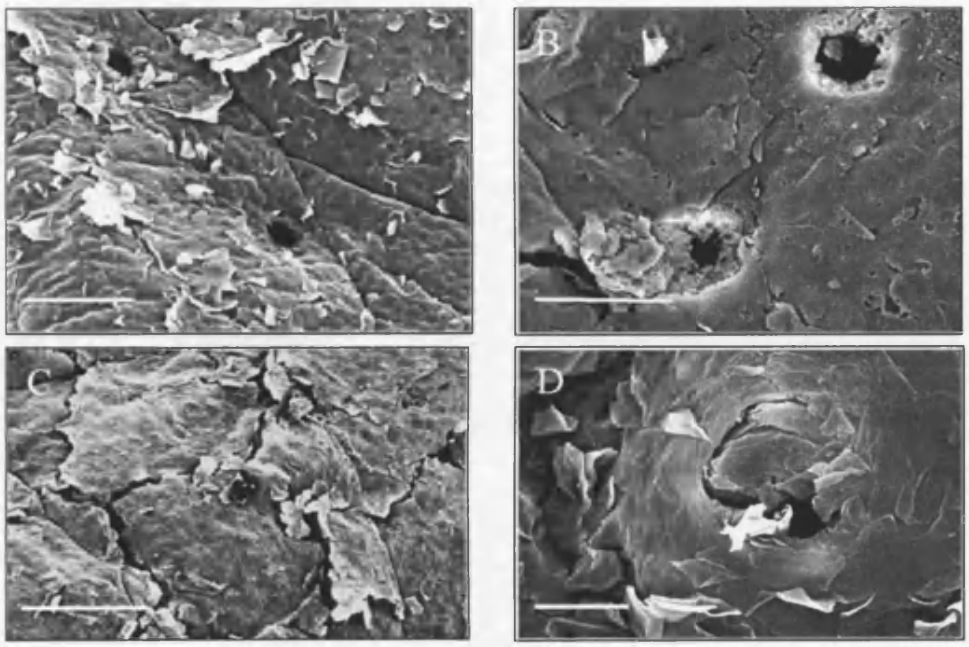


*Figure 2.12.* Scanning electron micrographs of heat separated human epidermal membrane that has been treated with frustum tipped (A, B) and pointed (C, D) wet-etch microneedle arrays. A, scale bar = 200μm (treated with TNI - Array 8); B, scale bar = 100μm (treated with TNI - Array 8); C, scale bar = 200μm (treated with TNI - Array 5); D, scale bar = 50μm (treated with TNI - Array 12). Skin was obtained from a 67 year old female donor.

Some of these disruptions were greater than 50μm in diameter. Those microchannels created by the pointed tips were more irregular in shape and possessed narrower diameters, approximately 30-50μm (Fig 2.12C & 2.12D).

When comparing the microconduits created by the two different types of array it was difficult to determine the effect of the tip structure on the dimensions and morphology of the microchannels. However, frustum tipped arrays produced greater levels of tissue disruption and therefore this type of array may be expected to facilitate more significant increases in skin permeability.

Artefacts are a renowned analytical problem when interpreting electron micrographs and therefore meticulous analysis of the images was essential. Therefore during investigations although initial observations of some membranes indicated successful penetration of microneedles (Fig 2.13A), under closer scrutiny the darkened areas, that appear as microchannels, revealed themselves to be merely indentations in the skin surface (Fig 2.13B). The pictured sample was treated with the frustum tipped microneedle array and so it is not unreasonable to assume that the frustum tips failed to penetrate the skin surface, as a result of their increased tip area, and may have been responsible for the creation of these indentations. When analysing microneedle treated skin it is therefore important to inspect each microdisruption and to establish a true 'break' in the skin surface by visualising damaged corneocytes surrounding the microconduit.

#### *2.4.3.4. SEM analysis of microneedle punctured human epidermal membrane*

Images of the microneedle array tips penetrating through the underside of the human epidermal membrane confirmed the ability of a wet-etch microneedle device to penetrate the skin barrier. It is worth noting however that the diameters of the microchannels were significantly greater than the width of the frustum shaped tips that protrude through the opening (Fig 2.14). This may be attributed to retraction of the device before sample analysis i.e. the device was applied under pressure to the skin surface and so upon removal of the pressure the devices retreats from the microchannels.

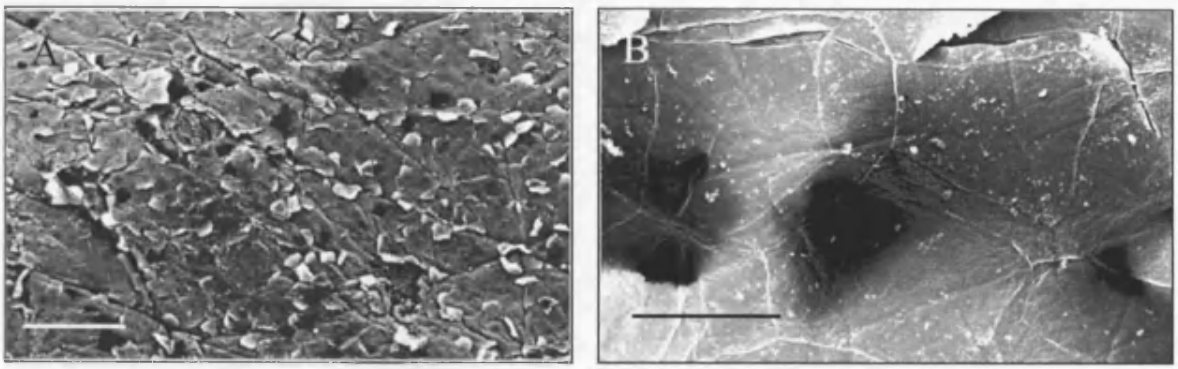


*Figure 2.13.* Scanning electron micrographs of apparent microdisruptions in the skin surface, which under closer examination reveal themselves as deformations in the membrane. A, scale bar = 200μm; B, scale bar = 20μm. Skin was obtained from a 67 year old female donor

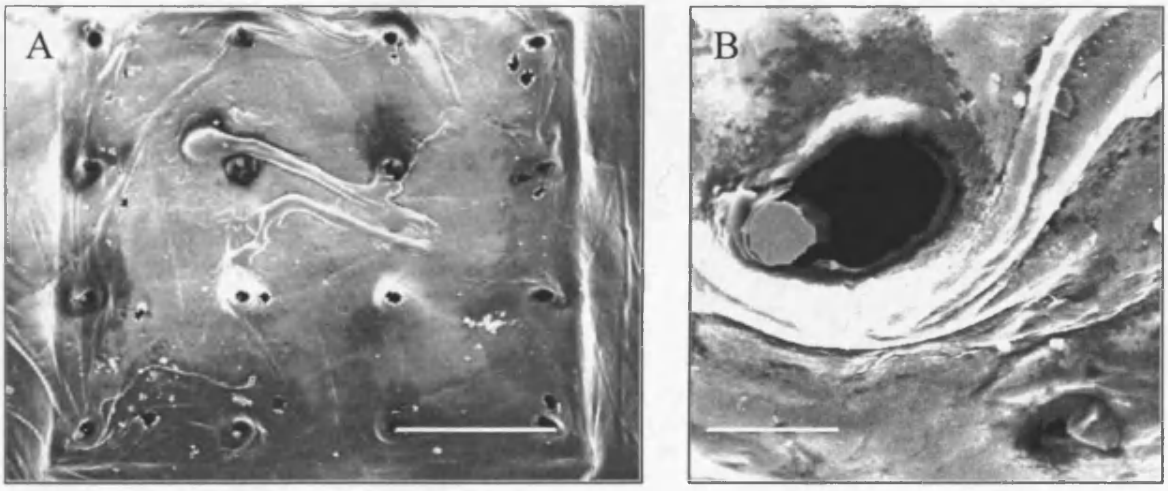


*Figure 2.14.* Scanning electron micrographs illustrating the ability of wet-etch microneedles to penetrate the epidermis with frustum-shaped tips (Treated with TNI - Array 4). A, scale bar = 1000μm; B, scale bar = 100μm. Skin was obtained from a 67 year old female donor.

### 2.4.4. Light microscopy of microneedle treated human skin

Tissue histology produces two-dimensional representations of a three dimensional system. Analysis of numerous sections and a selection of tissue samples were therefore required to build a detailed understanding of the tissue structure. It was also important to remember that artefacts may occur during the processing of the tissue that may distort the observed structure e.g. denaturation and crosslinking of proteins during fixation, the conversion of water to ice crystals during embedding and/or physical distortion during the sectioning process (Paulsen, 2000). The tissue sections discussed in the following text were therefore considered representative of all samples analysed.

#### *2.4.4.1. Histology of untreated human skin*

It is important to understand the architecture of human skin and its organisation in order to design an effective cutaneous delivery system. However skin structure is influenced by a number of factors including the patients' age and the anatomical site from which it is obtained (Roberts and Walters, 1998). Untreated breast skin from a variety of donor patients was therefore examined in order to appreciate the architecture of the tissue to be used throughout this investigation.

Low magnification images (Fig 2.15A) revealed the layered structure of skin. H&E staining of the tissue highlighted the nucleated areas of the skin tissue (Fig 2.15B). These images illustrated the practical difficulty in targeting therapies to the viable cells of the epidermis (dark blue region), the majority of the tissue being dominated by the elastic and collagen fibres of the dermis. The SC appeared as a continuous non-nucleated region (10-20μm thick) that covered the skin surface. Histology also identified two distinct layers within the dermis: a thin papillary layer containing cellular structures that positioned directly below the viable epidermis and the remainder of the dermis, which consisted primarily of non-nucleated connective tissue (Fig 2.15B).

Histology generally defines epidermal thickness as 75 to 600μm, dependent upon the area of the body (Junqueira and Carneiro, 2005b). The viable epidermis within breast

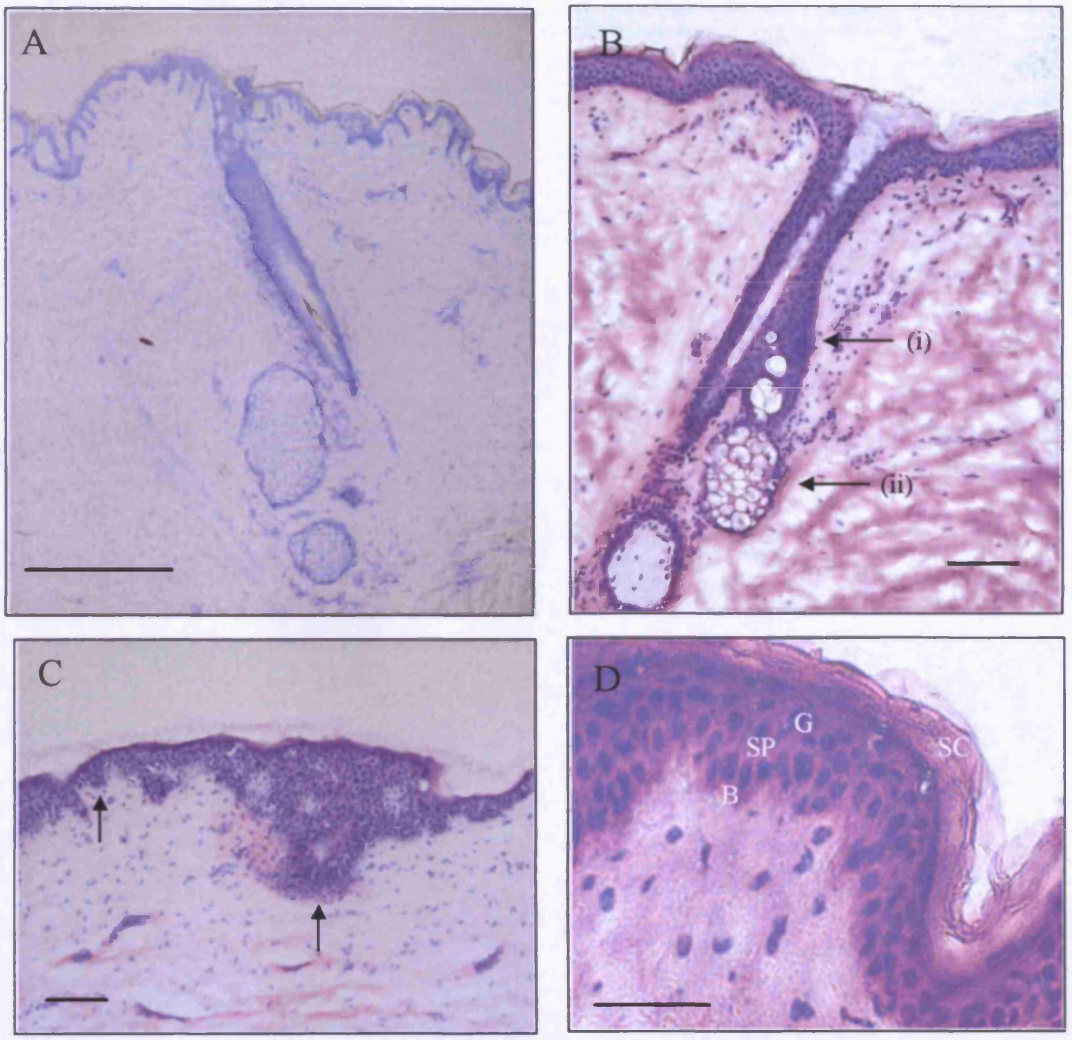


*Figure 2.15* Transverse sections (10-12μm) of untreated human breast skin, visualised by light microscopy. The selected micrographs were selected from different donors to provide an accurate representation of the breast tissue structure.

A. Toludine blue stained tissue at low magnification highlights the epidermal layer and a hair follicle. Scale bar = 500μm. Skin donor is a 30 year old female.

B. H&E staining facilitates visualisation of individual cells. (i) Hair follicle bulge; (ii) Sebaceous gland. Scale bar = 100μm. Skin donor is a 65 year old female.

C. H&E staining highlights the variability in the thickness of the viable epidermis (see arrows). Scale bar = 100μm. Skin donor is a 76 year old female.

D. High magnification images of H&E stained tissue reveals the cellular organisation of the viable epidermis. B= Basal layer; SP = Spinous layer; G = Granular layer; SC = Stratum corneum. Scale bar = 50μm. Skin donor is a 65 year old female.

tissue was just 50-100μm thick (Fig 2.15C). However the most noticeable feature of the viable epidermis was the variability in its thickness. This variability was present not only between different donors but also within the same tissue (Fig 2.15C). The keratinocyte 'depth' within the viable epidermis varied from just two cells, to more than twenty. This will be an important consideration in the design of microneedle devices for the localised delivery of nucleic acid formulations to this viable region.

It is possible that microneedle mediated delivery of a therapeutic agent may require that a specific cell type, within this viable epidermal layer, is targeted. Columnar shaped keratinocytes comprising the basal cell layer of the viable epidermis include stem cells (Fig 2.15D) (Ghazizadeh and Taichman, 2005), which are actively dividing and therefore represent the most lucrative target for gene therapies. The structure of the breast skin that was analysed suggested that microneedle devices may only need to penetrate to a depth of 50μm in some areas of the tissue in order to access the basal layer.

#### *2.4.4.2. Dry-etch microneedle treated human skin*

The distribution and extent of microchannels within microneedle-treated full thickness human skin was confirmed by post-application staining with methylene blue. This hydrophilic low MW dye diffused rapidly across the compromised SC barrier and was retained within the underlying microchannel. This provided a simple yet clear demonstration of the penetration efficiency of dry-etch microneedles (Fig 2.16A) and indicated that a significant proportion of the microneedle array successfully penetrated the outermost skin layer.

*En face* images of stained skin suggested that microneedle-created pores were approximately 50-100μm in diameter (Fig 2.16A). However, cryosections (Fig 2.16B & 2.16C) of the tissue indicated that lateral diffusion of the dye may have exaggerated this estimation. The diameter of the microchannel visualised by transverse sections (Fig 2.14B & 2.16C) was in close agreement with SEM images, at approximately 20-30μm wide with a channel depth of 100-120μm. Eosin and toluidine blue stained sections (Fig 2.16D-2.16F) identified the location of the microchannel within the skin architecture. In the majority of cryosections the conduit was restricted to the viable

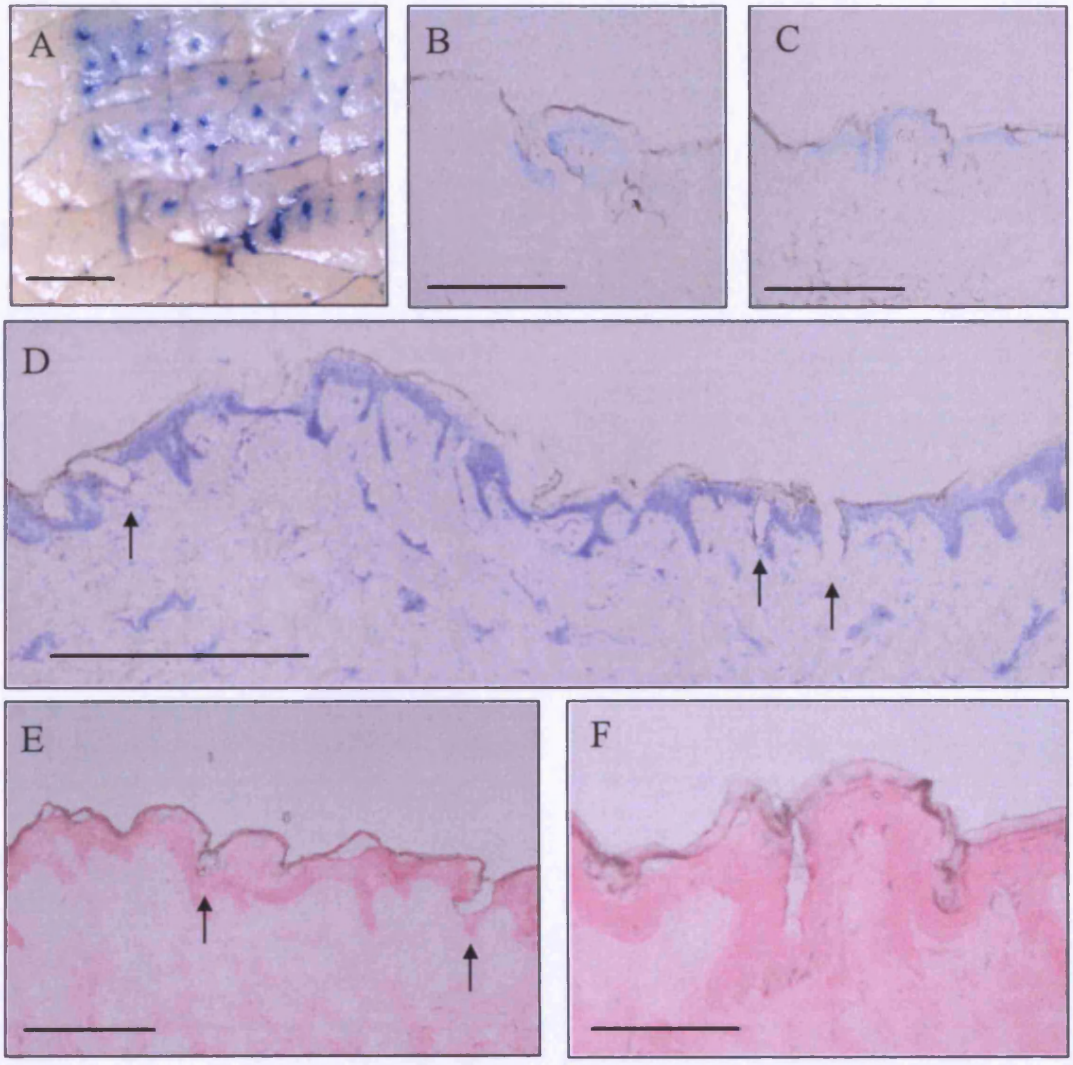


*Figure 2.16.* Light microscopy images of microchannels created within human skin, treated by the dry-etch microneedle device (Fig 2.6). Skin was obtained from a 30 year old female donor.

A. *En face* imaging of the skin surface following microneedle treatment and methylene blue application. Scale bar = 500μm.

B,C. Unstained cryosections (12μm) illustrating microchannels within the upper skin layers. Scale bar = 200μm.

D. Toludine blue staining of cryosections (12μm) highlights the tissue layers. Microchannels, highlighted by arrows, appear as physical disruptions in the stratum corneum and viable epidermis. Scale bar = 500μm.

E,F. Eosin staining of cryosections (12μm), illustrate microchannels (see arrows) confined to the viable epidermis. E, scale bar = 200μm; F, scale bar = 100μm.

epidermis. However, within some areas of the tissue these microchannels pierced the BMZ and penetrated into the upper layer of the dermis (the papillary layer).

#### *2.4.4.3. Wet-etch microneedle treated human skin*

Downward application of a wet-etch microneedle device to human tissue was less penetrative than the application of dry-etch devices. This may be explained by the lower density of microneedles and therefore the ability of the skin to deform around individual microneedles upon application of the device. However a rolling application, which greatly improved penetration efficiency, was developed (Fig 2.4). *En face* imaging suggested that the frustum tipped microneedles disrupted the skin surface to a greater degree than those with pointed tips, resulting in greater penetration of the methylene blue dye and larger, denser areas of staining (Fig 2.17A & 2.17B).

However, an important observation was the failure of all microneedles within an array to penetrate the skin surface and the different levels of skin damage induced by those that did penetrate. Histology confirmed this observation with microchannels created by the frustum tipped microneedles ranging from minor skin disruptions, similar to those visualised following dry-etch application (Fig 2.17C), to microchannels that were over 100μm wide (Fig 2.17D - 2.17F).

Another noteworthy point was the variability of penetration, depending upon the method of application. For example, a single smooth rolling motion with a wet-etch array, often resulted in preferred penetration of microneedles at the perimeter of the array pattern (Fig 2.18A). However, if the array was moved backwards and forwards slightly in a rocking motion, penetration efficiency in the central area of the array was improved (Fig 2.18A). The method of microneedle application was therefore noted as a fundamental parameter in the effective and reproducible penetration of a microneedle device.

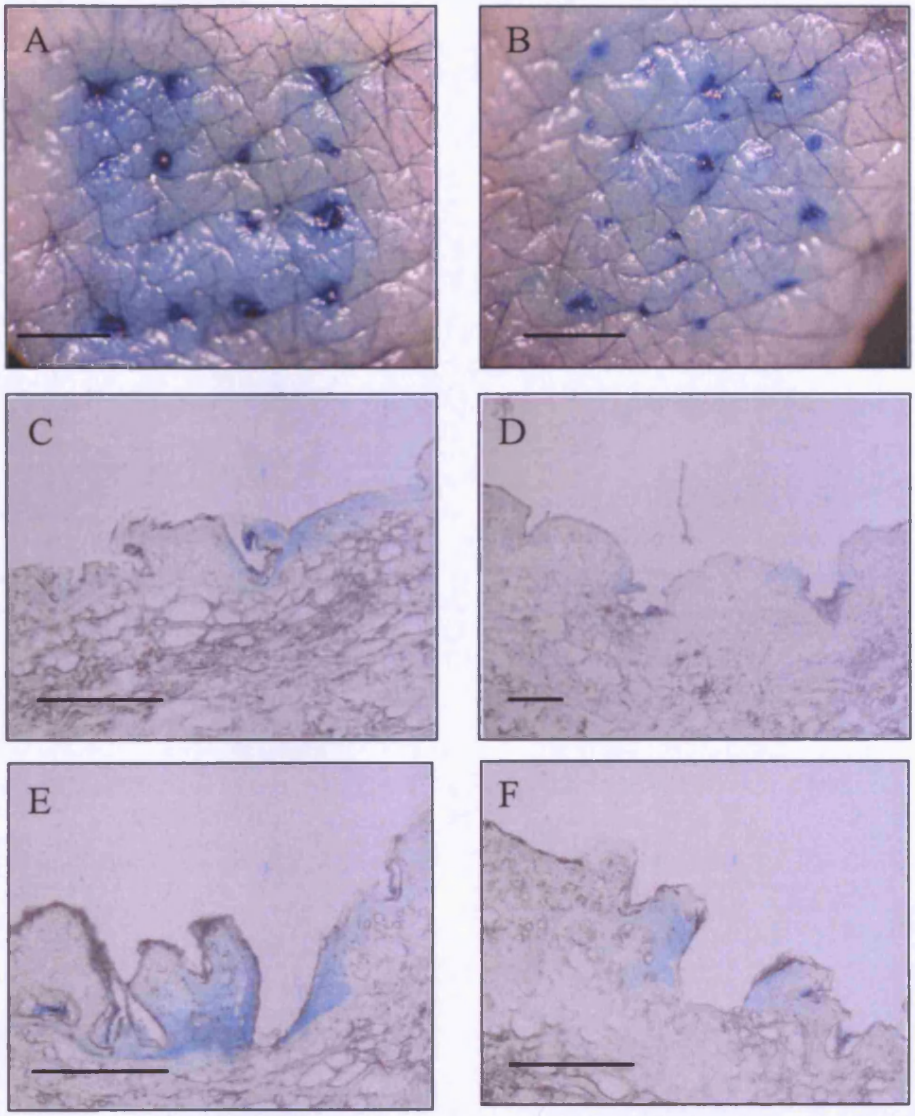


*Figure 2.17.* Light microscopy of microchannels created within human skin by the wet-etch microneedle device. Methylene blue dye highlights areas successfully penetrated by the microneedle array. Skin was obtained from a 57 year old female donor.

*A. En face* imaging of the skin surface following application of a wet etch array, with frustum shaped needle tips, (TNI - Array 1) in a single 'rolling' motion. Scale bar = 1000μm.

B. *En face* imaging of the skin surface following application of a wet etch array, with pointed needle tips, (TNI - Array 6) in a single 'rolling' motion, scale bar = 1000μm.

C, D, E, F. Unstained cryosections (12μm) of frustum treated human skin illustrating microchannels within the upper skin layers. Scale bar = 200μm.

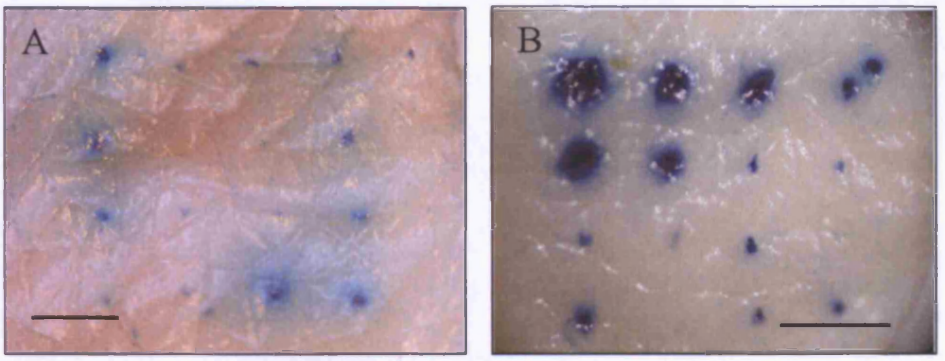


*Figure 2.18. En face* analysis of microchannels created by different application methods using wet-etch microneedle devices. Donor is a 61 year old female. Application of a wet-etch array, with sharp tipped microneedles (TNI - Array 21) in (A) a single 'rolling' motion and (B) a 'rolling' and then vibratory motion. Scale bar = 1000μm.

### 2.4.5. Microneedle integrity

Microneedle devices were examined for defects following their application to the skin surface. The mechanical properties of the microneedle array i.e. its strength and robustness must be optimised to ensure that the force involved in application of the device does not damage individual microneedles within the array (Wilke et al., 2005b). Such damage has implications both in the laboratory development of the device, arrays are repeatedly used in experiments and therefore reproducible penetration is required, and in the clinical setting, where individual microneedles remaining in the skin following device removal might be seen as a significant safety issue. Regular appraisal of the integrity of the microneedle array by light microscopy and SEM therefore ensured the device functionality. These observations also formed the basis for improvements in microneedle design, their engineering or their method of application to human skin.

#### *2.4.5.1. Dry-etch microneedle arrays*

Repeated use of the dry-etch devices manufactured by CSE resulted in a dramatic reduction in their capacity to puncture the skin surface. This was attributed to a coating of biological debris over the surface of the device that resulted in occlusion of the pointed needle tip (Fig 2.19A & 2.19B). Removal of biological contamination by submersion in Decon® 90 for a period exceeding 24hrs, followed by an overnight acetone rinse, restored the individual microneedle geometries and the device functionality (Fig 2.19C). However the fragility of silicon microneedles also resulted in irreparable physical damage to individual microneedles, particularly those located on the perimeter of the array pattern (Fig 2.6A).

Platinum coated dry etch devices, produced by TNI (Fig 2.19D), showed a much greater resistance to physical and biological damage following repeated applications to the human skin. It is not unreasonable to attribute this increase in robustness to differences in the array pattern and the structural modification of individual microneedles. Although physical damage to the device was minimal, those microneedles that were affected were again located primarily around the periphery of the array pattern. This suggested that forces imposed upon individual microneedles on their insertion into the skin are greater on peripheral microneedles of the dry-etch array.

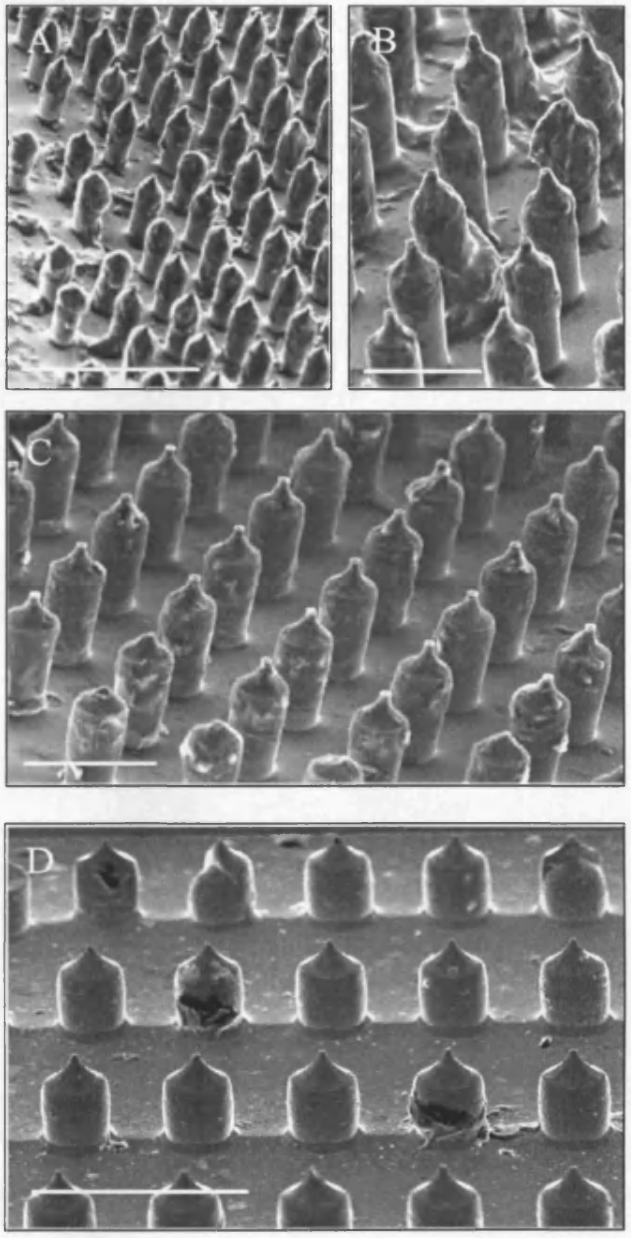


*Figure 2.19.* Scanning electron micrographs of dry-etch microneedle arrays following repeated application to human skin (A&B). Overnight treatment of the microneedle device results in restoration of the device characteristics (C&D). A, C, scale bar = 500μm; B, D, scale bar = 200μm.

### *2.4.5.2. Wet-etch microneedle arrays*

Wet-etch microneedles maintained their integrity following repeated applications to human skin. Mechanical abrasion and the previously described rinsing procedure (2.4.5.1) removed any traces of biological contamination. The strength of these microneedles has been attributed to their pyramidal shape and wide base (Wilke et al., 2005b).

However, although mechanical strength on the whole was increased, there was also a noticeable difference in the robustness of frustum tipped and pointed microneedles. The frustum tipped microneedles have been used in a range of experiments, including the lateral abrasion of the human skin surface i.e. dragging the microneedles across the skin surface, and have maintained their geometry (Fig 2.20A–2.20C). The pointed tips however were damaged by repeated use and did not withstand the forces imposed on the device by lateral abrasion experiments using human skin (Fig 2.20D-2.20F). These microneedles splintered or broke, most commonly at the microneedle tip, thereby rendering the device ineffective (Fig 2.21).

Silicon microneedles break at crystal planes, due to shear stresses imposed on individual microneedles during application (Wilke et al., 2005b). In the future production of wet-etch microneedles, it will therefore be important to consider such factors. It may be that there will be a compromise between the robust nature of the frustum tipped microneedle and the penetrative capabilities of the pointed microneedle array.

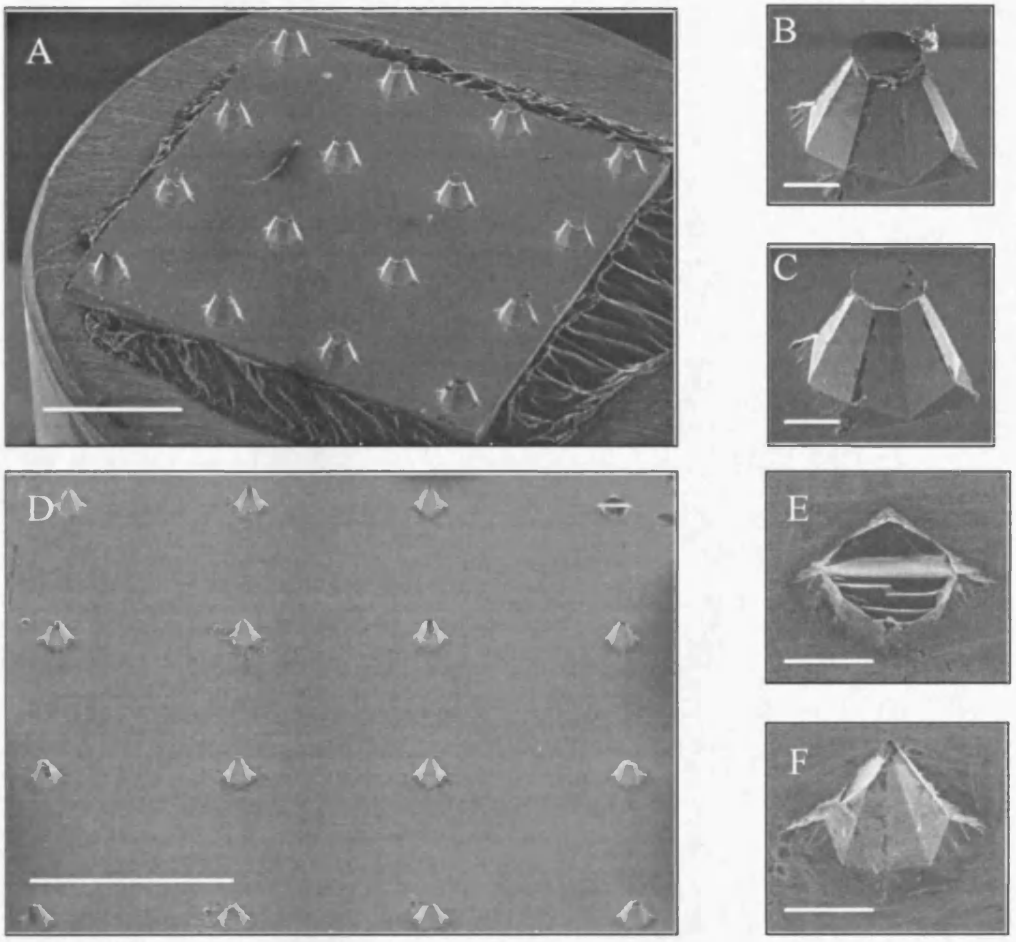


*Figure 2.20.* Scanning electron micrographs of wet-etch microneedle arrays following their application to human skin. Figures highlight the difference in the robustness of the frustum tipped (A-C) and sharp tipped (D-F) arrays. A, D, scale bar = 1000μm; B, C, E, F, scale bar = 100μm.

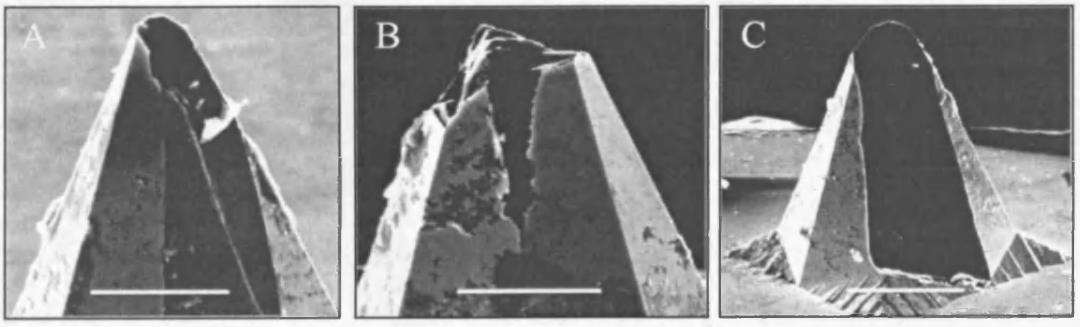


*Figure 2.21.* A series of scanning electron micrographs highlighting the damage to microneedle tips following repeated applications to the human skin. A, B, scale bar = 50μm; C, scale bar = 100μm.

## 2.5. CONCLUSIONS

Microneedles, created by dry-etch and wet-etch microfabrication processes, have demonstrated their ability to disrupt the skin barrier and facilitate the diffusion of a low MW dye into the epidermal skin layer. The creation of microchannel structures observed by histological analysis illustrated the basic capabilities of the device and encourages their employment in the cutaneous delivery of macromolecular formulations, with a view to facilitating epidermal gene delivery and expression.

However, although the observed microchannels were deemed suitable for investigation of cutaneous macromolecule delivery, the reproducibility of microneedle penetration was dependent upon numerous factors including the array pattern, microneedle density, microneedle geometries and the method and force of application. This was further complicated upon repeated use of devices by biological contamination and mechanical disruption to microneedle structures. The reproducibility of the microchannels that are created by arrays is likely to be an important factor governing the therapeutic progression of these devices. Therefore although cutaneous gene delivery using a microneedle array is the principal goal of this investigation, it is well understood that concurrent advances in the design of devices and the development of a reproducible application method will be of paramount importance for the progression of the microneedle device towards a clinically useful drug delivery platform.

# CHAPTER 3

# The diffusive characteristics of nanoparticle formulations through microconduits

## 3.1. INTRODUCTION

Significant advances in molecular biology and the resultant expansion in the biotechnology industry has stimulated progression of therapeutic entities from small chemical compounds to an expanding range of peptides, proteins and nucleic acids. However, effective clinical use of biomacromolecular therapeutics relies upon the development of novel technologies and formulations that can facilitate effective delivery of the therapeutic to its site of action. Delivery of therapeutics through the skin provides a portal for delivery that negates first pass metabolism by the liver. Novel strategies for the localised delivery of macromolecules through the outer skin barrier have therefore received notable recognition over recent years (Barry, 2001, Barry, 2002, Chiarello, 2004, Cross and Roberts, 2004, Prausnitz et al., 2004, Schuetz et al., 2005, Ting et al., 2004). This chapter aims, using a model system, to determine the physicochemical factors that influence the delivery of colloidal gene therapy formulations through conduits created in the skin by a microneedle device.

### 3.1.1. Understanding the diffusion of gene therapy complexes through the skin

An electrostatically charged colloidal gene complex, such as the LPD (Section 1.3.2), is likely to encounter a number of physical and biological obstacles that may retard its movement through aqueous microchannels created within the SC by a microneedle device. Predicted impediments to successful gene delivery include, (i) non-covalent interaction of the gene complex with the skin surface and tissue components, (ii) formulation instabilities, (iii) steric hindrances and (iv) degradation of pDNA by endonucleases. Recognising and understanding such barriers is of paramount importance in the development of drug delivery technologies and formulations that can facilitate efficient and effective cutaneous gene delivery.

The engineering of effective silicon microneedle devices for this study was a technically challenging manufacturing process, conducted in clean-room facilities over a period of several months (Section 2.1.1). During this interval, a series of predictive studies were designed to determine the importance of a colloidal particles size and surface charge (zeta potential) on its permeation through the microchannels of a representative synthetic porous membrane. The selection of a colloidal formulation and a membrane to

be used in this model was based upon the physical characteristics of the LPD formulation and the microneedle treated skin surface.

### 3.1.2. Selecting a model nanoparticle and a representative synthetic membrane

In order for data from a model system to be valuable in the prediction of nanoparticle permeation through microneedle treated skin, model design is critical. Fluorescent nanospheres, used previously as model nanoparticles (Alvarez-Roman et al., 2004, Kohli and Alpar, 2004), were therefore selected as a simple, well-defined, detectable and quantifiable representation of a colloidal gene therapy formulation.

Isopore® polycarbonate track-etched membranes were selected to represent microneedle treated skin (Fig 3.1). These membranes possess uniform cylindrical channels of measurable diameter and length {Apel, 2001 #48; Brendler, 1995 #51; Diez, 1989 #57}. Initial studies by Prausnitz and co-workers suggested that a device with an array of solid silicon microneedles, possessing sharp tips and a length of 150μm, produced conduits of 1μm diameter within the skin (Henry et al., 1998a). However, the application of alternative microneedle geometries to the human skin may create conduits with altered dimensions (Section 2.4). With this in mind, it was decided that model diffusion studies should assess the diffusion of colloidal particles through three pore sizes:-

1. 1.2μm pore size – based on the findings of Henry and co-workers (Henry et al., 1998a).
2. 10μm pore size – to determine the effects of an increased pore size on diffusion.
3. 100nm pore size – as a negative control.

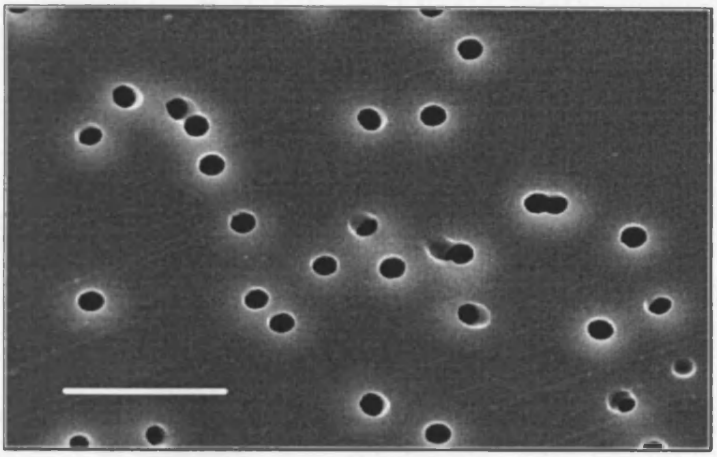

*Figure 3.1.* A scanning electron micrograph of a 10μm Isopore® polycarbonate track-etched membrane, scale bar = 50μm.

The permeation of colloidal particles through a membrane pore was not envisaged to be dependent upon the pore diameter alone. Electrostatic interaction between a nanoparticle and the membrane surface was also predicted to influence permeation. Therefore the surface charge (zeta potential) of the membrane and the nanoparticle were considered (Apel, 2001, Calvo et al., 1996). The skin surface has been described as a membrane of net negative charge with an isoelectric point of pH3-4. This was initially attributed to a greater proportion of negatively charged amino acid residues within the tissue (Burnette and Ongpipattanakul, 1987). However, electron dense desmosomes and desmosomal remnants are now considered to contribute significantly to this charge (Wertz and van den Bergh, 1998).

The Isopore® membrane has been described as a weak acid with a negative surface potential (Brendler et al., 1995). This is attributable to the exposure of carboxylic acid groups, within the pore structures, upon chemical etching of the polycarbonate membrane (Huismann et al., 2000, Keesom et al., 1988). Increased etching times, used to create larger pore sizes, therefore cause a resultant increase in the magnitude of the negative surface potentials (Keesom et al., 1988, Kim et al., 1997).

1. For pore sizes of 100nm and 200nm, the zeta potential becomes constant at approximately –10mV when the pH exceeds 6.

2. For 1μm pore membranes the zeta potential is constant when pH exceeds 6 at approximately –27mV.
3. Zeta potential approaches 0mV at ~ pH3–5 depending on the pore size (isoelectric point).

The population of charged carboxylic acid groups within membrane pores is small and hence the magnitude of the negative zeta potential for polycarbonate membranes remains relatively low. The polycarbonate membrane may not adopt a positive charge until extremely acidic pH values are achieved i.e. less than pH3. The surface of the membrane therefore retains a general hydrophobic character (Keesom et al., 1988).

Isopore® membranes were selected as a representative porous model of the microneedle treated skin that could be utilised in experiments to gain an appreciation of the influence of specific physicochemical parameters on the permeation of nanoparticles through microconduits. However, *in vivo* the permeation of nanoparticles into microneedle treated skin is expected to be much more complex. Therefore penetration of model nanoparticles across microneedle treated human epidermal membrane was also assessed.

### 3.1.3. Nanoparticle diffusion through human epidermal membrane

Successful non-invasive transcutaneous vaccination strategies (Glenn et al., 1998, Glenn et al., 2000, Scharton-Kersten T, 1999) have provoked interest in the development of topically applied nanoparticle formulations, containing pDNA, that can stimulate a protective immunity (Cui and Mumper, 2001, Cui and Mumper, 2002, Cui and Mumper, 2003). However current non-invasive DNA vaccination strategies suffer from unpredictable transfection efficiencies (Cui and Mumper, 2001, Shi et al., 1999) and it remains unclear how such particulate formulations penetrate the skin barrier (Domashenko et al., 2000, Hoffmann, 2000).

A recent diffusion study by Kohli *et al* assessed the ability of a topically applied fluorescent latex nanoparticle formulation to penetrate the untreated skin (porcine) surface (Kohli and Alpar, 2004). The investigators claim to have facilitated cutaneous delivery of negatively charged nanoparticles with 50nm and 500nm radii. However

200nm and 300nm radii nanoparticles failed to penetrate the membrane. The authors speculate that repulsion between the more intense 'negative charge density' on 50nm and 500nm particles and those on the negatively charged lipids in the skin facilitates increased permeation (Kohli and Alpar, 2004). However, only 0.1% of the nanoparticle formulation was detected in the receptor phase of Franz diffusion cells and so it is questionable if the detected levels of fluorescence are attributable to nanoparticle diffusion or background fluorescence. Histology also failed to detect fluorescent nanoparticles in the epidermis or dermis tissue, casting further doubt on the results.

A more recent study examined the penetration of negatively charged nanoparticles (20 & 200nm in diameter) through porcine skin using confocal laser scanning microscopy (Alvarez-Roman et al., 2004). Accumulation of particles was only observed in follicular openings and furrows on the skin surface. Investigators therefore acknowledged that although particle size, surface charge and hydrophobicity will affect penetration and deposition in a biological tissue, such as the skin, there was no evidence of SC penetration.

### 3.1.4. Techniques

#### *3.1.4.1. Photon Correlation Spectroscopy (PCS)*

If a colloidal suspension is illuminated with a laser, particles within that suspension will scatter light, which can then be measured by a detector. If the scattered light arrives at the detector with the same phase it causes constructive interference. However if the phase patterns oppose each other it causes destructive interference. Small particles that collide with solvent molecules move with a greater velocity than a larger particle and so this movement causes a greater fluctuation in the intensity of measurements. PCS therefore uses the difference in Brownian motion between a large and a small particle in order to determine their size.

#### *3.1.4.2. Zeta Potential*

A charged colloidal particle within an aqueous environment is associated with counterions, donated from the surrounding liquid environment (Fig 3.2). Therefore the electrical behaviour of a particle is dictated by ions that are bound in layers of

alternating charge around the particle. Counterions of the inner layer are tightly bound to the particle (Stern layer) due to their close contact with the particles charged surface. As they get further from the particle surface these counterion layers become less firmly bound (diffuse layer). Therefore as a particle moves within an aqueous media, those tightly bound ions remain bound to the particle surface while those in the diffuse layer remain behind. The potential at this boundary (the slipping plane) is the zeta potential.

Zeta potential is therefore a measure of the charge that a colloidal particle adopts within a defined aqueous media. It is dictated by the surface charge of the particle and the counterions present in the surrounding liquid. The basic principles of zeta potential measurement utilise the movement of charged particles within a colloidal system under the influence of an electric field i.e. electrophoresis.

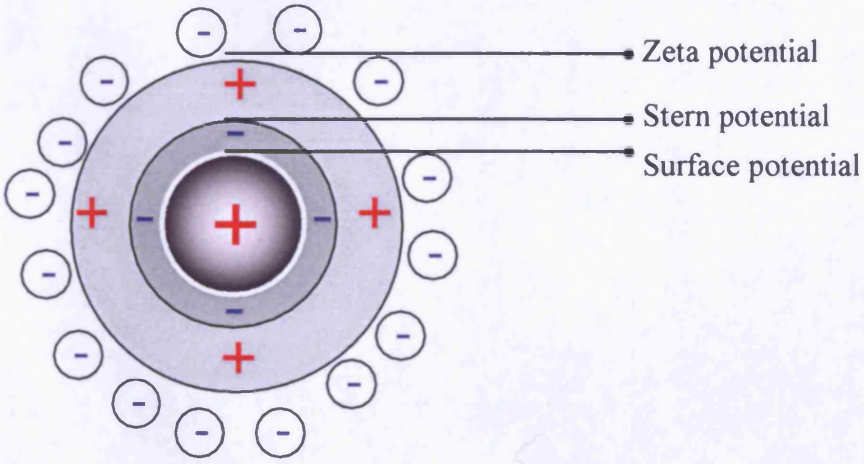


*Figure 3.2.* A schematic representation of a positively charged colloidal particle (black) suspended within an aqueous environment. The stern layer (grey), zeta potential (light grey) and the associated counterions are highlighted.

### *3.1.4.3. Fluorescence Microscopy*

Fluorescence microscopy is a selective detection method that permits visualisation of a small amount of a compound within a complex mixture of non-fluorescent material. Only compounds that contain a fluorophore can be analysed by this method. A

fluorophore has the ability to absorb light of a particular wavelength and to remit light of longer wavelengths. The process occurs in three basic steps, (i) light is absorbed from an excitatory light source and electrons are excited from the ground state to a higher electronic state (the excited state), (ii) internal conversion of energy due to the collision of the excited state compound with solvent molecules causes the loss of a small amount of energy and the molecule is converted to its 'lowest excited state' and (iii) electrons then return to the ground state and this results in the emission of a photon of energy. The excitation wavelength is therefore always shorter (higher energy) than the emission wavelength (lower energy). Excitation and emission wavelengths are specific to individual fluorophores. These must be determined prior to fluorescence microscopy (or spectrophotometry), to ensure that the sample is illuminated at the appropriate wavelength and that filters are available to view the sample with the exclusion of the illuminating light.

The major drawback to this method of analysis is the presence of background fluorescence and other fluorophores which interfere with effective analysis of your sample. The presence of interfering fluorophores is a well recognised issue in the analysis of biological samples, with those more complex samples such as whole skin tissue presenting greatest problems. For any fluorescence studies it is therefore essential that control samples are included to determine the relative contribution of endogenous/auto-fluorescence. During this investigation fluorescence microscopy has been utilised to determine the presence of fluorescent nanoparticles on the surface of Isopore® membranes, within histological sections of skin tissue and to identify cells successfully transfected with the pEGFP-N1 plasmid (Chapter 4).

## 3.2. AIMS AND OBJECTIVES

### Chapter Aim

The previous chapter characterised novel solid silicon microneedle devices that penetrated the human skin surface and thus created micron-sized conduits within the epidermal layer. This chapter aims, using a model system, to determine the physicochemical factors that influence the delivery of nanoparticles through such conduits and to demonstrate permeation of a nanoparticle formulation through microneedle treated human epidermal membrane. The results of these studies will indicate whether cutaneous delivery of a pDNA nanoparticle formulation, such as the LPD, is a realistic ambition.

### Chapter Objectives

- To determine the physicochemical properties of the LPD non-viral gene therapy vector.

- To develop and characterise a representative nanoparticle model of an LPD that can be visualised and quantified.

- To investigate the influence of physicochemical characteristics on the diffusion of a nanoparticle through a synthetic membrane containing pores of uniform diameter.

- To determine the ability of a microneedle array to enhance permeation of a nanoparticle formulation through the epidermal skin membrane.

## 3.3. MATERIALS AND METHODS

### 3.3.1. Materials

All reagents were obtained from Fisher (Loughborough, UK) and were, unless stated otherwise, of analytical grade.

The pCMVβ plasmid (7.2 kb) construct containing the *LacZ* reporter gene and the pEGFP-N1 plasmid (4.7kb) expressing the green fluorescent protein (GFP) reporter gene were obtained from Promega Corporation (Madison, WI) and propagated as detailed in Chapter 4 (Section 4.3.2).

1,2-Dioleoyl-3-triammonium-tropane (DOTAP) was purchased as the methyl sulphate salt from Avanti Polar Lipids (Alabaster, AL, USA). Protamine sulphate, fluorescent yellow/green polystyrene nanospheres (L-1280), propranolol hydrochloride, chloroform and greiner 96-well polypropylene plates were obtained from Sigma-Aldrich Chemical Company (Poole, UK). 2-(12-(7nitrobenz-2-oxa-1,3-diazol-4-yl)amino)dodecanoyl-1-hexadecanoyl-sn-glycero-3-phosphocholine ($NBDC_{12}$-HPC) was obtained from Molecular probes (Leiden, Netherlands)

All histology materials, including OCT embedding media, Histobond® adhesive microscope slide were obtained from RA Lamb Limited (Eastbourne, UK) or in the case of toluidine blue, Harris' haematoxylin, Gurrs' eosin aqueous solution 1%, Histomount® and xylene (low sulphur) from Lab 3 (Bristol, UK).

Equipment:-

Fluostar fluorometer (BMG laboratories, Offenburg, Germany)
Malvern 2000 Zetasizer (Malvern Instruments, Malvern, UK)
pH probe (Malvern Instruments, Malvern, UK)
Extrusion apparatus (Northern lipids, Vancouver, Canada)
Coulter $N_4$ Plus PCS Instrument (Coulter electronics, Luton, UK)
Leica CM305S Cryomicrotome (Leica Microsystems (UK) Limited, Milton Keynes, UK)
Olympus BX-50 system microscope (Olympus Optical, London,UK)
Olympus IX-5058F system microscope (Olympus Optical, London,UK)
Olympus DP-10 Camera (Olympus Optical, London,UK)
U-RFL-T-200 Olympus fluorescence burner (Olympus Optical, London,UK)
Olympus TH3 Power unit (Olympus Optical, London,UK)
Schott KL1500 fibre optic light source (Schott UK Limited, Stafford, UK)
Philips 208 Transmission Electron Microscope (Philips, Eindhoven, Netherlands)
Philips XL-20 Scanning Electron Microscope (Philips, Eindhoven, Netherlands)
Gold sputter coater (EM Scope, Kent, UK)
Ultrasonication bath (Ultrawave, Cardiff, UK)
U-300 spectrophotometer (Hitachi, Tokyo, Japan)

### 3.3.2. Nanoparticle preparation

#### *3.3.2.1. LPD non-viral gene delivery complex*

The LPD complex consists of a 3:2:1 mass ratio of DOTAP liposome: protamine sulphate: pDNA. pDNA (1mg/ml) was amplified in transformed *Escherichia coli (E.coli)* DH5α (Section 4.3.2.2). Protamine sulphate powder was dissolved in sterile deionised water to create a stock concentration of 1mg/ml and DOTAP liposomes were prepared to a final concentration of 1mg/ml.

To prepare DOTAP liposomes, 10mg of DOTAP was dissolved in ~10ml of chloroform in a round bottomed flask. The chloroform was then removed using a rotor–evaporator to produce a thin lipid film on the walls of the flask. The film was dried over a 90min period and subsequently hydrated with 10ml of sterile deionised water (37°C). The lipid suspension was then vortexed briefly and maintained at 37°C for 30mins to allow liposome formation to occur. A high-pressure extrusion apparatus containing an Isopore® polycarbonate track-etched membrane (100nm pore size) was used to produce unilamellar liposomes. Ten extrusion events produced liposomes with a diameter of approximately 100nm. Unimodal liposome size was measured using a Coulter $N_4$ plus PCS and size distribution processor (SDP) analysis was performed.

LPD complexes were prepared by sequential addition of components:-

- 3.8ml of deionised water added to 200µl pEGFP-N1 (1mg/ml).
    - 10min incubation.
- 400µl of protamine sulphate (1mg/ml) added.
    - 10min incubation.
- 600µl of DOTAP liposomes (1mg/ml).
    - 10min incubation.
- 1ml LPD complex added to 2ml of deionised water of known pH.

For zeta potential studies, the deionised water was included at a range of pH values, (adjusted with hydrochloric acid (0.01M) and sodium hydroxide (0.01M)).

For diffusion studies, fluorescent LPD gene complexes were prepared using a DOTAP liposome suspension containing 5%w/w of the fluorescent lipid $NBDC_{12}$-HPC. DOTAP liposomes were made in the same manner as detailed previously in this Section. However, the 10mg of lipid now contained 9.5mg DOTAP and 0.5mg of $NBDC_{12}$-HPC. The absorption and excitation wavelengths of the fluorescent lipid (460nm and 534nm respectively) allowed the quantitative analysis of liposomes using a fluorometer with excitation and emission filters set at 485nm and 520nm respectively.

#### *3.3.2.2. Fluorescent nanosphere*

Fluorescent nanospheres possess a surface bound fluorophore with maximum excitation and emission values of 470nm and 505nm respectively. These values were confirmed by excitation and emission scans using a U-300 spectrophotometer with a slit width of 2μm and a scan range of 200-800nm (Appendix II). Nanospheres were diluted using deionised water.

#### *3.3.2.3. Lipid coated nanospheres (LCN)*

A DOTAP lipid film was created (Section 3.3.2.1). Following this, 10ml of 5μl/ml nanosphere suspension (concentrate/water) was added to the flask, which was then vortexed for approximately 30secs and finally maintained at 37°C for 1hr. The suspension was then sonicated for 1hr and a Coulter $N_4$ plus PCS instrument was used to determine the size distribution of the resulting suspension. Excitation and emission spectra confirmed maintenance of the latex nanospheres fluorescent properties following the lipid coating procedure (Appendix II).

### 3.3.3. Transmission Electron Microscopy (TEM)

A pioloform-coated 200-mesh nickel grid was fixed between the tips of a metal forceps and 15μl of the nanoparticle formulation (LPD, nanosphere or LCN) was applied to the 'dull side' of the grid. After a contact time of 3mins, excess formulation was 'wicked' from the grid using filter paper. The grid was then placed on the surface of a filtered 2% aqueous uranyl acetate drop for 30secs, with the 'dull side' facing downward. The stain was then 'wicked' from the grid, which was rinsed twice in deionised water before analysis by TEM.

### 3.3.4. PCS size analysis

Measurements were performed using the Coulter $N_4$ Plus PCS instrument. Unimodal analysis provided a mean particle size and standard deviation for a monodisperse suspension. However for more complex distributions a size distribution processor (SDP) analysis was also used. Preparation of samples to be analysed by this technique i.e. (i) DOTAP liposomes, (ii) LPD complexes, (iii) fluorescent nanospheres and (iv) LCNs required dilution of the suspended sample in a clear-sided disposable cuvette, with filtered deionised water to a volume of 3ml.

### 3.3.5. Zeta potential

The zeta potential was determined for each of the nanoparticle formulations using the Malvern 2000 Zetasizer. Briefly, nanoparticle formulations were diluted with deionised water. A sample was then injected into a flow through cell, allowed to equilibrate for 30secs and then analysed repeatedly (N=5) before removal. The effect of pH on the stability of the nanosphere and LCN suspensions was investigated using a multi-purpose titrator. This allowed measurement of zeta potential under the influence of a progressive change in pH (achieved using hydrochloric acid (0.01M) and sodium hydroxide (0.01M) solutions).

### 3.3.6. Predictive diffusion studies using Isopore® membranes

Isopore® membranes were mounted between the donor and receptor chambers of static Franz diffusion cells of known receptor volume and diffusional area (Fig 3.3). Each membrane was 27mm in diameter and possessed a pore size of 100nm, 1.2μm or 10μm. The receptor compartment of each cell was filled with an aqueous solution and a magnetic stirrer bar was added. Sampling arms were covered with a foil cap and each diffusion cell was positioned on a magnetic stirrer plate, in a water bath maintained at 37°C. Each cell was allowed to equilibrate for at least 30mins before application of the formulation to the subsequently occluded donor chamber.

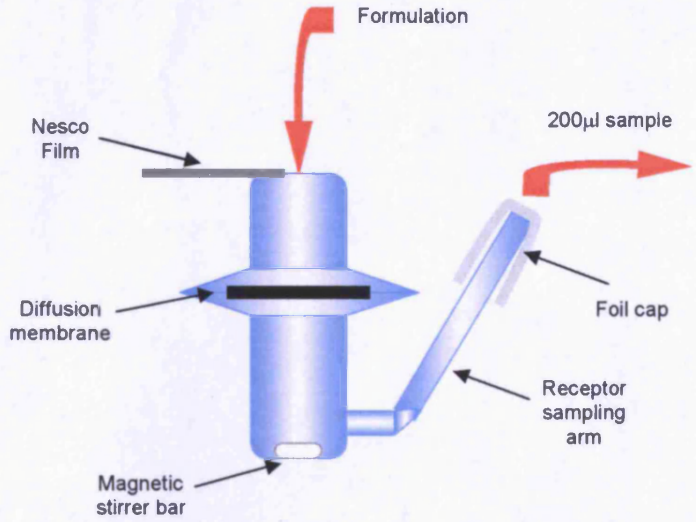


*Figure 3.3.* A schematic representation of the static Franz diffusion cell.

The applied formulations consisted of either fluorescent nanospheres, LCNs or fluorescent LPDs in an aqueous solution. The pH of the resulting formulation was adjusted to a target pH (depending on the study) using 0.01M hydrochloric acid or 0.01M sodium hydroxide solutions.

Degassed, deionised water filled the receptor compartment. The pH of the receptor phase was adjusted, using sodium hydroxide (1M) or hydrochloric acid (1M), to complement the formulation pH. Traditional buffer salts were not used to control pH due to their unpredictable effects on the zeta potential of a colloidal formulation. However, preliminary experiments assessing the pH value of the receptor phase before and after treatment indicated that the pH of the system was maintained throughout the experimental procedure.

Samples (200µl) were removed from the receptor arm at 30, 60, 120, 240, 360 and 720mins and replaced with an equal volume of receptor phase (37°C). A sample was also removed from the donor phase of each cell at the conclusion of the experiment. The final nanoparticle concentration in the donor and receptor phases was then used to calculate the theoretical amount of the formulation that was associated with the membrane. Samples were stored in a Greiner® black polypropylene 96-well plate and

analysed using a Fluostar® fluorometer. Calibration curves were constructed for each of the formulations in order to determine the limits of detection and were used to convert fluorescence values to nanoparticle concentrations.

Franz cells were dismantled following the removal of the final sample and selected membranes were retained for microscopic evaluation. Isopore® membranes, isolated from the Franz diffusion cells, were positioned on glass microscope slides, illuminated with a blue excitation light source and visualised using an Olympus BX-50 microscope. Photomicrographs were collected to provide a qualitative assessment of the membrane integrity and its fluorescence. Membranes were then mounted on aluminium stubs, gold sputter coated and assessed by SEM (Section 2.3.5). The receptor phase was also collected and the pH measured.

### 3.3.7. Heat separated human epidermal membrane diffusion studies

#### *3.3.7.1. Propranolol diffusion*

Human skin from a 67 year old female donor was removed from storage and allowed to defrost over a period of 1hr. Sub-cutaneous fat was removed by blunt dissection and the epidermal membrane was removed by heat separation and collected on aluminium foil (Section 2.3.5.1). Membranes to be treated by the microneedle device were then replaced on the dermal tissue and a wet-etch microneedle array (TNI – Array 5) was applied to the skin surface on five consecutive occasions. The treated areas (~2.5cm$^2$) were isolated from the epidermal membrane and mounted in Franz diffusion cells (N=6). Untreated epidermal membranes were also evaluated (N=4). The receptor compartment of the assembled cells was filled with PBS, pH7.4 and equilibrated in a water bath (37°C) for 30mins. Foil caps were placed on the receptor sampling arm and 0.5ml of formulation was added to the donor phase, which was then occluded. The study compared the diffusion of a 0.5mg/ml propranolol hydrochloride formulation through treated and untreated epidermal membranes and used deionised water as a negative control.

Samples from the receptor phase were analysed as previously detailed (Section 3.3.6) at 1, 2, 4, 6, 11 and 24hrs and also from the donor phase at the conclusion of the

experiment. Excitation and emission filters were set at 280nm and 330nm respectively during fluorescence spectrophotometry.

#### *3.3.7.2. Nanoparticle diffusion*

Microneedle (TNI – Array 8) treated human epidermal membranes (N=8), untreated membranes (N=2) and membranes punctured ten times with a hypodermic needle (N=2) were prepared and mounted in Franz diffusion cells (Section 3.3.7.1). The study investigated the diffusion of the fluorescent nanosphere formulation (Section 3.3.2.2) through treated and untreated epidermal membranes, using deionised water as a negative control for the formulation. In these experiments, the nanosphere formulation was utilised in its concentrated form.

Samples were removed from the receptor sampling arm at regular intervals over a period of 72hrs and analysed by fluorescence spectrophotometry (Section 3.3.6).

## 3.4. RESULTS AND DISCUSSION

### 3.4.1. Physicochemical properties of nanoparticle formulations

#### *3.4.1.1. Transmission electron microscopy*

TEM images suggested comparable diameters for the LPD gene therapy complex and model nanoparticle formulations (Fig 3.4). The 'finger-print' like appearance of LPD particles indicated a lipid lamellar surface structure (Fig 3.4C), which was also present in the LCNs (Fig 3.4B). Comparable surface morphology and size suggests that the LCN is an appropriate representative model of the LPD.

#### *3.4.1.2. Size analysis*

PCS indicated that the three studied nanoparticles possessed diameters of approximately 90-140nm, with model nanosphere formulations possessing slightly greater diameters than the LPD complex (Table 3.1). This confirmed TEM observations (Fig 3.4). Microconduits created within the skin surface by a microneedle device must therefore be significantly greater than the diameter of these nanoparticles if enhanced permeation across the SC is to be facilitated effectively.

*Table 3.1.* PCS size analysis of nanoparticle formulations (unimodal mean ± sd)

| IDENTITY | DOTAP:Protamine:pDNA (LPD complex) | Fluorescent Nanosphere | LCN |
|---|---|---|---|
| DIAMETER(nm) | 89.0±34.7 | 138.0±25.1 | 141.4±46.9 |

#### *3.4.1.3. Zeta potential*

The zeta potential for each of the formulations was assessed between pH2 and 12 (Fig 3.5). The isoelectric point of fluorescent nanospheres was just below pH5 (the pH value of a colloidal formulation at which the zeta potential becomes 0mV). Therefore by manipulating the pH of the colloidal formulation the zeta potential of the fluorescent nanosphere formulation can be reversed. Zeta potential values for both the LPD and the

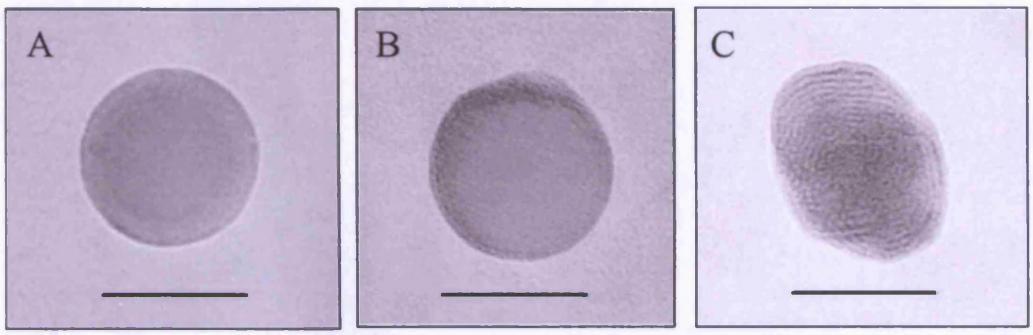


*Figure 3.4.* TEM images of; A, a fluorescent nanosphere; B, a lipid coated fluorescent nanosphere (LCN) and C, an LPD complex, scale bar = 100nm.

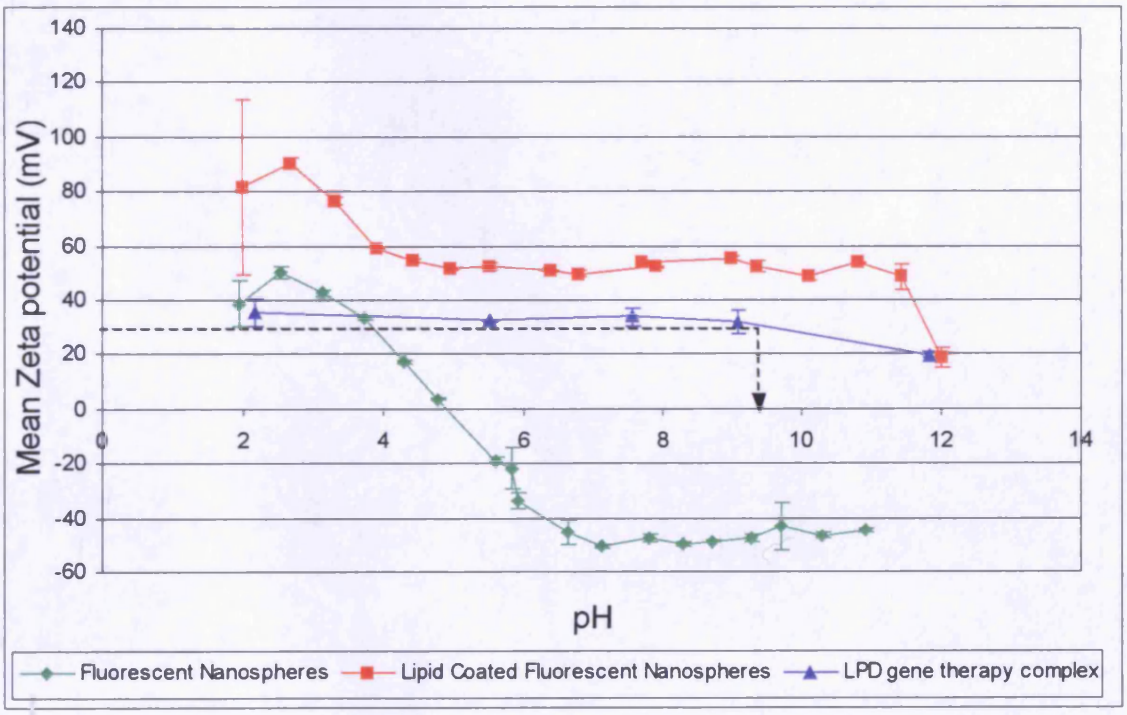


*Figure 3.5.* A graphical representation of zeta potential values for the three studied nanosphere formulations between pH2 and pH12. Dashed arrow indicates the pH at which the zeta potential of the LPD formulation drops below +30mV. Fluorescent nanosphere, lipid coated fluorescent nanosphere, mean ± sd (N=3); LPD complex, mean ± sd (N=5).

LCN however are resistant to changes in pH, remaining positive between pH2 and 12. The positive zeta potential of these nanoparticles is contributed by the cationic lipid (DOTAP) within the formulations. This supports those observations of comparable surface morphology made by TEM.

The other important parameter illustrated by this data is the control of pH within a colloidal formulation. Electrostatic repulsion between charged particles maintains the stability of a colloidal suspension. Therefore, to maintain a monodiperse colloidal system, the pH should be maintained at values that ensure a zeta potential of greater than approximately ±30mV (Fig 3.5). At pH values greater than 9, the zeta potential of the LPD formulation falls below +30mV, resulting in the aggregation of nanoparticles (data not shown). During microneedle mediated delivery, where aggregation of nanoparticles may result in occlusion rather than permeation through microconduits, the control of the formulation pH will therefore undoubtedly be important.

### 3.4.2. Predictive diffusion studies using Isopore® membranes

Diffusion studies analysing nanoparticle permeation through model Isopore® membranes indicated that a particles size and surface charge will influence its migration through microneedle treated skin.

Diffusion experiments were conducted at two selected pH values: -

- pH7.4 –Physiological pH, fluorescent nanospheres negatively charged.
- pH3 – Fluorescent nanospheres positively charged.

The zeta potential of the Isopore® membranes and nanoparticle formulations at each of the pH values were determined either by direct measurement or evaluation of the literature (Table 3.2). Between pH3 and 5 the membranes have a small negative zeta potential due to the presence of carboxylic acid groups within the track etched pores (Section 3.1.2). For track-etched membranes with larger pores (greater than 1μm) the negative surface charge is maintained at pH values as low as 3 (Keesom et al., 1988, Kim et al., 1997). This is particularly relevant for the 10μm pore Isopore® membrane used in these studies.

*Table 3.2.* A summary of the zeta potential values of nanoparticle formulations and Isopore® membranes at the studied pH values. * These are theoretical values. The zeta potential is likely to be at a reduced value at pH3, possibly approaching 0mV for the 100nm and 1.2μm pore membrane.

| | LPD | LCN | Nanosphere | Membrane |
|---|---|---|---|---|
| **pH 7** | Positive | Positive | Negative | Negative* |
| **pH 3** | Positive | Positive | Positive | Negative* |

### *3.4.2.1. Fluorescent nanosphere diffusion through Isopore® membranes*

At pH7.4, where both the nanospheres and the membrane surface have negative zeta potentials, diffusion through 10μm pores occured rapidly, with almost 80% of the applied formulation reaching the receptor phase after only 4hrs (Fig 3.6A). Rapid diffusion, facilitated by the significant difference between the pore and nanosphere diameters, highlighted the potential delivery capabilities of a microneedle device. Following this, the graph plateaus, indicating equilibration has been reached between donor and receptor phases.

The rate of diffusion through 1.2μm pores however was much reduced; approximately 60% of the formulation was detected in the receptor phase after the 12hr investigation period (Fig 3.6A). At this point the graph is still rising and therefore diffusion might be expected to continue to the plateau value that was observed for 10μm pores. It is likely that the reduction in diffusion was directly attributable to the decrease in pore size, although variation in charge density in the pores may have also contributed. For the 100nm pore membrane no migration of nanospheres into the receptor compartment was detected and microscopic examination suggested that nanospheres were accumulating on the upper surface of the membrane. This negative control confirmed the validity of the analytical method (Fig 3.6A).

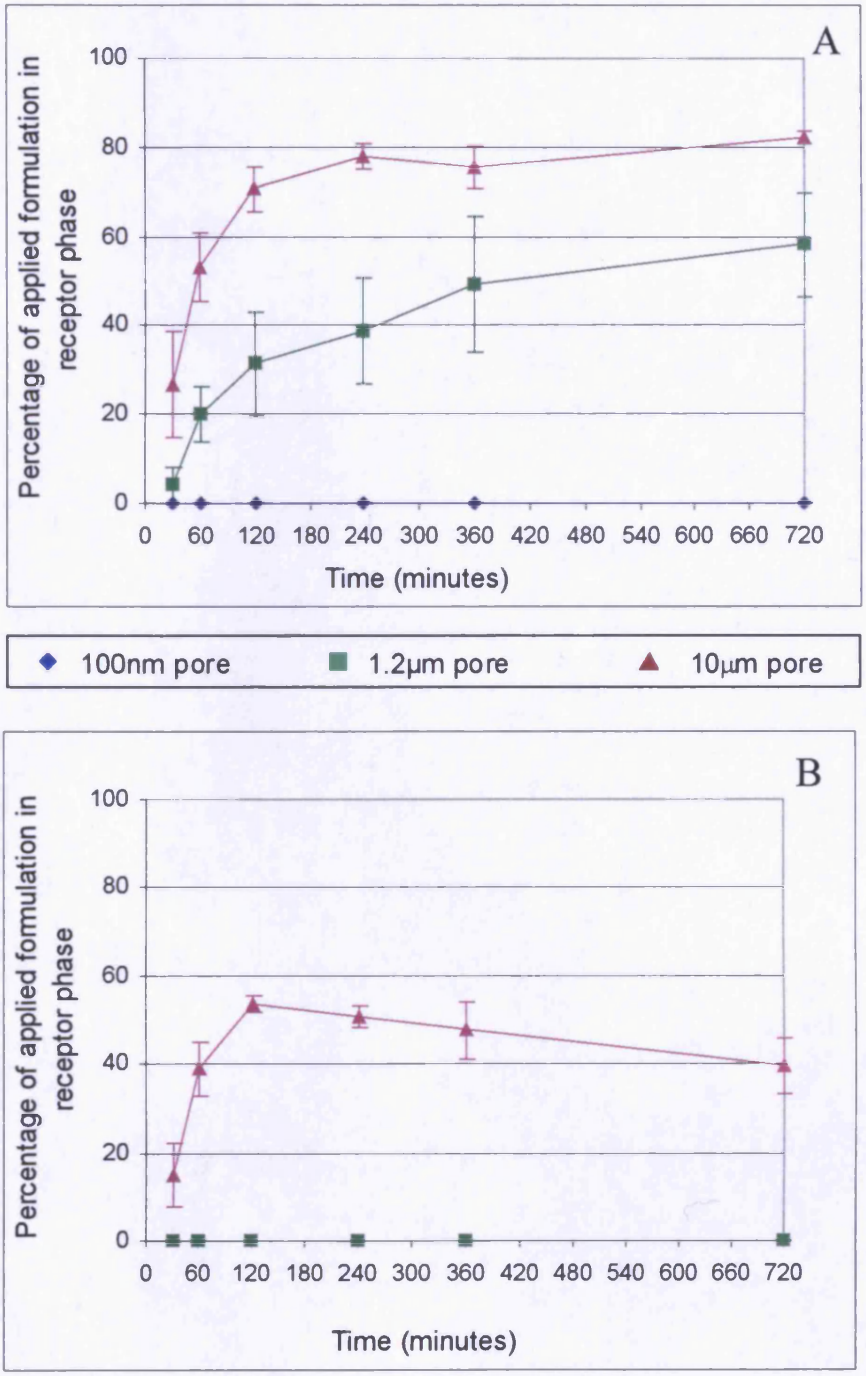


*Figure 3.6.* Diffusion profiles illustrating the percentage of the applied nanoparticle formulation detected within the receptor phase of Franz diffusion cells over a period of 12hrs. Isopore® membranes possessing three different pore sizes were used and the nanosphere formulation and receptor phases were maintained at either ~pH7.4 or ~pH3. A, pH3 mean ± sd (N=4); B, pH7.4 mean ± sd (N=4).

The curve shaped diffusion profiles (Fig 3.6A) indicated that, although initial diffusion through 1.2μm and 10μm membrane pores was rapid, after 2hrs the diffusive rate was gradually reduced. This will be an important consideration for the microneedle mediated delivery of a gene therapy formulation into the skin, where it will be important to deliver the formulation to the target cells rapidly in order to reduce its residence within the extracellular environment and its exposure to those factors that prevent successful transfection (Barry et al., 1999, Ruponen et al., 2003).

Reduction of the formulation and receptor phase solutions to pH3 caused a reversal of the nanospheres zeta potential (Fig 3.5) and a dramatic effect on the permeation characteristics of nanoparticles (Fig 3.6B). The diffusion of nanospheres through 10μm pores over the first 2hrs resulted in just 50% of the formulation reaching the receptor phase, in comparison to over 70% at pH7.4 (Fig 3.6B). However, more significantly, after 2 hrs diffusion was impeded and over the subsequent 10hrs fluorescence levels in the receptor phase decreased. The modification in diffusion characteristics, induced by the reduction in pH, was even more dramatic for the 1.2μm pores, where migration of the nanoparticles was undetectable during the time course of the experiment.

At pH 7.4 the negatively charged nanospheres were able to diffuse freely through the pores of the negatively charged membrane and the rate of diffusion was dictated primarily by the size of the pores, although electrostatic repulsion between the particle and the membrane is also likely to have occurred. However, at pH 3 the zeta potential of nanoparticles was reversed (Fig 3.5) and surface adsorption of positive nanoparticles to the negatively charged surface of membrane pores became a dominant factor. For 10μm pores, although the high pore diameter: particle diameter ratio (100) was insufficient to prevent particle migration, permeation was significantly retarded. A subsequent reduction in receptor phase concentrations following the 2hr time-point may be attributable to the electrostatic interaction of nanoparticles with the underside of the membrane. Nanoparticle permeation through 1.2μm pores was prohibited, possibly due to occlusion of the membrane pores by surface adsorption of nanoparticles (Fig 3.6). Mass balance data achieved at the conclusion of the experiments i.e. the measured donor and the receptor phase concentrations and the calculated membrane bound fraction of the applied formulation (Table 3.3) supported this hypothesis.

| nano-sphere | potential (mV) | | | | 12hrs | | | | |
|---|---|---|---|---|---|---|---|---|---|
| | | 100nm | 1.2μm | 10μm | 100nm | 1.2μm | 10μm | 100nm | 1.2μm |
| **pH ~3** | 39.1 ± 4.6 | 70.1 ±8.4 | 50.5 ±7.6 | 4.1 ±1.5 | 0 ± 0 | 0.1 ± 0 | 39.6 ±6.4 | 29.9 ± 8.4 | 49.5 ± 7.7 |
| **PH ~7.4** | -39.0 ± 5.7 | 91.2 ± 7.4 | 37.9 ± 16.2 | 8.9 ± 0.2 | 0± 0 | 58.3 ± 11.7 | 82.3 ± 1.2 | 8.8 ± 7.4 | 3.8 ± 4.6 |

Measurements indicate that at the conclusion of experiments, conducted at pH3, 50% of the applied formulation may be associated with the membrane. Whereas, 7.4 less than 10% of the formulation was calculated to be membrane b Fluorescence microscopy of Isopore® membranes recovered following the exper confirmed these observations (Fig 3.7). Membranes maintained at pH3 showed i levels of fluorescence in comparison to those maintained at pH7.4, attributabl 'surface coating' with fluorescent nanoparticles. Interestingly, SEM images 100nm and 1.2μm membranes supported this observation (Fig 3.8), both meml being more densely populated with nanospheres when maintained within the acidic conditions.

It is therefore apparent that the pH, and resulting zeta potential, of a col formulation can have significant effects on the diffusive properties of colloidal pa through a porous membrane. These factors must therefore be considered when ut microneedle devices to deliver nanoparticle formulations, such as gene th complexes, and possibly macromolecules across the skin surface and highlig importance of optimising physicochemical properties of a pharmaceutical formula

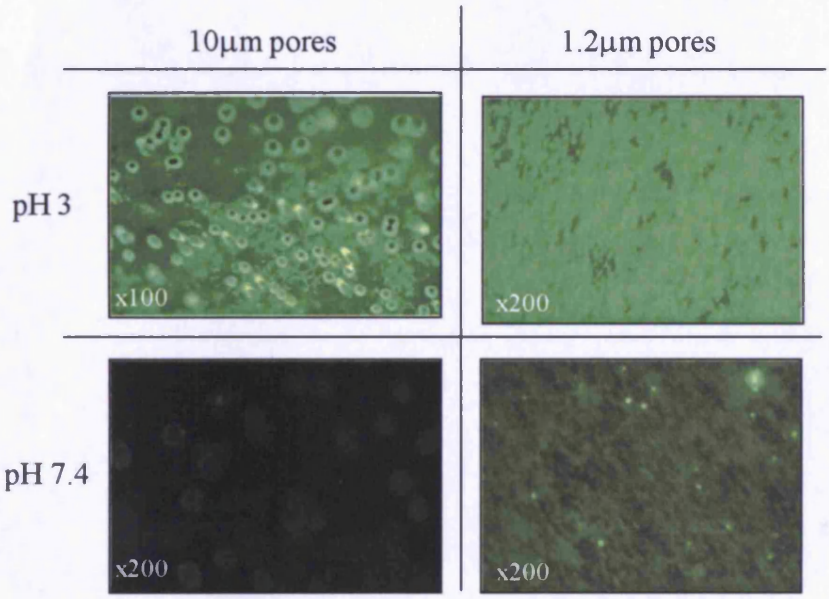


*Figure 3.7.* Fluorescent images of Isopore® membranes isolated from Franz diffusion cells subsequent to diffusion experiments conducted at pH3 and pH7.4. Pore size and pH are indicated within the table structure and magnifications are detailed as inserts.

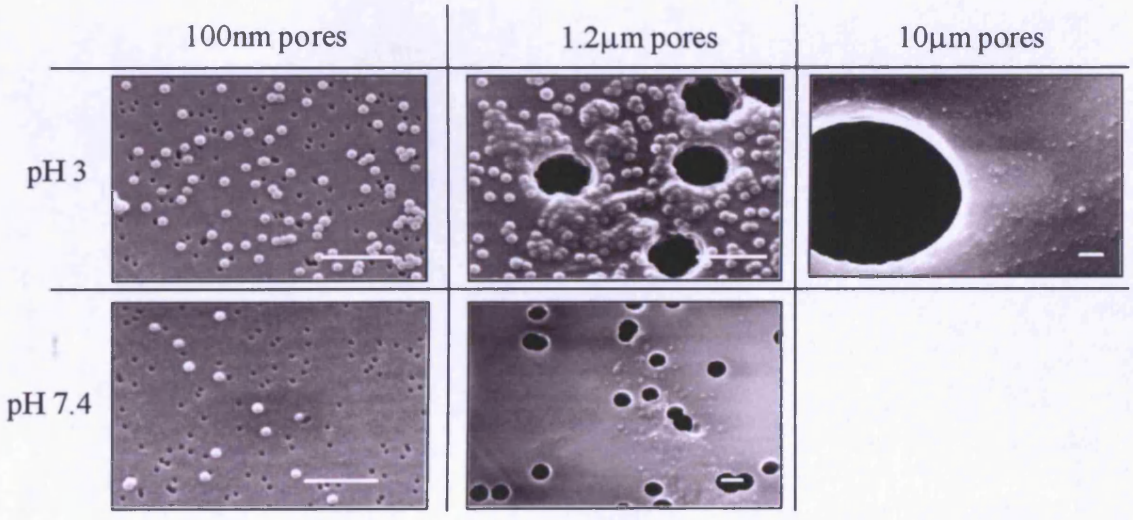


*Figure 3.8.* SEM images of Isopore® membranes isolated from Franz diffusion cells subsequent to diffusion experiments conducted at pH3 and pH7.4. Pore size and pH are indicated within the table structure. Scale bar = 1μm.

### *3.4.2.2. LCN diffusion through Isopore® membranes*

The data obtained for the latex nanosphere formulation suggested that at pH7.4 the positive surface potential of LCNs might retard or even prevent their movement through the pores of the negatively charged Isopore® membrane. However, although diffusion occurred at a slower rate than latex nanospheres, the negative potential of the membrane did not result in retention of the LCN formulation, as was expected (Fig 3.9). Over 12hrs, ~70% of the formulation passed through the 10μm pores and ~50% of the formulation through the 1.2μm conduits (Fig 3.9).

A reduction in the pH of the system from pH7.4 to pH3 appeared to have little effect on the diffusive characteristics of the LCN. This was confirmed by the mass balance calculation conducted at the conclusion of the experiment (Table 3.4).

*Table 3.4.* A summary of the distribution of the LCN within the Franz cell at the conclusion of diffusion experiments. Values are expressed as mean ± sd (N=5).

| LCN | Zeta potential (mV) | Percentage in DONOR phase at 12hrs | | | Percentage in RECEPTOR phase at 12 hrs | | | Calculated membrane BOUND percentage | | |
|---|---|---|---|---|---|---|---|---|---|---|
| | | 100nm | 1.2μm | 10μm | 100nm | 1.2μm | 10μm | 100nm | 1.2μm | 10μm |
| pH ~3 | 76.7 ± 1.5 | 89.7 ± 7.4 | 24.3 ± 11.0 | 12.2 ± 2.6 | 0 ± 0 | 59.9± 2.0 | 79.5 ± 2.9 | 8.3 ± 8.8 | 15.8 ± 10.41 | 8.3 ± 0.8 |
| pH ~7.4 | 49.5 ± 1.0 | 84.0 ± 6.1 | 31.8 ± 9.4 | 14.1 ± 1.5 | 0 ± 0 | 51.8 ± 9.1 | 69.8 ± 8.1 | 13.6 ± 9.5 | 16.4 ± 2.5 | 16.1 ± 7.0 |

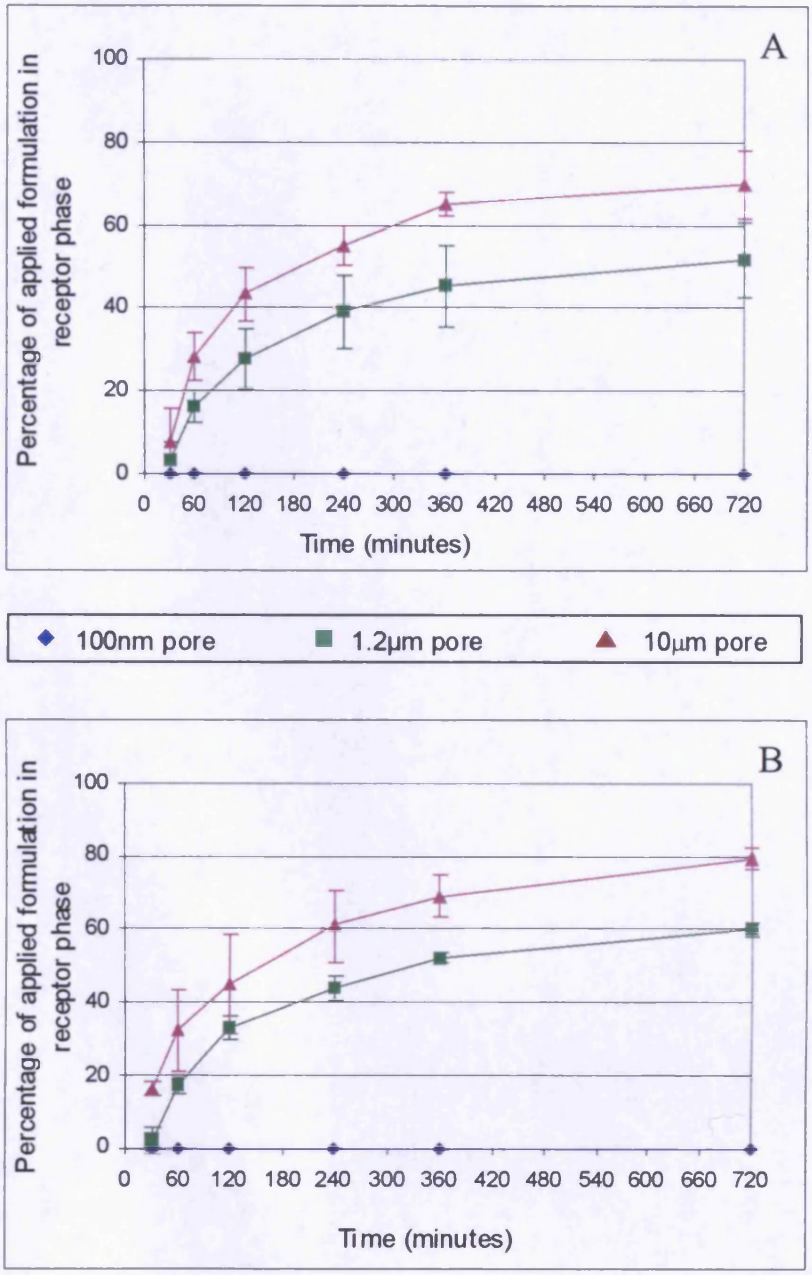


*Figure 3.9.* Diffusion profiles detailing the percentage of the applied LCN formulation detected within the receptor phase of Franz diffusion cells over a period of 12hrs. The LCN formulation and the receptor phase were maintained at pH7.4/pH3 and the Isopore® membranes possessed 100nm, 1.2µm or 10µm pores. A, pH3 mean ± sd (N=5) for 100nm and mean ± sd (N=4) for 1.2 µm and 10µm; B pH7.4, mean ± sd (N=5) for all pore sizes.

lipid suspension. Topical application of the LCN formulation may have there resulted in interaction of excess 'free' cationic lipid with the membrane surface, endowing the surface of the polycarbonate membrane with comparable physicochen characteristics to the LCN. This would negate the opposing surface potentials of membrane and nanoparticle, as observed in experiments with nanospheres at pH3 3.6), and therefore facilitate more reproducible diffusion profiles for the LCN at pH values, as witnessed (Fig 3.9).

### *3.4.2.3. Fluorescent LPD diffusion through Isopore® membranes*

Diffusion of an LPD gene therapy complex through the microchannels of the Isop membrane was assessed by inclusion of a fluorescent lipid within the lipos component of the LPD formulation. The shapes of diffusion profiles at pH7.4 comparable to those achieved with the LCN, with data indicating that ~ 80% and of the applied formulation reached the receptor phases of diffusion cells containing 10μm and 1.2μm Isopore® membranes respectively (Fig 3.10) (Table 3.5). suggested that delivery of an LPD gene complex through microneedle treated containing microchannels with diameters greater than 1μm, was a realistic possibilit

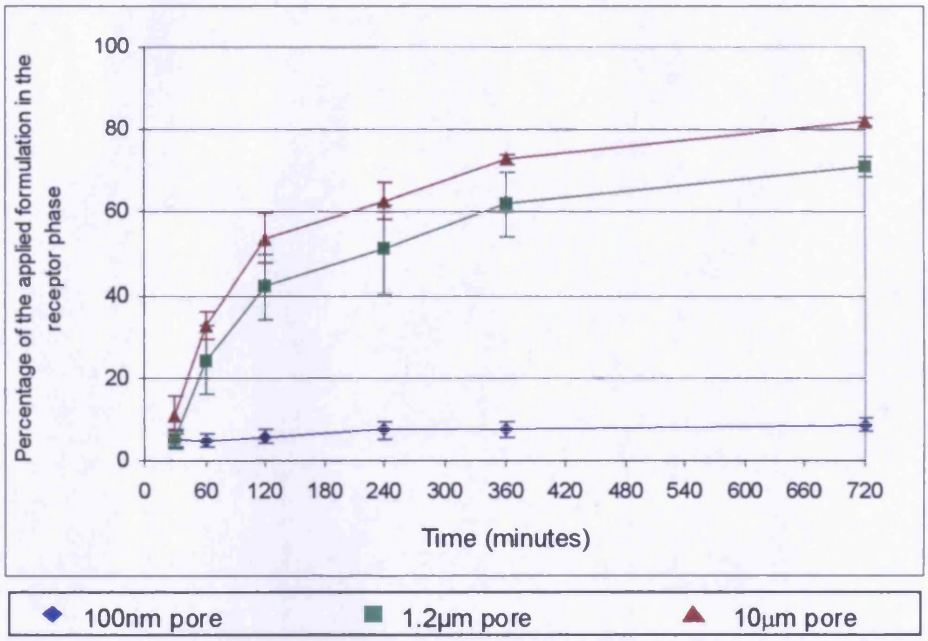


*Figure 3.10.* Diffusion profiles detailing the percentage of the applied nanoparticle formulation detected within the receptor phase of Franz diffusion cells over a period of 12hrs. Isopore® membranes possess three different pore sizes. The diffusion cell was maintained at ~pH7.4. Mean ± sd (N=5) for 100nm and 1.2μm; mean ± sd (N=3) for 10μm.

Data also indicated that ~10% of the formulation diffused through the 100nm pores, which was included as a negative control. There are a number of possible explanations for this:-

1. The mean diameter of the LPD is just below 100nm (Section 3.4.1.2.). Therefore, the smaller complexes within this heterogeneous population may be capable of permeating through the membrane pores.
2. LPD complexes can deform and pass through the membrane pores.
3. Fluorescent lipid remains 'free' within the suspension or within liposomes that are not incorporated within the LPD formulation and are allowed to permeate through 100nm pores.

It is likely that a small proportion of fluorescence signal within the receptor phase of the analysed 1.2μm and 10μm membrane systems was contributed by 'free' fluorescent lipid or liposome within the formulation. The diffusion profiles may therefore be slightly exaggerated and the final receptor concentrations of functional LPDs are likely to be ~5-10% lower than stated.

*Table 3.5.* A summary of the distribution of the fluorescent LPD within the Franz cell at the conclusion of diffusion experiments. Values are expressed as mean ± sd (N=5).

| LPD | Zeta potential | Percentage in DONOR phase at 12hrs | | | Percentage in RECEPTOR phase at 12 hrs | | | Calculated membrane BOUND percentage | | |
|---|---|---|---|---|---|---|---|---|---|---|
| | | 100nm | 1.2μm | 10μm | 100nm | 1.2μm | 10μm | 100nm | 1.2μm | 10μm |
| pH ~7.4 | 33.9±3.2 | 83.9 | 26.5 | 15.2 | 8.8 | 71.2 | 81.9 | 7.3 | 2.4 | 3.0 |

### *3.4.2.4. Summary of Isopore® diffusion studies*

The diffusion of fluorescent nanospheres and the LCNs across Isopore® membranes has highlighted the influence that physicochemical properties may have on the diffusion of a nanoparticle complex through microchannels, forged in the skin epidermis by a microneedle device. The diffusion characteristics of fluorescent nanospheres in particular have exemplified this. A reduction in pH reversed the zeta potential of the nanoparticle, encouraged electrostatic interaction with the membrane surface and resulted in impeded permeation. However the presence of the cationic lipid within the LCN and LPD formulations reduced the simplicity of the model system and therefore obscured evaluation of the influence of physicochemical properties upon permeation through the membrane.

### 3.4.3. Heat separated human epidermal membrane diffusion studies

#### *3.4.3.1. Propranolol diffusion through human epidermal membrane*

Demonstrating the ability of a silicon microneedle device to penetrate the outermost layers of human skin (Section 2.4) does not confirm its ability to enhance the permeation of compounds/particles across the skin barrier. Therefore, although it is instinctive to assume that microchannels fashioned by the device will promote permeation of therapeutics across the SC, it was important to prove the microneedles delivery capabilities. Propranolol is an easily analysed therapeutic molecule that has been the subject of a number of transdermal permeation studies (Modamio et al., 2000, Rama Rao et al., 2003, Stott et al., 2001) and therefore was selected as a model, small drug molecule to be delivered across microneedle treated human epidermal membrane.

As might be expected the permeation of topically applied propranolol hydrochloride through untreated human epidermal membrane was low, with less than 2% of the applied formulation detected in the receptor phase after 24hrs (Fig 3.11). However, permeation of the compound through microneedle treated epidermal membranes was enhanced significantly. More than 15% of the applied formulation was detected in the receptor phase after 24hrs (Fig 3.11). However, the associated standard deviations suggested that there was a noteworthy level of variation between diffusion cells. This may be attributed to variability in the penetration efficiency of the pointed tipped wet-etch microneedle array (Section 2.4.3.3).

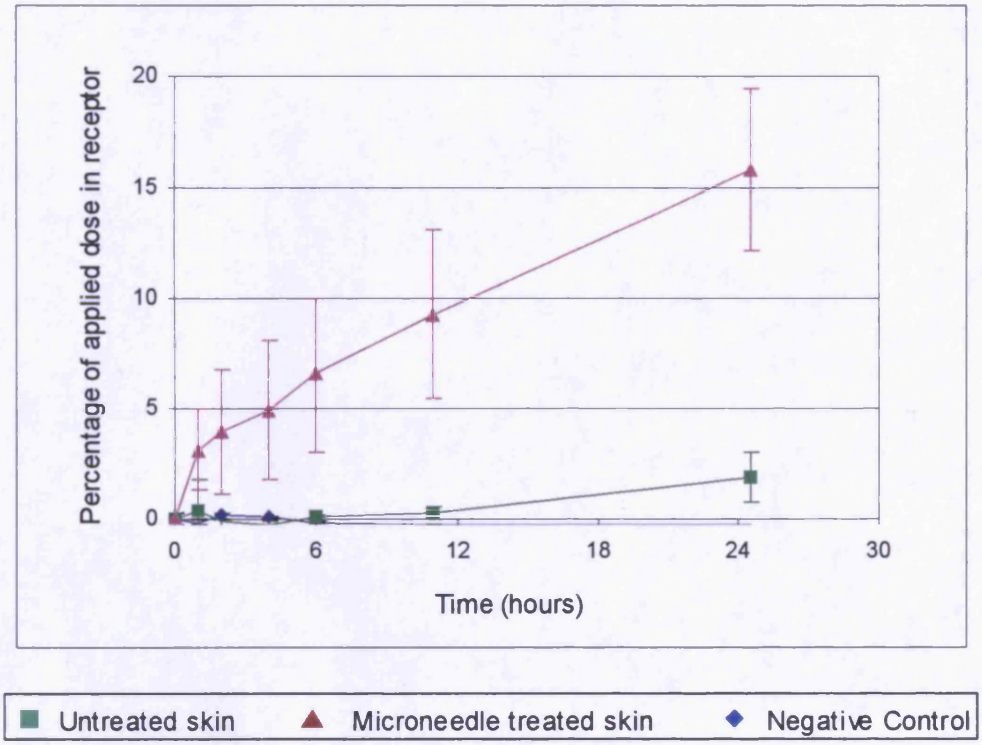


*Figure 3.11.* Diffusion profiles detailing the percentage of the applied propranolol hydrochloride dose detected within the receptor phase of Franz diffusion cells. Diffusion of propranolol hydrochloride through untreated and wet-etch microneedle treated (TNI-Array 5) membranes was compared. Mean ± sd (N=4) for untreated an microneedle treated membranes; mean ± sd (N=2) for the negative control.

### *3.4.3.2. Nanosphere diffusion through human epidermal membrane*

The successful diffusion of fluorescent nanoparticles across the 10μm pores of an Isopore® membrane and the proven ability of a microneedle device to promote permeation of propranolol hydrochloride across the human epidermal membrane was encouraging. The passage of fluorescent nanospheres across microneedle treated, untreated and hypodermic needle treated human epidermal membranes was therefore analysed (Fig 3.12).

Fessi and co-workers (Alvarez-Roman et al., 2004), this indicated that the epider barrier is essentially resistant to the passive diffusion of negatively char nanoparticles.

Penetration of the epidermal membrane by a hypodermic needle permitted permea of nanospheres through the skin, ~10% of the formulation reaching the receptor phas just 3hrs (Fig 3.12). However, fluorescence levels in the receptor phase gradu declined to a detectable level of ~6% of the applied formulation over the timecours the experiment.

Most significantly, results confirmed the ability of frustum tipped microneedles facilitate nanoparticle delivery, with more than 20% of the applied nanospl formulation traversing the epidermal barrier over the 6hr period. In agreement v hypodermic needle penetration, the detectable receptor phase levels were subseque halved over the next 18hrs. Only approximately 10% of the applied formulation therefore detected within the receptor phase at the 24hr time point.

This phenomenon was consistent with the diffusion profile obtained using fluoresc nanosphere predictive studies at pH3 (Fig 3.6), where electrostatic interaction of nanosphere formulation with the synthetic membrane resulted in blockage of the po a halt in permeation and the subsequent reduction in receptor phase levels nanoparticle interaction with the underside of the membrane. The skin, as a biolog tissue, is much more complex and therefore it is more difficult to rationalise the c with such confidence. However it is not unreasonable to account for the reduction diffusion and the decrease in receptor concentration seen in hypodermic microneedle studies to such physicochemical factors.

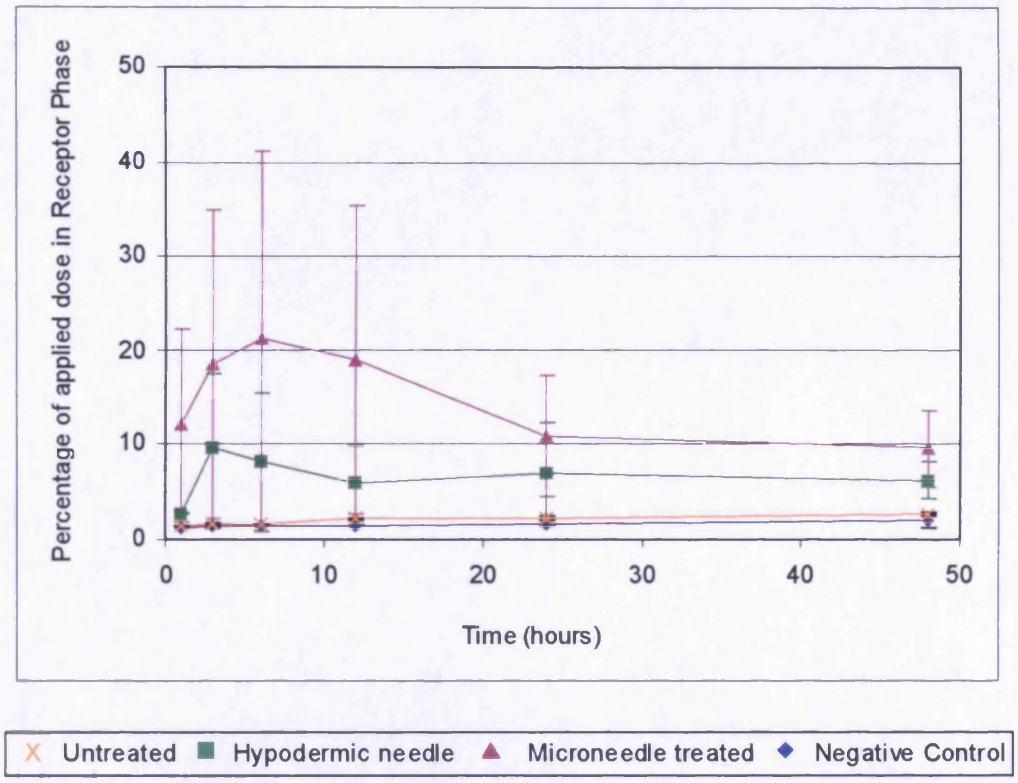


*Figure 3.12.* Diffusion profiles detailing the percentage of the applied nanosphere formulation detected within the receptor phase of Franz diffusion cells over a period of 48hrs. Mean ± sd (N=2) for untreated and needle treated membranes; mean ± sd (N=4) for microneedle treated (TNI-Array 8) and negative control membranes.

Another significant feature of the data was the large standard deviations associated with microneedle treated membranes. Biological variability and the poor reproducibility of microneedle penetration, which SEM images reveal may be even more significant for the frustum tipped microneedles (Section 2.4.4.3), were likely to be major contributory factors. However, the unusual diffusion profile and the significant variability prompted SEM analysis of the epidermal membranes used in this investigation.

Low magnification images of the untreated epidermal membrane confirmed the integrity of the membrane (Fig 3.13A). Upon closer inspection, it became apparent that the SC was coated in the fluorescent nanosphere formulation, individual nanospheres adhering to corneocytes on the skin surface and collecting within the dermatoglyphics

(Fig 3.13B). The identification of discrete nanoparticles on the skin surface indicated that the formulation retained its colloidal stability in the diffusion cells, in a manner synonymous with that visualised in the predictive Isopore® diffusion studies (Section 3.4.2.1).

The epidermal membrane, treated with the hypodermic needle, possessed a number of uniform circular microchannels, 50-100μm in diameter, which were likely to have facilitated the passage of nanoparticles through the membrane during diffusion experiments (Fig 3.13C & 3.13D). Microneedle treated membranes contained micro-disruptions of comparable diameter to those created by the hypodermic needle (Fig 3.14A & 3.13D). However there was a greater population of micro-disruptions, thus explaining the increase in the observed nanoparticle permeation (Fig 3.12).

Microchannels created by the frustum tipped microneedle arrays were visualised as both simple circular conduits (Fig 3.14D) and less symmetrical disruptions associated with lateral tears in the membrane (Fig 3.14A). Closer inspection of the skin surface revealed the layered structure of corneocytes surrounding microchannels and the obvious disruption of SC integrity (Fig 3.14B, 3.14C, 3.14E & 3.14F). More interestingly however was the appearance of adsorbed nanospheres between the disrupted corneocytes and the presence of nanoparticle aggregates on the interior surface of the microchannels (Fig 3.14B, 3.14C, 3.14E & 3.14F). Nanoparticle aggregates appear to have accumulated in the 10μm disruption, proximal to the microchannel (Fig 3.14B). Aggregation may have been caused by factors induced by microneedle damage to the tissue e.g. the release of biological components from the tissue or a change in pH. Disruption of the SC, exposure of the underlying epidermal cells and the release of cellular components from the damaged cells may therefore be responsible for a reduction in colloidal formulation stability and the blockage of microchannels by aggregates.

Although permeation halted (Fig 3.12), possibly due to destabilisation of the colloidal suspension within the biological environment and/or adherence to the tissue surface, the creation of microconduits across the epidermal barrier by the device has nonetheless facilitated permeation of charged nanoparticles.

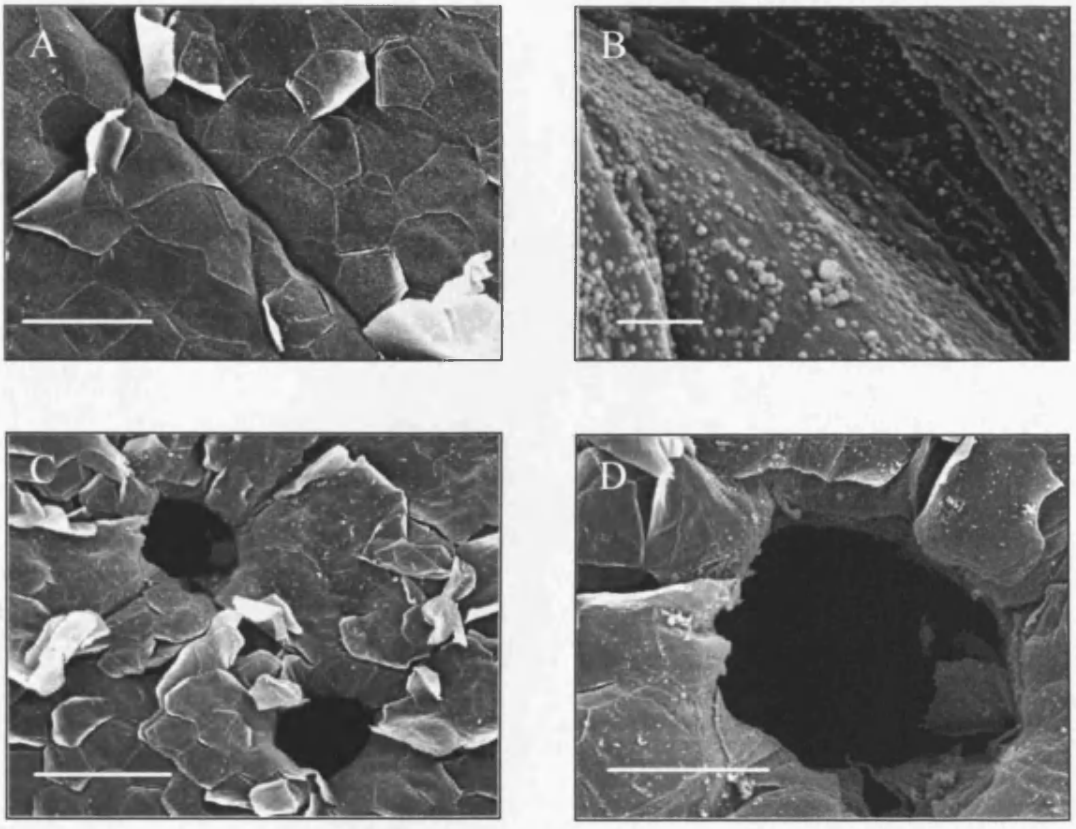


*Figure 3.13.* Scanning electron micrographs of epidermal membranes used in diffusion experiments (Section 3.4.3.2). Untreated epidermal membranes (A, B) and those treated with a hypodermic needle (C, D) following topical nanosphere application are pictured. A, D scale bar = 50µm; B scale bar = 2µm; C scale bar = 100µm.

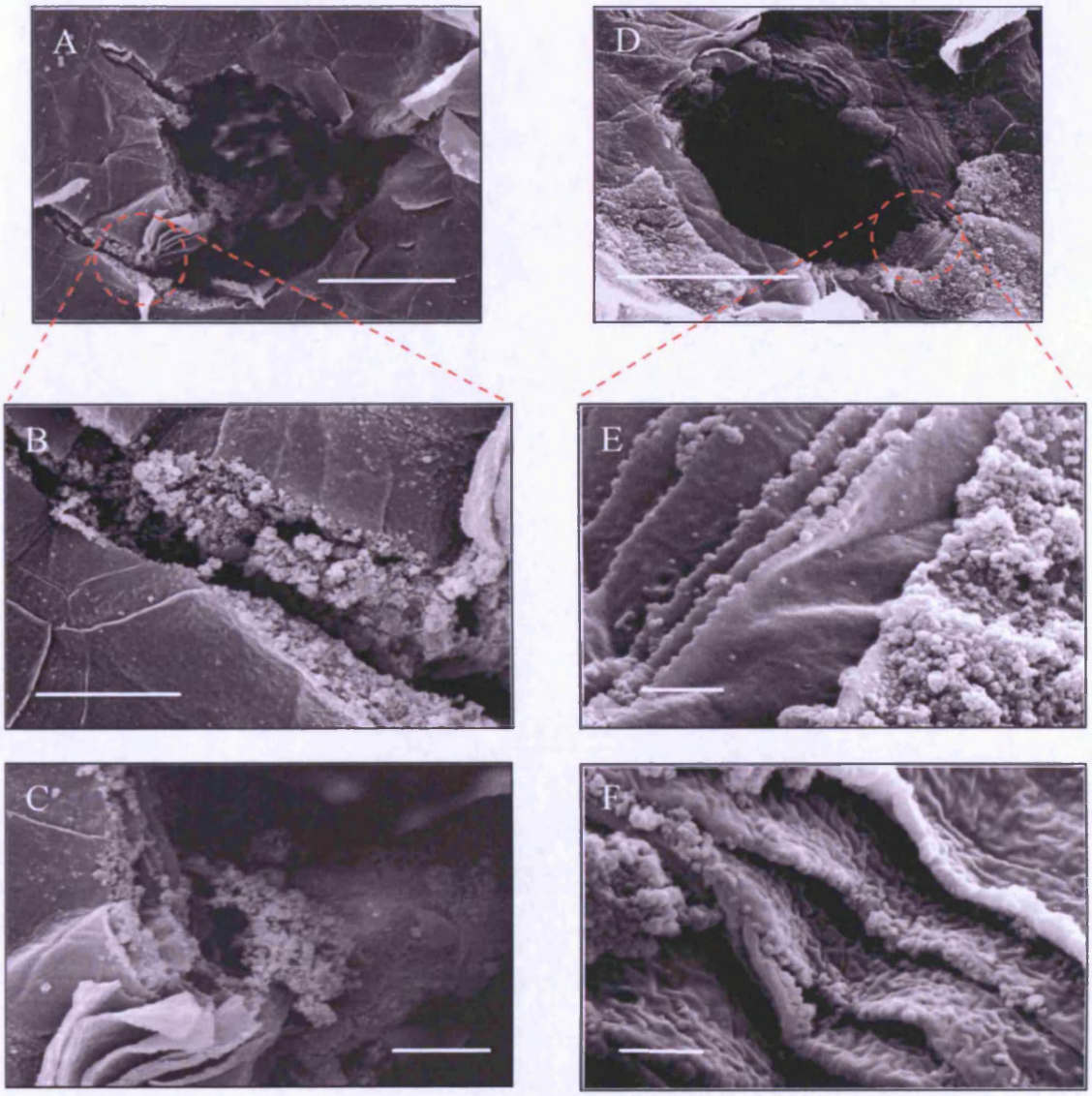


*Figure 3.14.* Scanning electron micrographs of epidermal membranes used in diffusion experiments (Section 3.4.3.2). A fluorescent nanosphere formulation was applied topically to epidermal membranes which were subsequently treated with a frustum tipped wet-etch microneedle device (TNI-Array 5). A, D scale bar = 50µm; B, C, scale bar = 10µm; E, F, scale bar = 2µm.

## 3.5. CONCLUSIONS

Investigations using Isopore® membranes and three model nanoparticle formulations suggest that charged colloidal gene complexes can potentially be delivered through uniform microneedle fashioned microconduits. However, the cutaneous delivery of a colloidal formulation will not be dependent simply upon the creation of conduits within the skin that have a greater diameter than the nanoparticles. Predictive investigations illustrated the importance that formulation parameters including particle size, formulation pH and zeta potential may have on microneedle mediated delivery across the SC.

The microneedle enhanced delivery of propranolol hydrochloride across the epidermal barrier demonstrated the ability of the device to promote transdermal delivery of small drug molecules. Nanoparticle permeation across microneedle treated human epidermal membrane proved to be less uniform and more unpredictable. However, these studies encourage continued investigation of the microneedle device as a novel drug delivery platform for cutaneous delivery of colloidal formulations.

However to facilitate cutaneous gene expression, i.e. expression of an exogenous nucleic acid formulation within the viable epidermis, a gene therapy formulation only needs to be delivered across the SC barrier. The subsequent chapter therefore evaluates the ability of microneedles to deliver and retain nanoparticles within the viable epidermis of full thickness human skin and examines methods by which reporter gene activity within the tissue may be detected.

# CHAPTER 4

# Assessment of functionality of reporter plasmids, microneedle devices and *ex vivo* human skin for cutaneous transfection studies

## 4.1. INTRODUCTION

The principle aim of these studies was to facilitate cutaneous delivery and subsequent expression, of an exogenous pDNA formulation using a microneedle device. To assess the microneedle-mediated delivery of a non-viral gene complex to the epidermal layer of human skin and the subsequent transfection of viable cells therein it was therefore essential to, (i) demonstrate effective delivery of a nanoparticle formulation to the viable epidermis using a microneedle device, (ii) develop a method of organ culture that can maintain the viability of cells within excised human skin and (iii) develop a robust methodology that can detect reporter gene expression within skin. These issues were approached in turn and have been addressed within this chapter.

### 4.1.1. Reporter pDNA

pDNA, isolated from bacteria, has been manipulated by recombinant DNA technology to create genetic sequences that can be propagated in a transformed bacterial host (most commonly *E.coli*), isolated and then purified. Plasmid constructs are well-characterised vectors that are used to introduce exogenous transgenes into a target mammalian cell and promote their subsequent expression (Uherek and Wels, 2000).

Plasmids therefore possess a number of common constituents within their genetic sequence:-

1. An antibiotic selection site – an antibiotic resistance gene, e.g. ampicillin, permits selection of those bacteria containing the plasmid.
2. A prokaryotic origin of replication – For generation of multiple copies of the plasmid following the transformation of bacterial cells.
3. A promoter sequence – provides recognition sites for the RNA polymerase enzyme and therefore has an important role in transcription.
4. A multicloning site – A site into which a therapeutic transgene is inserted.

Plasmids exist as extrachromosomal closed circular loops of DNA, distinct from the bacterial/mammalian genome (episomal). Once the pDNA has been delivered into the target cell and has entered the nucleus, it utilises the cellular machinery to translate the nucleic acid sequence into an encoded protein. Functional plasmids typically possess 5-

10,000 base pairs, have a zeta potential of -30 to -100mV and a hydrodynamic diameter of approximately 100nm (Piskin et al., 2004).

To develop novel gene delivery methods it is fundamental to distinguish expression of an exogenous genetic sequence from the continued transcription and translation of endogenous genes. Reporter sequences encode for proteins that possess a detectable phenotype, which can provide qualitative and/or quantitative measures of transfection efficiency. Ideally, reporter genes are not endogenous to the cell under investigation and their product can be detected at low concentrations in a rapid, simple and reproducible manner. pCMVβ, pEGFP-N1 and pGL3 reporter plasmids were evaluated for future cutaneous gene delivery experiments (Chapter 5).

pCMVβ

This reporter plasmid, propagated in *E. coli*, contains the bacterial *lacZ* transgene, which encodes for the bacterial β-galactosidase enzyme (MacGregor and Caskey, 1989). β-galactosidase activity can be detected *in situ* by histochemical techniques that rely on the oxidation of a substituted indoyl galactosidase, within the presence of a ferriferrocyanide catalyst, to a visible reaction product. The most popular substrate, 4-bromo-5-chloro-3-indoyl-β-D-galactopyrosanide (X-gal), is converted by the enzyme to a blue reaction which can be identified within a tissue by light microscopy.

pEGFP-N1

The pEGFP-N1 reporter plasmid encodes for a protein which, upon optimal excitation at 488nm, emits a detectable fluorescent green signal. This reporter system is widely utilised in gene therapy studies as it does not require a substrate to stimulate detection and therefore is simple to analyse (van Roessel and Brand, 2002). The green fluorescent protein (GFP) can be detected *in situ* within living cells by illumination under a blue excitation filter on a fluorescence microscope or quantified within a monodisperse cell suspension using flow cytometry.

pGL3

The pGL3 plasmid contains a reporter sequence encoding for the bioluminescent firefly luciferase (*Photinus Pyralis*) enzyme (Wet et al., 1985). In the presence of adenosine triphosphate (ATP) and oxygen co-substrates luciferase oxidises beetle luciferin substrate, causing a resultant emission of light (550-570nm). The light expressed by this reaction remains constant for a short period of time and its intensity can therefore be measured using a luminometer. The intensity of light that is produced is proportional to the concentration of the enzyme and hence the reporter system can provide a quantitative measure of transfection (Fortunati et al., 1996, Liu et al., 1997, Manthorpe et al., 1993, Mikszta et al., 2002).

### 4.1.2. Skin Models

Limited and unpredictable availability of human skin for experimental studies is a limitation within the field of transdermal delivery that has resulted in the continued assessment of suitable animal models (Panchagnula et al., 1997). Porcine ear skin is considered to be a representative model of the human skin structure and is frequently used in predictive permeation studies (Dick and Scott, 1992, Sekkat, 2002, Wester and Noonan, 1980). Porcine skin has also been utilised successfully in localised gene expression studies (Babiuk et al., 2003, Hengge et al., 1995, Hengge et al., 1998, Hengge et al., 1996). Murine models provide useful tools for the study of genodermatoses (Arin and Roop, 2004, Jiang and Uitto, 2005).

However differences in architecture and biology between human and animal skin are well recognised (Panchagnula et al., 1997). Therefore for experiments to produce data that is truly predictive of the *in vivo* environment investigations should preferably be conducted in human tissue. Excised human skin was therefore selected to investigate microneedle facilitated cutaneous gene delivery. To date cutaneous transfection studies using human skin, either in organ culture (Hengge et al., 1996) or grafted onto rodents (Sawamura et al., 1999), has been limited. The development of a functional *ex vivo* human skin model to assess localised delivery and expression of exogenously applied nucleic acid formulations was therefore considered imperative to the validity of the results achieved.

The availability of human skin for experimental studies has relied upon collaboration with clinicians both at the Royal Gwent Hospital, Newport and Llandough Hospital, Cardiff and the Vale NHS trust. Skin tissue was obtained, with informed patient consent and NHS Trust and local ethical committee approval, from breast reduction and mastectomy procedures. The expression of exogenous genes within excised skin relies upon epidermal cells maintaining functional cellular machinery that can process the nucleic acid, i.e. the cells must be 'living', and therefore immediate availability of human skin, following removal from the donor, was crucial to the planned experiments.

### 4.1.3. 'Viable' *ex vivo* human skin

Following removal of the tissue from the donor autolysis begins immediately (Tomita et al., 2004), with keratinocytes ultimately dying due to accumulation of toxic metabolites and a lack of nutrition (Sterne et al., 2000). Deterioration in tissue specimens may be caused by:-

1. Physical trauma – during excision of the skin.
2. Nutrition and perfusion deprivation.
3. Hypoxia.
4. Loss of biochemical and neural stimulation.
5. Desiccation.
6. Infection, particularly if the skin is stored in nutrient media (Cetin et al., 2000).

The successful 'uptake' of human skin allografts for reconstructive surgery, burns and wound treatment is directly linked to the skin viability prior to grafting (Bravo et al., 2000). The conditions used to maintain the viability of *ex vivo* human skin for grafting procedures was therefore considered.

A universal method to promote tissue viability during the transport and storage of human skin grafts remains uncertain, with skin banks in different countries using different protocols. Storage protocols for 'fresh' skin (fresh skin being tissue used following removal from the donor without freezing) prior to grafting range from, a 3 to 15 day accepted storage period, at 4°C (Castagnoli et al., 2003, Cetin et al., 2000, Sterne et al., 2000) or 37°C (Bravo et al., 2000), in saline (Bravo et al., 2000, Cetin et al., 2000,

Sterne et al., 2000) or nutrient medium (Ben-Bassat et al., 2001, Castagnoli et al., 2003) and in a flattened or rolled state (Sterne et al., 2000).

The viability of human skin can be examined using a number of methods (Messager et al., 2003) including histological analysis (Castagnoli et al., 2003, Sterne et al., 2000), trypan blue exclusion (Cetin et al., 2000), the tetrazolium reduction/MTT [3-(4,5-dimethylthiazol-2-yl)-2,5-diphenyltetrazolium bromide] assay (Cetin et al., 2000), oxygen consumption assay (Bravo et al., 2000, Zieger et al., 1993), lactate dehydrogenase activity (Halprin and Ohkawara, 1966) and pH changes (Issachar et al., 1997). However, it is important to consider the functionality of the assay when interpreting viability data. Viability assays may indicate if the cellular membrane of keratinocytes remains intact, if intracellular enzymes remain functional or if respiratory capability is maintained. However, they do not indicate the 'true' viability of the cell i.e. can the cell transcribe and translate a DNA sequence, synthesise the encoded peptide and finally create the functional protein? The expression of a pDNA formulation within the epidermis of excised human skin necessitates such levels of viability. Detectable expression of a reporter plasmid in human tissue following intradermal administration was therefore considered to be a more appropriate marker of tissue viability than the more 'traditional' viability assays (Section 5.4.1).

### 4.1.4. Human skin organ culture models

Organ culture of skin involves removal of the tissue from the donor, transport to the laboratory, normally within media maintained at 4°C (Backvall et al., 2002, Kent et al., 2001, Reece et al., 1998), and rapid incubation of the tissue within defined experimental conditions that can maintain the viability of the tissue, *ex vivo* (Varani, 1998).

Although some studies indicate that skin can be maintained by submersion in nutrient media (Kivinen et al., 2003, Ma et al., 2003), the majority of organ culture protocols incubate the tissue at the air-liquid interface, i.e. the dermis is bathed in nutrient media and the epidermis remains in contact with the air (Companjen et al., 2001, Moll, 2003, Moll et al., 1998, Rijnkels et al., 2001). The Trowell-type organ culture (Trowell, 1954, Trowell, 1959) is a well established method where skin is maintained on steel grids that are covered by lens tissue paper (Companjen et al., 2001, Larregina et al., 2001, Tammi

and Maibach, 1987). The important features of this experimental set-up are the dimensions/condition of skin biopsies, the constituents of the nutrient media and the incubation conditions:-

1.Skin biopsies – Split-thickness skin, i.e. skin from which a considerable portion of the dermis has been removed either by a dermatome (Ben-Bassat et al., 2001, Bravo et al., 2000, Sterne et al., 2000) or skin graft knife (Backvall et al., 2002, Kent et al., 2001), is prepared prior to organ culture to ensure that nutrient media can permeate to the epidermal cells that overly the dermis. Skin biopsies with 2-3mm$^2$ surface areas are considered optimal to prevent necrosis of the central portion of the tissue (Backvall et al., 2002, Moll, 2003, Moll et al., 1998, Varani, 1998), although biopsies up to 1-2cm$^2$ have been successfully cultured (Hengge et al., 1996, Reece et al., 1998).

2.Nutrient media – A range of basal nutrient media containing various supplements have been utilised in the organ culture of skin tissue, with the optimal media yet to be determined. However, a review by Varani (Varani, 1998) highlights the importance of a high level of calcium ions in the media (>1mM) to ensure fibroblast viability. It is the fibroblasts, located within the dermal tissue, that are thought to preserve the tissue structure. The basal media (DMEM 25mM HEPES) selected for these studies possessed a calcium chloride concentration of 1.8mM and has been successfully employed in other skin organ culture methodologies (Backvall et al., 2002, Ma et al., 2003, Moll et al., 1998, Rijnkels et al., 2001) used to maintain the viability of human skin.

3.Incubation – The tissue is routinely incubated at 37°C and 5% $CO_2$ and the media is changed every 24-72 hrs (Kivinen et al., 2003, Ma et al., 2003, Moll, 2003, Moll et al., 1998, Rijnkels et al., 2001, Varani, 1998). Under these conditions, human skin has been shown to maintain its morphology and the ability to synthesise DNA for up to 7 days (Gaylarde et al., 1975, Tammi et al., 1979).

The organ culture methodology developed to maintain the viability of excised human skin in these studies was based upon investigations examining cutaneous gene expression *ex vivo* (Hengge et al., 1996, Kent et al., 2001, Larregina et al., 2001).

### 4.1.5. Techniques

#### *4.1.5.1. Mammalian cell culture*

The *in vitro* propagation of monolayers of immortalised mammalian cells within cell nutrient media provides a model of the cellular environment that is used routinely in gene therapy studies to screen vector formulations and nucleic acid therapeutics.

Cultured cells are grown in a monolayer on the surface of a plastic cell culture flask until they approach approximately 90% confluency. At this time point a proteolytic enzyme is used to gently remove the cells from the flask surface, thus creating a monodisperse suspension that can be divided over a greater surface area. This ensures that cells are supplemented with sufficient growth media and are maintained predominantly within the growth phase of their cell cycle. Repeated 'splitting' of cells in this manner is referred to as passaging.

To study the functionality of reporter plasmids in mammalian cell lines a vector formulation, such as the LPD (Section 1.3.2), is often used to promote cell uptake. Cell transfection typically involves removal of nutrient media from a sub-confluent (i.e. when cells are within the growth phase of the cell cycle) cell monolayer and topical treatment of the cells with the vector formulation. Successfully transfected cells are then identified by detection of the encoded reporter protein.

In these studies an immortalised human lung epithelial carcinoma cell line, A-549 and an immortalised human keratinocyte cell line, HaCaT have been utilised to assess the functionality of reporter pDNA systems. A-549 cells are a well characterised mammalian cell line that displays the morphological and biochemical features of pulmonary type II cells. These have been used routinely within our laboratory (Birchall et al., 2000) and were therefore selected to illustrate the functionality of an LPD

formulation and the pDNA contained therein. The HaCaT keratinocyte cell line provided a more representative model of those target cells located within human skin.

#### *4.1.5.2. Flow Cytometry*

This technique determines both the light scattering and fluorescent parameters of a particle suspension and can therefore be used to assess the fluorescent properties of a cell population treated with formulations containing pEGFP-N1. Moreover this offers a quantitative measure of transfection efficiency, the percentage of fluorescent cells resulting from expression of the plasmid distinguishable from the remainder of the cell population. A monodisperse cell suspension is irradiated with a laser set to the excitation of the specified fluorophore. This generates a fluorescent emission that is collected by photo-detectors and converted into an electrical signal. Scattering of light by the colloidal suspension is also detected and is converted into a signal that relates to the finite number of cells present in the sample. This information is then converted into analysable data inferring the mean fluorescence of each cell and the proportion of cells within the analysed population that display fluorescent properties.

#### *4.1.5.3. Bioluminescence*

In a manner similar to fluorescence (Section 3.1.4.3), bioluminescence is associated with the emission of photons due to the transition of electrons from high to low excitation states. However the chemical reaction that induces the excitation state in bioluminescent samples occurs much more slowly and therefore it is the initial reaction upon addition of the enzyme substrate, the 'flash', which is measured by a luminometer. Luminometers detect emitted photons and process the signal to a quantitative measurement. The pGL3 plasmid, which encodes for the firefly luciferase enzyme, can therefore be used to determine the efficiency of cellular transfection by analysis of homogenates using a luciferase assay system and a luminometer.

## 4.2. AIMS AND OBJECTIVES

### Chapter Aims

Studies aim to confirm the functionality of the LPD non-viral vector formulation and the intraepidermal delivery capabilities of microneedle devices. The techniques required to detect expression of reporter plasmids in human skin were also considered.

### Chapter Objectives

- To isolate, purify, quantify and demonstrate the integrity of supercoiled reporter plasmids, propagated in transformed *E.coli.*

- To assess the functionality of pCMVβ, pEGFP-N1 and pGL3 by detection of the expressed protein, following treatment of mammalian cells with the LPD non-viral vector.

- To develop an organ culture methodology to maintain the viability of human skin *ex vivo.*

- To facilitate cutaneous delivery of a nanoparticle formulation to the viable epidermis of *ex vivo* human skin, using a microneedle device.

- To determine the ability of a microneedle array to facilitate cutaneous delivery of a functional biological macromolecule to the viable epidermis within *ex vivo* human skin.

- To establish a robust methodology for the detection of the bacterial β-galactosidase enzyme within *ex vivo* human skin.

## 4.3. MATERIALS AND METHODS

### 4.3.1. Materials

All reagents were obtained from Fisher (Loughborough, UK) and were of analytical grade, unless otherwise stated.

The 7.2 kb pCMVβ plasmid construct containing the *lacZ* reporter gene, the 4.7kb pEGFP-N1 plasmid expressing the green fluorescent protein (GFP) reporter gene and the 5.3Kb pGL3 plasmid were obtained from Promega® Corporation (Madison, WI). Quantilum recombinant luciferase enzyme, the luciferase assay system, DH5α *E.coli* and the recombinant β-galactosidase enzyme were obtained from the Promega® Corporation (Madison, WI). The Qiagen® Plasmid 2500 Mega Kit was obtained from Qiagen® (Crawley, UK).

1,2-Dioleoyl-3-triammonium-tropane (DOTAP) was purchased as the methyl sulphate salt from Avanti Polar Lipids (Alabaster, AL, USA).

Protamine sulphate, BSA, bichichonic acid (BCA), fluorescent yellow/green polystyrene nanospheres (L-1280), fluorescent red polystyrene nanospheres (L-9279), phosphatidylethanolamine dipalmitoyl-sulforhodamine B , chloroform, Greiner® 96-well polypropylene plates, the bright-line haemocytometer and components of the X-gal staining solutions were obtained from Sigma-Aldrich Chemical Company (Poole, UK).

Cell culture plastics were obtained from Corning-Costar (High Wycombe, UK). MEM (EAGLES) 25mM HEPES, Dulbecco's Modified Eagle's Medium (DMEM 25mM HEPES), foetal bovine serum and penicillin-streptomycin solution were obtained from Invitrogen Corporation (Paisley, UK). All histology materials, including OCT embedding media, Histobond® adhesive microscope slide were obtained from RA Lamb Limited (Eastbourne, UK) or in the case of toluidine blue, Harris' haematoxylin, Gurrs' eosin aqueous solution 1%, Histomount® and xylene (low sulphur) from Lab 3 (Bristol, UK).

Equipment:-

Fluostar Optima Plate Reader (BMG Labtech, Aylesbury, UK)
Eppendorf Biophotometer (Eppendorf, Cambridge, UK)
FACScalibur System (Beckton Dickinson, California, UK)
Extrusion apparatus (Northern lipids, Vancouver, Canada)
Philips XL-20 Scanning Electron Microscope (Philips, Eindhoven, Netherlands)
Philips 208 Transmission Electron Microscope (Philips, Eindhoven, Netherlands)
Gold sputter coater (EM Scope, Kent, UK)
Bal-Tec CPD030 Critical Pont Drier (Balzers, Lichenstein)
Olympus IX-50585 Inverted Microscope System (Olympus Optical, London, UK)
Olympus BX-50 Microscope System (Olympus Optical, London, UK)
Olympus DP10 Microscope Digital camera system (Olympus Optical, London, UK)
Olympus U-RF-L-T Power Supply Unit (Olympus Optical, London, UK)
Anthos Labtec HT2 96 well plate reader (Anthos, Salzburg, Austria)
Avanti J-20XP centrifuge (Beckmann Coulter, Miami, USA)
Sanyo Orbital incubator (Sanyo, Loughborough, UK)
Ultra-violet (UV) transilluminator (BioRad GelDoc, Hercules, CA).
Leica CM305S cryomicrotome (Leica Microsystems Limited, Milton Keynes, UK)
Schott KLI500 fibre optic light source (Schott UK Limited, Stafford, UK)
Stemi 2000-C stereomicroscope (Zeiss, Welwyn Garden City, UK)
Olympus Camedia C-4040 Zoom Digital Camera (Olympus Optical, London, UK)

### 4.3.2. Plasmid preparation

#### *4.3.2.1. Creating competent DH5α E.coli*

An aliquot of *E.coli* was thawed on ice and streaked onto a Luria agar plate which was subsequently incubated for 24hrs at 37°C. A single colony of bacteria was then selected and cultured overnight in 10ml of Luria broth, maintained at 37°C. 100ml of fresh Luria broth was then inoculated with 5ml of this *E.coli* culture which was incubated at 37°C for 2.5hrs and agitated at 800r.p.m. The culture was then divided between two sterile centrifuge tubes and centrifuged at 3000r.p.m. for 5mins. The supernatants were subsequently discarded and 12.5ml of ice cold calcium chloride (0.1M) was used to gently resuspend the bacterial pellets. The suspensions were maintained on ice for a total of 2mins before centrifugation at 3000r.p.m. for 10mins. The supernatants were discarded and the bacteria resuspended in 5ml of ice cold calcium chloride. These suspensions were maintained on ice for a total of 2.5hrs before the addition of 5ml of glycerol (40%v/v in deionised water) to each suspension.

#### *4.3.2.2. Transformation of DH5α E.coli*

Transformation, the introduction of pDNA into a population of competent *E.coli* organisms, was used to create stocks of bacteria that could propagate exogenous plasmids. This process relies upon antibiotic resistance genes, contained within the plasmid structure, to selectively isolate and/or propagate transformed bacteria. For pEGFP-N1 the selective antibiotic is kanamycin and for pCMVβ and pGL3 the selective antibiotic is ampicillin. This resistance gene is essential for the selection of successfully transformed bacteria.

Briefly, 200μl of competent cells (removed from storage at -86°C and thawed on ice) were transferred to a sterile 15ml centrifuge tube within sterile conditions (under a Bunsen flame). To this, 1μl of a 10ng/ml solution of the pDNA was added. The suspension was incubated on ice for 30mins and subsequently immersed within a water bath (maintained at 42°C) before replacement in the ice for a further 2mins. Luria broth (3ml) was then added to the bacterial suspension which was incubated for 45mins in a shaking water bath at 37°C. A selective agar plate, containing either ampicillin

(pCMVβ, pGL3) or kanamycin (pEGFP-N1) at a concentration of 100μg/ml was then inoculated with 150μl of the bacterial suspension, which was spread over the plate and allowed to dry underneath a Bunsen flame for 30mins. The inoculated plate was finally incubated at 37°C for 20hrs.

A single colony of transformed bacteria was selected from the agar plate using a sterile loop and subsequently cultured in 10ml of antibiotic selective (ampicillin or kanamycin 100μg/ml) Luria broth for a further 20hrs at 37°C. Aliquots (0.5ml) of the overnight culture were then placed in a sterile microcentrifuge tube and suspended in 500μl of sterile 30%v/v glycerol (in PBS). Finally the aliquots of transformed bacteria were stored at -86°C.

#### *4.3.2.3. Plasmid propagation and isolation*

The propagation of successfully transformed bacteria relies upon selection of the transformed bacteria with an antibiotic to which the plasmid structure confers resistance. As previously stated, for pCMVβ and pGL3 the selective antibiotic is ampicillin and for pEGFP-N1, kanamycin.

Two Luria agar plates (2x25ml) containing 100μg/ml of the selective antibiotic were streaked with the transformed *E.coli*. These plates were inverted and incubated for 16-24hrs at 37°C before storage for up to 48hrs at 2-8°C.

Two 5ml Luria broths containing 100μg/ml of the selective antibiotic, were inoculated with a single colony of *E.coli* from the selection plate. The broths were then incubated at 37°C under constant agitation in an orbital incubator at 300r.p.m for 8hrs. Four conical flasks, each containing 125ml of Luria broth with the selective antibiotic at a concentration of 100μg/ml, were then inoculated with 1ml of the previous *E.coli* broth and agitated in an orbital incubator, maintained at 37°C, at 300r.p.m. for a total of 16hrs.

pDNA was then isolated from the 500ml bacteria culture using the Qiagen®-Tip 2500 Mega Kit and the enclosed protocol (September 2000), which itself was adapted from a

procedure developed by Caplen and colleagues (Caplen et al., 1994). Briefly, the overnight culture was divided between two balanced centrifuge bottles and centrifuged at 6,000g for 15mins at 4°C. The supernatant waste was then decanted and destroyed by chlorination (addition of Presept® tablets).

The bacterial pellet was then re-suspended in 50ml of a tris-EDTA buffer containing the RNAase enzyme (P1), to create a homogenous suspension. Lysis of bacterial cells continued upon addition of 50ml of a sodium hydroxide-SDS buffer (P2). After 5mins, lysis was halted by addition of 50ml of a chilled acidic potassium acetate buffer (P3). The suspension was then mixed by six inversions of the container and maintained on ice for a total of 30mins, with six inversions every 5mins ensuring a homogenous suspension. This buffer neutralises the lysate and causes precipitation of denatured cellular debris within salt-detergent complexes. At this stage the plasmid remains in solution.

The resulting suspension was then centrifuged at 20,000g for 30mins at 4°C to remove the precipitated debris. Following centrifugation, the supernatant was carefully filtered through a Whatman Number 1 filter paper into a sterile beaker. The filtrate was then poured into the Qiagen®-tip barrel and the waste filtrate was collected underneath the tip. The tip, on which the pDNA was now 'loaded', was then washed with 200ml of a 'medium-salt' pH7 buffer (QC) to remove any remaining impurities and small metabolites. The pDNA was finally eluted from the tip using 35ml of a 'high salt' elution buffer at pH8.5 (QF) and collected in a sterile beaker.

Propran-2-ol (24.5ml) was then added to the beaker at room temperature to precipitate the pDNA and the solutions were divided between two sterile 50ml centrifuge tubes which were centrifuged at 15,000g for 30mins at 4°C. The supernatant was carefully decanted and each sample pellet was subsequently rinsed with 3.5ml of ethanol (70%). The sample was then centrifuged at 15,000g for 10mins at 4°C. The ethanol rinse and subsequent centrifugation step were then repeated. Following removal of ethanol for the second time, the pellet was allowed to air dry for approximately 15mins. Finally, the DNA pellet was re-dissolved in 1ml (0.5ml in each centrifuge tube) of warmed tris-EDTA buffer, pH8, and the two solutions were combined.

#### *4.3.2.4. Plasmid quantification*

The concentration and purity of the isolated plasmid solution was analysed by UV absorbance at 260nm and 280nm using an Eppendorf® Biophotometer. The UV absorbance value of the double stranded DNA solution at 260nm ascertains the concentration of the pDNA solution whereas the ratio between the absorbance at 260nm and 280nm ($^{260nm}/_{280nm}$) provides an indication of the sample quality, an absorbance ratio of >1.8 accepted as an effectively pure pDNA solution. Sample analysis involved measurement of the UV absorbance of 50µl of a 1 in 50 dilution of the harvested plasmid solution within a disposable UVette® eppendorf.

#### *4.3.2.5. Agarose gel electrophoresis*

Gel electrophoresis determined the integrity and identity of the pDNA following preparation. Agarose gel (1g) was dissolved in 100ml of a tris-borate EDTA (TBE) solution by heating in a microwave oven for a period of 1min, following which the solution was allowed to cool to approximately 50°C. Two drops of ethidium bromide (approximately 1µg) were then added to the agarose solution which was mixed well and subsequently poured into the electrophoresis tray, containing a well comb. The gel was then allowed approximately 1hr to solidify and subsequently immersed in TBE buffer within the electrophoresis tank. The comb was gently removed from the gel, creating wells into which samples were loaded. Samples contained 10µl of the plasmid under analysis (at a concentration of 1mg/ml) and 1µl of gel loading buffer (bromophenol blue). Hyperladder VI (5µl) was added to an adjacent well. The tank was then connected to a voltage source and run at 100Volts for up to 90mins. The gel was then isolated from the tank and visualised under a UV transilluminator.

### 4.3.3. Mammalian cell culture methods

#### *4.3.3.1. Cell maintenance*

Cells (A-549 and HaCaT) were stored at -80°C as a homogenous suspension in a nutrient medium containing glycerol. Upon removal from storage, cells were thawed on ice and added slowly (dropwise) to nutrient media within a 25cm$^2$ cell culture flask. Nutrient media for cell culture consisted of 2%v/v penicillin-streptomycin, 10%v/v foetal bovine serum (FBS) and 88%v/v Dulbecco MEM (DMEM). Cell monolayers were maintained within nutrient media (replenished at 48hr intervals) at 37°C and 5%$CO_2$ and allowed to reach >75% confluency before being divided and seeded (passaged) into new cell culture flasks. This maintained cells within the log phase of growth and ensured survival.

#### *4.3.3.2. Cell seeding*

Cell monolayers, maintained in 25cm$^2$ cell culture flasks were washed three times in sterile PBS. The cell monolayer was then rinsed for 60secs with trypsin-EDTA (1ml) and the flask was placed in an incubator (37°C:5%$CO_2$) for 5mins. Following incubation, the flask was mechanically agitated to release the cell monolayer from the surface. Cells were then resuspended in 10ml of growth media (2%v/v penicillin-streptomycin, 10%v/v FBS and 88%v/v Dulbecco DMEM). A 0.5ml aliquot was removed from the flask to conduct a haemocytometer cell count, which was conducted under a bright field light microscope. For transfection, each well of a 24 well cell culture plate was seeded at a density of 50,000cells/cm$^2$ (i.e. 72,000 cells/well) and was maintained in 1ml of nutrient media. For routine cell maintenance, approximately 1 million cells were seeded into cell culture flasks and maintained in 7-8ml of nutrient media.

#### *4.3.3.3. Cell transfection protocol*

Cells were allowed to reach 75% confluency (A-549 approximately 70hrs post-seeding, HaCaT approximately 70-140hrs post-seeding based on previously determined cell growth studies) prior to transfection. Transfection timings, passage numbers and the identity of the cell line used in this chapter are detailed in the legends that accompany

those figures. Three plasmids were used for transfection studies, pCMVβ, pGL3 and pEGFP-N1. All were prepared in tris-EDTA buffer (pH7.4) at a concentration of 1mg/ml for mammalian cell culture transfection studies.

Three formulations were utilised in cell culture studies:-

1. LPD complexes were prepared as outlined previously (Section 3.3.2.1) to a concentration of 100μg plasmid/ml of formulation (30μg/300μl). Briefly, to prepare sufficient vector to transfect 6 wells of a 24-well plate: -
    - Pipette 30μl of plasmid (1mg/ml) into a centrifuge tube.
    - Add 120μl of sterile water.
    - Add 60μl of protamine sulphate (1mg/ml).
    - Allow 10mins for the formulation to equilibrate.
    - Add 90μl of DOTAP liposome (1mg/ml).
    - Allow 10mins for the formulation to equilibrate.
2. Naked pDNA (1mg/ml) was diluted to a concentration of 30μg/300μl by the addition of sterile water.
3. Sterile water (300μl) was included as a negative control.

For pEGFP-N1 studies using a fluorescent LPD complex, the rhodamine labelled lipid, phosphatidylethanolamine dipalmitoyl-sulforhodamine B, was included at a concentration of 5%w/w within the DOTAP liposome preparation prior to creation of the LPD (Section 3.3.2.1).

Following preparation of 300μl of formulation, 5.7ml of warmed DMEM was added to produce a final plasmid concentration of 5μg/ml. Media was then removed from each well of the 24-well plate and the cell monolayer was rinsed twice with sterile PBS, to ensure removal of serum, before addition of 1ml of the formulation to each of the selected wells. The rinse step is critical in the transfection process since serum can interact with cationic lipids resulting in instability of the vector formulation and a subsequent reduction in transfection efficiency (Felgner et al., 1987, Gao and Huang, 1996, Yang and Huang, 1997). The plate was then incubated (37°C:5%$CO_2$) for a period of 6hrs after which time the formulation was removed from the cell surface and, following a brief rinse, replaced with nutrient media. Twenty four hours after treatment

of the cell monolayer the media was removed and cells were processed to detect the plasmid product.

#### *4.3.3.4. β-galactosidase detection*

Following transfection, cells were fixed over a 15min period using 180µl of freshly prepared 0.25%v/v glutaraldehyde solution per well. Following two PBS rinses, 90µl of freshly prepared X-gal staining solution (prepared using the Invitrogen® manufacturers protocol) was added to each well and the plate was incubated (37°C:5%$CO_2$) until blue pigmentation became apparent (0.5-2hrs). X-gal solution was then replaced with sterile PBS and cells were visualised under the Olympus IX-50 light microscope.

#### *4.3.3.5. GFP detection*

Fluorescence Activated Cell Sorting (FACS) Analysis

For (FACS) experiments, cell culture plates were transfected using the following formulations:-

1. PBS (Negative Control).
2. LPD containing the rhodamine-labelled DOTAP liposome and the pCMVβ plasmid.
3. LPD containing the pEGFP-N1 plasmid.
4. LPD containing the rhodamine labelled DOTAP liposome and the pEGFP-N1 plasmid.

At 24hrs post-treatment, cells were washed twice with PBS and covered with 30µl trypsin-EDTA/well for 2mins. Cells were then incubated for 15mins and re-suspended in 1ml of growth media. The cell suspension was pipetted up and down to create a homogenous monodisperse suspension, transferred to falcon FACS tubes and maintained on ice. Analysis of the sample was carried out using the FACSCalibur system.

Fluorescence Microscopy

HaCaT cells, grown in a 24-well cell culture plate were treated with the following formulations:

1. PBS (Negative control).

2. LPD containing the pEGFP-N1 plasmid.
3. LPD containing the rhodamine labelled DOTAP liposome and the pEGFP-N1 plasmid.

At 1 or 24 hrs post treatment, the formulation was removed from the well of the plate, the cells were rinsed in PBS and the cell monolayer was then visualised under both fluorescence (blue and green excitation) and bright field microscopy, using the Olympus IX-50. Alternative use of bright-field and fluorescence filters permitted visualisation of HaCaT cell morphology, the location of the rhodamine fluorophore (contained in the LPD complex) and the identification of cells expressing pEGFP-N1.

#### *4.3.3.6. Luciferase Detection*

Following treatment of cells with pGL3 formulations, the Promega® luciferase detection Kit was used, as detailed in the manufacturers' protocol, to determine the levels of transfection within cell populations. Briefly, 24hrs after treatment, the cells were washed twice with PBS and subsequently covered with 80µl of reporter lysis buffer. The cell culture plate was then gently agitated for 5mins and placed on ice for 2hrs and then in the freezer for a further 2hrs. Following this period, the plate was removed and allowed to thaw over 30-45mins. Cells were finally harvested from the plate surface using a cell scraper and transferred to microcentrifuge tubes, which were vortexed prior to centrifugation at 13,000r.p.m. for 15secs. The supernatant was then removed, placed in a microcentrifuge tube and stored at -80°C. For assay, samples were thawed on ice and aliquots (50µl) were placed in a white 96-well plate which was subsequently analysed using the Fluostar Optima®. An autoinjector added 100µl of luciferase substrate per well, the plate was then agitated and the eliminated light units were recorded.

A BCA protein assay determined the protein content within each sample (Smith et al., 1985). This permitted calculation of the relative light units (RLU) per unit protein for each population of cells studied. Briefly, 10ml of BCA was added to 0.2ml of $CuSO_4$ solution (4%w/v) and mixed for 30secs to create the assay reagent. Standard BSA solutions of increasing concentrations (from 0-2mg/ml) were prepared and 20µl of each concentration was added, in triplicate, to the wells of a colourless 96-well plate. Cell lysate samples (20µl), previously analysed by luminometry, were also added to the

plate. To these samples, 200µl of the BCA assay reagent was added and the plate was briefly agitated before incubation for 30mins at 37°C:5% $CO_2$. Following incubation, the samples were allowed to cool to room temperature over a period of 1hr and the UV absorbance of samples and BSA calibrants were analysed at 570nm using the Anthos 96-well plate spectrophotometer. The equation of the line, calculated for the BSA calibration curve, was then used to convert absorbance values for the cell lysate samples to protein content, which was manipulated to calculate RLU.

### 4.3.4. *Ex vivo* human skin organ culture

Human skin was obtained from breast reduction and mastectomy procedures with informed patient consent and full ethical approval. The tissue was placed immediately in nutrient skin media (DMEM supplemented with 5% FBS and 1% Penicillin/Streptomycin) and transported on ice to the laboratory.

Sub-cutaneous fat was removed from the tissue by blunt dissection and the tissue was dried briefly. The skin was then pinned to a dissection board and a significant proportion of the dermis was removed using a stainless steel razor blade. The 'split thickness' skin (approximately 2mm thick) was then treated with the formulation/device of interest, divided into approximately $1cm^2$ areas and maintained in a Trowell-type organ culture set-up (Fig 4.1). Details of the protocol for organ culture were adapted from methodologies utilised by Kent *et al* (Kent et al., 2001), Backvall *et al* (Backvall et al., 2002) and Larregina *et al* (Larregina et al., 2001).

After treatment the skin was positioned on lens tissue paper supported by a sterile steel mesh, within a six well culture plate. Each well contained 7.5ml of freshly prepared nutrient media which soaked the lens tissue paper by a wicking effect. Skin was incubated at the air-liquid interface for approximately 24hrs at 37°C:5%$CO_2$ before analysis.

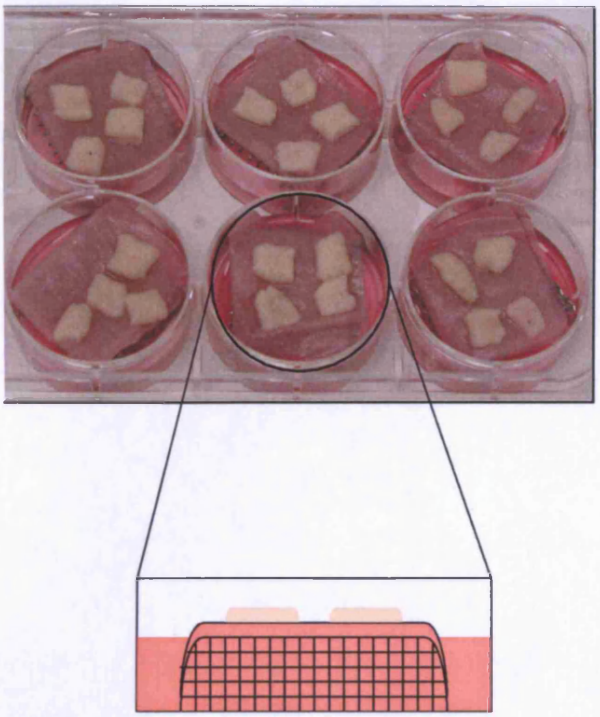

*Figure 4.1.* Split thickness human skin, obtained from surgical procedures, was maintained in a Trowell-type organ culture set-up. The tissue was maintained at the air-liquid interface at 37°C for 24-48hrs.

### 4.3.5. Cutaneous nanoparticle delivery

#### *4.3.5.1. Fluorescent nanosphere formulation*

These studies aimed to identify the location of a nanoparticle formulation within the skin structure following localised delivery by a microneedle device or an intradermal injection. The ideal nanoparticle model to be used in these studies would be the fluorescent LPD or the LCN formulation, owing to their comparability with the LPD in both dimension and surface morphology (Section 3.4.1). However, limited fluorescence signal prevented visualisation of the formulation within the skin tissue by histological evaluation. The formulation used in these studies was a concentrated (stock) fluorescent red nanosphere (approximately 100nm diameter) suspension.

#### *4.3.5.2. Intradermal Injection of fluorescent nanospheres*

Fresh human skin from a female donor, of unknown age, was injected with 50µl of the latex nanosphere formulation using a 1ml syringe and 29G hypodermic needle. Skin was then maintained in organ culture for 8hrs, rinsed, fixed and embedded in OCT medium within a cryomould surrounded by solid carbon dioxide. Cryosections (10-12µm) were obtained and mounted on superfrost plus® slides. Tissue sections were illuminated by a blue excitation light source and analysed by fluorescence microscopy.

#### *4.3.5.3. Microneedle mediated delivery of fluorescent nanospheres*

##### *4.3.5.3.1. Dry etch microneedles*

Fresh human skin from a female donor, of unknown age, was treated topically with 50µl of the fluorescent nanosphere formulation followed by a single application of a dry-etch microneedle device (CSE-Array A). Skin was then maintained in organ culture for 16hrs and processed to create histological sections that were analysed under blue illumination by fluorescence microscopy.

##### *4.3.5.3.2. Wet etch microneedles*

Fresh human skin, from a 76 year old female donor, was treated topically with 10µl of the fluorescent nanosphere formulation followed by 10 applications of the wet-etch microneedle device. This was conducted using frustum tipped (TNI-Array 8) and pointed tipped (TNI-Array 5) microneedles. Skin was then maintained in organ culture for 20hrs and processed to create histological sections that were analysed, under blue illumination, by fluorescence microscopy.

### 4.3.6. Detecting β-galactosidase in human skin

#### *4.3.6.1. Invivogen® protocol*

Human skin from a 48 year old donor was collected and sub-cutaneous fat was removed by blunt dissection. The tissue was then divided into 1cm$^2$ areas and treated topically with the microneedle device followed by a PBS formulation. Skin was then maintained within organ culture for a period of 46hrs and subsequently processed using the commercial *lacZ* staining kit, obtained from Invivogen®, and the manufacturers' protocol.

Human skin was placed in PBS/$MgCl_2$ solution, on ice, for a short period. Each piece of skin was then fixed in 2ml glutaraldehyde 0.5%v/v for 2hrs and subsequently rinsed in PBS/$MgCl_2$ (2mM) over a period of 6hrs. Each skin biopsy was then placed in 2ml of X-gal staining solution at 37°C for a total period of 43hrs. All solutions were freshly prepared using components supplied within the Invivogen Kit® (Table 4.1).

Table 4.1. The components of the X-gal staining solution provided with the Invivogen® staining kit.

| **Volume** | **100ml** |
|---|---|
| Potassium ferricyanide [0.6M] | 1ml |
| Potassium ferrocyanide [0.6M] | 1ml |
| $MgCl_2$ [1M] | 0.2ml |
| Ipegal [10%] | 0.2ml |
| Sodium Deoxycholate [10%] | 0.1ml |
| X-gal solution [40mg/ml]* | 2.5ml |
| 10X PBS | 10ml |
| $H_2O$ | 85ml |

*X-gal powder is made up to a 40mg/ml solution with N-N-dimethylformamide

#### *4.3.6.2. Optimising detection of the β-galactosidase enzyme*

Over the previous 10 years Dr Ulrich Hengge and his laboratory have produced a number of publications investigating exogenous gene expression within the skin and are recognised as major contributors to this field of research. Early studies by the group highlight the ability to transfect porcine (Hengge et al., 1995) and human (Hengge et al., 1996) skin, maintained in organ culture conditions, with the pCMVβ plasmid. The X-gal staining methodology used by Hengge and colleagues was therefore adopted in the studies detailed within this section.

In 1997, Weiss and co-workers recognised the difficulties in detection of the β-galactosidase enzyme (Weiss et al., 1997). Use of the *lacZ* reporter gene and detection of the bacterial β-galactosidase enzyme within gene transfer studies is now commonplace. However the activity of an endogenous mammalian enzyme, located within the lysosomes of cells, often confounds those results achieved. This effect has been noted in a wide range of cell and tissue types (Weiss et al., 1999). Experiments conducted by Weiss and co-workers aimed to reduce/abolish the activity of the endogenous enzyme and this optimised protocol was therefore adopted for use in these studies.

Female skin from a 78 year old donor was collected and 6 areas ( approximately 1cm$^2$), were removed from the tissue. The following formulations (10μl) were injected intradermally into the superficial layers of the skin using a 25G Microlance® needle:-

1. Positive control: β-galactosidase enzyme (1Unit/100μl) (N=3).
2. Negative control: PBS (N=3).

Tissues were then rinsed and fixed. Two skin areas (one positive control and one negative control) were then immersed in 2ml of a staining solution (Table 4.2). The tissue was stained for 12hrs and then rinsed in PBS for 1hr before analysis.

| | | | |
|---|---|---|---|
| Potassium ferricyanide [0.6M] | 50 | 42 | 25 |
| Potassium ferrocyanide [0.6M] | 50 | 42 | 25 |
| $MgCl_2$ [1M] | 10 | 10 | 10 |
| Ipegal [10%] | 10 | 0 | 10 |
| Sodium Deoxycholate [10%] | 5 | 0 | 5 |
| PBS [x10] | 500 | | |
| Tris-HCl buffer (pH8.50) [200mM] | | 2500 | |
| $NaH_2PO_4$ (pH7.3) [200mM] | | | 2500 |
| Water | 4250 | 2150 | 2300 |
| Incubation Conditions | 37°C | 37°C | Room temperat |

#### *4.3.6.3. Visualising the β-galactosidase enzyme in ex vivo human skin*

*En face* analysis

Following X-gal staining, the tissue was rinsed briefly in 2ml PBS and visuali
*face*, mounted on a glass slide or between two glass slides, using a light microscop

1. For low magnification images, a Stemi 2000-C stereomicroscope was at
   to an Olympus Camedia C-4040 zoom digital camera, the surface of the s
   was illuminated using a Schott KL1500 fibre optic light source and
   images were stored on a Flashpath® graphics card.

Following *en face* analysis, the tissue was embedded within OCT media, cryosec and H&E stained to identify the cellular architecture of the tissue (Section 2.3.9).

### 4.3.7. Microneedle mediated cutaneous β-galactosidase delivery

Human skin from a 43 year old female donor was transported to the laboratory c treated with dry-etch microneedles (CSE-Array A) and treated topically with 40µl galactosidase (1Unit/100µl in a bicene buffer [50mM] containing 100µg/ml of This process was repeated, this time applying PBS as a negative control. Each s was placed in the chamber of a 6-well cell culture plate and maintained at the air- interface in organ culture conditions for 24hrs. The tissue was then rinsed, fixe stained using the previously developed 'Weiss' protocol (Section 4.3.6.2). Sa were then analysed (Section 4.3.6.3).

260nm and 280nm. All plasmid samples isolated from *E.coli* and deemed suitat transfection studies possessed an initial concentration of between 2.5 and 3.5mg/r a ($^{260nm}/_{280nm}$) ratio greater than 1.8. The configuration of pDNA solutions was an by agarose gel electrophoresis i.e. relaxed circular DNA, open circular DN supercoiled (Fig 4.2). The intense bands in lanes 1 and 2 suggest that the gr proportion of the plasmid isolated from the transformed bacteria is in the super form (also called covalently closed DNA, where DNA is fully intact) (Fig 4.2A). T of relaxed circular (where DNA is fully intact, but has been 'relaxed') and open ci forms (one strand of DNA has been cut) of the pDNA are visualised as muc intense bands that migrate at a reduced rate. Transfection studies using lipid-based therapy vectors have demonstrated greater success using pDNA in the supercoiled (Even-Chen and Barenholz, 2000, Zuidam and Barenholz, 1998). Initial failu transfect mammalian cells in this study were attributed to a degradation o supercoiled plasmid into its less effective configurations (Fig 4.2B - lane 5) highlighted the importance of continued analysis of pDNA samples by agaro electrophoresis during this study.

### 4.4.2. Determining the functionality of reporter plasmids in mammalian cell culture

Following transformation of bacteria, plasmids (pCMVβ, pEGFP-N1 and pGL3) propagated, isolated and their concentrations, configurations and integrity determined (Section 4.3.2). However before application of these reporter plasm cutaneous transfection studies, it was important to ascertain their functionality more reproducible and controlled environment of mammalian cell culture.

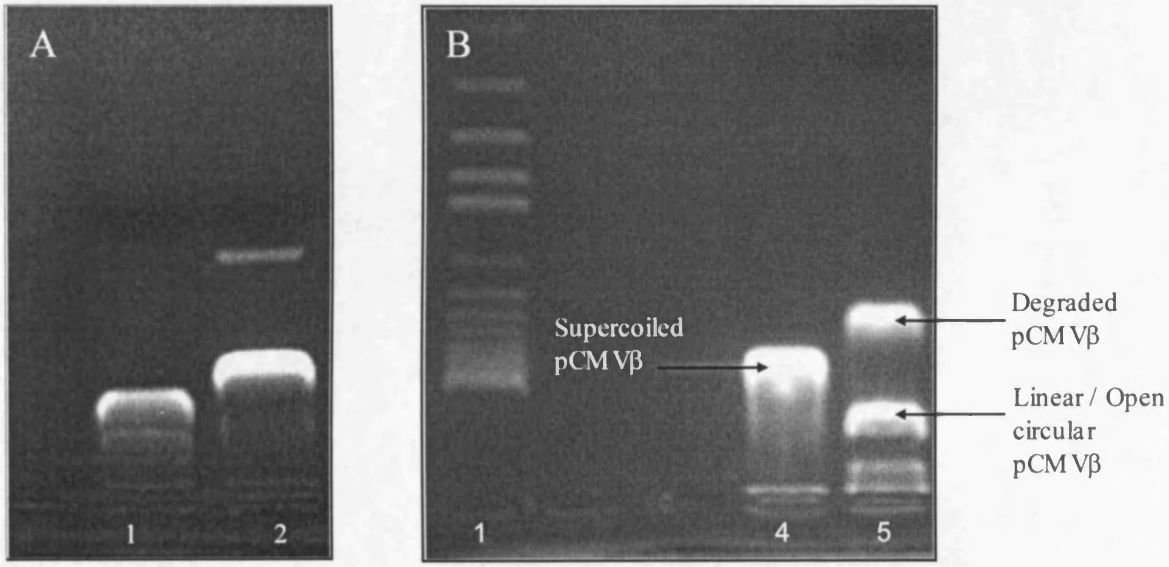


*Figure 4.2.*

A. Agarose gel electrophoresis illustrated the integrity of the pCMVβ (7.2Kb) (lane 1) and pEGFP-N1 plasmid (4.7Kb) (lane 2) used in transfection studies. The small band pictured ahead of the supercoiled plasmid band in lane 2 indicated the presence of a small amount of fragmented DNA within the formulation.

B. Agarose gel electrophoresis was used to determine the configuration of the pCMVβ plasmid (7.2Kb) isolated from stocks of transformed DH5α *E.coli* (lane 4). The Hyperladder IV was pictured in lane 1.

#### *4.4.2.1. β-galactosidase*

A-549 cells, successfully transfected with pCMVβ incorporated within an LPD vector, were visibly discriminated *in situ* by enzymatic conversion of the X-gal substrate to a blue pigment (Fig 4.3A). Investigations using the HaCaT cell line confirmed the ability of an LPD formulation to transfect human keratinocytes *in vitro* (Fig 4.3B – 4.3D). However, the characteristics of cell growth within a population were not uniform. Cells appeared as a confluent monolayer (Fig 4.3B), as a monodisperse layer (Fig 4.3C) and also as clusters (Fig 4.3D). The unpredictable growth characteristics of the cells prevented optimisation of transfection levels. There was no visible transfection of cells treated with the naked pCMVβ formulation, i.e. in the absence of non-viral condensing elements.

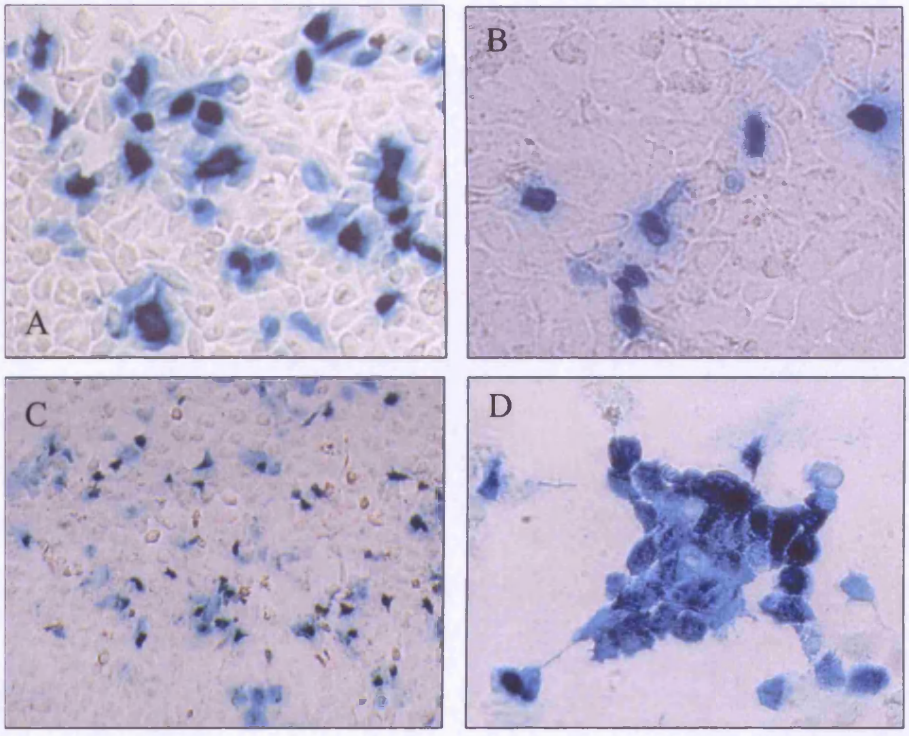


*Figure 4.3.* Detectable transfection of (A) A-549 (passage103) and (B-D) HaCaT (passage 60) cell lines with the pCMVβ plasmid, incorporated within an LPD vector. Transfection was analysed 24hrs after topical application of the formulation. Magnifications A, X200; C X100; B, D, X400.

#### *4.4.2.2. pEGFP-N1*

The encoded product of the pEGFP-N1 reporter plasmid was detectable *in situ*, with no cell processing or assay required for its detection. Those successfully transfected cells adopted a bright green fluorescence (Fig 4.4A & 4.4B). The inclusion of a rhodamine labelled cationic lipid, within DOTAP liposomes that were used to formulate the LPD, supplemented the formulation with fluorescent red properties. This permitted visualisation of the LPD location within the cell monolayer and interaction of the vector with the keratinocyte cell membrane.

Intense areas of red fluorescence surrounding cells treated just 1hr previously with the LPD formulation, indicated rapid interaction of the positively charged LPD complex with the negatively charged cell membrane (Fig 4.4C). At this stage there was no evidence of successful transfection with the pEGFP-N1 plasmid. However after 24hrs GFP was clearly identifiable within a number of cells (Fig 4.4B & 4.4E). Persistence of red fluorescence in association with the cell membrane indicated a continued presence of the vector, or at least components of the LPD, with the cell (Fig 4.4F). However the functionality of the LPD and the location of the rhodamine label, extra or intracellularly were not determined.

Flow cytometry studies provided quantitative indicators of gene expression and reinforced the necessity of a vector formulation to facilitate successful transfection of cells maintained in culture (Fig 4.5). Each plot in Fig 4.5 represents a single cell population, isolated from the well of a 24-well cell culture plate, 24hrs after topical application of one of four formulations. FACS data achieved for the control formulation i.e. those cells treated with PBS alone, determined the background level of fluorescence within a cell population (Fig 4.5A). Treatment of cells with an LPD formulation, containing rhodamine labelled DOTAP liposomes and pCMVβ, resulted in an upward shift in approximately 40% of the HaCaT cell population (Fig 4.5B). This shift represented those cells that possessed fluorescent red properties due to association with the rhodamine-labelled LPD formulation, or at least the cationic liposome component of the formulation. Treatment of cells with an LPD formulation containing pEGFP-N1 caused a right shift in the position of approximately 10% of the cell population (Fig

4.5C). These cells possessed fluorescent green properties and were therefore deemed to have been successfully transfected with pEGFP-N1. This level of transfection is in general agreement with visible levels of transfection noted in fluorescence microscopy studies.

Application of an LPD formulation, containing the rhodamine labelled liposome and housing pEGFP-N1, induced both an upward and right shift of a significant proportion (approximately 11%) of the fluorescent cell population (Fig 4.5D). The cells in the top right quadrant are therefore directly associated with the rhodamine labelled lipid component of the LPD formulation and have subsequently been transfected to express GFP. There was limited evidence of successful transfection in cells that were not associated with the rhodamine component of the LPD (Fig 4.5D – bottom right quadrant). Significantly, just over 50% of the cell population that was associated with the LPD formulation did not express GFP (Fig 4.5D – top left quadrant). This is indicative of the inefficiency of the non-viral gene therapy vector. Replicate analysis for each formulation analysed (N=6) supported these observations (Fig 4.6).

#### *4.4.2.3. pGL3*

Although pEGFP-N1 provided a plasmid that was useful for quantitative analysis of transfection in mammalian culture studies, the analytical method (flow cytometry) is not easily extrapolated to biological tissue. Reporter plasmids encoding for the luciferase enzyme, such as pGL3, are therefore used frequently for quantitative cutaneous transfection studies (Babiuk et al., 2002, Dileo et al., 2003, Li et al., 2003, Mikszta et al., 2002, Williams et al., 1991). Detection of successful expression requires cell isolation, lysis to extract the luciferase enzyme and detection of light emitted upon addition of the luciferase substrate.

Transfection using pGL3, incorporated within an LPD vector, proved successful (Fig 4.7). A 'flash' response was recorded from those treated cells 2secs after addition of the substrate and levels of emitted light were maintained for over 20secs. However, although this demonstrated the functionality of the plasmid, the variability in transfection efficiencies was notable (highlighted by the sd results in Fig 4.7). Cells treated with naked pGL3 or the LPD formulation containing an alternative reporter gene

(negative control) failed to produce any detectable levels of transfection. These results were in agreement with previous data obtained using the pEGFP-N1 and pCMVβ plasmids.

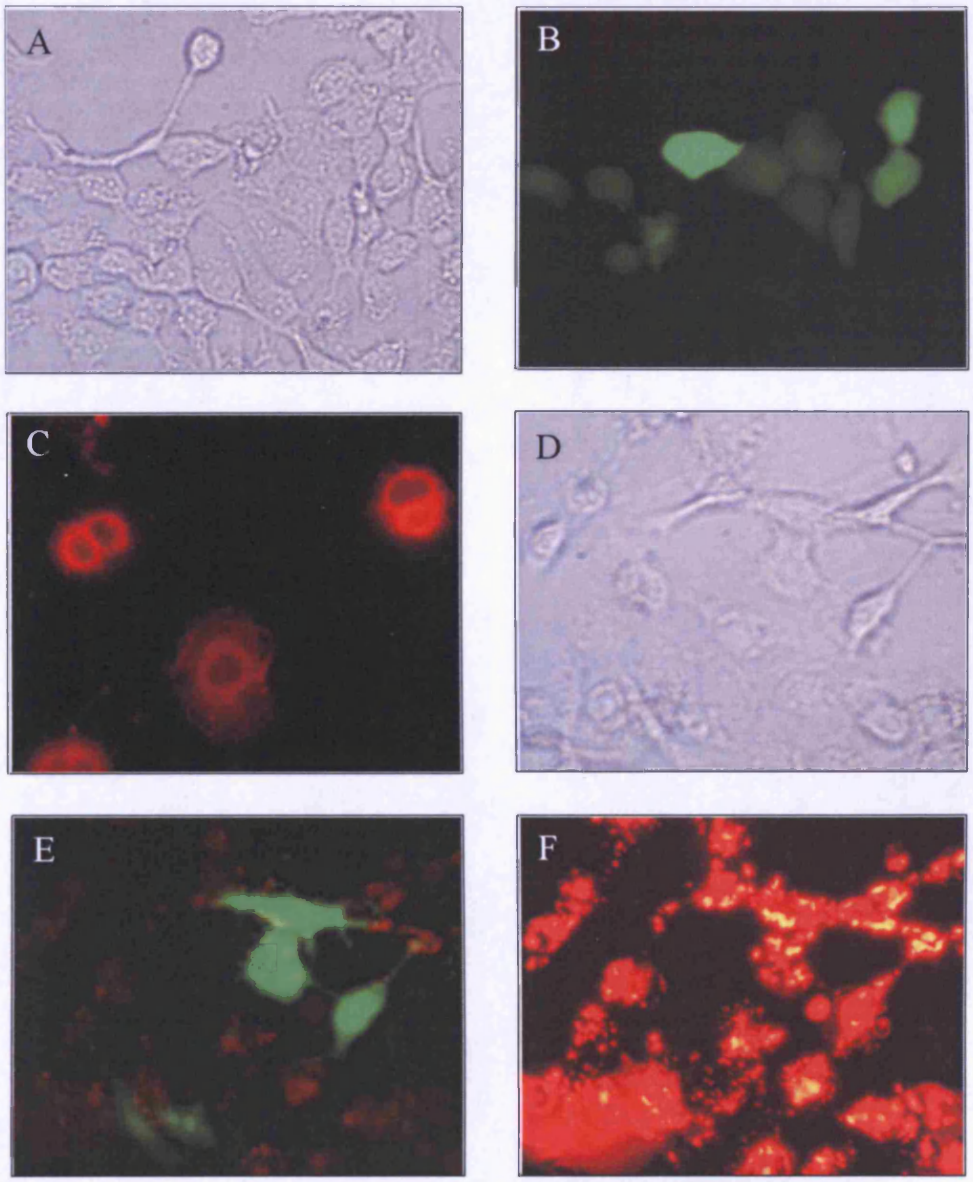


*Figure 4.4.* Detectable transfection of HaCaT cell lines (passage 61, transfected 70hrs post-seeding), with the pEGFP-N1 plasmid, incorporated within an LPD vector. Transfection was analysed at 1hr (C) and 24hrs (A-B, D-F) after topical application of the formulation. Images depict cells treated with an LPD (A, B) or a rhodamine-labelled LPD (C-F) and were pictured using light (A, D), blue fluorescence (B, E) or green fluorescence (C, F) microscopy. Magnification X400.

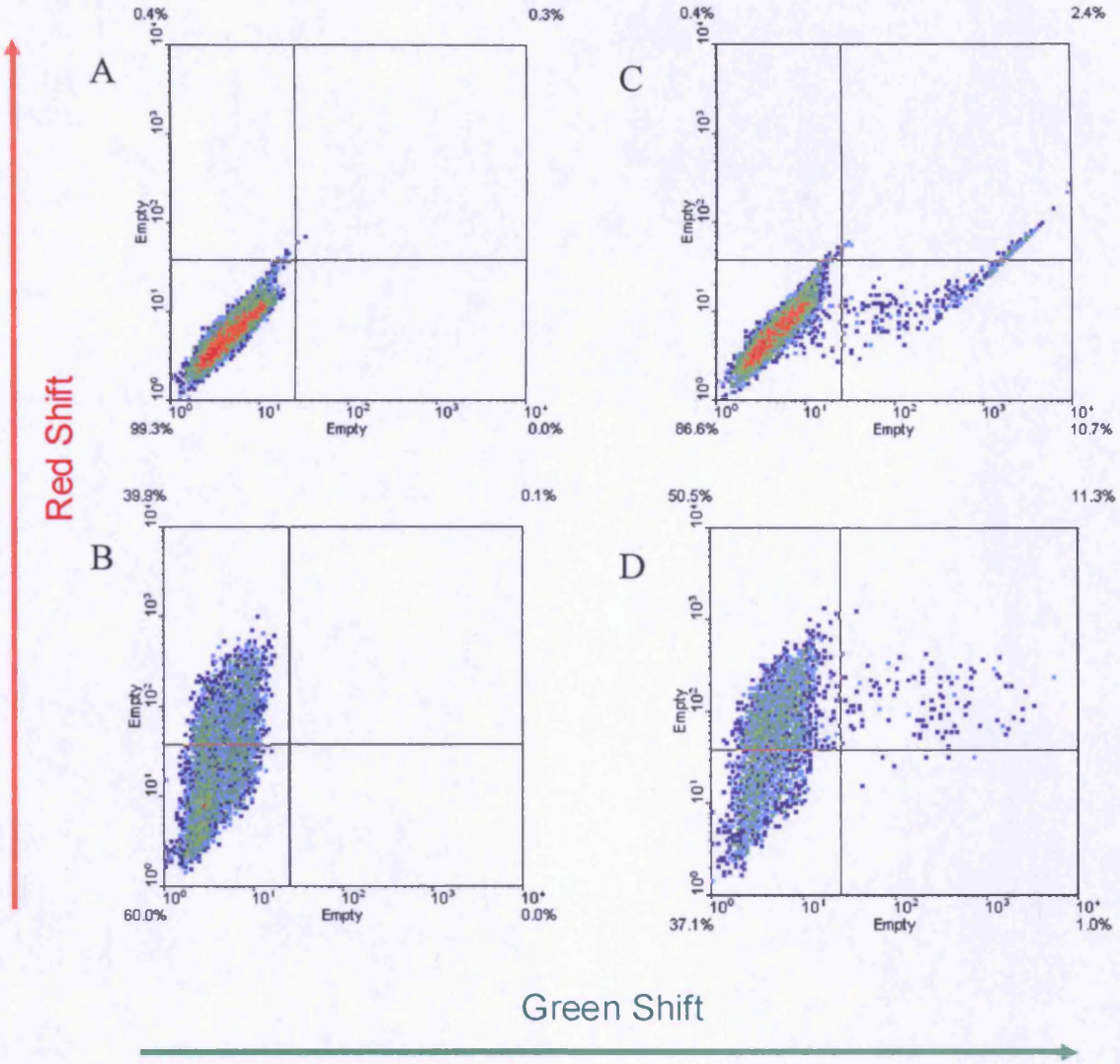


*Figure 4.5.* FACS analysis of HaCaT cells treated with four different formulations (passage 63, transfected 141hrs post-seeding). Each dot plot is representative of a single cell population to which a different formulation was applied; A=blank formulation (negative control), B=Rhodamine-labelled LPD containing pCMVβ, C=LPD containing pEGFP-N1, D=Rhodamine-labelled LPD containing pEGFP-N1.

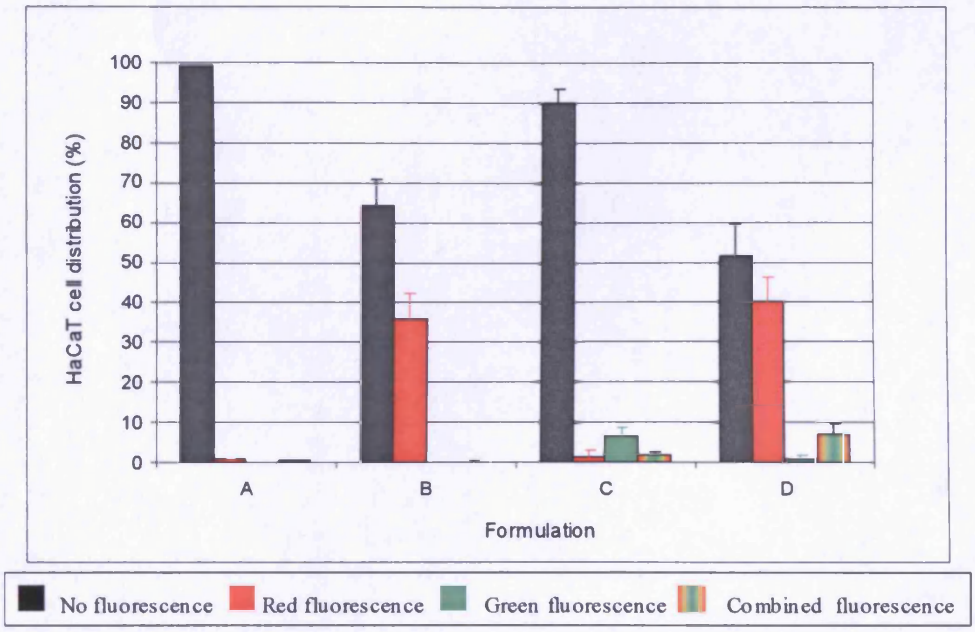


*Figure 4.6.* Combined FACS data for treated HaCaT cells. A=Blank treatment; B=Rhodamine-labelled LPD containing pCMVβ plasmid; C=LPD containing pEGFP-N1; D=Rhodamine-labelled LPD containing and pEGFP-N1, mean ± sd (N=6).

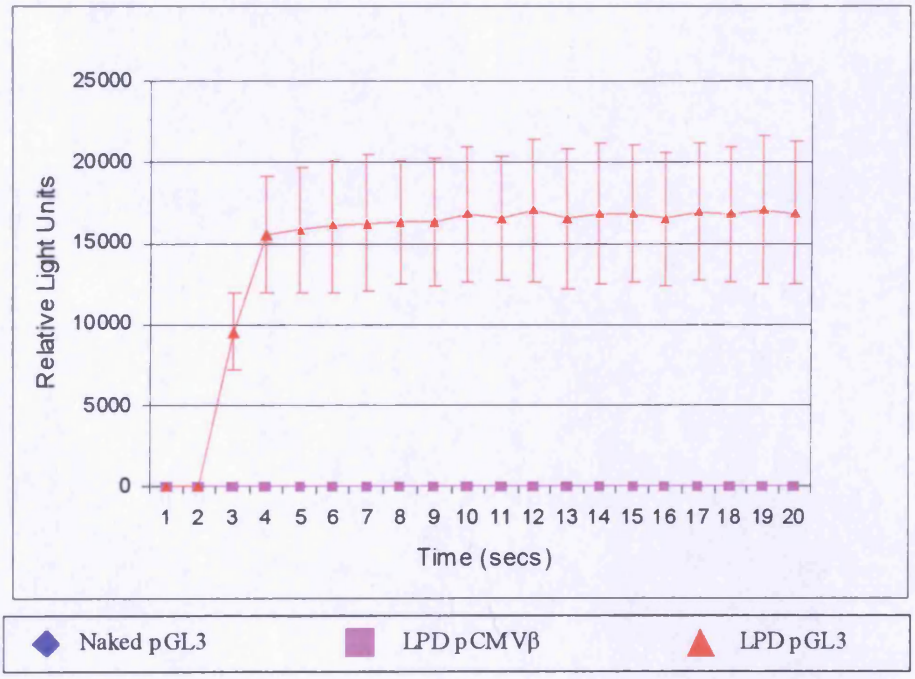


*Figure 4.7.* The relative light units released by A-549 cells (transfection 74hrs post-seeding, passage 96) following treatment with naked pGL3 (N=3), LPD pCMVβ (N=3) or LPD pGL3 (N=8) formulations, mean ± sd.

### 4.4.3. Cutaneous Nanoparticle Delivery

*In vitro* studies illustrated the functionality of each of the reporter plasmids studied and enabled progression of the investigation towards the analysis of transfection within human skin tissue. However, although mammalian cells are an accepted *in vitro* model, the complexity of the skin, the organisation of keratinocytes within the three dimensional architecture of the viable epidermis and the necessity to deliver the formulation across the SC barrier makes the transfection of cells within the organ a significantly greater challenge.

The previous chapter demonstrated the ability of a microneedle array to deliver small molecules and nanoparticle formulations across human epidermal membrane. However successful cutaneous expression of exogenous pDNA relies upon delivery of a formulation across the SC and its subsequent retention within the viable epidermis. The previously characterised microneedle devices, dry- and wet-etch (pointed and frustum tipped), were therefore used to examine localised delivery of a nanoparticle formulation to the viable epidermis of *ex vivo* human skin.

#### *4.4.3.1. Nanoparticle permeation into untreated human skin*

Histological analysis of intact human skin treated topically with a fluorescent nanoparticle formulation revealed a uniform distribution of the formulation over the entire skin surface (Fig 4.8). These observations are in agreement with Alvarez-Roman *et al* (Alvarez-Roman et al., 2004). At no point were fluorescent nanoparticles visualised below the SC.

#### *4.4.3.2. Intradermal injection of fluorescent nanospheres*

Direct intradermal injection of macromolecular therapeutics, including nucleic acid formulations is a well established cutaneous delivery technique (Chesnoy and Huang, 2002, Hengge et al., 2001, Kremer et al., 1999, McCluskie et al., 1999, Meuli et al., 2001, Sawamura et al., 2005, Sawamura et al., 2002b, Woodley et al., 2004). However this method of delivery is dependent upon the skill of the administrator. These studies were therefore used to determine the reproducibility of the technique and the location of deposition upon intradermal injection of a nanoparticle formulation.

Following intradermal injection, the nanoparticle formulation was retained within a discrete reservoir in the upper dermis (Fig 4.9A). Dissemination to the surrounding tissue was limited. Delivery to viable cells of the epidermis relied upon interaction of the formulation with cells that surround the 'needle track' (Fig 4.9B), possibly as a result of the backpressure created upon bolus administration. During removal of the needle, this pressure also resulted in deposition of a proportion of the formulation on the overlying skin surface. It was therefore postulated that transfection of cells with nanoparticle formulations, such as non-viral gene therapy complexes, will occur primarily in those cells that surround the needle track and that the majority of the formulation would be delivered, ineffectively, to the dermal region. This is unsurprising when considering a needle of millimetre dimensions is being used to deliver a formulation to a micron-scale target area.

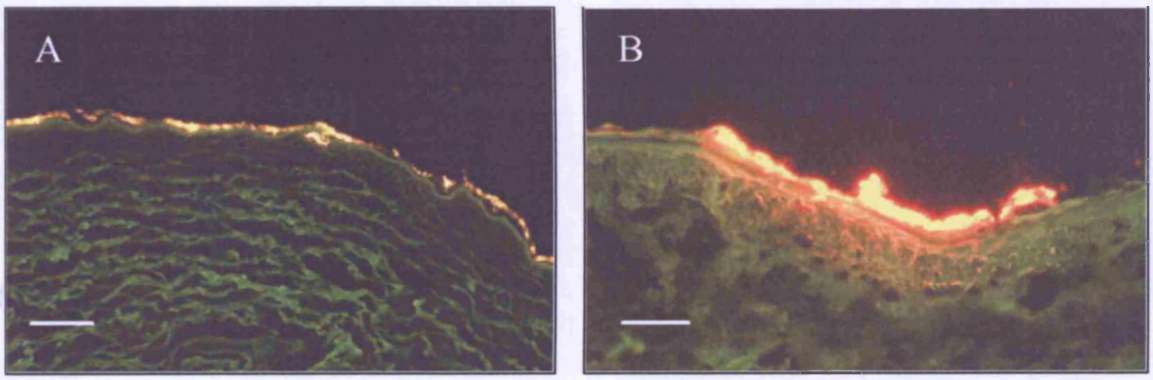


*Figure 4.8.* Human skin, treated topically with a fluorescent red concentrated nanosphere formulation. A, scale bar = 200μm; B, scale bar = 50μm. Skin was obtained from a female donor of unknown age.

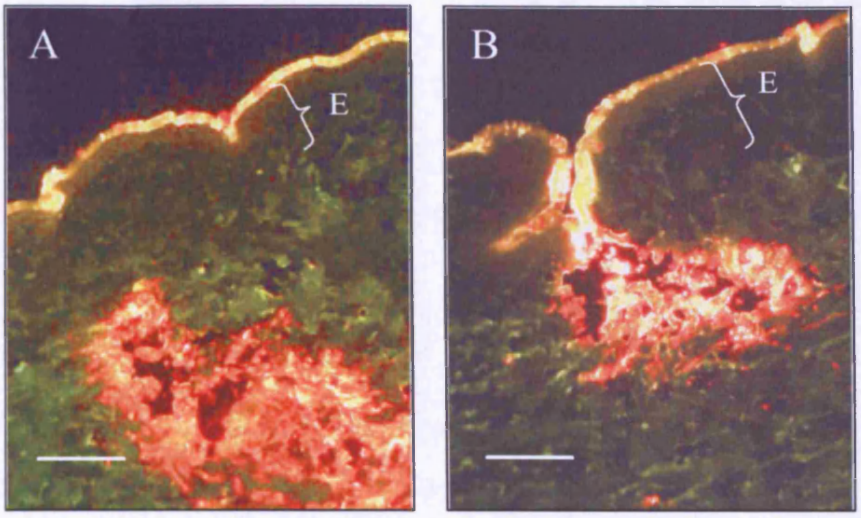


*Figure 4.9.* Transverse sections of human skin, injected with a concentrated fluorescent red nanosphere formulation. E=Epidermis, scale bar = 100μm. Skin was obtained from a female donor of unknown age.

#### *4.4.3.3. Dry-etch microneedle mediated nanoparticle delivery*

Histological evaluation of human skin, treated with a microneedle device and fluorescent nanoparticles, was used to asses the delivery capabilities of the microneedle array. However, when interpreting histological sections it is important to remember the contribution of processing parameters to the tissues final appearance. Therefore hundreds of cryosections were analysed from each tissue sample and the images considered most representative of the tissue architecture and microchannel structure were selected for photomicrographs.

Treatment of human skin with a fluorescent nanosphere formulation and application of a dry-etch microneedle array (CSE-Array A) illustrated the ability of the device to facilitate epidermal delivery of a colloidal formulation (Fig 4.10). Microchannels appeared as non-uniform conduits, approximately 100-200μm in length and 30-40μm in diameter (Fig 4.10A-4.10C). Direct interaction of the fluorescent nanoparticle formulation with tissue components that occupy the interior of microchannels (observed as red or co-localised yellow against the autofluorescent green background) highlighted the potential of the device for the cutaneous delivery of nanoparticles. However there

was no fluorescent signal recorded in the epidermal tissue remote of microchannel structures, thus indicating restricted intercellular movement of nanoparticles.

The autofluorescence of human skin (Felner, 1976), particularly in the SC and connective tissue of the dermis was also illustrated (Fig 4.10). Mechanical disruption of the tissue, such as that resulting from microneedle penetration, appeared to increase levels of fluorescence within the surrounding tissue. This proved useful in the identification of microchannels during analysis of cryosections but detrimental to future investigations using pEGFP-N1 for transfection studies in human skin.

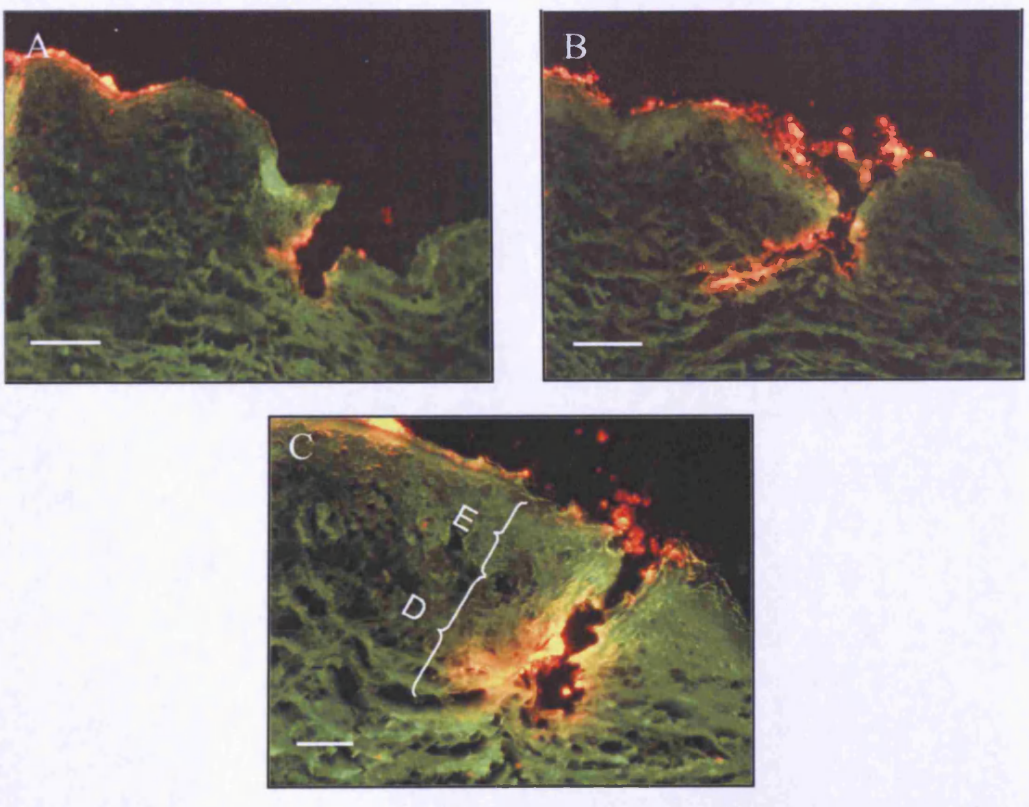


*Figure 4.10.* Transverse sections of human skin, treated topically with a concentrated fluorescent red nanosphere formulation followed by application of a dry-etch microneedle device. E=Epidermis and D=Dermis in image (C). A, B, scale bar = 100μm; C, scale bar = 50μm. Skin was obtained from a female donor of unknown age.

#### *4.4.3.4. Wet-etch microneedle mediated nanoparticle delivery*

##### *4.4.3.4.1. Frustum tipped microneedles*

The penetrative capabilities of wet-etch microneedles was also demonstrated by the localised delivery of nanoparticles into human skin. Images recorded at low magnifications (x40) permitted visualisation of the width of each tissue sample, allowing the relative level of membrane disruption to be appreciated (Fig 4.11). Higher magnification images (x100) permitted closer inspection of the microchannel morphology (Fig 4.11).

The heterogeneity of microchannels, created by the array, was clearly identifiable by comparing the disruptions in different areas of the tissue (Fig 4.11A-4.11D). Minimally invasive microchannels, approximately 100μm in depth and 50μm in diameter, were confined primarily to the viable epidermis (Fig 4.11A & 4.11B). These conduits retained the colloidal formulation within the epidermal region and restricted interaction of nanoparticles to those viable cells that constitute the interior walls of the epidermal microchannel. More significant disruptions, extending up to 200μm in depth, facilitated permeation of the formulation across the epidermis and into the underlying dermal layer (Fig 4.11C & 4.11D). However although disruptions resulted in significant levels of the formulation permeating into the dermal region, detection of nanoparticles within the epidermal region remained evident.

##### *4.4.3.4.2. Pointed tipped microneedles*

Pointed tipped microneedle devices caused less disruption of the skin surface and a reduced conduit depth (Fig 4.12). This resulted in a greater proportion of microchannels that were restricted to the viable epidermis (Fig 4.12A & 4.12B). Maintaining the integrity of the BMZ prevented permeation of the nanoparticles into the dermal region. This may be expected to restrict non-viral gene therapy vectors to the viable epidermis and hence promote localised transfection.

Interestingly, microdisruptions that pierced the BMZ only facilitated permeation of the nanoparticle into the dermal tissue directly beneath the microchannel. The formulation was therefore often visualised as a columnar area of fluorescence, located directly

below the microchannel (Fig 4.12C & 4.12E). Limited movement of the nanoparticle formulation within the dermis was analogous to observations made following intradermal injection (Fig 4.8). Restriction of the formulation to its site of deposition, in the dermis, may be attributable to electrostatic interaction of nanoparticles with the connective tissue structures.

In conclusion, the cutaneous delivery of gene therapy complexes aims to target those cells of the viable epidermis. Studies with fluorescent nanospheres indicated that minimal disruption of the tissue by a microneedle device can promote localised epidermal delivery of nanoparticles to this target region. However inter- and intra-individual variability in the thickness of this epidermal layer and the heterogeneity of microchannels created by the device resulted in the inevitable extension of a proportion of microchannels into the papillary dermis. Progressive improvements to the microneedle device and advances in pharmaceutical formulation must therefore improve the reproducibility of penetration in order to promote exclusive delivery to the viable epidermis.

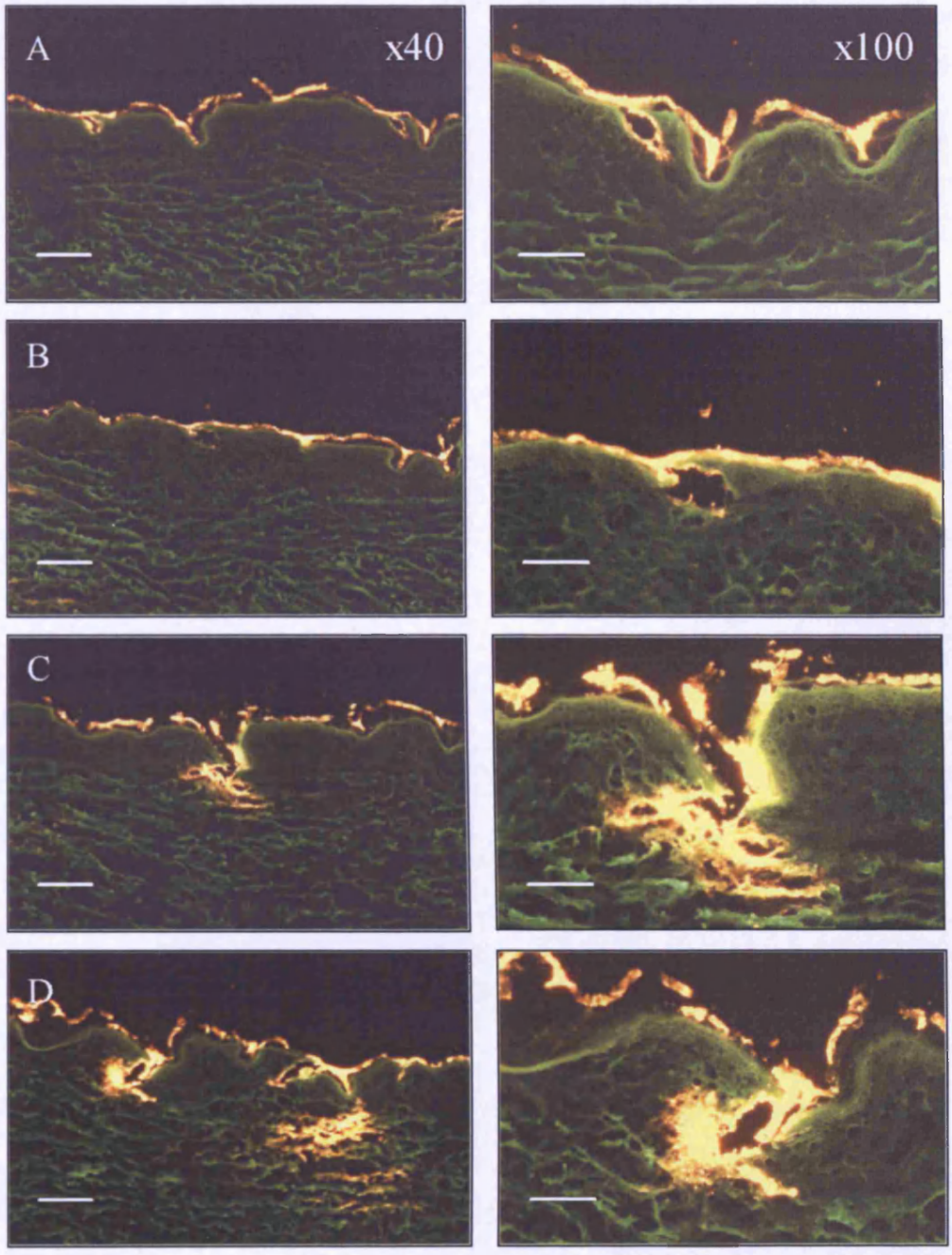


*Figure 4.11.* Transverse sections of human skin treated with a concentrated fluorescent red nanosphere formulation followed by the application of a frustum tipped microneedle array (TNI - Array 8). Matched images pictured at x40, scale bar = 200μm; x100, scale bar = 100μm. Skin was obtained from a 76 year old female donor.

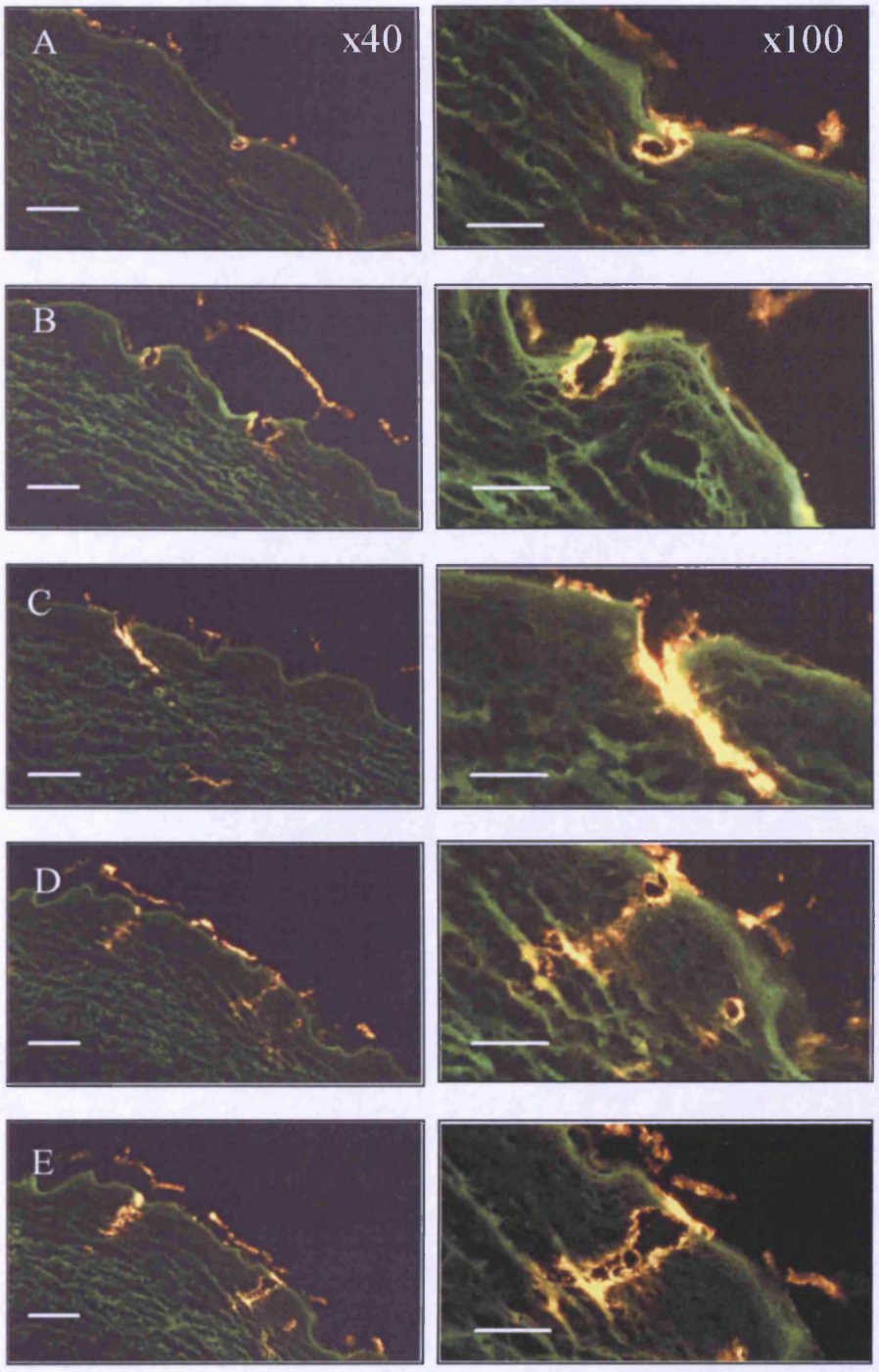


*Figure 4.12.* Transverse sections of human skin treated with a fluorescent red concentrated fluorescent nanosphere formulation followed by the application of a sharp tipped microneedle array (TNI - Array 5). Images are pictured at x40, scale bar = 200μm & x100, scale bar = 100μm. Skin was obtained from a 76 year old female donor.

### 4.4.4. Detecting β-galactosidase in *ex vivo* human skin

The successful incorporation of functional pDNA within LPD vectors and the ability of microneedle devices to facilitate delivery of such nanoparticle formulations to the viable cells of the epidermis are fundamental requirements for effective microneedle mediated cutaneous gene delivery. However, the success of this investigation also relied on the ability to successfully detect expression of reporter genes within human skin. The pEGFP-N1 plasmid is detected *in situ* using fluorescence microscopy. However, as previously indicated, human tissue possesses autofluorescent properties (Section 4.4.3.3). The pCMVβ reporter system was therefore selected to determine the extent and location of gene expression in human skin cells following cutaneous gene delivery.

The staining methodology utilised in mammalian cell culture studies cannot be directly extrapolated to *ex vivo* studies, where target cells are maintained within the epidermis in a three dimensional architecture, sandwiched between the SC and dermal tissue layers. Inefficient penetration of the staining solution to all epidermal cells and adverse interaction with the tissue must also be considered in the detection of those cells expressing the *lacZ* gene.

#### *4.4.4.1. Invivogen® protocol*

Following 12hrs of Invivogen® *lacZ* staining, *en face* images of untreated skin samples revealed a low level of endogenous staining (Fig 4.13A), particularly apparent around hair follicles (Fig 4.13B). Further staining of the negative control, up to 43hrs (Fig 4.13C & 4.13D), resulted in significant levels of endogenous surface staining. Therefore an alternative detection methodology was developed and validated to ensure that X-gal could facilitate unambiguous identification of cells within the tissue that contained the pCMVβ encoded bacterial β-galactosidase enzyme.

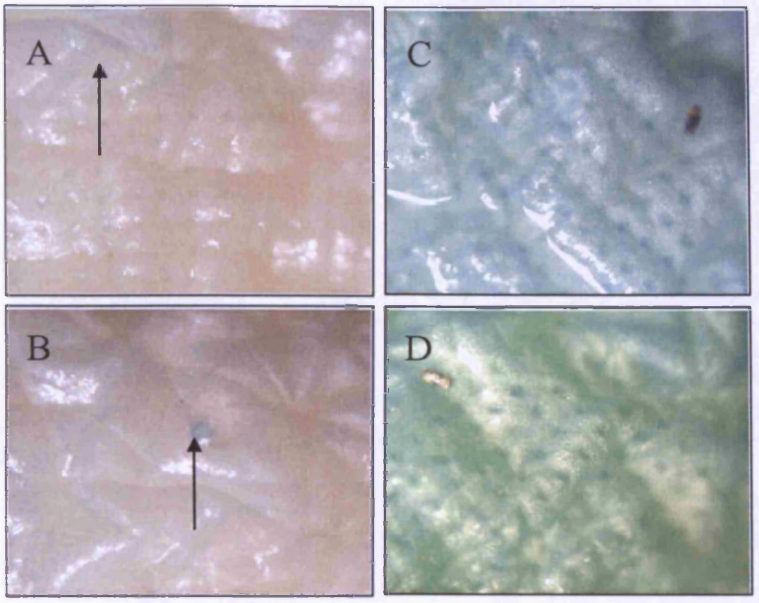


*Figure 4.13. En face* light microscopy images of microneedle treated human skin, to which a PBS solution has been applied. The skin is processed using the Invivogen® *lacZ* staining kit and immersed in the X-gal solution for (A), (B) 12hrs, (C) 35hrs and (D) 43hrs. Arrows indicate areas of positive staining. Skin was obtained from a 48 year old female donor.

#### *4.4.4.2. Optimising detection methods for the β-galactosidase enzyme*

Detection of the bacterial β-galactosidase enzyme by X-gal staining methods is dependent on a number of factors (Weiss et al., 1999):-

1. Fixation technique (glutaraldehyde versus paraformaldehyde versus formalin) could discriminate between endogenous and exogenous activity.
2. Overnight fixation reduced β-galactosidase activity to undetectable levels, therefore 30mins-2hrs in glutaraldehyde is recommended for whole tissues.
3. Altering the temperature and duration of X-gal exposure does not provide a reliable method of distinguishing between endogenous and exogenous enzyme activity.

4. Exposure of paraffin sections rather than the whole tissue to the X-gal solution results in poor β-galactosidase activity.
5. Endogenous enzyme activity is optimal at acidic pH values whilst exogenous activity is promoted at alkaline pH values.
6. The pH of PBS buffers are reduced during incubation with the tissue, particularly over considerable staining periods.
7. Tris–HCl buffer (100mM) preserves the selected alkaline pH value during the staining interval.
8. Commercial Kits suggest X-gal incubation times of 2-4hrs to reduce endogenous staining. However, both endogenous and exogenous activity is often eliminated.

This detailed investigation revealed the importance of the buffer used in X-gal staining procedures. By maintaining the pH of the X-gal staining solution at 8.0-8.5 unambiguous detection of exogenous β-galactosidase activity in lung tissue was achieved. This principle proved to be transferable to the detection of the β-galactosidase enzyme within the skin (Fig 4.14).

Control experiments suggested that minor changes in staining conditions can have major effects on the ratio of exogenous to endogenous β-galactosidase levels that are detected (Fig 4.14). The Invivogen® staining protocol produced significant levels of endogenous staining (Fig 4.14A). Such levels may mask subtle indications of successful keratinocyte transfection by the pCMVβ plasmid. The Hengge staining protocol reduced the level of endogenous stain considerably, possibly due to the lower incubation temperature (Fig 4.14B). However, the tissue that has been processed using the protocol developed by Weiss and co-workers displayed no evidence of endogenous stain (Fig 4.14C). This was attributed to retention of the pH between 8.0 and 8.5 during the incubation period. Maintenance of alkaline conditions upon immersion of the skin tissue produces optimal conditions for the bacterial β-galactosidase enzyme, produced by pCMVβ, and negates the effects of the mammalian enzyme which has acidic pH optima (Weiss et al., 1999).

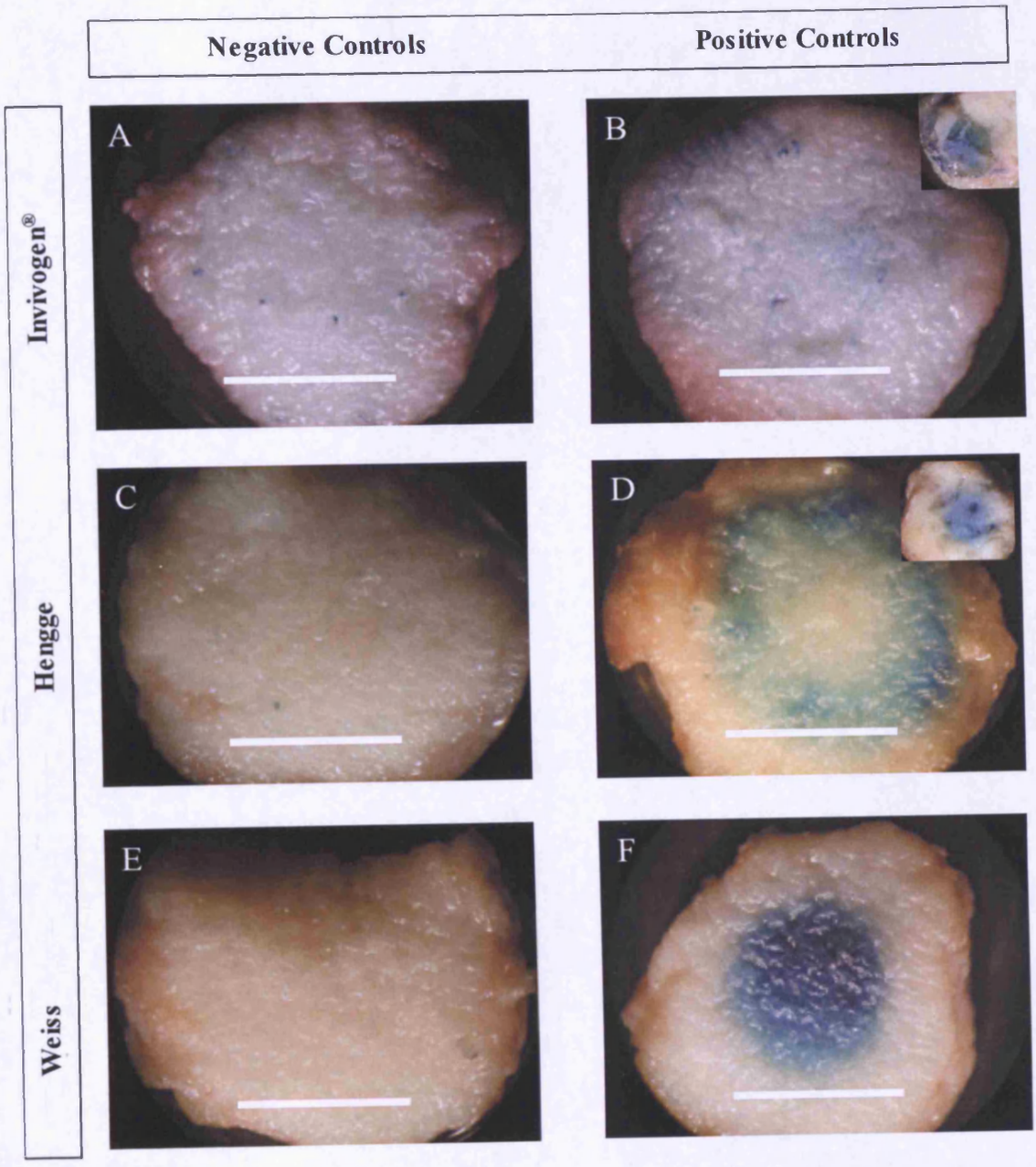


*Figure 4.14. En face* images of the human skin surface following intradermal injection of PBS (negative controls) or the β-galactosidase enzyme (positive controls). Detection of β-galactosidase activity with the Invivogen® (A, B), Hengge (C, D) and Weiss (E, F) protocols were analysed. Inserted images in B and D are of the underside of the tissue i.e. the dermis. Scale bar = 500μm. Female donor is a 78 year old female.

Intradermal injection of the β-galactosidase enzyme, included as a positive control, resulted in the development of an intense blue pigmentation using all three staining protocols. However distribution of the stain within the tissue was dictated by the accuracy of delivery. For Invivogen® and Hengge staining protocols the stain was most apparent in the dermal region, indicating that the enzyme was injected below the epidermal layer (Fig 4.14B & 4.14D) and for Weiss methodology the stain was located in the upper skin layers (Fig 4.14F). This supported previous observations, suggesting that intradermal injection, although variable, can deliver macromolecules to the upper area of the skin (Fig 4.9). Interestingly, unlike fluorescent nanoparticles, the enzyme was able to diffuse from its site of injection and therefore was detected throughout the epidermal layer (Fig 4.15).

### 4.4.5. Microneedle mediated cutaneous β-galactosidase delivery

The β-galactosidase enzyme was selected as a model protein to demonstrate the ability of a microneedle device to deliver a biologically active macromolecule into the epidermal region and to detect discrete areas of exogenous β-galactosidase enzyme *in situ*. Blue pigmentation was visible in a uniform pattern of discretely stained areas (Fig 4.16A). Transverse sections confirmed the ability of a microneedle device to disrupt the SC barrier and demonstrated the localised delivery of β-galactosidase up to 80μm below the skin surface (Figure 4.14B - 4.16D). Interestingly, membrane disruption by the dry-etch array appeared to be minimal and the enzyme was therefore retained exclusively within the confines of the epidermal region. A negative control served to confirm the absence of endogenous β-galactosidase activity. Cutaneous delivery of the β-galactosidase enzyme and its subsequent detection supported the previously recognised capabilities of the microneedle array and more importantly verified the methodology that will be employed in subsequent reporter gene studies to detect the pCMVβ encoded enzyme within the skin.

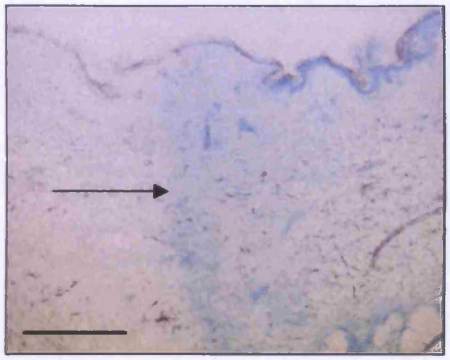

*Figure 4.15.* A 50μm cryosection of human skin, following intradermal injection of the β-galactosidase enzyme (positive controls), was stained using the protocol of Weiss and co-workers. Arrow indicates the detected boundary of the bolus intradermal β-galactosidase injection. Scale bar = 500 μm. Human skin was obtained from a 78 year old female donor.

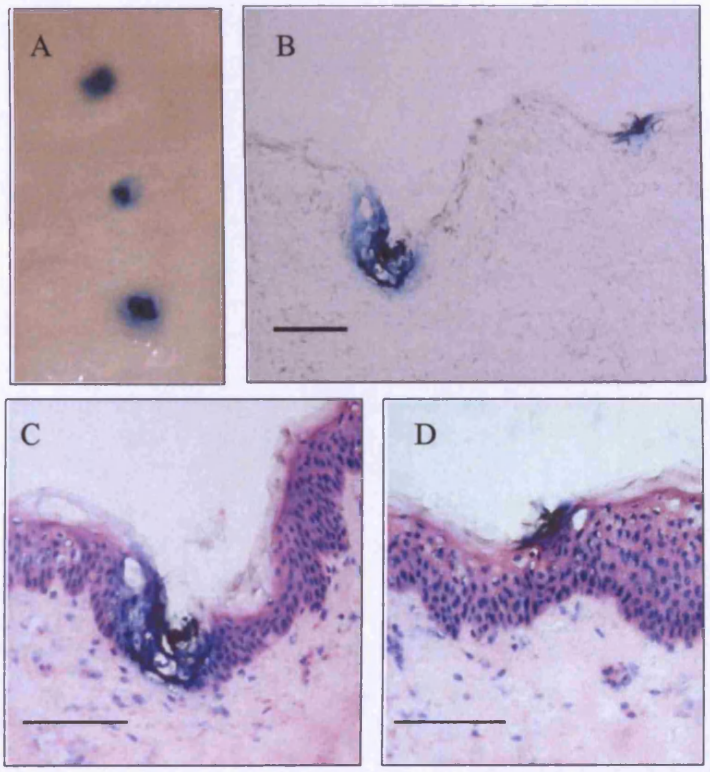


*Figure 4.16.* Dry-etch microneedle treated (CSE-Array A) human skin treated topically with the β-galactosidase enzyme. *En face* imaging (A), an unstained transverse cryosection (B) and H&E stained cryosections (C & D) illustrated the deposition pattern and localisation of the enzyme upon microneedle mediated delivery to the skin. Scale bar = 100μm. Human skin was obtained from a 43 year old female donor.

## 4.5. CONCLUSIONS

Three reporter plasmids were propagated, harvested and their functionality demonstrated in mammalian cell culture using an immortalised human keratinocyte cell line. These studies highlighted the importance of vector formulations, such as the LPD, in the successful transfection of keratinocytes *in vitro*. *Ex vivo* human skin however provides a more representative model of the *in vivo* environment and will be used in subsequent skin gene expression studies. The Trowell-type organ culture method has been adopted and adapted, in order to promote skin viability throughout the experimental time course (Gaylarde et al., 1975, Tammi et al., 1979).

Intradermal injection of nucleic acid therapeutics is an established but invasive method of cutaneous delivery. Initial studies using nanoparticle formulations suggested that the delivery capabilities of the microneedle array device compare favourably to intradermal injection. Successful microneedle mediated delivery of a nanoparticle formulation into human skin encouraged investigation of the device as an alternative minimally invasive platform for localised delivery of gene therapy formulations.

To investigate the cutaneous transfection of viably maintained *ex vivo* human skin, using a microneedle device, effective methods of detection are required. pCMVβ is an established reporter plasmid that encodes for the β-galactosidase enzyme. A robust methodology has been developed that permits unambiguous detection of the exogenous β-galactosidase enzyme.

# CHAPTER 5

# Cutaneous Gene Delivery Studies

## 5.1. INTRODUCTION

Recognition of the skin as an immunocompetent organ, responsive to localised nucleic acid vaccination strategies (Tang et al., 1992), and continued understanding of the genetic abnormalities associated with skin disease (Khavari, 1998, Magnaldo and Sarasin, 2002) has provoked considerable interest in cutaneous gene therapy (Hengge, 2005). However expression of an exogenous gene within the tissue requires effective delivery of a nucleic acid formulation to the viable epidermis and the efficient transfection of the cells therein.

To date the most successful methods of cutaneous gene delivery have been biolistic techniques (Fynan et al., 1993, Tang et al., 1992) and direct intradermal injection (Raz et al., 1994). However a number of limitations to these delivery methods have been identified, most notably their inability to deliver formulations exclusively to the epidermal layer and the significant practical constraints associated with each of the techniques. Microneedle array devices can deliver macromolecular and nanoparticle formulations to the epidermal region in a simple and potentially pain free manner (Smart and Subramanian, 2000). Their suitability as delivery platforms for cutaneous gene therapies has therefore been assessed in this Chapter.

### 5.1.1. Biolistic cutaneous gene delivery

In the early 1990's biolistic gene delivery, used for gene transfer in plants (Klein et al., 1987), was adapted for cutaneous immunisation (Fynan et al., 1993, Tang et al., 1992) and remains the most established delivery method for DNA vaccination (Dileo et al., 2003, Fynan et al., 1993, Lin et al., 2000, Pertmer et al., 1995, Wang et al., 2004). Numerous investigations, principally in animal models, have illustrated the ability of this technology to facilitate the localised expression of exogenous genes in skin (Chen et al., 2000, Dean and Chen, 2004, Fensterle et al., 1999, Han et al., 2000, Kitagawa et al., 2003, Rakhmilevich et al., 1996, Roberts et al., 2005, Tacket et al., 1999). The potential of biolistic DNA vaccination is therefore being assessed in pre-clinical and Phase I clinical trials (http://www.powdermed.com/developmentOverview.htm, 2006).

The principle of biolistic delivery is to propel pDNA coated microparticles (often gold) at high velocity, within a stream of helium gas, through the SC barrier and into the

underlying tissue. However, limitations to particle mediated transfection include, (i) failure of particles to traverse the SC barrier (Kendall et al., 2004), (ii) variability in the depth of microparticle delivery (Kendall et al., 2004), (iii) reduction in cell viability following administration (Raju et al., 2006), (iv) the unknown fate of non-biodegradable carrier particles within the treated tissue, (v) limited dosing capacity (resulting in repeated applications) (Baca-Estrada et al., 2000) and (vi) device impracticalities i.e. high cost and the requirement of a helium propellant system. These shortcomings encourage continued improvement to the device (Kendall, 2006) and have also stimulated interest in alternative novel cutaneous delivery methods.

### 5.1.2. Intradermal pDNA injection as a method of cutaneous gene delivery

Direct intradermal injection of a naked pDNA solution and the subsequent transfection of epidermal cells was first illustrated in mouse models in 1994 (Raz et al., 1994). However, it was studies by Hengge and co-workers in subsequent years that recognised the potential of this simplistic delivery strategy (Hengge et al., 1996). Investigations using murine, porcine and, most significantly, *ex vivo* human skin recorded localised expression of the β-galactosidase expressing reporter plasmid throughout the epidermis as early as 4hrs after treatment (Hengge et al., 1996). Expression was located in those cells surrounding the point of injection and predominated in the stratum spinosum layer, although transfection of basal and stratum granulosum cells was also evident.

These preliminary investigations were succeeded by a study comparing the expression of the pCMVβ reporter plasmid in both canine mucosa and porcine skin (Hengge et al., 1998). Interestingly, following injection of 20μg of the plasmid formulation the mucosal cells produced more encoded protein than the skin; 3.75μg of β-galactosidase detected within an 8mm biopsy of the buccal mucosa and just 100ng detected within skin. This was attributed to the lower proliferative potential of epidermal cells within the skin (Hengge et al., 1998).

Several studies by Sawamura and co-workers have also assessed intradermal pDNA injection for localised gene delivery (Meng et al., 1999, Meng et al., 2002, Sawamura et al., 2005, Sawamura et al., 2002a, Sawamura et al., 1998) and have demonstrated successful transfection of epidermal cells using a range of plasmids, from 0.6Kb to 9Kb

in size (Sawamura et al., 2002b). However elegant experiments using a rhodamine-labelled GFP expressing plasmid also highlighted the inefficiencies of the technique (Sawamura et al., 2002b). Although nearly all cells of the epidermis appeared to be interacting with the plasmid 4hrs after injection, this was not converted into significant levels of transfection.

Obstacles presented within the extracellular domain (Barry et al., 1999, Ruponen et al., 2003) and during the intracellular trafficking of exogenous DNA from the cell surface to the nucleus are well recognised (Howell et al., 2003, Lechardeur et al., 1999, Lechardeur et al., 2005, Wiethoff and Middaugh, 2003). For non-mitotic cells, including keratinocytes, it is estimated that at least 100,000 plasmids must be delivered to the cytoplasm of each cell to ensure passive penetration of plasmid material into the nucleus (Lechardeur et al., 2005). It is therefore not unreasonable to assume that the tortuous transition of a plasmid from its point of delivery in the superficial dermis, through the BMZ and across the epidermal cell membrane (Sawamura et al., 2002a) does not deliver sufficient quantities of a plasmid to facilitate efficient transfection. Therefore although direct intradermal injection is a useful tool, some even suggesting that it will have a place in the clinic in the future (Sawamura et al., 2002a), recent studies continue to highlight transfection inefficiencies as the principle hurdle to therapeutic progression (Meng et al., 2002, Meykadeh et al., 2005).

A number of strategies have been employed to heighten transfection efficiencies following intradermal injection of naked pDNA. These include subsequent electroporation of the tissue to improve cell membrane penetration (Babiuk et al., 2003, Drabick et al., 2001, Glasspool-Malone et al., 2000), the inclusion of nuclease inhibitors to reduce pDNA degradation by endonucleases (Barry et al., 1999, Glasspool-Malone et al., 2000) and the use of pDNA solutions of increasing ionic strength (Chesnoy and Huang, 2002) (thought to promote transfection by reducing interaction with tissue components and thus improving cellular delivery). However, although all of these strategies promoted cutaneous pDNA delivery, the resulting transfection efficiency remained low and unpredictable.

### 5.1.3. Topical application of formulations for cutaneous gene delivery

#### *5.1.3.1. Naked DNA*

Topical application of a nucleic acid formulation to facilitate efficient expression of the exogenous gene within the underlying viable epidermis would be the most desirable method of delivery, based upon the simplicity of formulation and ease of application. However, penetration of macromolecular therapies is restricted by the inherent barrier properties of the SC. A recent study demonstrated permeation of ~20ng plasmid/cm$^2$ through dermatomed human skin over a 24hr period and recorded measurable levels of the transcribed mRNA, both within the localised skin and lymph tissue (Kang et al., 2004). However, a permeation of 20ng plasmid/cm$^2$ translated to only 0.01% of the applied pDNA dose.

Topical application of naked pDNA to untreated skin therefore typically results in inefficient and irreproducible transfection of cells, primarily associated with the hair follicle (Fan et al., 1999, Udvardi et al., 1999). The physicochemical properties of pDNA (zeta potential of -30mV to -70mV, a hydrodynamic diameter of ~100nm and a MW of 1-10 million) (Piskin et al., 2004) and the barrier properties of the functional human skin barrier suggest that topical application of an aqueous pDNA solution to untreated human skin will never become a plausible method of facilitating efficient, reproducible cutaneous transfection. Topical pDNA application therefore often serves as a negative control in cutaneous transfection studies (Choi et al., 2006, Li and Hoffmann, 1995, Meykadeh et al., 2005, Mikszta et al., 2002).

#### *5.1.3.2. Non-viral vectors*

Lipoplexes have been utilised in cutaneous transfection strategies as a convenient, inexpensive vector that can increase the penetration of nucleic acids across the SC and more importantly promote the transfection of viable cells in the underlying epidermis without significant disruption of the skin surface. The hair follicle has been recognised as a portal for the entry of cationic liposome-DNA complexes and hence topical lipoplex application facilitates the transfection of keratinocytes within the follicular structure (Alexander and Akhurst, 1995, Domashenko et al., 2000, Li and Hoffmann, 1995). Partition of lipid based complexes into the sebum that surrounds the hairshaft

and subsequent interaction of the complex with the surrounding cells has been proposed as the delivery pathway (Birchall et al., 2000). Cells within the anagen phase, when the follicle is actively growing and cells are dividing, have been identified as particularly susceptible to transfection (Alexander and Akhurst, 1995, Domashenko et al., 2000, Hoffmann, 2000, Li and Hoffmann, 1995). A number of lipid based vesicles are therefore currently being analysed for cutaneous gene delivery, including conventional cationic liposomes (Babiuk et al., 2002, Baca-Estrada et al., 2000, Birchall et al., 2000, Shi et al., 1999), non-ionic liposomes (Niosomes) (Raghavachari and Fahl, 2002, Vyas et al., 2005), biphasic lipid delivery systems (Babiuk et al., 2002, Foldvari et al., 2006b) and transferosomes (Cevc et al., 1995, Kim et al., 2004). However although promising, the transfection efficiencies for topical lipoplexes remains low (Foldvari et al., 2006a, Meykadeh et al., 2005).

Other notable non-viral topical vector formulations include chitosan-based nanoparticles (Cui and Mumper, 2001) and microemulsion systems (Cui and Mumper, 2002). Both types of particle enhance cutaneous transfection in comparison to topically applied pDNA. However although they offer a number of distinct advantages, including reproducibility of nanoparticle formation, high DNA entrapment rates and biocompatibility of formulation components, transfection levels remain relatively inefficient. Recent studies have also assessed the inclusion of adjuvants (Cui and Mumper, 2003) and the use of biolistic methods of cutaneous delivery (Cui et al., 2003, Mumper and Cui, 2003) to improve the transfection efficiencies of these non-viral formulations.

Notably, prior to topical application of naked pDNA and non-viral gene therapy vectors investigators often utilise mechanical methods to disrupt the skin surface and thus enhance delivery. Tape/adhesive stripping (Liu et al., 2001, Udvardi et al., 1999, Watabe et al., 2001, Yu et al., 1999), depilatory products (Alexander and Akhurst, 1995, Shi et al., 1999) and abrasion (Yu et al., 1999) before topical application of formulations has been used to promote cutaneous gene expression (Choi et al., 2006, Foldvari et al., 2006b).

#### *5.1.3.3. Viral vectors*

Viral vectors have been successfully exploited as vehicles for delivering exogenous nucleic acid sequences to the skin (Ghazizadeh and Taichman, 2000, Hengge and Mirmohammadsadegh, 2000, Shi et al., 1999, Smith et al., 1985, Tang et al., 1997). However the questionable safety profile and the inflammatory response of the host organism to these viral vectors (Raper et al., 2003) has steered a significant number of investigators towards safer and potentially more simplistic non-viral methods.

### 5.1.4. Minimally invasive methods of cutaneous gene delivery

As previously discussed, microneedle mediated cutaneous delivery of nucleic acid formulations remains relatively unexplored (Section 1.5.7). Mikstza and colleagues have transfected keratinocytes in murine skin by lateral application of microenhancer arrays (MEA) across the skin surface, subsequent to the topical application of a pDNA solution encoding the firefly luciferase enzyme (Mikszta et al., 2002). This 'microabrasion' application method resulted in transfection levels comparable to intradermal injection and up to 2,800 fold greater than control samples. However to achieve this level of transfection at least six passages of the device across the skin surface were required. This study also assessed the ability of the MEA device to facilitate DNA immunisation. MEA delivery of the hepatitis B surface antigen (HBsAg) encoding plasmid to a mouse model resulted in antibody titres that were significantly greater and less variable than those achieved with intradermal injection (Mikszta et al., 2002). Such improvements in transfection levels are supported by studies using a puncture mediated method (similar to the tattooing process) (Ciernik et al., 1996) and microseeding (in which DNA is delivered by oscillating needles to a depth of 2mm) (Eriksson et al., 1998).

## 5.2. AIMS AND OBJECTIVES

### Chapter Aims

Previous chapters have demonstrated the cutaneous delivery capabilities of microneedle devices and have proven the functionality of nucleic acid formulations. Studies within this chapter aim to demonstrate transfection of epidermal cells within *ex vivo* human skin tissue and to investigate the suitability of a microneedle array device as a means of facilitating localised delivery and expression of a reporter plasmid. Naked pDNA and the LPD non-viral vector will be assessed in these studies.

### Chapter Objectives

- To transfect excised human skin by intradermal injection of a naked pDNA solution, thereby demonstrating tissue viability and reporter plasmid functionality.

- To translate the *in vitro* transfection capabilities of an LPD vector, noted in Chapter 4, to *ex vivo* human skin.

- To evaluate wet-etch and dry-etch microneedle arrays for the cutaneous delivery of nucleic acid formulations and their subsequent expression within human skin.

## 5.3. METHODS

### 5.3.1. Materials

All reagents were obtained from Fisher (Loughborough, UK) and were of analytical grade, unless otherwise stated.

The pCMVβ plasmid (7.2 kb), the pEGFP-N1 plasmid (4.7kb) and the recombinant β-galactosidase enzyme were obtained from Promega Corporation (Madison, WI). The Qiagen® Plasmid Mega Kit was obtained from Qiagen® (Crawley, UK).

1,2-Dioleoyl-3-triammonium-tropane (DOTAP) was purchased as the methyl sulphate salt from Avanti Polar Lipids (Alabaster, AL, USA). Protamine sulphate, BSA, chloroform and components of the X-gal staining solution were obtained from Sigma-Aldrich Chemical Company (Poole, UK).

Cell culture plastics were obtained from Corning-Costar (High Wycombe, UK). MEM (EAGLES) 25mM HEPES, Dulbecco's Modified Eagle's Medium (DMEM 25mM HEPES), FBS, trypsin-EDTA and penicillin-streptomycin solution were obtained from Invitrogen Corporation (Paisley, UK). Histology materials were obtained from RA Lamb Limited (Eastbourne, UK) with the exception of toluidine blue, Harris' haematoxylin, Gurrs' eosin aqueous solution 1%, Histomount® and xylene (low sulphur) which were purchased from Lab 3 (Bristol, UK).

Equipment:-

Fluostar Optima Plate Reader (BMG Labtech, Aylesbury, UK)
Eppendorf Biophotometer (Cambridge, UK)
FACScalibur System (Beckton Dickinson, California, UK)
Extrusion apparatus (Northern Lipids, Vancouver, Canada)
Olympus IX-50 Inverted Microscope System (Olympus Optical, London, UK)
Olympus BX-50 Microscope System (Olympus Optical, London, UK)
Olympus DP10 Microscope Digital camera system (Olympus Optical, London, UK)
Olympus U-RF-L-T Power Supply Unit (Olympus Optical, London, UK)
Anthos Labtec HT2 96 well plate reader (Anthos, Salzburg, Austria)
Schott KL1500 fibre optic light source (Schott UK Limited, Stafford, UK)
Stemi 2000-C stereomicroscope (Zeiss, Welwyn Garden City, UK)
Olympus Camedia C-4040 Zoom Digital Camera (Olympus Optical, London, UK)

### 5.3.2. *Ex vivo* cutaneous transfection investigations

#### *5.3.2.1. Ex vivo organ culture*

Following removal from the donor, fresh excised human skin was placed immediately in nutrient skin media (DMEM supplemented with 5% FBS and 1% penicillin/ streptomycin) and transported on ice to the laboratory. Under containment 2 conditions sub-cutaneous fat was removed from the tissue by blunt dissection and the tissue was dried. The skin was then pinned to a dissection board and a significant proportion of the dermis was removed using a stainless steel razor blade and discarded. The formulation under investigation and control formulations were then applied to the split-thickness skin using either a hypodermic needle or a microneedle array. The combination of formulations and devices discussed during these studies are detailed in subsequent sections. The tissue was then divided into treatment areas (~1$cm^2$) and maintained at the air-liquid interface at 37°C:5%$CO_2$ in organ culture for 24hrs prior to detection of the reporter gene (Section 4.3.4).

Experiments were conducted using human tissue from a number of donors, using various concentrations of plasmid solutions and a range of microneedle array devices. Therefore the age of the skin donor, the concentration and identity of the formulation applied and the device selected to facilitate cutaneous delivery are detailed within the figure legend to which they relate.

#### *5.3.3.2. Ex vivo transfection methods (Non-microneedle)*

During this investigation a number non-microneedle methods of cutaneous pDNA delivery have been investigated. Delivery techniques have included intradermal injections, topical application of an LPD and a lateral hypodermic scrape amongst others. The concentration of pDNA solutions and the identity of reporter plasmids used in the experiments discussed in this Chapter have been summarised in the table overleaf (Table 5.1). The text accompanying the table describes each of the formulations used, the experimental controls and the method of cutaneous application.

Table 5.1. Experimental protocols used in the discussed studies that examined the transfection of *ex vivo* human skin with non-microneedle methods of delivery. The figure within this chapter to which each of the methodologies relates has been included.

| Figure | Formulation | Controls | Cutaneous application method |
|---|---|---|---|
| **5.2** | pCMVβ solution (1mg/ml) | Negative: PBS<br>Negative: pEGFP-N1 solution | Intradermal Injection (dipped) |
| **5.3** | pCMVβ solution (1mg/ml) | Negative: PBS<br>Positive: β-galactosidase enzyme | Intradermal Injection |
| **5.4** | pEGFP-N1 solution (1mg/ml) | Negative: PBS Buffer | Intradermal Injection |
| **N/A** | LPD complex (pCMVβ) | Negative: pEGFP-N1 solution<br>Positive: pCMVβ concentrated solution | Intradermal Injection & Topical Application |
| **5.5** | Concentrated pCMVβ solution | Negative: PBS | Lateral Hypodermic Scrape |

- **Intradermal injection**: The lower section (~50%) of a 200µl pipette tip was removed and a hypodermic needle (Microlance® 3 0.5x25G) was attached to the remaining tip. This in turn was attached to a pipette (2-20µl) to permit exact volumes to be injected intradermally into the skin. Intradermal injection involved insertion of the needle at an acute angle to the skin surface in order to deliver the formulation as close to the skin surface as practically possible.

- **Intradermal injection (dipped)**: Before intradermal injection (described previously), the hypodermic needle was immersed in red fluorescent nanospheres (100nm diameter, 1µl concentrate/10µl deionised water) for 5secs.

- **Lateral Hypodermic Scrape**: The hypodermic needle was immersed in a concentrated plasmid solution for 30secs. The tip was then inserted vertically into the uppermost skin layer and dragged laterally across the skin surface.

- **LPD complex:** LPD gene therapy complexes contained 2.5μg of pCMVβ in 30μl of the colloidal suspension in a 1:2:3w/w ratio of pDNA to protamine to DOTAP liposome, as previously described (Section 3.3.2.1). The formulation was applied to the skin by intradermal injection and topical application. 30 μl and 60μl formulation volumes were investigated.

- **pCMVβ solution**: A 1mg/ml plasmid solution within TE buffer at pH8.0. A concentrated solution was 2.5-3.0mg/ml.

- **β-galactosidase enzyme:** A solution of the bacterial β-galactosidase enzyme (1Unit/100μl) was included in early studies as a positive control.

### *5.3.3.3. Ex vivo transfection methods (Microneedle devices)*

A number of microneedle devices and application methods have been employed during these investigations. For simplicity, these studies have been summarised in Table 5.2 (wet-etch microneedles) and Table 5.3. (dry-etch microneedles). During investigations, the orientation of the skin sample and the application of the device were progressively adapted to mimic the *in vivo* skin environment more closely and to improve the penetration of the microneedle device. The subsequent text describes the formulations used, the orientation of the skin, the microneedle applicator and the application technique for both types of microneedle device studied (Table 5.2 & 5.3).

All reporter plasmid formulations were prepared by plasmid propagation and isolation procedures (Section 4.3.2). The concentrations used were between 2.5-3.5mg/ml for all experiments. The specific plasmid concentration utilised within individual experiments is detailed in the related figure legend. Alternative reporter plasmids were used as controls.

**Wet –etch Microneedles**

For details of the experimental parameters within wet-etch microneedle studies, the reader is referred to Table 5.2.

- **Microneedle applicators:** The microneedle arrays were attached to applicators to enable the device to be applied in a more controlled manner. Initial studies attached ~0.5cm$^2$ arrays to a syringe plunger using a cyanoacrylate adhesive (plunger). However, the majority of studies used wet-etch devices where arrays were attached to steel cylindrical columns (2-5cm in length) using an epoxy resin (rod).

- **Rolling application:** Wet-etch microneedles were applied to skin using the rolling application method (Section 2.3.8). Briefly, this involved maintaining split-thickness human skin under tension over a curved cork platform. The plasmid solution was pipetted onto the skin surface and the device was then

applied to the topically treated area. The microneedle array was positioned at a 45° angle to the skin surface and rotated forward through an angle of approximately 90°, finishing at a 45° angle to the skin surface in the opposing direction. Downward force was maintained throughout the application. This was considered to be a single application. To apply the device to the skin a second time the contact of the microneedle and the skin was maintained and the device was then rotated in the opposite direction. Therefore, in studies investigating the influence of repeated microneedle application on transfection efficiency, where the array was applied on ten occasions, the array was moved repeatedly forwards and backwards in this 'rocking' motion.

- **Lateral application:** For lateral application, split-thickness human skin (Section 4.3.4) was maintained under tension on a cork dissection board in a flattened state. The formulation to be investigated was topically applied to the skin surface. The microneedle device was then applied in a downward motion to the edge of the treated area, under relatively constant pressure, for a period of approximately 2secs and subsequently moved laterally across the skin surface (Fig 5.1).

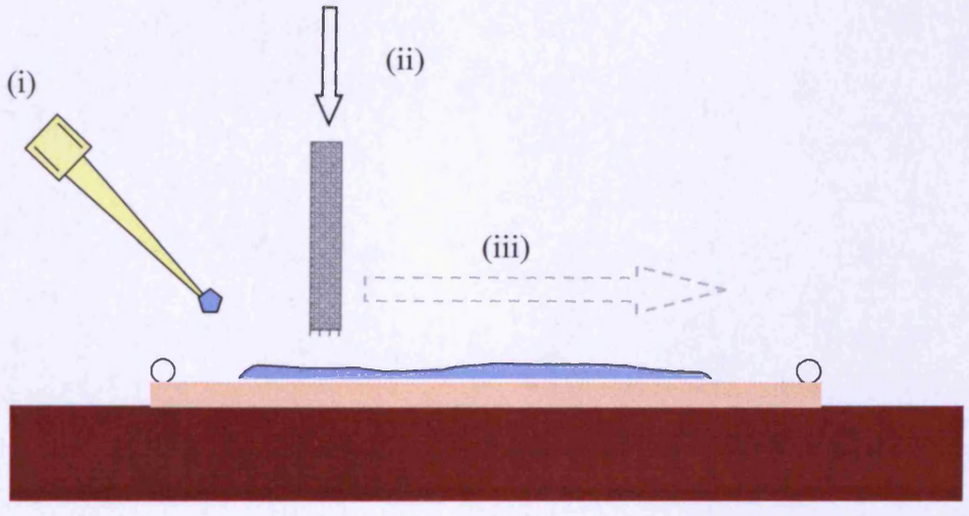


*Figure 5.1.* A schematic representation of the lateral transfection process using wet-etch microneedle devices, (i) the formulation was applied and distributed over the tissue surface, (ii) the microneedle device was applied in a downward motion to the skin tissue, (iii) the device was moved in a lateral motion over the topically treated area.

Table 5.2. A summary of experimental protocols for investigations using **wet**-etch microneedles. The figure within this chapter to which each of the methodologies relates has been included.

| **Figure** | **Formulation** | **Controls** | **Skin set-up** | **Applicator** | **Tip Shape** | **TNI Array ID** | **Application method (No of applications)** |
|---|---|---|---|---|---|---|---|
| **5.10** | Conc pCMVβ solution | Conc pEGFP-N1 | Curved skin | Plunger | Frustum | 1 | Rolling (2) |
| **5.11** | Conc pCMVβ solution | Conc pEGFP-N1 | Curved skin | Rod | Frustum | 2 | Rolling (1) |
| **5.12** | Conc pCMVβ solution | Conc pEGFP-N1 | Curved skin | Plunger | Frustum & Sharp | 1 & 6 | Rolling (2) |
| **5.13** | Conc pCMVβ solution | Conc pEGFP-N1 | Curved skin | Rod | Frustum | 3 | Rolling (10) |
| **5.14** | Conc pCMVβ solution | Conc pEGFP-N1 | Flat skin | Rod | Frustum | 2 | Lateral (1) |
| **5.15 (A-D) 5.15A-H** | Conc pCMVβ solution | Conc pEGFP-N1 | Flat skin | Rod | Frustum | 6 | Lateral (1) |
| **5.15E 5.16I** | Conc pCMVβ solution | Conc pEGFP-N1 | Flat skin | Rod | Frustum | 8 | Lateral (1) |

**Dry-etch Microneedles**

For details of the experimental parameters within dry-etch microneedle studies, the reader is referred to Table 5.3.

- **Microneedle applicators:** the dimensions of the dry-etch microneedles (0.5x1cm) did not permit attachment to the steel rods used previously for wet-etch arrays. These arrays were therefore mounted upon aluminium stubs (normally used to mount samples for SEM analysis) using double sided adhesive tape.

- **Rolling application:** Arrays were applied to the skin using a rolling application method, as previously detailed for the wet-etch arrays. The only difference was that split-thickness skin to which the array was applied was maintained on a flattened cork support, in a similar manner to that previously detailed for the lateral application.

#### *5.3.3.4. β-galactosidase detection in human skin tissue*

The skin was processed, 24 hours after treatment, to identify those cells successfully transfected with pCMVβ (Section 4.3.6.2). On removal from the staining solution the sample was rinsed, positioned on a glass microscope slide and visualised *en face* (Section 4.3.6.3). Selected skin samples were sandwiched between two glass slides. This reduced the dermatoglyphics of samples, thereby improving visualisation of blue pigmented areas on the skin surface. Samples were then cryosectioned and tissue histology was examined using techniques described previously (Section 4.3.6.3).

Prior to *en face* imaging, selected tissue samples were also counterstained with Nuclear Fast Red (NFR), a low MW dye normally used in histological techniques. A 5%w/v solution of NFR in deionised water was applied topically to the microneedle treated area and removed after 30mins. The surface of the skin was then swabbed repeatedly with ethanol and the sample was mounted between two microscope slides and visualised *en face* (Section 4.3.6.3). NFR penetrates disruptions in the SC, stains the underlying tissue and therefore permitted visualisation of microneedle fashioned conduits in the skin.

Table 5.3. A summary of experimental protocols utilised during investigations with **dry**-etch microneedles. The figure within this chapter to which each of the experimental procedures relates has been included.

| **Figure** | **Formulation** | **Controls** | **Skin set-up** | **Applicator** | **Cork ID** | **Application method** |
|---|---|---|---|---|---|---|
| **5.17**<br>**5.18** | Conc pCMVβ solution | Conc pEGFP-N1 | Flat split skin | Aluminium Stub | 15 | Rolling (2) |
| **5.19**<br>**5.20** | Conc pCMVβ solution | Conc pEGFP-N1 | Flat split skin | Aluminium Stub | 15 | Rolling (2) |

#### *5.3.3.5. GFP detection in human skin tissue*

Following administration of pEGFP-N1 to the skin and an incubation period of 24hrs in organ culture, the skin was rinsed briefly in PBS and embedded in OCT medium. The tissue was then cryosectioned and visualised by fluorescence microscopy (Section 4.3.6.3).

## 5.4. RESULTS AND DISCUSSION

### 5.4.1. Intradermal injection of pDNA formulations into human skin

#### *5.4.1.1. Evidence of cutaneous transfection*

Before assessing the potential of the microneedle device as a platform for cutaneous gene delivery, it was fundamental to establish the functionality of the plasmid reporter system in human skin and in doing so demonstrate the viability of the excised tissue in organ culture. Direct intradermal injection of naked pDNA is an established method of delivery for the localised expression of exogenous reporter genes (Hengge et al., 1996). Previous experience with this delivery technique (Section 4.3.5.2 & 4.3.6.2) indicated that a significant proportion of the dose would be delivered into the dermal region. Contact of a nucleic acid formulation with viable epidermal cells therefore relied upon upward migration of the formulation from its delivery point in the superficial dermis and/or direct interaction with cells that surround the 'needle track'.

Following intradermal administration of a pCMVβ solution (1mg/ml), the skin was maintained in culture for 24hrs to permit transcription and translation of the *lacZ* gene and subsequently exposed to the X-gal substrate. Successful expression of the reporter plasmid was observed as discrete blue areas of pigmentation, up to 250μm in diameter (Fig 5.2A), within the upper layers of the skin (Fig 5.2B). Subsequent H&E staining highlighted the cellular architecture of the tissue and revealed localisation of the pigment to the viable epidermis (Fig 5.2C). Tissues injected with the pEGFP-N1 reporter plasmid, as a control, did not display any signs of blue pigmentation (data not shown). Prior to pCMVβ injection, the needle was 'dipped' in a fluorescent red nanoparticle suspension. This was used to determine the proximity of the transfection point to the location of the hypodermic needle upon delivery of the plasmid solution. Traces of red fluorescence, located in the dermal region underlying the point of transfection (Fig 5.2D), confirmed that the discrete area of blue pigmentation was directly associated with the point of intradermal injection.

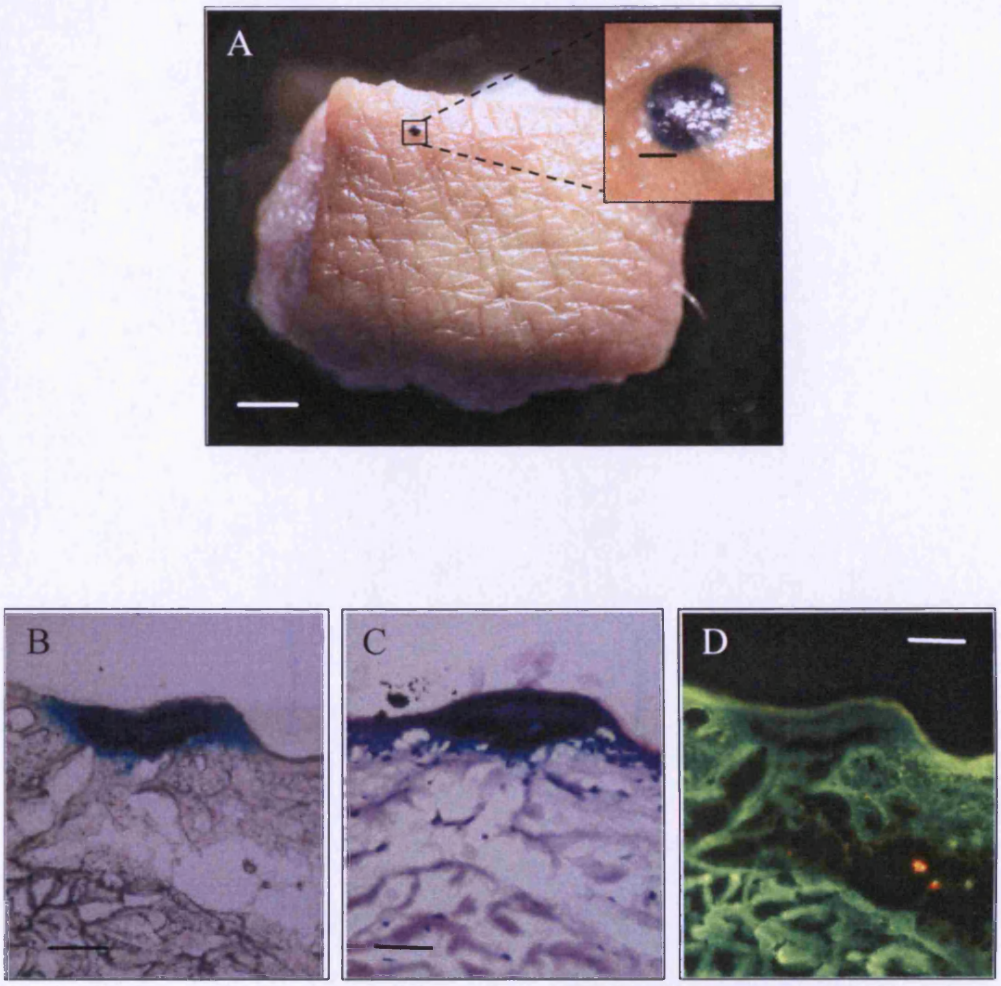


*Figure 5.2.* Successful transfection following intradermal injection of 10µl pCMVβ (1mg/ml) using a hypodermic needle that was dipped in a fluorescent nanosphere formulation prior to administration. A, scale bar = 1mm (inset scale bar = 100µm). Cryosections of the tissue revealed the location of the transfection point and the tissue architecture B, C, D, scale bar = 50µm. Donor skin was obtained from a 58 year old female.

Further studies using a different donor tissue confirmed these observations (Fig 5.3). The two areas of transfection observed following intradermal injection of the pCMVβ formulation were associated with a major disruption of the skin surface (Fig 5.3B & 5.3D). It may be assumed that the disruption was caused by penetration of the hypodermic needle into the tissue. Histological evaluation indicated that viable epidermal cells were transfected at the point of the needles entrance into the skin (needle track) and also in a cellular region at the tip of the needle, from which the formulation was delivered (Fig 5.3C & 5.3E). The two areas of transfection noted were therefore produced by a single injection.

Transfection following intradermal pCMVβ injection was always witnessed in discrete cellular areas associated with the point of injection. This was attributed to a combination of promoted intracellular delivery and restricted dissemination of the intact formulation from its site of deposition (Hengge et al., 2001, Lin et al., 2001, Mirmohammadsadegh et al., 2002). Large membrane disruption (Budker et al., 2000), where the cell membrane is temporarily disrupted by the mechanics of the delivery technique, and hydrodynamic pressure (Zhang et al., 2004), where the plasmid is forced through transient pores in the cell membrane, have been proposed as mechanisms of intracellular plasmid delivery following direct pDNA injection.

The pEGFP-N1 plasmid, encoding for GFP, was selected as an alternative reporter system to confirm observations made with pCMVβ. However the autofluorescence of human skin (Fig 5.4A), which appeared heightened by mechanical disruption of the skin surface, resulted in significant levels of endogenous green fluorescence surrounding the point of injection (Fig 5.4B). This compromised exclusive detection of GFP and the reporter plasmid was therefore discarded as a method by which to detect cutaneous transfection using microneedle devices.

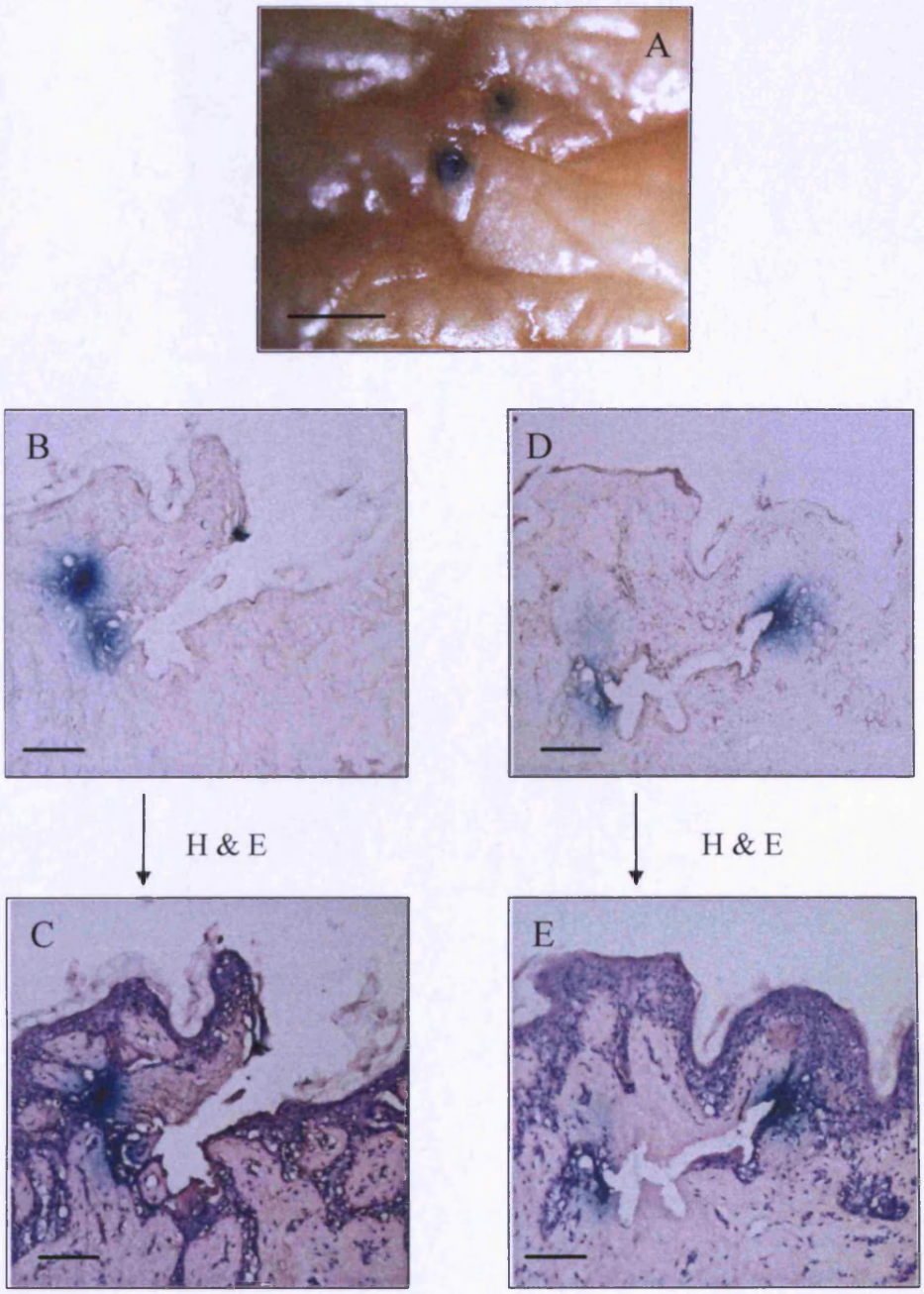


*Figure 5.3.* Successful transfection following intradermal injection of 20µl of pCMVβ (1mg/ml) can be detected *en face* following X-gal staining. A; scale bar = 500µm. Cryosections of the tissue revealed the exact location of transfection (B & D) and H&E staining permits visualisation of the surrounding tissue architecture (C & E). B-E scale bar = 100µm. Donor skin was obtained from a 51 year old female.

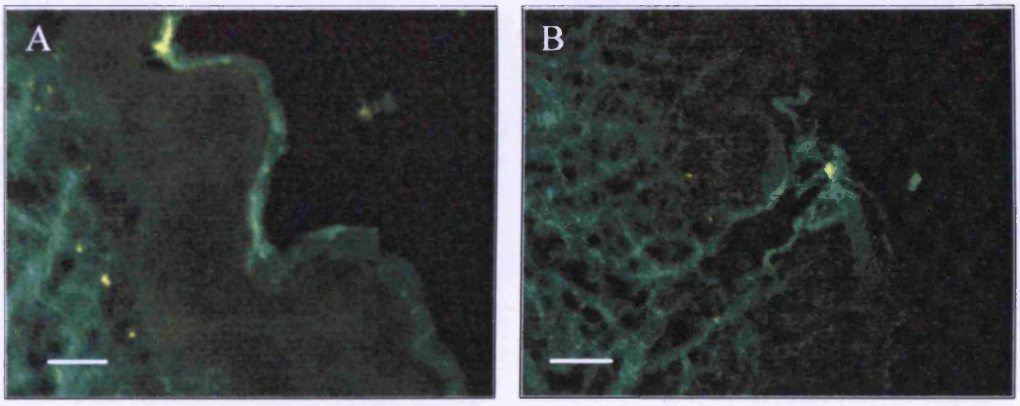


*Figure 5.4.* Cryosections of human tissue following intradermal injection of 50µl of pEGFP-N1 (1mg/ml). A, scale bar = 50µm; B, scale bar = 100µm. Donor skin was obtained from a 54 year old female.

In conclusion, successful expression of exogenous pDNA within *ex vivo* human skin confirmed the cellular viability of human skin maintained within organ culture and validated the applicability of this model for future studies. Detection of the pCMVβ encoded β-galactosidase enzyme and the omission of endogenous pigmentation in control samples confirmed the usefulness of this reporter plasmid. However, although the location and intensity of blue pigmentation identified the co-ordinates, and to a degree the relative levels of transfection, it did not permit identification of individually transfected cells. However diffuse colouration, attributed to permeation of the β-galactosidase enzyme into the extracellular environment, is consistent with other studies that have utilised this reporter system (Hengge et al., 1995, Hengge et al., 1998, Hengge et al., 1996).

#### *5.4.1.2. Inefficient cutaneous transfection*

In this investigation over one hundred intradermal injections have been conducted, using fourteen donor tissues, over a period of six months (Appendix II – TableA1). However, successful transfection of human tissue was only evident on 17 occasions. Inefficient and poorly reproducible transfection was attributed to limitations of intradermal injection as a method for localised gene delivery (Meng et al., 2002, Meykadeh et al., 2005). However, although transfection efficiency was poor it is likely to be an underestimate of *in vivo* transfection. Removal of skin from the donor organism reduces tissue viability, resulting in a concomitant reduction (up to ten times) in the achievable transfection levels (Hengge et al., 1998, Hengge et al., 1996), and detection of the pCMVβ reporter gene also has acknowledged limitations, the X-gal staining procedure only identifies ~80% of successfully transfected cells within skin tissue samples (Couffinhal et al., 1997).

The architecture of the skin (Fig 5.2 & Fig 5.3), itself highly variable between the examined donor tissues, may have also contributed to the poor reproducibility of transfection. Logically, tissues with thinner epidermal layers may be considered more difficult to transfect due to a reduced population of viable cell candidates and a smaller target area for cutaneous transfection. Inherent inter- and intra- individual differences in skin structure is a significant challenge to the design of all novel cutaneous delivery systems. The objective is therefore to develop a platform that can deliver therapeutics to a heterogeneous tissue in a reproducible manner.

#### *5.4.1.3. Assessing plasmid dose*

Preliminary investigations, conducted in the same donor tissue indicated that increasing the concentration of the pCMVβ solution (from 1mg/ml to 2.5mg/ml) promoted identifiable cutaneous transfection. However amassing of the experimental data achieved over the investigated period did not support these initial observations (Appendix II-Table A1). Hengge and co-workers suggest that intradermal injection of up to 20μg of pDNA in a volume of 50-100μl is optimal, higher concentrations providing negligible improvements to transfection levels (Hengge et al., 1995). However, Sawamura and co-workers oppose this observation, indicating that 6μg in 30μl is the optimal dose (Sawamura et al., 2002b). Investigations that utilise electroporation to enhance transfection following intradermal injection use up to 200μg of pDNA in 100μl (Drabick et al., 2001, Dujardin and Preat, 2004). The optimal pDNA dose and volume remains undetermined and therefore concentrated plasmid solutions were selected for the majority of studies discussed in the subsequent text.

### 5.4.2. Selecting a nucleic acid formulation to facilitate transfection of human skin

Human keratinocytes maintained in mammalian cell culture required a non-viral vector, the LPD, to facilitate cell transfection (Section 4.4.2). However, this did not translate to human skin studies. Both topical application and intradermal injection of LPD formulations failed to demonstrate detectable levels of the β-galactosidase enzyme at 24hrs post-treatment (data not shown). In a parallel experiment, in the same donor tissue, intradermal injection of naked pCMVβ facilitated observable levels of transfection (Section 5.4.1.1). This is a direct reversal of observations made in mammalian cell culture. Failure of the LPD complex *ex vivo* may be attributed to the reduced plasmid concentration in the formulation (28.7μg/10μl in concentrated pDNA compared to 2.5μg/30μl in the LPD). The concentration of pDNA in the LPD complex was restricted due to precipitation of LPD vectors at increased concentrations and small sample volumes. An optimal topical dose of ~8μg/30ml has been suggested for cationic complexes (Alexander and Akhurst, 1995, Birchall et al., 2000). However, conflicting studies indicate that only 3μg of a reporter plasmid is required to facilitate detectable cutaneous transfection (Sawamura et al., 2002b).

The failure of topically applied and injected LPD formulations to facilitate identifiable cutaneous transfection within human skin therefore prompted employment of naked pDNA for studies using microneedle devices. Recognition of naked pDNA injections, in the absence of additional carrier systems, as an effective nucleic acid delivery system in both skin and muscle tissue is increasing (Basner-Tschakarjan et al., 2004, Budker et al., 2000, Mirmohammadsadegh et al., 2002). It has even been suggested that keratinocytes possess a specific ability to take up and process naked pDNA by a novel receptor-mediated process. However, the identity of the receptor, mechanisms of transmembrane movement and intracellular trafficking remain unknown (Basner-Tschakarjan et al., 2004, Budker et al., 2000, Wolff and Budker, 2005).

### 5.4.3. Lateral disruption of the skin surface

Topical application of naked pDNA to human skin was used as a control in numerous experiments during the course of this investigation (data not shown) and, in agreement with previously published data, this failed to facilitate detectable levels of localised transfection (Choi et al., 2006, Li and Hoffmann, 1995, Meykadeh et al., 2005, Mikszta et al., 2002). It therefore became apparent that delivery of the formulation across the SC barrier was critical to the effective transfection of epidermal cells. Intradermal injection of pDNA was poorly reproducible (highly dependent upon the skill of the administrator) and evidence of transfection was restricted to a single point of injection. Microneedle array devices were therefore considered to offer a more controlled method of delivery that could expose larger areas of the viable epidermis to the pDNA formulation following multiple penetrations of the skin surface.

As a prelude to gene delivery investigations using microneedles, a hypodermic needle was immersed in a concentrated solution of pCMVβ and 'scratched' along the skin surface. Two of the four treated areas displayed discrete points of transfection directly associated with the needle track (Fig 5.5A). This was not replicated using the 1mg/ml formulation. Transverse sections revealed significant tissue damage, the epidermal layer separating from the underlying dermis in the treated area (Fig 5.5B). This might be expected to retard transfection efficiency as successful expression of pDNA is dependent upon the functionality of cells within the tissue.

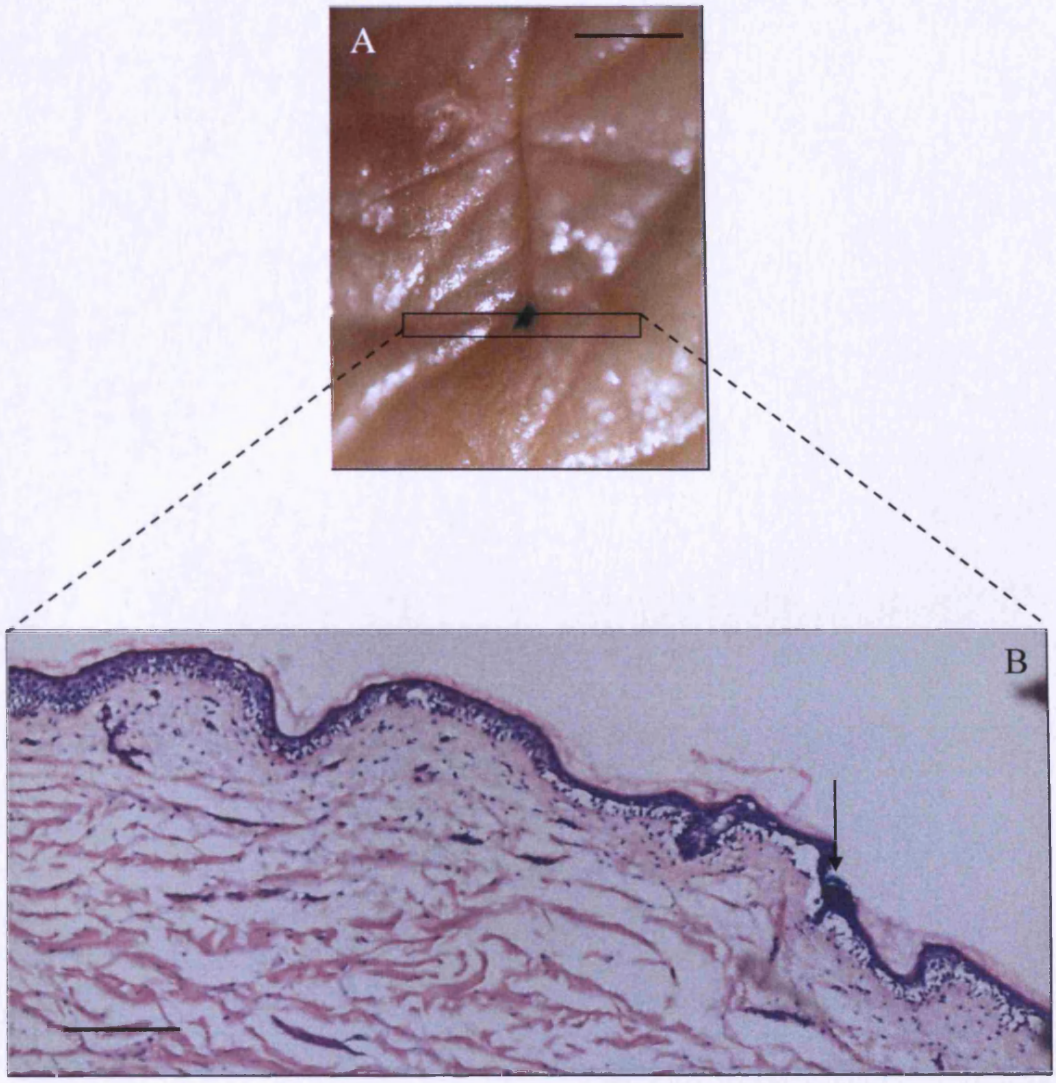


*Figure 5.5.* Successful transfection, indicated by arrow, following lateral application of a hypodermic needle (dipped prior to application in pCMVβ (2.9mg/ml)) across *ex vivo* human skin. A, scale bar = 500μm; B, scale bar = 200μm. Donor skin was obtained from a 77 year old female.

### 5.4.4. Microneedle transfection

The transfection of human skin tissue with pCMVβ, following both intradermal injection and the lateral disruption method, encouraged investigation of the microneedle device as a means to improve the reproducibility and efficiency of transfection in a less invasive fashion. A number of wet- and dry-etch microneedle devices were assessed and several application methods used to promote delivery of the pCMVβ formulation.

#### *5.4.4.1. Wet-etch microneedles*

##### *5.4.4.1.1. Rolling wet-etch microneedle application*

Application of a frustum tipped wet-etch microneedle device facilitated successful cutaneous gene delivery and subsequent expression in human skin (Fig 5.6A & 5.6B). A uniform pattern of pigmented transfection points was indicative of the spacing between microneedles within the array (Fig 5.6A & 5.6B). Each transfected area was over 100μm in diameter and the pigment was located in close proximity to microneedle disruptions within the viable epidermis (Fig 5.6C & 5.6D). Microchannels were approximately 50μm in diameter and on occasion extended from the skin surface to the papillary dermis (Fig 5.6C & 5.6D). It should be noted that no evidence of successful transfection was observed in any control samples included in this experiment or in the microneedle studies that are discussed in the remainder of this Chapter (data not shown). The exclusive transfection of cells proximal to the microconduit suggested that the pDNA formulation was retained in close proximity to its point of delivery. This was synonymous with those observations made following intradermal pDNA injection (Section 5.4.1.1). Elevated transfection levels within the localised region may also be explained by enhanced intracellular delivery of pDNA resulting from temporary mechanical disruption to cell membranes upon contact with individual microneedle structures (Budker et al., 2000).

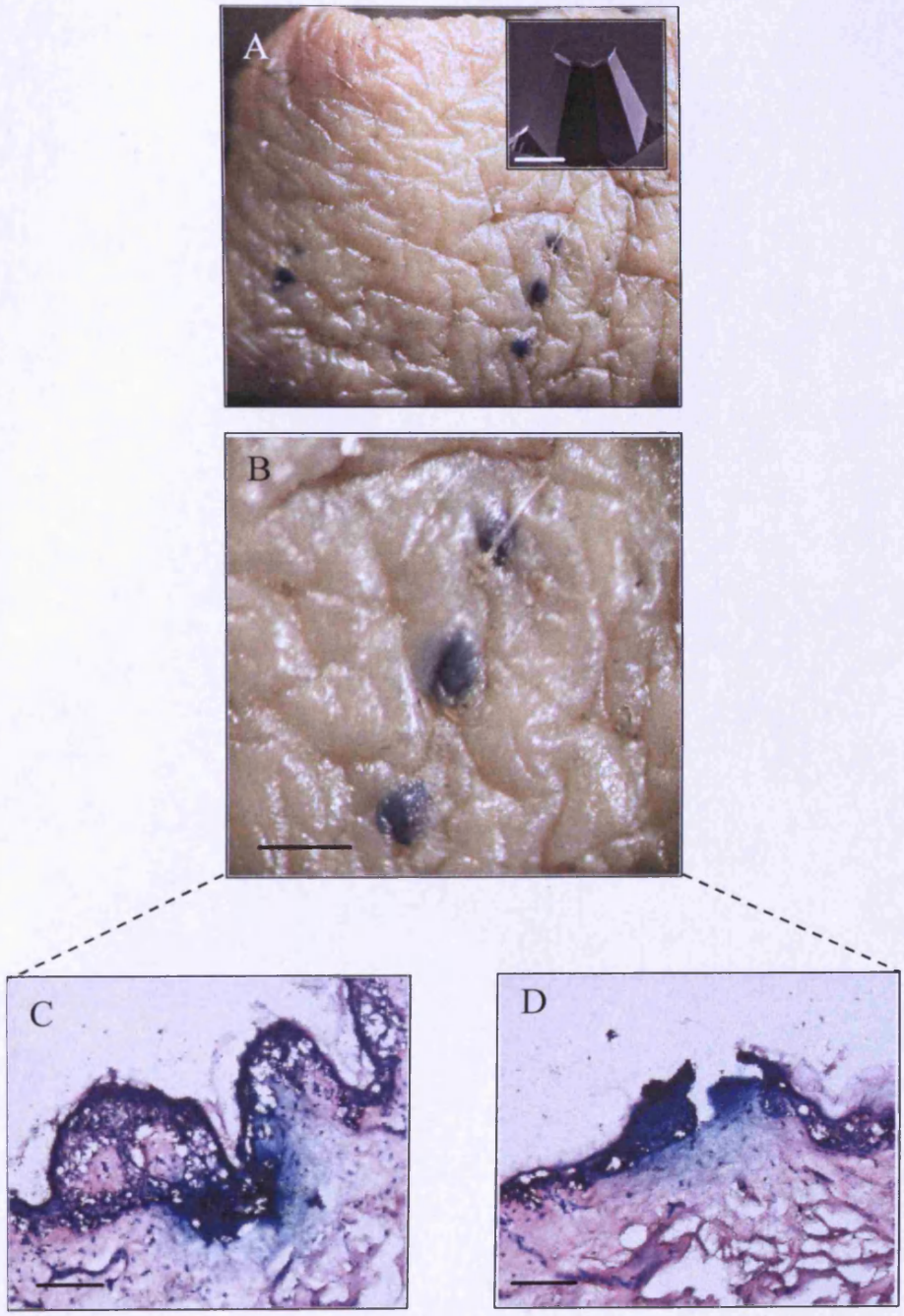


*Figure 5.6. En face* images and H&E stained cryosections following wet-etch microneedle application (TNI – Array 1) to human skin, pre-treated topically with 10µl pCMVβ (2.5mg/ml). B, scale bar = 200µm; C, D, scale bar = 100µm Donor skin was obtained from a 52 year old female. (The shape of individual microneedles used in this study is included as an insert in image A, scale bar = 100 µm).

Expression of the *lacZ* gene in alternative donor tissues confirmed the functionality of the device (Fig 5.7). Unlike intradermal injection (Fig 5.2 & 5.3) or lateral application of a hypodermic needle across the tissue surface (Fig 5.5), the tissue architecture proximal to the point of microneedle insertion was maintained (Fig 5.7C & 5.7D). This supported the fundamental concept of the microneedle device as a minimally invasive delivery system.

During microneedle studies, 1mg/ml pCMVβ formulations were less effective than more concentrated solutions (2.5-3.5mg/ml). More interestingly, transfection of the skin tissue was only evident when the formulation was applied to the skin surface prior to application of the device. The failure of pDNA to transfect cells upon topical application to a microneedle treated area may be explained by a combination of factors including ineffective penetration of the pDNA into microconduits, limited permeation of the pDNA through microconduits, poor uptake by local cells, degradation by endonucleases and/or interaction with tissue components within the external environment. The adherence of pDNA to the SC may also retain the nucleic acid on the skin surface and thus prevent epidermal permeation (Foldvari et al., 2006b, Kuo and Chou, 2004). It may therefore be postulated that application of the device to an area of skin pre-treated with the pCMVβ formulation results in active transfer of the formulation from the skin surface, through the SC and possibly into the underlying epidermal cells.

However although microneedle arrays facilitated cutaneous expression of exogenous nucleic acid formulations, the procedure was poorly reproducible. Not all treated samples displayed visible signs of transfection and not all microneedles within a single array device facilitated transfection. As frustum-tipped microneedles may not efficiently penetrate into skin tissue (Section 2.4.3.3), further studies were conducted using pointed tipped microneedles.

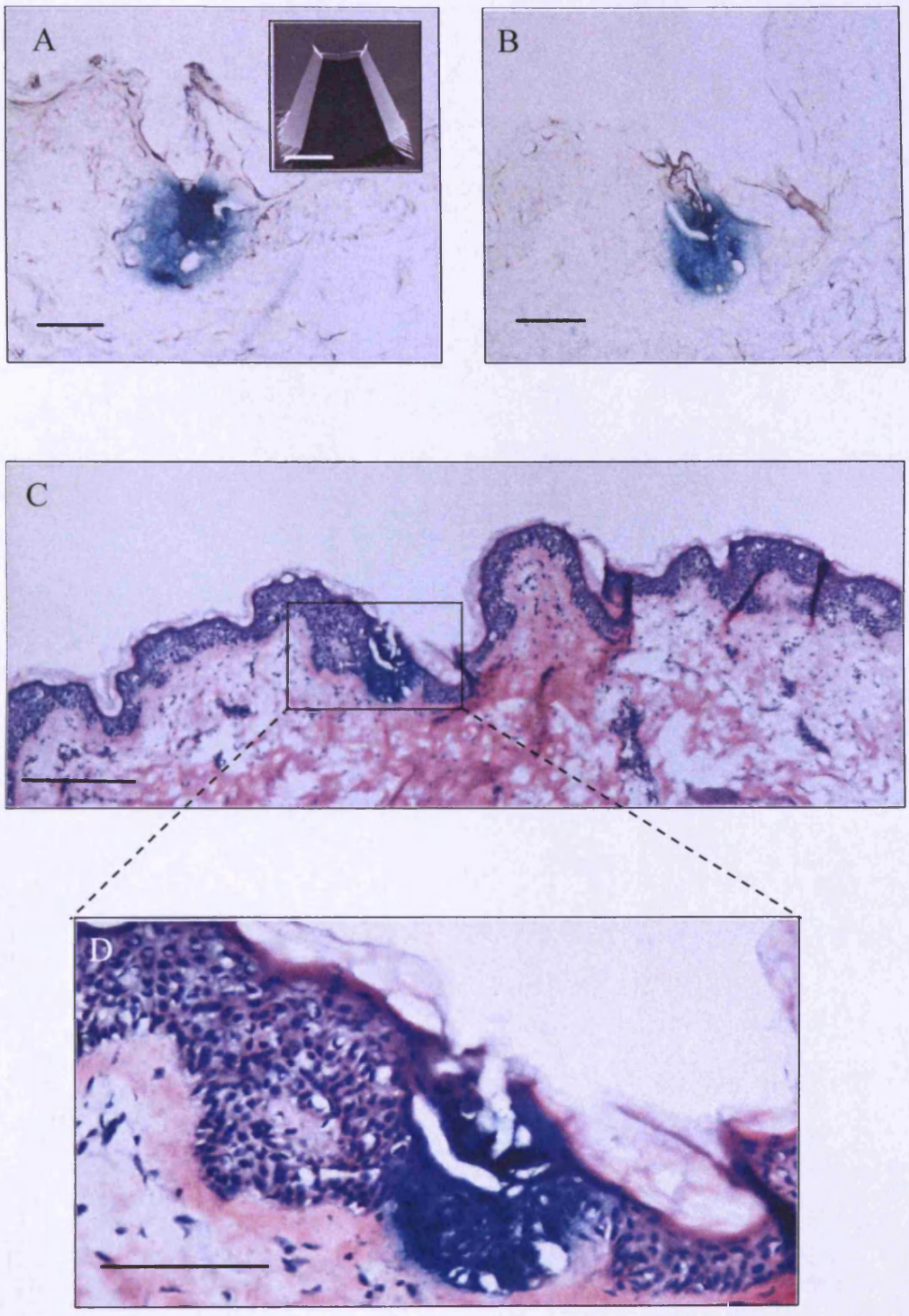


*Figure 5.7.* Unstained and H&E stained cryosections following wet-etch microneedle application (TNI – Array 2) to human skin, pre-treated topically with 10µl pCMVβ (2.5mg/ml). A, B, D, scale bar = 100µm; C, scale bar = 250µm. Donor skin was obtained from a 72 year old female. (The shape of individual microneedles used in this study is included as an insert in image A, scale bar = 100 µm).

Discrete areas of blue pigmentation were noted throughout the viable epidermis, in close proximity to microconduits created by a pointed microneedle array (Fig 5.8). Counterstaining with NFR permitted detection of successful microdisruptions in the SC and indicates successful penetration of all microneedles (Fig 5.8B). Two identifiable areas of transfection from a potential sixteen may be considered inefficient. However, it must be remembered that such observations are synonymous with the established inefficiencies of non-viral gene therapy and are therefore unlikely to be attributable solely to the limitations of the device.

The transfection levels witnessed in initial studies with wet-etch microneedle array devices were unpredictable and inefficient. Concentrated pDNA solutions and the analysis of multiple skin samples were required to obtain positive evidence of transfection. Alternative methods of microneedle application were therefore investigated in an attempt to improve transfection efficiency.

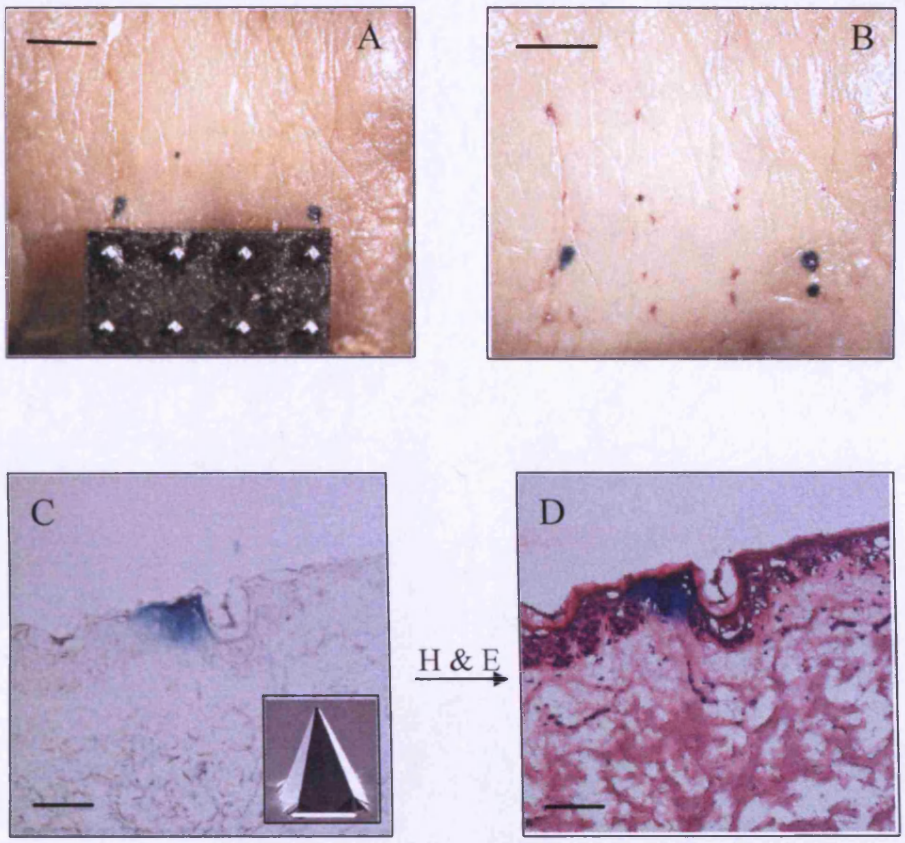


*Figure 5.8. En face* images and cryosections following wet-etch microneedle application (TNI – Array 6) to human skin, pre-treated topically with 10µl pCMVβ (2.87mg/ml). TNI - Array 6 was pictured alongside the skin in image A. The skin pictured in image B was treated topically with NFR to highlight disruptions in the skin surface. A, B, scale bar = 1mm; C, D, scale bar = 100µm. Donor skin was obtained from a 72 year old female. (The shape of individual microneedles used in this study is included as an insert in image C, scale bar = 100 µm).

*5.4.4.1.2. Multiple wet-etch microneedle application*

Multiple applications of microneedle devices to skin tissue specimens, pre-treated with a concentrated pDNA solution, produced a notable increase in the quantity of transfection points but also a greater heterogeneity in the diameter and intensity of these pigmented areas (Fig 5.9). This may be attributable to inconsistencies in delivery of the formulation using the microneedle device and/or the architecture of the skin at the point of transfection.

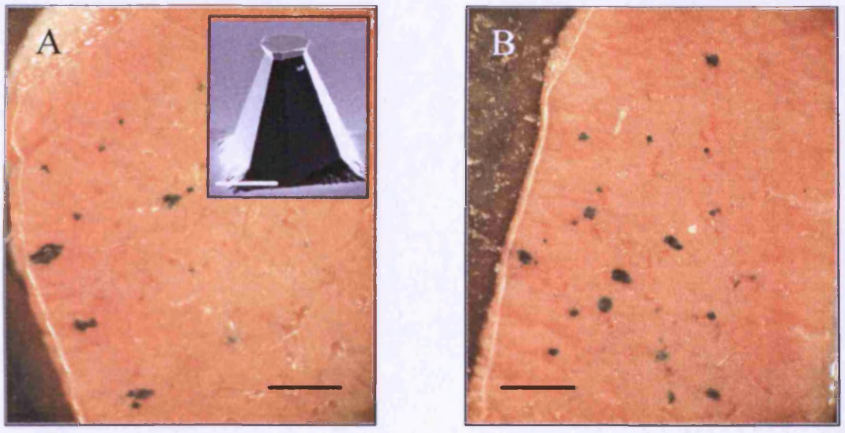


*Figure 5.9. En face* images following four wet-etch microneedle (TNI – Array 3) rolling applications to human skin, pre-treated topically with 40µl pCMVβ (2.5mg/ml). A, B scale bar = 1mm. Donor skin was obtained from a 48 year old female. (The shape of individual microneedles used in this study is included as an insert in image A, scale bar = 100 µm).

At present the levels of transfection observed following this method of pCMVβ delivery remain irreproducible, some human skin tissue samples demonstrated minimal or even no signs of transfection following treatment whilst others displayed significant evidence of transfection (Fig 5.9). Nevertheless, these studies highlight the ability of a microneedle array to facilitate concurrent transfection at multiple points in human skin. Progressive improvements to the design of microneedle devices, a greater understanding of cutaneous transfection and optimisation of the pDNA formulations will be required to facilitate more predictable levels of cutaneous gene expression following wet-etch microneedle treatment.

*5.4.3.1.3. Lateral wet-etch microneedle application*

Lateral application of the microneedle device across the skin surface resulted in significant physical disruption of the tissue (Fig 5.10A). However, in doing so this facilitated heightened levels of cutaneous transfection. All experiments displayed evidence of β-galactosidase expression although, levels again varied between donor tissues and between individual samples. As noted previously (Section 2.4.5.2), the integrity of the microneedle device was maintained following repeated lateral application to the skin surface, thereby allaying safety concerns regarding the fragmentation of microneedles within the skin.

Initial studies with the robust frustum shaped microneedles resulted in over 15 identifiable points of transfection (Fig 5.10B), directly associated with lateral disruptions in the skin surface (Fig 5.10C). Further studies emphasised the potential of this technique for cutaneous gene delivery, with over 50 distinguishable points of transfection located within or alongside microneedle 'tracks' (1.5-2cm in length) (Fig 5.11 & 5.12D). However, no points of transfection were noted in any other areas of the tissue. The reason why positively transfected areas of tissue occur at discrete loci along the length of the microneedle 'track' remains unclear. Further work is required to ascertain if the formulation is delivered homogenously along the length of the microneedle track and/or if transfection points are associated with cellular areas that recover following mechanical disruption by the device.

Transverse sections suggested that lateral application caused significant disruption of the epidermal architecture, with damage extending into the papillary dermis (Fig 5.12A & 5.12B). It is interesting to note however that the integrity of the skin was maintained in the areas of tissue between the lateral abrasions. This was in contrast to observations made following lateral abrasion of the tissue with a hypodermic needle (Fig 5.4). Therefore, although this is obviously a more invasive method of delivery than the original microneedle concept (Section 1.5.1), further work to determine the recovery of skin following application, the risks of infection and the levels of tissue damage are warranted before it is discounted as a potential method to promote cutaneous gene delivery.

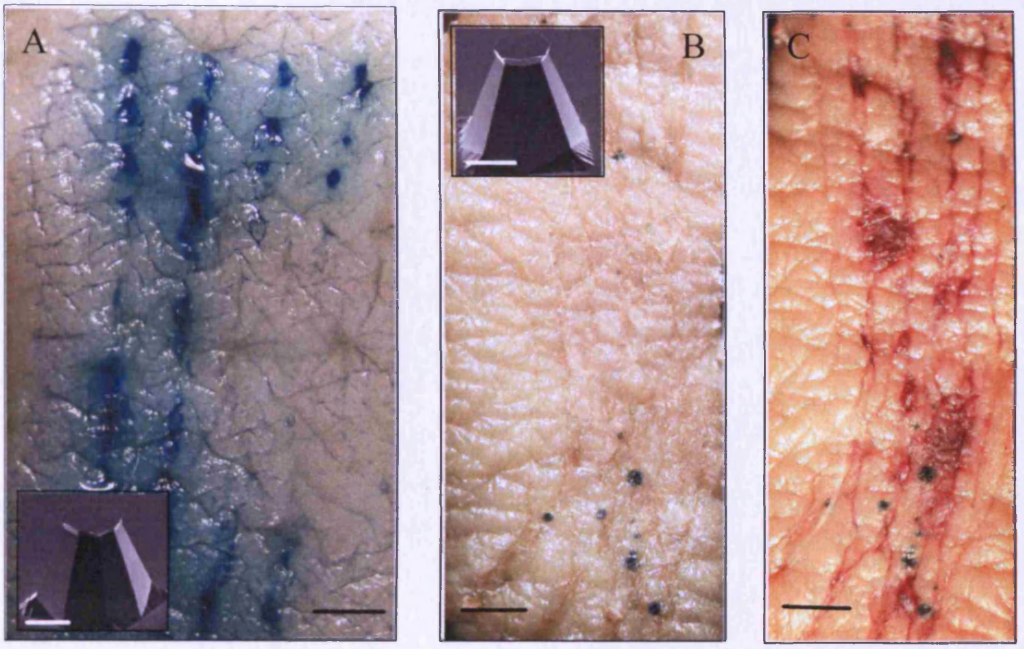


*Figure 5.10.* A. An *en face* image following application of a wet etch array (TNI - Array 1), in a lateral motion, followed by topical application of methylene blue. A, scale bar = 1mm. Donor skin was obtained from a 57 year old female. (The shape of individual microneedles used in this study is included as an insert in image A, scale bar = 100 μm). B, C. *En face* images following application of a wet-etch microneedle array (TNI - Array 2), in a lateral motion, to human skin pre-treated topically with pCMVβ (2.5mg/ml). The skin pictured in image C has also been treated topically with NFR to highlight disruptions in the skin surface. B, C scale bar = 1mm. Donor skin was obtained from a 68 year old female. (The shape of individual microneedles used in this study is included as an insert in image B, scale bar = 100 μm).

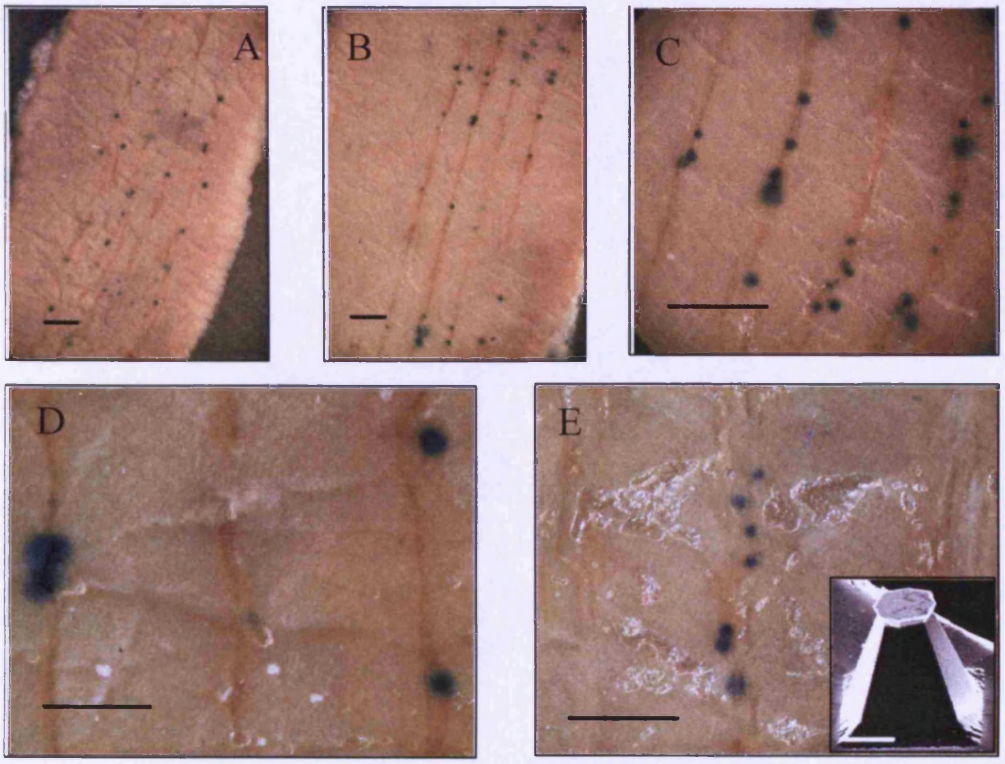


*Figure 5.11. En face* images following application of a wet-etch array (TNI - Array 8), in a lateral motion to human skin, pre-treated topically with 20µl pCMVβ solution (3.5mg/ml). A, B, C scale bar = 1mm; D, E scale bar = 500µm. Donor skin was obtained from a 76 year old female (A-D) and an 80 year old female (E). (The shape of individual microneedles used in this study is included as an insert in image E, scale bar = 100 µm).

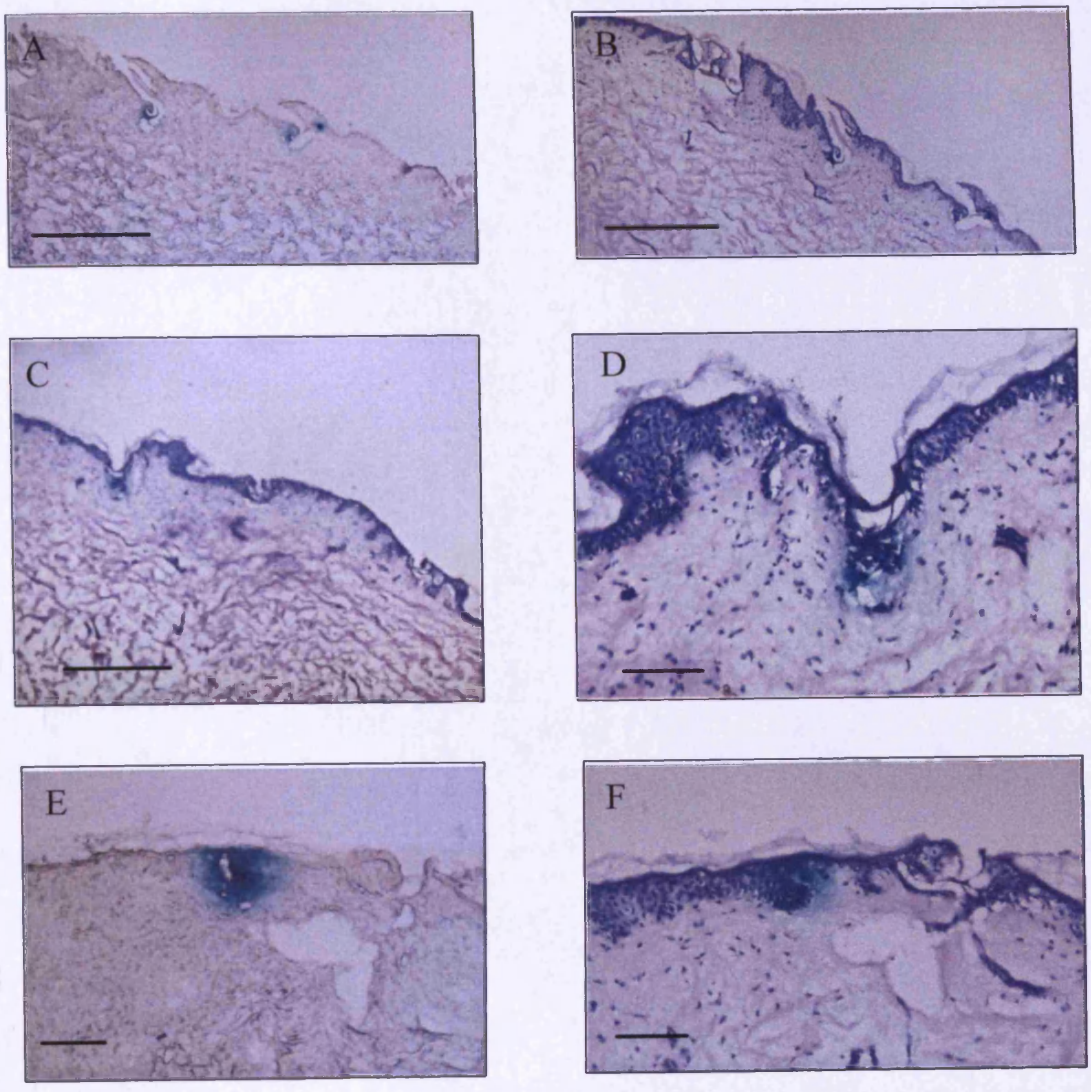


*Figure 5.12.* Cryosections taken following application of a wet-etch array (TNI - Array 8), in a lateral motion, across human skin pre-treated topically with 20µl pCMVβ solution (3.5mg/ml). A and F are unstained cryosections whilst all other sections are H&E stained. A, B, C scale bar = 500µm; D, E, F, scale bar = 100µm. Donor skin was obtained from a 76 year old female.

Experiments conducted in different donor tissues illustrated the contribution of the skin architecture to the reproducibility and efficiency of transfection (Fig 5.13). Significantly more transfection points of greater intensity were witnessed in the skin pictured in Fig 5.13A, compared to that pictured in Fig 5.13B. A reduction in the epidermal width means a narrower target region for localised delivery, a resultant decrease in the numbers of cells surrounding microneedle fashioned disruptions and therefore a reduced population of cells exposed to the exogenous pDNA formulation (Fig 5.13B). A thinner epidermis may also be associated with increased tissue fragility. Therefore irreparable damage to epidermal cells following application of the microneedle device may have also contributed to the reduced transfection levels witnessed in this donor tissue.

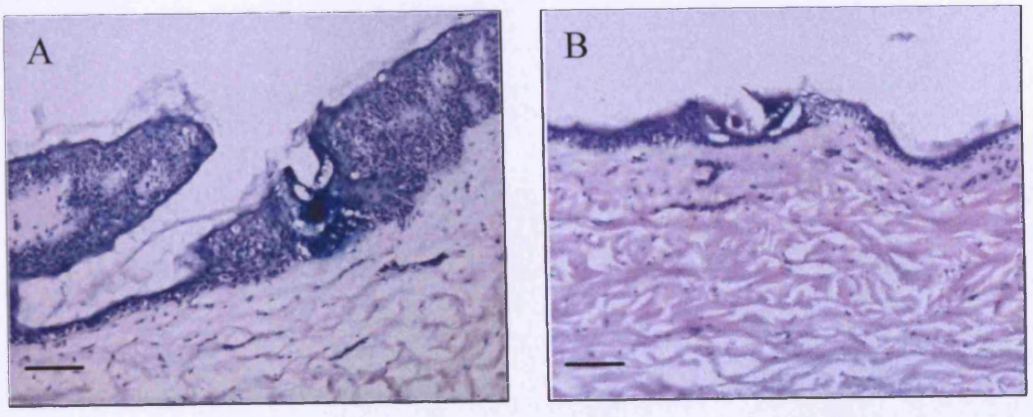


*Figure 5.13.* Cryosections following application of a wet-etch array (TNI - Array 8), with frustum shaped microneedles, across human skin pre-treated topically with 20µl pCMVβ solution (3.5mg/ml). A, B scale bar = 100µm. Donor skin was obtained from a 76 year old female (A) and an 80 year old female (B).

#### *5.4.3.2. Dry-etch microneedles*

Successful exogenous gene delivery to human skin by wet-etch microfabricated microneedles and improved transfection following increased disruption of the SC layer prompted investigation of dry-etch needles as a method of facilitating cutaneous gene delivery. These devices possess a 15 x 16 arrangement of microneedles which were expected to produce a considerable increase in the frequency of microconduits in the skin surface and a resultant increase in the number of observable transfection points.

Penetration of the dry-etch microneedle device facilitated localised expression of pCMVβ in the tissue surrounding the created microdisruptions (Fig 5.14). However NFR counterstaining also identified a large number of microchannels that failed to display any associated evidence of β-galactosidase expression and thus again highlighted the inefficiencies of cutaneous gene expression. Increased magnifications revealed co-localisation of the blue pigmentation with the NFR stain, thus confirming the transfection of cells directly associated with microchannels (Fig 5.14C).

This was confirmed by histological evaluation (Fig 5.15A & 5.15D). Although the length of microprojections (250-280μm) in the dry-etch array were comparable to that of the wet-etch, the dimensions of microconduits and the disruption of the tissue architecture following application of the dry-etch device was less than that observed with its wet-etch counterpart (Fig 5.15). The reduction in invasiveness was attributed to the shape of individual microprojections and/or the increased density of microneedles within the array pattern. Previous investigators have noted a 'bed of nails' effect when using microneedle arrays with high densities of microprojections (Yang and Zahn, 2004).

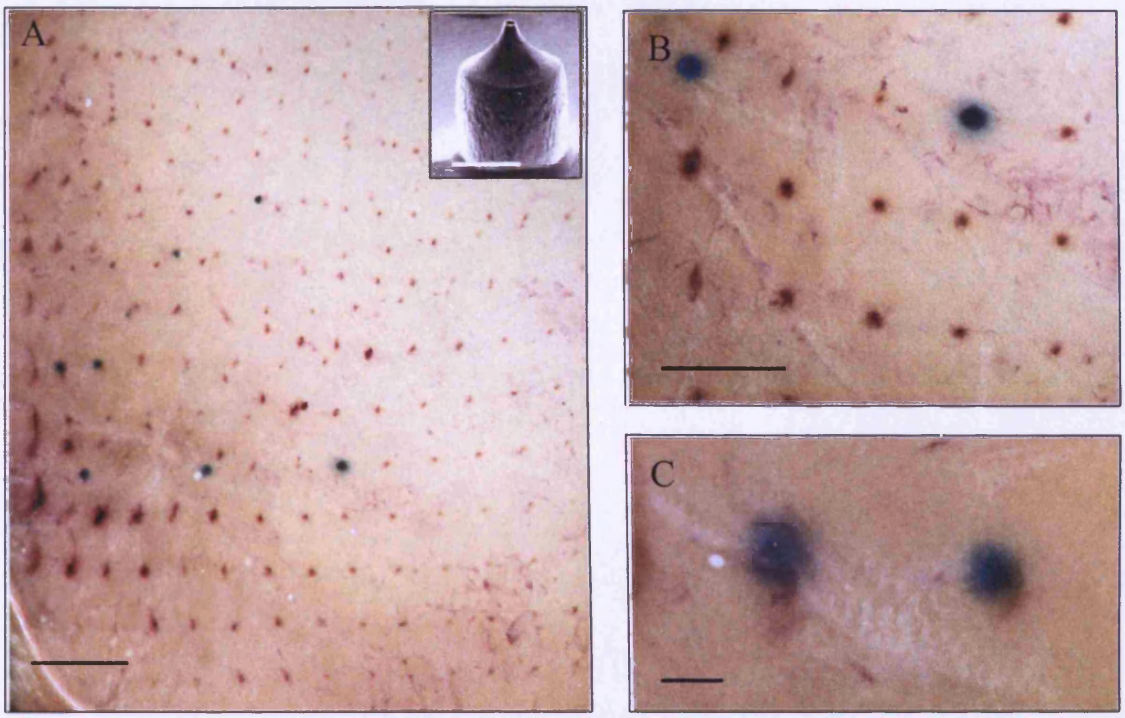


*Figure 5.14. En face* images following application of dry-etch microneedles (TNI – Array 15) to human skin, pre-treated topically 20 µl of pCMVβ (1mg/ml). The skin has also been treated topically with NFR to highlight microneedle disruptions in the skin surface. A, scale bar = 1mm; B scale bar = 500µm; C scale bar = 100µm. Donor skin was obtained from a 52 year old female. (The shape of individual microneedles used in this study is included as an insert in image A, scale bar = 100 µm).

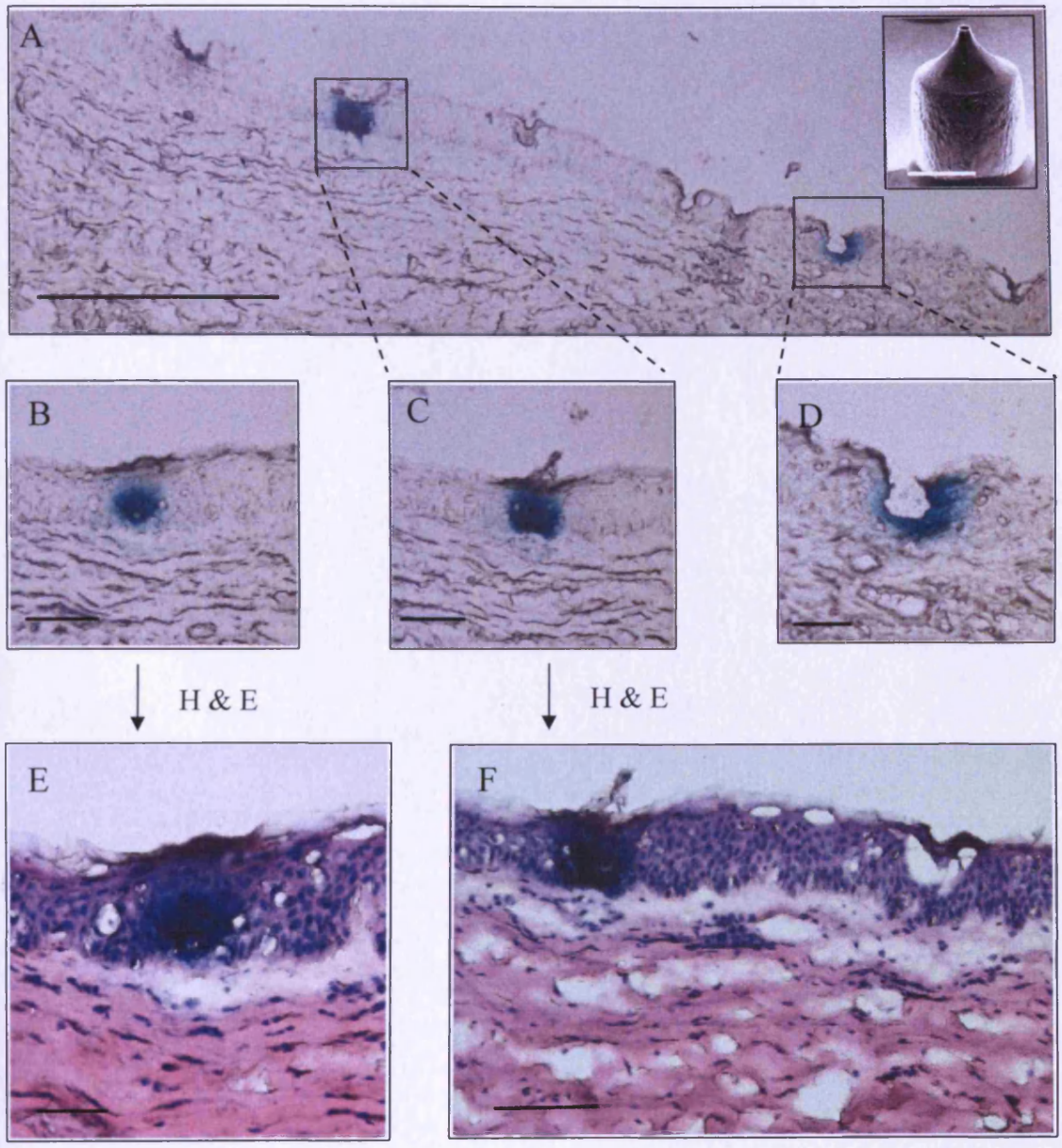


*Figure 5.15.* Cryosections following application of a dry-etch microneedle device (TNI – Array 15) to human skin treated topically with 20µl of pCMVβ (1mg/ml). Sections E&F have been H&E stained to visualise tissue architecture. A, scale bar = 500µm; B, C, F scale bar = 100µm; D, E scale bar = 50µm. Donor skin was obtained from a 52 year old female. (The shape of individual microneedles used in this study is included as an insert in image A, scale bar = 100 µm).

The relative inefficiencies of dry-etch microneedles as facilitators of cutaneous transfection were confirmed in subsequent studies. All tissue samples showed evidence of transfection (N=4) but the number and intensity of pCMVβ transfection points varied both between and within samples, with only 7-8 transfection points observed following penetration of up to 240 microneedles (Fig 5.16A).

Histology of dry-etch microneedle treated human tissue identified transfected areas with a focus of pigmentation in the lower layers of the viable epidermis i.e. the basal layer and stratum spinosum (Fig 5.15E & 5.15F). Interestingly, in the subsequent experiment transverse sections identified disparate areas of transfection within the skin architecture (Fig 5.16B-5.16E). Pigmentation located exclusively within the upper epidermal layers (Fig 5.16C), the papillary dermis (Fig 5.16D) and the basal epidermis (Fig 5.16E) suggested that cells can potentially be transfected at any point throughout the epidermal region. Transverse sections of the larger pigmented area also revealed two intense areas of transfection within a single transfection point (Fig 5.17). Successful transfection of cells in the upper layers, where keratinocytes are in the latter stages of cornification, was surprising. Prior to these investigations, cells within this layer were considered to be essentially 'non-viable' with regard to gene therapy. Investigations therefore indicate that specific regions of the skin may be transfected exclusively with a nucleic acid formulation. However, improvements to the delivery device and advances in non-viral nucleic acid formulations will be required to reduce the impact of inter and intra-individual differences in the skin structure on the targeted, reproducible transfection of localised skin cells.

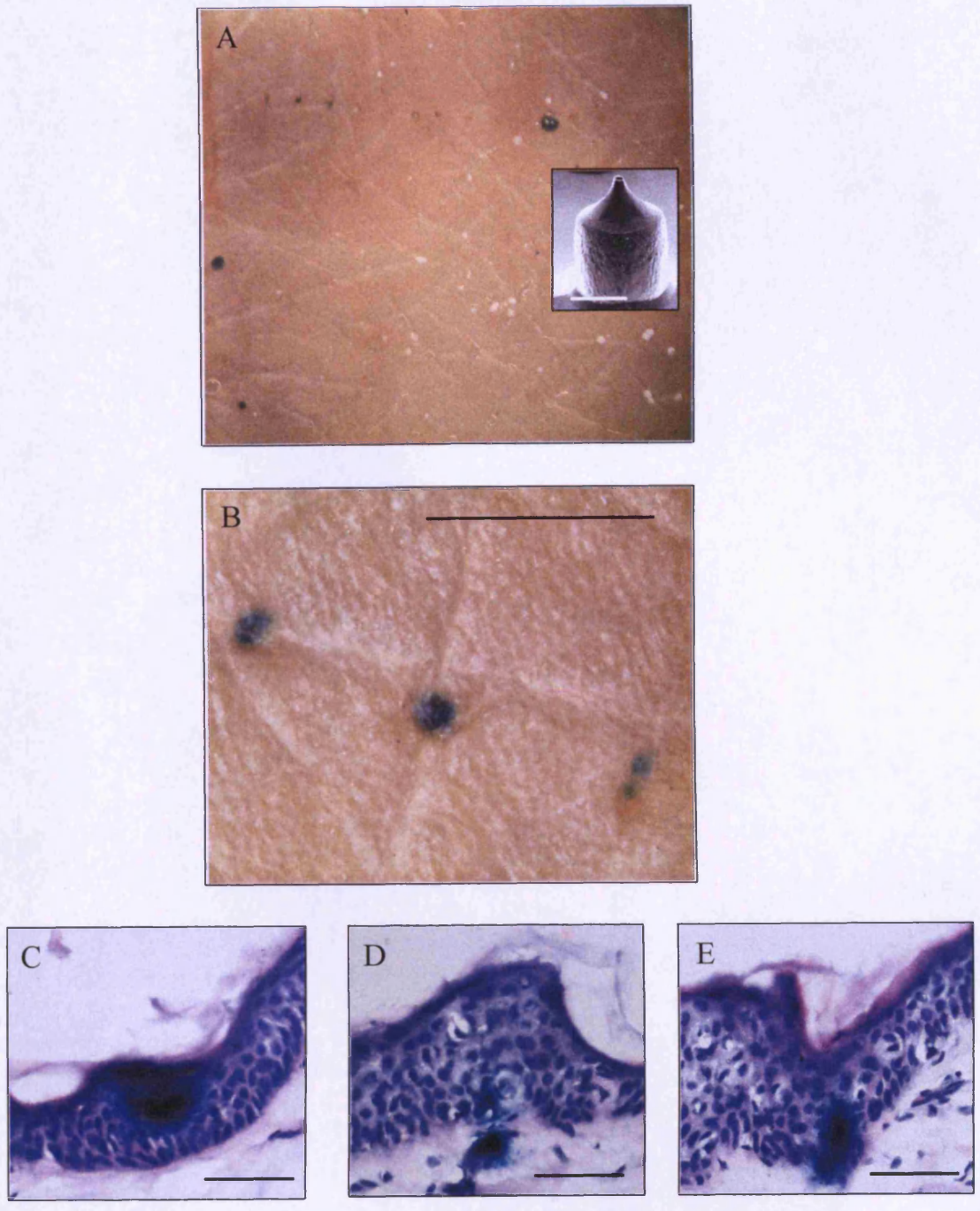


*Figure 5.16. En face* images and cryosections following application of a dry-etch microneedle device (TNI – Array 15) to human skin, pre-treated topically with 20µl pCMVβ (2.5mg/ml). Sections C-E are H&E stained. B, scale bar = 1mm; C, D, E scale bar = 50µm. Donor skin was obtained from 58 year old female. (The shape of individual microneedles used in this study is included as an insert in image A, scale bar = 100 µm).

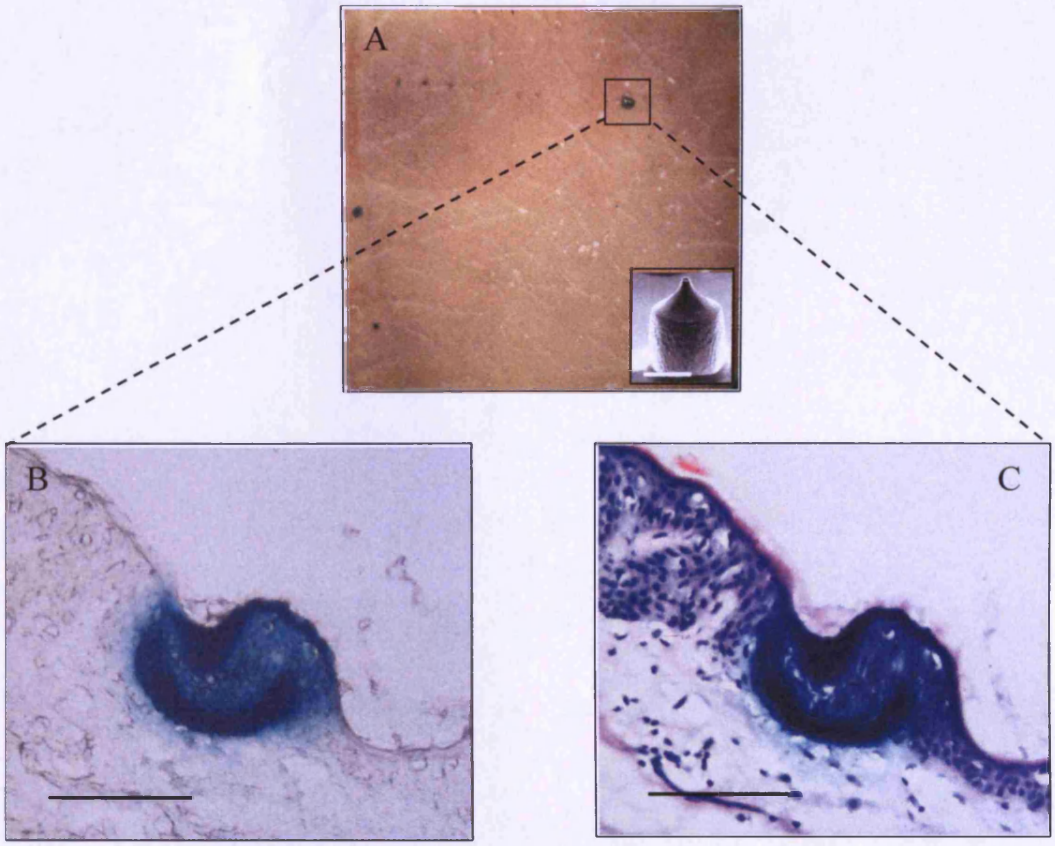


*Figure 5.17.* An *en face* image and cryosections following application of a dry-etch microneedle device (TNI – Array 15) to human skin, pre-treated topically with 20µl pCMVβ (2.5mg/ml). Section C has been H&E stained. B, C scale bar = 100µm. Donor skin was obtained from a 58 year old female. (The shape of individual microneedles used in this study is included as an insert in image A, scale bar = 100 µm).

## 5.5. CONCLUSIONS

Investigations using human keratinocytes, maintained in mammalian cell culture, required an LPD vector formulation to facilitate detectable levels of transfection. However, topical application, intradermal injection and microneedle mediated cutaneous delivery of the LPD formulation failed to facilitate identifiable expression within excised human skin. Conversely, intradermal injection of naked pCMVβ facilitated transfection of epidermal cells at the point of injection (Hengge et al., 1995, Hengge et al., 1996). The functionality of a naked pDNA formulation in human skin illustrated the importance of conducting investigations in representative experimental models. Results obtained from *ex vivo* human skin can therefore be more confidently, but tentatively, extrapolated to the clinical setting.

Transfection of discrete areas of human skin following, intradermal injection of a naked pDNA formulation, was unpredictable and inefficient. Application of a microneedle array to the skin can facilitate concurrent transfection of epidermal cells in several areas of the tissue. Transfection was directly associated with microchannels created by the device, it may even be postulated that mechanical disruption of cell membranes promoted transfection at the point of microneedle insertion. However microneedle mediated cutaneous transfection was inefficient and poorly reproducible and, although increasing the frequency of microneedle application and/or applying the device laterally can promote transfection, significant advances are required.

It is unclear whether unpredictable transfection efficiencies are a result of inter-/intra-individual differences in the skin structure, ineffective delivery of pDNA across the SC by the microneedle array, the inefficient transfection of cells by non-viral vector formulations or by a combination of such factors. Continued improvements to the delivery capabilities of microneedle arrays and optimisation of nucleic acid formulations are therefore required to address such inefficiencies.

# CHAPTER 6

# Discussion

## 6.1. GENERAL DISCUSSION

Subsequent to a seminal report by Prausnitz and co-workers in 1998 (Henry et al., 1998a), the microneedle array device has stimulated significant interest as a novel means to increase the permeability of the skin barrier to a range of therapeutic candidates, including macromolecules. During this period the concept of the device, as a pain and blood free method for creating microconduits through the outer skin layers, has been established. However, the technology remains in its infancy and therefore the optimal design of microneedle arrays, therapeutic candidates to be delivered by this method and their potential role within the clinical setting has not been fully elucidated. The aim of this investigation was to demonstrate the ability of a solid silicon microneedle array to facilitate exogenous gene expression within human skin, with the ultimate ambition of utilising devices as non-invasive gene delivery platforms for therapeutic strategies such as DNA vaccination.

The development of microneedle arrays, used in this study, relied upon close collaboration and regular communication with engineers that were responsible for the manufacture of devices. Initial attempts to fabricate microneedles, using dry-etch techniques (Henry et al., 1998a), resulted in heterogeneous and fragile microneedle structures that failed to penetrate the skin surface and often splintered or broke during application. However, optimisation of dry-etching conditions and the development of a wet-etching manufacturing procedure generated more robust microneedles that maintained their integrity following repeated applications to the skin surface.

Wet- and dry-etch microfabrication techniques can produce microneedle devices with different physical characteristics. The dry-etch devices used in these studies consisted of microprojections with pointed tips and cylindrical bodies, arranged in a densely populated array pattern (up to 400 needles on a $1cm^2$ array). The dimensions of individual microneedles ranged from 150μm to 250μm in length and 50μm to 160μm in diameter. Wet-etch devices comprise consisted of just nine or sixteen pyramidal microneedles, approximately 280μm in height with base diameters of up to 200μm. Generally, these microneedles were larger and more robust than their dry-etch counterparts and could also be created with either pointed or frustum shaped tips.

In agreement with published data, needle spacing, needle geometry and the method of array application significantly influenced the penetrative capabilities of microneedles (Park et al., 2005, Yang and Zahn, 2004). Dry-etch devices were less invasive, microchannels rarely exceeding depths of greater than 100μm. Frustum tipped wet-etch devices however created microchannels that were frequently over 50μm in diameter and extended approximately 200μm into the treated human skin. It is perhaps unsurprising that wet-etch devices produced more significant tissue damage, given their morphology and the greater insertion forces required for penetration of frustum shaped tips into the skin (Davis et al., 2004). Ideally a minimal level of invasiveness, based upon the spatial frequency of microchannels and their magnitude, would be determined for each microneedle device and its proposed therapeutic application.

The method of application is fundamental to the efficiency and reproducibility of microneedle penetration. Dry-etch devices penetrated the skin surface upon application of downward pressure. However this application method failed to translate successfully to wet-etch devices. This may be explained by the increased spacing between individual microneedles within the wet-etch array and the ability of the skin to deform 'around' the needle. This may be further complicated by the elasticity of skin and the dermatoglyphics of the tissue surface. It may seem logical to increase the microneedle density in order to facilitate penetration. However, the manufacturing methods utilised in wet-etching technology restrict microneedle density within these arrays and the optimal microneedle density is yet to be determined.

It is not only the array characteristics that determine the penetration efficacy of a device, but also its method of application to the skin surface. For example, adoption of a 'rolling application' greatly improved skin penetration of wet-etch devices. The pressure of microneedle application, the application technique and the tension of the skin, onto which the device is applied, are therefore all likely to contribute to the penetrative capabilities of individual microneedles within an array. Within the laboratory these parameters are controlled by the user and reproducible application therefore relies upon repeated experience with the devices. However, for microneedle devices to progress to the clinic and possibly public use, a uniform method of application that can ensure reproducible penetration is required. A microneedle

applicator must therefore be developed in synergy with advances in the design and engineering of microneedle arrays.

Repeated application of microneedle arrays to human skin resulted in contamination of the device with biological debris, mechanical damage to individual microneedles, (particularly at the periphery of the array) and a subsequent reduction in penetration efficiency. The structural fragility of silicon microneedles may result in ineffective delivery of a formulation and will certainly raise concerns regarding the deposition of silicon, a material with unproven biocompatibility, in skin. However, optimisation of the array characteristics and the continued development of polymer (Park et al., 2005) and metal (Cormier et al., 2004) microneedle arrays may produce more robust, clinically acceptable, cost effective and disposable devices that are more suitable for use in clinical practice.

For non-viral gene therapy applications, therapeutic DNA is commonly formulated into nanoparticle structures. The restrictive SC barrier would prevent effective delivery of such nanoparticles into skin. Microchannels, created in the skin by a microneedle device, provide a potential route through which such materials can permeate in order to access the underlying cells of the viable epidermis. Studies using model membranes, in Chapter 3, indicated that migration of a nanoparticle across microneedle treated skin was influenced, in part, by the dimensions of the microconduit, the surface charge of the particles and the surface charge of the skin membrane. Nanoparticles (approximately 100nm in diamter) diffused rapidly across aqueous filled microconduits that were significantly greater than the particle diameter (10μm). However for 1.2μm microconduits, a reduced channel size and adsorption to the membrane surface resulted in retention of nanoparticles and retarded permeation across the membrane.

In human epidermal studies, the increased complexity of the biological environment and non-uniform penetration of the skin by microneedle devices resulted in significant variability in nanoparticle permeation through the epidermal membrane. Cumulative adhesion of nanoparticles to the skin surface and the formation of colloidal aggregates within microconduits appeared to occlude membrane microchannels and prohibit trans-epidermal penetration of applied nanoparticles. It is instinctive to assume that creating

an aqueous conduit of greater diameter than the therapeutic will facilitate effective intra/transdermal delivery. However studies indicated that the physicochemical properties of a nanoparticle formulation and its interaction with components of the biological tissue may significantly influence its permeation through microneedle treated skin.

*In vitro* transfection of HaCaT cells using the pCMVβ, pEGFP-N1 and pGL3 reporter plasmids demonstrated the functionality of an LPD vector in effective gene transfer and permitted validation of the techniques employed to detect the encoded protein. However *in vitro* transfection results are often not translated to the more complex biological environment and therefore animal models are more commonly used in cutaneous gene therapy studies. Unfortunately, significant differences in the architecture and biology of human and animal skin mean that results obtained from animal models do not always extrapolate directly to *in vivo* human skin. This was of particular relevance in our studies where the parameters of the delivery technology, i.e. microneedle length and composition, are specifically designed and optimised to enable delivery to human skin. During this investigation, establishment of a successful method of organ culture to maintain the viability of excised human skin has therefore provided a representative laboratory model that can be utilised in the assessment of cutaneous gene delivery strategies.

Intradermal injection of naked pDNA was successfully employed in the mid 1990's to overcome the SC barrier and transfect cells in the underlying viable epidermis of *ex vivo* human skin (Hengge et al., 1995). Observations from Chapters 4 and 5 suggest that cutaneous gene expression relies primarily upon interaction of the formulation with those cells surrounding the needle track and that the majority of the dose will be deposited, ineffectively, in the connective tissue of the dermis region. Transfected cells were generally restricted to discrete areas, possibly associated with increased intracellular delivery resulting from mechanical disruption of cell membranes and/or the hydrodynamic delivery of nucleic acid.

Cell transfection following intradermal injection of pDNA was unpredictable and irreproducible. Limited permeation of the pDNA formulation from the point of delivery,

degradation of the delivered nucleic acid by endonucleases present within the tissue (Barry et al., 1999), interaction of the formulation with components of the tissue architecture, an inability to deliver a sufficient number of plasmid copies to cells within the tissue (Lechardeur et al., 2005) or inefficiencies of non-viral gene delivery may all contribute to this inefficiency. The microneedle array creates more penetrations in the skin surface, over a larger area, and therefore was predicted to deliver the exogenous nucleic acid formulation to a greater number of epidermal cells.

Cutaneous delivery of naked pCMVβ by wet-etch microneedle arrays and subsequent staining for the reporter gene product confirmed gene expression throughout all cellular layers of the viable epidermis in areas proximal to microneedle mediated conduits. This suggests that even keratinocytes in the latter stages of differentiation, when cells are synthesising increasing numbers of intracellular keratin filaments and organelles are effectively degrading, are responsive to transfection with exogenous pDNA. Dry-etch arrays have demonstrated the ability to transfect discrete cellular regions within the viable epidermis, e.g. papillary dermis, basal epidermis and the stratum spinosum. However, it would be premature to conclude that microneedle devices can be designed to reproducibly transfect cells in specific regions of the tissue. In fact, it may be argued that intra- and inter-variability in epidermal architecture may never permit the delivery and expression of gene therapeutics to targeted regions of the viable epidermis.

Interestingly, topical application of a nucleic acid formulation following microneedle treatment of skin did not facilitate detectable exogenous gene expression in any of the experiments conducted. Cutaneous transfection was only observed when the pDNA formulation was applied to the skin surface prior to microneedle treatment. This phenomenon may be explained by microneedle assisted penetration of the pDNA formulation to the epidermal region. Promoted delivery may also be supplemented by a concomitant enhancement in intracellular penetration, resulting from mechanical disruption to cell membranes by individual microneedles. Active assisted delivery of a nucleic acid formulation may therefore be required to facilitate cutaneous transfection and so the development of hollow microneedles may be timely (Davis et al., 2005, Martanto et al., 2006, Wang et al., 2006). A hollow microneedle offers a potentially controlled environment through which a therapeutic can be actively delivered to the

target tissue. This would eliminate reliance upon passive diffusive properties of a formulation and may increase intracellular gene delivery under hydrodynamic pressure. However, future studies will need to consider the shear forces imposed upon pDNA during injection from a micron sized aperture (Trebotich et al., 2003) and the possible interaction of formulations with the interior surface of the microneedle structure.

Numerous points of transfection were observed following topical pDNA application and microneedle treatment of the skin surface. However, the efficiency and reproducibility of exogenous gene expression was generally poor. Multiple application or lateral disruption of the tissue resulted in increased disruption of the skin surface and notable increases in detectable gene expression but transfection remained unpredictable. A commonly employed and well characterised non-viral gene vector, the LPD complex, was therefore used to condense pDNA and promote cell transfection and DNA uptake. However, intradermal injection and microneedle mediated delivery of this formulation failed to facilitate detectable levels of gene expression in human skin. These observations are in direct contrast with mammalian cell culture studies where a non-viral vector was essential for successful pDNA expression. Although suggested mechanisms for this phenomenon exist, including receptor-mediated uptake and large membrane disruption, the efficacy of naked pDNA within skin tissue remains poorly understood (Basner-Tschakarjan et al., 2004, Budker et al., 2000, Mirmohammadsadegh et al., 2002). Clearer elucidation of the mechanisms by which naked pDNA facilitates transfection of keratinocytes within human skin is required in order to enhance delivery strategies.

Unpredictable microneedle mediated gene expression in human skin is not solely attributed to limitations in the delivery capabilities of the device. The intra- and inter-individual differences in the structure of human skin that have been observed in this investigation are well documented (Roberts and Walters, 1998). This results in the exposure of variable numbers of epidermal cells to the nucleic acid formulation and a resultant disparity in the detectable transfection levels, within and between samples. This may be regarded as an inherent problem to the successful progression of microneedle mediated gene delivery to the clinic and indeed for cutaneous malignancies or the treatment of inheritable disease states, where treatment may rely upon the

transfection of all or a significant percentage of cells in the target region, this presents a significant barrier. However in the case of DNA vaccination, a reproducible minimum level of cellular transfection that can stimulate an effective immune response may be sufficient. Given the residence of LCs in the viable epidermis, it may be argued that the depth of pDNA delivery is as important as the levels of gene expression. Optimising the number of microneedle penetrations to expose as many viable epidermal cells, including LCs, as possible and creating an effective pharmaceutical formulation to promote efficient transfection of epidermal cells, may therefore enhance the efficacy of a cutaneous DNA vaccination. The ultimate goal would be to produce an efficacious, pain-free, disposable, microneedle vaccination that can be self-administered and does not possess the infection risks that are associated with injections.

During this investigation the capabilities of solid silicon microneedle devices for the cutaneous delivery of macromolecules, including non-viral gene therapies, has been demonstrated. However, despite illustrating proof-of-principle, further advances in engineering techniques, materials and design of microneedle arrays is required to ensure more reproducible and controlled penetration of the skin. Using microneedles for cutaneous gene delivery will also rely upon concurrent advances in gene delivery technologies. Indeed, it may be argued that the potential of a microneedle device for cutaneous gene therapy will only be realised subsequent to developments in the efficiency of gene therapy vectors. However, the emergence of the first commercial gene therapy product in China (Peng, 2005, Wilson, 2005) and the continued improvement of cutaneous non-viral gene vectors (Lisziewicz et al., 2006, Lisziewicz et al., 2005) permits optimism towards the development of clinically useful and efficacious cutaneous gene therapies.

## 6.2. FUTURE STUDIES

The cutaneous delivery and expression of exogenous pDNA is currently inefficient and poorly reproducible. This may be attributable to the limitations of the microneedle device, the inefficiencies associated with non-viral gene therapy, the reduced viability of *ex vivo* skin or a combination of such factors.

Continued dialogue with microneedle engineers is essential to the development of a microneedle array. Further work is required to optimise penetration characteristics of microneedle devices and to understand how the morphology and geometry of microneedle arrays affects their insertion into human skin.

The staining methodology used to detect the β-galactosidase enzyme in this study resulted in a diffuse area of pigmentation that may miscalculate transfection levels (Couffinhal et al., 1997). Future studies should utilise anti-β-galactosidase antibodies to locate individually transfected cells within the epidermis. This may be combined with histological measures to determine the viability of epidermal cells in excised human skin tissue and following application of a microneedle array (Jacobs et al., 2002, Jacobs et al., 2001, Jacobs et al., 2000). It would be particularly interesting to ascertain the viability of those cells that surround the microneedle channel following insertion of the device and to determine if irreparable damage to cells results a diminished ability to express the exogenous plasmid or whether transient damage to cell membranes facilitates intracellular uptake and promotes transfection.

These improvements may also be supplemented by improvements in pharmaceutical formulation. The currently employed, primitive, methods of pDNA application may contribute to ineffective transfection and therefore the development of semi-solid formulations or the creation of a coated microneedle device may improve the uniformity of gene delivery. For example, recent investigation of a calcium phosphate coated microneedle structure (Shirkhanzadeh, 2005) may be combined with the use calcium phosphate as a non-viral gene delivery vector (Roy et al., 2003) to produce a coated microneedle device that can protect nucleic acid formulation from degradation and

facilitate controllable release, *in situ,* to the viable cells surrounding a microneedle fashioned microconduit.

Although the pCMVβ reporter plasmid has been successfully employed to facilitate microneedle mediated exogenous gene expression within human skin, observations need to be supported by the use of alternative reporter plasmids and the use of systems that can infer quantitative measures of gene expression. Autofluorescent areas created within human skin upon disruption of the membrane prevented unambiguous detection of the GFP protein, encoded from pEGFP-N1, and therefore its employment as a secondary qualitative indicator of transfection was compromised during this study. The luciferase reporter plasmid was employed *in vitro* to provide quantitative assessment of gene expression levels. However, time constraints and the increased practical difficulties associated with extracting the luciferase enzyme from skin tissue prevented its successful use in *ex vivo* studies. A quantitative measure of exogenous gene expression within human skin would permit optimisation of delivery and formulation strategies and determine the concentration of protein that can be expressed following microneedle mediated delivery. Development of a robust quantitative assessment of exogenous gene expression is therefore of paramount importance to progression of these studies within the laboratory.

Physical disruption of the skin barrier has raised a number of safety concerns within the transdermal delivery community. The holes created by syringe insertion are expected to heal within 24-48 hours (Baxter and Mitragotri, 2005) and so it is not unreasonable to predict that microneedle holes, which are of significantly smaller dimensions, might be expected to heal in a reduced time. In the future it will therefore be important to assess the response of the skin to microneedle induced tissue damage and to assess the risks that may, or may not, be associated with disruption of the skin barrier function.

Aggarwal, P. & Johnston, C. R. (2004) Geometrical effects in mechanical characterizing of microneedles for biomedical applications. *Sensors and Actuators B,* **102,** 226-234.

Aguiar, J. C., Hedstrom, R. C., Rogers, W. O., Charoenvit, Y., Sacci, J. B., Jr., Lanar, D. E., Majam, V. F., Stout, R. R. & Hoffman, S. L. (2001) Enhancement of the immune response in rabbits to a malaria DNA vaccine by immunization with a needle-free jet device. *Vaccine,* **20,** 275-80.

Alarcon, J. B., Waine, G. B. & Mcmanus, D. P. (1999) DNA Vaccines: technology and application as anti-parasite and anti-microbial agents. *Advances in Parasitology,* **42,** 343-410.

Alexander, M. Y. & Akhurst, R. J. (1995) Liposome-mediated gene transfer and expression via the skin. *Human Molecular Genetics,* **4,** 2279-85.

Alonso, L. & Fuchs, E. (2003a) Stem cells in the skin: waste not, Wnt not. *Genes and Development,* **17,** 1189-200.

Alonso, L. & Fuchs, E. (2003b) Stem cells of the skin epithelium. *Proceedings of the National Academy of Science, USA,* **100 Suppl 1,** 11830-5.

Alvarez-Roman, R., Naik, A., Kalia, Y. N., Guy, R. H. & Fessi, H. (2004) Skin penetration and distribution of polymeric nanoparticles. *Journal of Controlled Release,* **99,** 53-62.

Andree, C., Swain, W. F., Page, C. P., Macklin, M. D., Slama, J., Hatzis, D. & Eriksson, E. (1994) *In vivo* transfer and expression of a human epidermal growth factor gene accelerates wound repair. *Proceedings of the National Academy of Science, USA,* **91,** 12188-92.

Apel, P. (2001) Track etching technique in membrane technology (Invited Talk). *Radiation Measurements,* **34,** 559-566.

Arin, M. J. & Roop, D. R. (2004) Inducible mouse models for inherited skin diseases: implications for skin gene therapy. *Cells Tissues Organs,* **177,** 160-8.

Babiuk, S., Baca-Estrada, M., Babiuk, L. A., Ewen, C. & Foldvari, M. (2000) Cutaneous vaccination: the skin as an immunologically active tissue and the challenge of antigen delivery. *Journal of Controlled Release,* **66,** 199-214.

Babiuk, S., Baca-Estrada, M. E., Pontarollo, R. & Foldvari, M. (2002) Topical delivery of plasmid DNA using biphasic lipid vesicles (Biphasix). *Journal of Pharmacy and Pharmacology,* **54,** 1609-14.

Babiuk, S., Baca-Estrada, M. E., Foldvari, M., Baizer, L., Stout, R., Storms, M., Rabussay, D., Widera, G. & Babiuk, L. (2003) Needle-free topical electroporation improves gene expression from plasmids administered in porcine skin. *Molecular Therapy,* **8,** 992-8.

Baca-Estrada, M. E., Foldvari, M., Babiuk, S. L. & Babiuk, L. A. (2000) Vaccine delivery: lipid-based delivery systems. *Journal of Biotechnology,* **83,** 91-104.

Backvall, H., Wassberg, C., Berne, B. & Ponten, F. (2002) Similar UV responses are seen in a skin organ culture as in human skin in vivo. *Experimental Dermatology,* **11,** 349-56.

Banchereau, J. & Steinman, R. M. (1998) Dendritic cells and the control of immunity. *Nature,* **392,** 245-252.

Banga, A. K. & Prausnitz, M. R. (1998) Assessing the potential of skin electroporation for the delivery of protein- and gene-based drugs. *Trends in Biotechnology,* **16,** 408-12.

Barry, B. W. (2001) Review: Novel mechanisms and devices to enable successful transdermal drug delivery. *European Journal of Pharmaceutical Sciences,* **14,** 101-114.

Barry, B. W. (2002) Drug delivery routes in skin: a novel approach. *Advanced Drug Delivery Reviews,* **54,** S31-S40.

Barry, M. E., Pinto-Gonzalez, D., Orson, F. M., Mckenzie, G. J., Petry, G. R. & Barry, M. A. (1999) Role of endogenous endonucleases and tissue site in transfection and CpG-mediated immune activation after naked DNA injection. *Human Gene Therapy,* **10,** 2461-80.

Basner-Tschakarjan, E., Mirmohammadsadegh, A., Baer, A. & Hengge, U. R. (2004) Uptake and trafficking of DNA in keratinocytes: evidence for DNA-binding proteins. *Gene Therapy,* **11,** 765-74.

Bates, M. (2004) Needle-free drug delivery system blasts through the skin. *Pharmaceutical technology,* 18-20.

Baxter, J. & Mitragotri, S. (2005) Jet-induced skin puncture and its impact on needle-free jet injections: Experimental studies and a predictive model. *Journal of Controlled Release,* **106,** 361-373.

Belting, M., Sandgren, S. & Wittrup, A. (2005) Nuclear delivery of macromolecules: barriers and carriers. *Advanced Drug Delivery Reviews,* **57,** 505-27.

Ben-Bassat, H., Chaouat, M., Segal, N., Zumai, E., Wexler, M. R. & Eldad, A. (2001) How long can cryopreserved skin be stored to maintain adequate graft performance? *Burns,* **27,** 425-31.

Birchall, J. C., Kellaway, I. W. & Gumbleton, M. (2000) Physical stability and *in vitro* gene expression efficiency of nebulised lipid-peptide-DNA complexes. *International Journal of Pharmaceutics,* **197,** 221-31.

Birchall, J. C., Marichal, C., Campbell, L., Alwan, A., Hadgraft, J. & Gumbleton, M. (2000) Gene expression in an intact *ex vivo* skin tissue model following percutaneous delivery of cationic liposome-plasmid DNA complexes. *International Journal of Pharmaceutics,* **197,** 233-8.

Birchall, J., Coulman, S., Anstey, A., Gateley, C., Sweetland, H., Gershonowitz, A., Neville, L. & Levin, G. (2006) Cutaneous gene expression of plasmid DNA in excised human skin following delivery via microchannels created by radio frequency ablation. *International Journal of Pharmaceutics,* **312,** 15-23.

Bos, J. D. & Meinardi, M. M. H. M. (2000) The 500 Dalton rule for the skin penetration of chemical compounds and drugs. *Experimental Dermatology,* **9,** 165-169.

Bratthauer, G. L. (1999) Preparation of frozen sections for analysis. *Methods in Molecular Biology,* **115,** 57-62.

Bravo, D., Rigley, T. H., Gibran, N., Strong, D. M. & Newman-Gage, H. (2000) Effect of storage and preservation methods on viability in transplantable human skin allografts. *Burns,* **26,** 367-78.

Bremseth, D. L. & Pass, F. (2001) Delivery of insulin by jet injection: recent observations. *Diabetes Technology and Therapeutics,* **3,** 225-232.

Brendler, E., Ratkje, S. K. & Hertz, H. G. (1995) Streaming potentials of Nuclepore membranes by the electric wok method. *Electrochimica Acta,* **41,** 169169-176.

Budker, V., Budker, T., Zhang, G., Subbotin, V., Loomis, A. & Wolff, J. A. (2000) Hypothesis: naked plasmid DNA is taken up by cells in vivo by a receptor-mediated process. *Journal of Gene Medicine,* **2,** 76-88.

Burnette, R. R. & Ongpipattanakul, B. (1987) Characterization of the permselective properties of excised human skin during iontophoresis. *Journal of Pharmaceutical Sciences,* **76,** 765-773.

Calvo, J. I., Hernandez, A., Pradanos, P. & Tejerina, F. (1996) Charge adsorption and zeta potential in cyclopore membranes. *Journal of Colloid and Interface Science,* **181,** 399-412.

Caplen, N. J., Gao, X., Hayes, P., Elaswarapu, R., Fisher, G., Kinrade, E., Chakera, A., Schorr, J., Hughes, B., Dorin, J. R., Porteous, D. J., Alton, F. W., Geddes, D. M., Coutelle, C., Williamson, R., Huang, L. & Gilchrist, C. (1994) Gene therapy for cystic fibrosis in human by liposome-mediated DNA transfer: the production of resources and the regulatory process. *Gene Therapy,* **1,** 139-147.

Castagnoli, C., Alotto, D., Cambieri, I., Casimiri, R., Aluffi, M., Stella, M., Alasia, S. T. & Magliacani, G. (2003) Evaluation of donor skin viability: fresh and cryopreserved skin using tetrazolioum salt assay. *Burns,* **29,** 759-67.

Cetin, C., Kose, A. A., Aral, E., Ercel, C., Tandogdu, O., Karabagli, Y. & Ozyilmaz, M. (2000) The effects of saline and plasma on skin graft keratinocyte viability. *British Journal of Plastic Surgery,* **53,** 418-9.

Cevc, G., Schatzlein, A. & Blume, G. (1995) Transdermal drug carriers: basic properties , optimization and transfer efficiency in the case of epicutaneously applied peptides. *Journal of Controlled Release,* **36,** 3-16.

Chabri, F., Bouris, K., Jones, T., Barrow, D., Hann, A., Allender, C., Brain, K. & Birchall, J. (2004) Microfabricated silicon microneedles for nonviral cutaneous gene delivery. *British Journal of Dermatology,* **150,** 869-77.

Chaote, K. A. & Khavari, P. A. (1997) Direct Cutaneous Gene Delivery in a Human Genetic Skin Disease. *Human Gene Therapy,* **8,** 1659-1665.

Chen, D., Burger, M., Chu, Q., Endres, R., Zuleger, C., Dean, H. & Payne, L. G. (2004) Epidermal powder immunization: cellular and molecular mechanisms for enhancing vaccine immunogenicity. *Virus Research,* **103,** 147-53.

Chen, D., Endres, R. L., Erickson, C. A., Weis, K. F., Mcgregor, M. W., Kawaoka, Y. & Payne, L. G. (2000) Epidermal immunization by a needle-free powder delivery technology: immunogenicity of influenza vaccine and protection in mice. *Nature Medicine,* **6,** 1187-1190.

Chen, D., Maa, Y. F. & Haynes, J. R. (2002) Needle-free epidermal powder immunization. *Expert Review of Vaccines,* **1,** 265-76.

Chen, T., Langer, R. & Weaver, J. C. (1999) Charged microbeads are not transported across the human stratum corneum in vitro by short high-voltage pulses. *Bioelectrochemistry and Bioenergetics,* **48,** 181-192.

Chesnoy, S. & Huang, L. (2002) Enhanced cutaneous gene delivery following intradermal injection of naked DNA in a high ionic strength solution. *Molecular Therapy,* **5,** 57-62.

Chiarello, K. (2004) Breaking the barrier: Advances in transdermal technology. *Pharmaceutical Technology,* **28,** 46-56.

Choi, M. J., Kim, J. H. & Maibach, H. (2006) Topical DNA vaccination with DNA/lipid based complex *Current Drug Delivery,* **3,** 37-45.

Christophers, E. & Kligman, A. (1963) Preparation of isolated sheets of human stratum corneum. *Archives of Dermatology,* **88,** 702-704.

Ciernik, I. F., Krayenbuhl, B. H. & Carbone, D. P. (1996) Puncture-mediated gene transfer to the skin. *Human Gene Therapy,* **7,** 893-899.

Collas, P. & Alestrom, P. (1997) Rapid targeting of plasmid DNA to zebrafish embryo nuclei by the nuclear localization signal of SV40 T antigen. *Molecular Marine Biology And Biotechnology,* **6,** 48-58.

Companjen, A. R., Van Der Wel, L. I., Wei, L., Laman, J. D. & Prens, E. P. (2001) A modified ex vivo skin organ culture system for functional studies. *Archives of Dermatological Research,* **293,** 184-90.

Cork, M. (2004) Gene-environment interactions in atopic eczema. *Perspectives in Percutaneous Penetration.* Montpellier, STS publishers.

Cormier, M., Johnson, B., Ameri, M., Nyam, K., Libiran, L., Zhang, D. D. & Daddona, P. (2004) Transdermal delivery of desmopressin using a coated microneedle array patch system. *Journal of Controlled Release,* **97,** 503-11.

Couffinhal, T., Kearney, M., Sullivan, A., Silver, M., Tsurumi, Y. & Isner, J. M. (1997) Histochemical staining following *LacZ* gene transfer underestimates transfection efficiency. *Human Gene Therapy,* **8,** 929-934.

Cross, S. E. & Roberts, M. S. (2004) Physical enhancement of transdermal drug application: Is delivery technology keeping up with pharmaceutical development. *Current Drug Delivery,* **1,** 81-92.

Cui, Z. & Mumper, R. J. (2001) Chitosan-based nanoparticles for topical genetic immunization. *Journal of Controlled Release,* **75,** 409-419.

Cui, Z. & Mumper, R. J. (2002) Topical immunization using nanoengineered genetic vaccines. *Journal of Controlled Release,* **81,** 173-184.

Cui, Z. & Mumper, R. J. (2003) The effect of co-administration of adjuvants with a nanoparticle-based genetic vaccine delivery system on the resulting immune responses. *European Journal of Pharmaceutics and Biopharmaceutics,* **55,** 11-8.

Cui, Z., Baizer, L. & Mumper, R. J. (2003) Intradermal immunization with novel plasmid DNA-coated nanoparticles via a needle-free injection device. *Journal of Biotechnology,* **102,** 105-15.

Davis, S. P., Landis, B. J., Adams, Z. H., Allen, M. G. & Prausnitz, M. R. (2004) Insertion of microneedles into skin: measurement and prediction of insertion force and needle fracture force. *Journal of Biomechanics,* **37,** 1155-63.

Davis, S. P., Martanto, W., Allen, M. G. & Prausnitz, M. R. (2005) Hollow metal microneedles for insulin delivery to diabetic rats. *IEEE Transactions on Biomedical Engineering,* **52,** 909-915.

Dean, D. A., Strong, D. D. & Zimmer, W. E. (2005a) Nuclear entry of nonviral vectors. *Gene Therapy,* **12,** 881-90.

Dean, H. J., Fuller, D. & Osorio, J. E. (2003) Powder and particle-mediated approaches for delivery of DNA and protein vaccines into the epidermis. *Comparitive Immunology, Microbiology & Infectious Diseases,* **26,** 373-88.

Dean, H. J. & Chen, D. (2004) Epidermal powder immunization against influenza. *Vaccine,* **23,** 681-686.

Dean, H. J., Haynes, J. & Schmaljohn, C. (2005b) The role of particle-mediated DNA vaccines in biodefense preparedness. *Advanced Drug Delivery Reviews,* **57,** 1315-1342.

Dellambra, E., Pellegrini, G., Guerra, L., Ferrari, G., Zambruno, G., Mavilio, F. & De Luca, M. (2000) Toward epidermal stem cell-mediated *ex vivo* gene therapy of junctional epidermolysis bullosa. *Human Gene Therapy,* **11,** 2283-7.

Dick, I. P. & Scott, R. C. (1992) Pig ear skin as an *in vitro* model for human skin permeability. *Journal of Pharmacy and Pharmacology,* **44,** 640-645.

Diez, L. M., Villa, F. M., Giminez, A. H. & Garcia, F. T. (1989) Streaming potential of some polycarbonate microporous membranes when bathed by LiCl, NaCl, $MgCl_2$ and $CaCl_2$ aqueous solutions. *Journal of Colloid and Interface Science,* **132,** 27-33.

Dileo, J., Miller, T. E., Chesnoy, S. & Huang, L. (2003) Gene transfer to subdermal tissues via a new gene gun design. *Human Gene Therapy,* **14,** 79-88.

Domashenko, A., Gupta, S. & Cotsarelis, G. (2000) Efficient delivery of transgenes to human hair follicle progenitor cells using topical lipoplex. *Nature Biotechnology,* **18,** 420-423.

Doukas, A. G. & Kollias, N. (2004) Transdermal drug delivery with a pressure wave. *Advanced Drug Delivery Reviews,* **56,** 559-579.

Dowty, M. E., Williams, P., Zhang, G., Hagstrom, J. E. & Wolff, J. A. (1995) Plasmid DNA Entry Into Postmitotic Nuclei of Primary Rat Myotubes. *Proceedings of the National Academy of Science, USA,* **92,** 4572-4576.

Drabick, J. J., Glasspool-Malone, J., Somiari, S., King, A. & Malone, R. W. (2001) Cutaneous transfection and immune responses to intradermal nucleic acid vaccination are significantly enhanced by *in vivo* electropermeabilization. *Molecular Therapy,* **3,** 249-255.

Dujardin, N. & Preat, V. (2004) Delivery of DNA to skin by electroporation. *Methods in Molecular Biology,* **245,** 215-26.

Elias, P. M. (1983) Epidermal lipids, barrier function, and desquamation. *Journal of Investigative Dermatology,* **80,** 44s-49s.

Elias, P. M. (2005) Stratum corneum defensive functions: An integrated view. *Journal of Investigative Dermatology,* **125,** 183-200.

Eriksson, E., Yao, F., Svensjo, T., Winkler, T., Slama, J., Macklin, M. D., Andree, C., Mcgregor, M., Hinshaw, V. & Swain, W. F. (1998) *In vivo* gene transfer to skin and wound by microseeding. *The Journal of Surgical Research,* **78,** 85-91.

Even-Chen, S. & Barenholz, Y. (2000) DOTAP cationic liposomes prefer relaxed over supercoiled plasmids. *Biochimica et Biophysica Acta,* **1509,** 176-188.

Fan, H., Lin, Q., Morrissey, G. R. & Khavari, P. A. (1999) Immunization via hair follicles by topical application of naked DNA to normal skin. *Nature Biotechnology,* **17,** 870-872.

Faneca, H., Simoes, S. & Pedroso De Lima, M. C. (2004) Association of albumin or protamine to lipoplexes: enhancement of transfection and resistance to serum. *Journal of Gene Medicine,* **6,** 681-92.

Fang, J. Y., Lee, W. R., Shen, S. C., Wang, H. Y., Fang, C. L. & Hu, C. H. (2004) Transdermal delivery of macromolecules by erbium:YAG laser. *Journal of Controlled Release,* **100,** 75-85.

Felgner, P. L., Gadek, T. R., Holm, M., Roman, R., Chan, H. W., Wenz, M., Northrop, J. P., Ringold, G. M. & Danielsen, M. (1987) Lipofection: A highly efficient, lipid-mediated DNA-transfection procedure. *Proceedings of the National Academy of Science, USA,* **84,** 7413-7417.

Felner, M. J. (1976) Green autofluorescence in human epidermal cells. *Archives of Dermatology,* **112,** 667-670.

Fensterle, J., Grode, L., Hess, J. & Kaufmann, S. H. E. (1999) Effective DNA vaccination against listeriosis by prime/boost inoculation with the gene gun. *The Journal of Immunology,* **163,** 4510-4518.

Ferrari, S., Pellegrini, G., Mavilio, F. & De Luca, M. (2005) Gene therapy approaches for epidermolysis bullosa. *Clinics in Dermatology,* **23,** 430-436.

Foldvari, M., Babiuk, S. & Badea, I. (2006a) DNA delivery for vaccination and therapeutics through the skin. *Current Drug Delivery,* **3,** 17-28.

Foldvari, M., Kumar, P., King, M., Batta, R., Michel, D., Badea, I. & Wloch, M. (2006b) Gene delivery into human skin *in vitro* using biphasic lipid vesicles. *Current Drug Delivery,* **3,** 89-93.

Fortunati, E., Bout, A., Zanta, M. A., Valerio, D. & Scarpa, M. (1996) In vitro and in vivo gene transfer to pulmonary cells mediated by cationic liposomes. *Biochim Biophys Acta,* **1306,** 55-62.

Fuchs, E. (1990) Epidermal differentiation: the bare essentials. *Journal of Cell Biology,* **111,** 2807-2814.

Fujiwara, A., Hinokitani, T., Goto, K. & Arai, T. (2005) Partial ablation of porcine stratum corneum by argon-fluoride excimer laser to enhance transdermal drug permeability. *Lasers in Medical Science,* **19,** 210.

Fynan, E. F., Webster, R. G., Fuller, D. H., Haynes, J. R., Santoro, J. C. & Robinson, H. L. (1993) DNA vaccines: Protective immunizations by parenteral, mucosal and gene-gun innoculations. *Proceedings of the National Academy of Science, USA,* **90,** 11478-11482.

Gambardella, L. & Barrandon, Y. (2003) The multifaceted adult epidermal stem cell. *Current Opinion in Cell Biology,* **15,** 771-7.

Gao, X. & Huang, L. (1995) Cationic liposome-mediated gene transfer. *Gene Therapy,* **2,** 710-722.

Gao, X. & Huang, L. (1996) Potentiation of cationic liposome-mediated gene delivery by polycations. *Biochemistry,* **35,** 1027-1036.

Gardeniers, J. G. E., Berenschot, J. W., De Boer, M. J., Yeshurun, Y., Hefetz, M., Van't Oever, R. & Van Den Berg, A. (date unknown). Silicon micromachined hollow microneedles for transdermal liquid transfer, http://ieeexplore.ieee.org/iel5/7726/21214/00984224.pdf?arnumber=984224 [www], [cited 13th January2003], last update date unknown.

Garmory, H. S., Perkins, S. D., Phillpotts, R. J. & Titball, R. W. (2005) DNA vaccines for biodefence. *Advanced Drug Delivery Reviews,* **57,** 1343-1361.

Gaylarde, P. M., Sarkany, I. & A., G. (1975) Cell migration and DNA synthesis in organ culture of human skin. *British Journal of Dermatology,* **92,** 375-380.

Gerstel, M. S. & Place, V. A. (1976) Drug Delivery Device, US Patent 3,964,482.

Ghazizadeh, S. & Taichman, L. B. (2000) Virus-mediated gene transfer for cutaneous gene therapy. *Human Gene Therapy,* **11,** 2247-51.

Ghazizadeh, S. & Taichman, L. B. (2005) Organization of stem cells and their progeny in human epidermis. *Journal of Investigative Dermatology,* **124,** 367-72.

Giri, M., Ugen, K. E. & Weiner, D. B. (2004) DNA vaccines against human immunodeficiency virus type 1 in the past decade. *Clinical Microbiology Reviews,* **17,** 370-89.

Glasspool-Malone, J., Somiari, S., Drabick, J. J. & Malone, R. W. (2000) Efficient nonviral cutaneous transfection. *Molecular Therapy,* **2,** 140-146.

Glenn, G. M., Kenney, R. T., Ellingsworth, L. R., Frech, S. A., Hammond, S. A. & Zoeteweij, J. P. (2003) Transcutaneous immunization and immunostimulant strategies: capitalizing on the immunocompetence of the skin. *Expert Review of Vaccines,* **2,** 253-67.

Glenn, G. M., Scharton-Kersten, T., Vassell, R., Mallett, C. P., Hale, T. L. & Alving, C. R. (1998a) Cutting Edge: Transcutaneous immunization with cholera toxin protects mice against lethal mucosal toxin challenge. *The Journal of Immunology,* **161,** 3211-3214.

Glenn, G. M., Scharton-Kersten, T., Vassell, R., Mallett, C. P., Hale, T. L. & Alving, C. R. (1998b) Skin immunization made possible by cholera toxin. *Nature,* **391,** 851.

Glenn, G. M., Taylor, D. N., Li, X., Frankel, S., Montemarano, A. & Alving, C. R. (2000) Transcutaneous Immunization: A human vaccine delivery strategy using a patch. *Nature Medicine,* **6,** 1403-1406.

Green, C. L. & Khavari, P. A. (2004) Targets for molecular therapy of skin cancer. *Seminars in Cancer Biology,* **14,** 63-9.

Greenhalgh, D. A., Rothnagel, J. A. & Roop, D. R. (1994) Epidermis: an attractive target tissue for gene therapy. *Journal of Investigative Dermatology,* **103,** 63S-69S.

Haake, A., Scott, G. A. & Holbrook, K. A. Chapter 2: Structure and Function of the Skin: overview of the epidermis and dermis. In: FREINKEL, R. K. & WOODLEY, D. T., editors. The Biology of the Skin. 1st ed. New York: The Parthenon Publishing Group, 2001.

Haider, I., Pettis, R. J., Davison, N., Clarke, R. & Zahn, J. D. (date unknown). Biomedical and fluid flow characterization of microneedle-based drug delivery devices, http://asb-biomech.org/onlineabs/abstracts2001/pdf/080.pdf [www], [cited 24th October 2002], last update date unknown.

Halprin, K. M. & Ohkawara, A. (1966) Lactate production and lactate dehydrogenase in the human epidermis. *Journal of Investigative Dermatology,* **47,** 222-226.

Han, R., Reed, C. A., Cladel, N. M. & Christensen, N. D. (2000) Immunization of rabbits with cottontail rabbit papillomavirus E1 and E2 genes: protective immunity induced by gene gun-mediated intracutaneous delivery but not by intramuscular injection. *Vaccine,* **18,** 2937-44.

Hengge, U. R., Chan, E. F., Foster, R. A., Walker, P. S. & Vogel, J. C. (1995) Cytokine gene expression in epidermis with biological effects following injection of naked DNA. *Nature Genetics,* **10,** 161-6.

Hengge, U. R., Walker, P. S. & Vogel, J. C. (1996) Expression of naked DNA in human, pig and mouse skin. *The Journal of Clinical Investigation,* **97,** 2911-2916.

Hengge, U. R., Pfutzner, W., Williams, M., Goos, M. & Vogel, J. C. (1998) Efficient expression of naked plasmid DNA in mucosal epithelium: prospective for the treatment of skin lesions. *Journal of Investigative Dermatology,* **111,** 605-8.

Hengge, U. R., Taichman, L. B., Kaur, P., Rogers, G., Jensen, T. G., L.A., G., Rees, J. L. & Christiano, A. M. (1999) How realistic is cutaneous gene therapy? *Experimental Dermatology,* **8,** 419-431.

Hengge, U. R. & Mirmohammadsadegh, A. (2000) Adeno-associated virus expresses transgenes in hair follicles and epidermis. *Molecular Therapy,* **2,** 188-94.

Hengge, U. R., Dexling, B. & Mirmohammadsadegh, A. (2001) Safety and pharmacokinetics of naked plasmid DNA in the skin: studies on dissemination and ectopic expression. *Journal of Investigative Dermatology,* **116,** 979-82.

Hengge, U. R. (2005) Progress and prospects of skin gene therapy: a ten year history. *Clinics in Dermatology,* **23,** 107-114.

Henry, S., Mcallister, D. V., Allen, M. & Prausnitz, M. R. (1998a) Microfabricated Microneedles: A novel approach to transdermal drug delivery. *Journal of Pharmaceutical Sciences,* **87,** 922-925.

Henry, S., Mcallister, D. V., Allen, M. & Prausnitz, M. R. (1998b) Micromachined microneedles for the transdermal delivery of drugs. 11th IEEE Micro Electro Mech. Syst.Workshop Heidelberg. 1998.

Herndon, T., Gonzalez, S., Gowrishankar, T. R., Anderson, R. & Weaver, J. (2004) Transdermal microconduits by microscission for drug delivery and sample acquisition. *BMC Medicine,* **2,** 12.

Hilliges, M., Wang, L. & Johansson, O. (1995) Ultrastructural evidence for nerve fibers within all vital layers of the human epidermis. *Journal of Investigative Dermatology,* **104,** 134-137.

Hingson, R. A., Davis, H. S. & Rosen, M. (1963) Historical development of jet injection and envisioned uses in mass immunization and mass therapy based upon 2 decades experience. *Military Medicine,* **128,** 516.

Hoffmann, R. M. (2000) The hair follicle as a gene therapy target. *Nature Biotechnology,* **18,** 20-21.

Hoffmann, R. M. (2003) Immune reactions in skin and hair follicle gene therapy. *Molecular Therapy,* **7,** 294-295.

Howarth, M. & Elliott, T. (2004) The processing of antigens delivered as DNA vaccines. *Immunological Reviews,* **199,** 27-39.

Howell, D. P., Krieser, R. J., Eastman, A. & Barry, M. A. (2003) Deoxyribonuclease II is a lysosomal barrier to transfection. *Molecular Therapy,* **8,** 957-63.

Http://www.Alteatherapeutics.Com/ (2005). [www], [cited 15 March 2005], last update date 15th April 2004.

Http://www.Nanopass.Com/ (2005). [www], [cited 2nd November2005], last update date unknown.

Http://www.Powdermed.Com/Developmentoverview.Htm (2006). [www], [cited 26th March 2006], last update date unknown.

Http://www.Silexmicrosystems.Com/Mems.Asp?Page=S3 (2006). [www], [cited 4th April 2006], last update date unknown.

Http://www.Wiley.Co.Uk/Genmed/Clinical/ (2006). [www], [cited 17th March 2006], last update date January 2006.

Huismann, I. H., Pradanos, P., Calvo, J. I. & Hernandez, A. (2000) Electroviscous effects, streaming potential and zeta potential in polycarbonate track-etched membranes. *Journal of Membrane Science,* **178,** 79-92.

Irvine, A. D. & Mclean, W. H. (2003) The molecular genetics of the genodermatoses: progress to date and future directions. *British Journal of Dermatology,* **148,** 1-13.

Issachar, N., Gall, Y., Borell, M. T. & Poelman, M.-C. (1997) pH measurements during lactic acid stinging test in normal and sensitive skin. *Contact Dermatitis* **36,** 152-155.

Jacobs, J. J. L., Lehe, C., Cammons, K. D. A., Das, P. K. & Elliott, G. R. (2000) Methyl green-pyronine staining of porcine organotypic skin explant cultures: An alternative model for screening for skin irritants. *ATLA,* **28,** 279-292.

Jacobs, J. J., Lehe, C., Cammans, K. D., Yoneda, K., Das, P. K. & Elliott, G. R. (2001) An automated method for the quantification of immunostained human Langerhans cells. *Journal of Immunological Methods,* **247,** 73-82.

Jacobs, J. J., Lehe, C., Cammans, K. D., Das, P. K. & Elliott, G. R. (2002) An in vitro model for detecting skin irritants: methyl green-pyronine staining of human skin explant cultures. *Toxicology In Vitro,* **16,** 581-8.

Jeschke, M. (2003). Non-viral gene therapy to improve wound healing, www.uni-regensburg.de/Fakultaeten/Medizin/Chirurgie/ [www], [cited 26th March 2003], last update date unknown.

Jiang, Q. J. & Uitto, J. (2005) Animal models of epidermolysis bullosa--targets for gene therapy. *Journal of Investigative Dermatology,* **124,** xi-xiii.

Jones, P. H., Harper, S. & Watt, F. M. (1995) Stem cell patterning and fate in human epidermis. *Cell,* **80,** 83-93.

Jonkman, M. F. (1999) Hereditary skin diseases of hemidesmosomes. *Journal of Dermatological Science,* **20,** 103-21.

Junqueira, L. C. & Carneiro, J. Chapter 1: Histology and its methods of study. In: JUNQUEIRA, L. C. & CARNEIRO, J., editors. Basic Histology. 11th ed. New York: McGraw-Hill, 2005a, 1-20.

Junqueira, L. C. & Carneiro, J. Chapter 18: Skin. In: JUNQUEIRA, L. C. & CARNEIRO, J., editors. Basic Histology. 11th ed. New York: McGraw-Hill, 2005b, 360-372.

Kaiser, J. (2004) Influenza: Girding for disaster: Searching for all-powerful flu weapons. *Science,* **306,** 395.

Kalia, Y. N., Naik, A., Garrison, J. & Guy, R. H. (2004) Iontophoretic drug delivery. *Advanced Drug Delivery Reviews,* **56,** 619-658.

Kang, M. J., Kim, C. K., Kim, M. Y., Hwang, T. S., Kang, S. Y., Kim, W. K., Ko, J. J. & Oh, Y. K. (2004) Skin permeation, biodistribution, and expression of topically applied plasmid DNA. *Journal of Gene Medicine,* **6,** 1238-46.

Kari, B. (1986) Control of blood glucose levels in alloxan-diabetic rats by iontophoresis of insulin. *Diabetes Technology & Therapeutics,* **35,** 217-221.

Kaur, P. & Li, A. (2000) Adhesive properties of human basal epidermal cells: an analysis of keratinocyte stem cells, transit amplifying cells, and postmitotic differentiating cells. *Journal of Investigative Dermatology,* **114,** 413-20.

Kaushik, S., Hord, A. H., Denson, D. D., Mcallister, D. V., Smitra, S., Allen, M. G. & Prausnitz, M. R. (2001) Lack of pain associated with microfabricated microneedles. *Anaesthesia and Analgesia,* **92,** 502-504.

Keesom, W. H., Zelenka, R. L. & Radke, C. J. (1988) A zeta-potential model for ionic surfactant adsorption on an ionogenic hydrophobic surface. *Journal of Colloid and Interface Science,* **125,** 575-585.

Kendall, M., Mitchell, T. & Wrighton-Smith, P. (2004) Intradermal ballistic delivery of micro-particles into excised human skin for pharmaceutical applications. *Journal of Biomechanics,* **37,** 1733-41.

Kendall, M. (2006) Engineering of needle-free physical methods to target epidermal cells for DNA vaccination. *Vaccine,* **24,** 4644-4647.

Kent, S. J., Cameron, P. U., Reece, J. C., Thompson, P. R. & Purcell, D. F. (2001) Attenuated and wild-type HIV-1 infections and long terminal repeat-mediated gene expression from plasmids delivered by gene gun to human skin ex vivo and macaques in vivo. *Virology,* **287,** 71-8.

Khavari, P. A. (1998) Gene Therapy for Genetic skin disease. *The Journal of Investigative Dermatology,* **110,** 462-467.

Kim, A., Lee, E. H., Choi, S. H. & Kim, C. K. (2004) *In vitro* and *in vivo* transfection efficiency of a novel ultradeformable cationic liposome. *Biomaterials,* **25,** 305-13.

Kim, K. J., Fane, A. G., Nystrom, M. & Pihlajamaki, A. (1997) Chemical and electrical characterization of virgin and protein-fouled polycarbonate track-etched membranes by FITR and streaming-potential measurements. *Journal of Membrane Science,* **134,** 199-208.

Kitagawa, T., Iwazawa, T., Robbins, P. D., Lotze, M. T. & Tahara, H. (2003) Advantages and limitations of particle-mediated transfection (gene gun) in cancer immuno-gene therapy using IL-10, IL-12 or B7-1 in murine tumor models. *Journal of Gene Medicine,* **5,** 958-65.

Kivinen, P. K., Nilsson, G., Naukkarinen, A. & Harvima, I. T. (2003) Mast cell survival and apoptosis in organ-cultured human skin. *Experimental Dermatology,* **12,** 53-60.

Klein, T., Wolf, E., Wu, R. & Sanford, J. (1987) High velocity microprojectiles for delivering nucleic acids into living cells. *Nature,* **327,** 70-73.

Kohli, A. K. & Alpar, H. O. (2004) Potential use of nanoparticles for transcutaneous vaccine delivery: effect of particle size and charge. *International Journal of Pharmaceutics,* **275,** 13-7.

Kremer, L., Dupre, L., Wolowczuk, I. & Locht, C. (1999) In vivo immunomodulation following intradermal injection with DNA encoding IL-18. *The Journal of Immunology,* **163,** 3226-31.

Kuo, S. & Chou, Y. (2004) A novel polymer microneedle and PDMS micromolding Technique. *Tamkang Journal of science and engineering,* **7,** 95-98.

Kutzler, M. A. & Weiner, D. B. (2004) Developing DNA vaccines that call to dendritic cells. *The Journal of Clinical Investigation,* **114,** 1241-4.

Kwissa, M., Kampen, J., Zurbriggen, R., Gluck, R., Reimann, J. & Schirmbeck, R. (2000) Efficient vaccination by intradermal or intramuscular inoculation of plasmid DNA expressing hepatitis B surface antigen under desmin promoter/enhancer control. *Vaccine,* **18,** 2337-2344.

La Montagne, J. R. & Fauci, A. S. (2004) Intradermal influenza vaccination--can less be more? *New England Journal of Medicine,* **351,** 2330-2.

Lajtha, L. G. (1979) Stem cell concepts. *Differentiation,* **14,** 23-34.

Larregina, A. T. & Falo, L. D. (2005) Changing paradigms in cutaneous immunology: Adapting with dendritic cells. *Journal of Investigative Dermatology,* **124,** 1-12.

Larregina, A. T., Watkins, S. C., Erdos, G., Spencer, L. A., Storkus, W. J., Beer Stolz, D. & Falo, L. D., Jr. (2001) Direct transfection and activation of human cutaneous dendritic cells. *Gene Therapy,* **8,** 608-17.

Lavon, I. & Kost, J. (2004) Ultrasound and transdermal drug delivery. *Drug Discovery Today,* **9,** 670-6.

Lechardeur, D., Sohn, K. J., Haardt, M., Joshi, P. B., Monck, M., Graham, R. W., Beatty, B., Squire, J., O'brodovich, H. & Lukacs, G. L. (1999) Metabolic instability of plasmid DNA in the cytosol: a potential barrier to gene transfer. *Gene Therapy,* **6,** 482-97.

Lechardeur, D., Verkman, A. S. & Lukacs, G. L. (2005) Intracellular routing of plasmid DNA during non-viral gene transfer. *Advanced Drug Delivery Reviews,* **57,** 755-67.

Lee, S., Mcauliffe, D. J., Flotte, T. J., Kollias, N. & Doukas, A. G. (1998) Photomechanical transcutaneous delivery of macromolecules. *Journal of Investigative Dermatology,* **111,** 925-929.

Lee, W. R., Shen, S. C., Wang, K. H., Hu, C. H. & Fang, J. Y. (2002) The effect of laser treatment on skin to enhance and control transdermal delivery of 5-fluorouracil. *Journal of Pharmaceutical Science,* **91,** 1613-26.

Lee, W. R., Shen, S. C., Kuo-Hsien, W., Hu, C. H. & Fang, J. Y. (2003) Lasers and microdermabrasion enhance and control topical delivery of vitamin C. *Journal of Investigative Dermatology,* **121,** 1118-25.

Levin, G., Gershonowitz, A., Sacks, H., Stern, M., Sherman, A., Rudaev, S., Zivin, I. & Phillip, M. (2005) Transdermal delivery of human growth hormone through RF-microchannels. *Pharmaceutical Research,* **22,** 550-5.

Li, L. & Hoffmann, R. M. (1995) The feasibility of targeted selective gene therapy of the hair follicle. *Nature Medicine,* **1,** 705-706.

Li, Z., Ning, W., Wang, J., Choi, A., Lee, P. Y., Tyagi, P. & Huang, L. (2003) Controlled gene delivery system based on thermosensitive biodegradable hydrogel. *Pharmaceutical Research,* **20,** 884-8.

Lian, T. & Ho, R. J. (2003) Design and characterization of a novel lipid-DNA complex that resists serum-induced destabilization. *Journal of Pharmaceutical Science,* **92,** 2373-85.

Lin, M. T. S., Pulkkinen, L., Uitto, J. & Yoon, K. (2000) The gene gun: current applications in cutaneous gene therapy. *International Journal of Dermatology,* **39,** 161-170.

Lin, W., Cormier, M., Samiee, A., Griffin, A., Johnson, B., Teng, C. L., Hardee, G. E. & Daddona, P. E. (2001) Transdermal delivery of antisense oligonucleotides with microprojection patch (Macroflux) technology. *Pharmaceutical Research,* **18,** 1789-93.

Lisziewicz, J., Trocio, J., Whitman, L., Varga, G., Xu, J., Bakare, N., Erbacher, P., Fox, C., Woodward, R., Markham, P., Arya, S., Behr, J. P. & Lori, F. (2005) DermaVir: a novel topical vaccine for HIV/AIDS. *Journal of Investigative Dermatology,* **124,** 160-9.

Lisziewicz, J., Kelly, L. & Lori, F. (2006) Topical DermaVir vaccine targeting dendritic cells. *Current Drug Delivery,* **3,** 83-88.

Liu, Y., Mounkes, L. C., Liggitt, H. D., Brown, C. S., Solodin, I., Heath, T. D. & Debs, R. J. (1997) Factors influencing the efficiency of cationic liposome-mediated intravenous gene delivery. *Nature Biotechnology,* **15,** 167-73.

Liu, L. J., Watabe, S., Yang, J., Hamajima, K., Ishii, N., Hagiwara, E., Onari, K., Xin, K. Q. & Okuda, K. (2001) Topical application of HIV DNA vaccine with cytokine-expression plasmids induces strong antigen-specific immune responses. *Vaccine,* **20,** 42-8.

Lleres, D., Weibel, J. M., Heissler, D., Zuber, G., Duportail, G. & Mely, Y. (2004) Dependence of the cellular internalization and transfection efficiency on the structure and physicochemical properties of cationic detergent/DNA/liposomes. *Journal of Gene Medicine,* **6,** 415-28.

Lombry, C., Dujardin, N. & Preat, V. (2000) Transdermal delivery of macromolecules using skin electroporation. *Pharmaceutical Research,* **17,** 32-37.

Luttge, R., Gardeniers, J. G. E., Vrouwe, E. X. & Van Den Berg, A. (2003) Microneedle array interface to ce on chip. *7th International Conference on Miniaturized Chemical and Biochemical Analysis Systems.* Calafornia, USA.

Ma, H., Xu, R., Cheng, H., Kuo, H. S., During, M. & Fang, R. H. (2003) Gene transfer into human keloid tissue with adeno-associated virus vector. *Journal of Trauma,* **54,** 569-73.

Macgregor, G. R. & Caskey, C. T. (1989) Construction of plasmids that express E. coli beta-galactosidase in mammalian cells. *Nucleic Acids Research,* **17,** 2365.

Madison, K. C. (2003) Barrier function of the skin: "la raison d'etre" of the epidermis. *Journal of Investigative Dermatology,* **121,** 231-41.

Magnaldo, T. & Sarasin, A. (2002) Genetic reversion of inherited skin disorders. *Mutation Research,* **509,** 211-220.

Magnaldo, T. & Sarasin, A. (2004) Xeroderma pigmentosum: from symptoms and genetics to gene-based skin therapy. *Cells Tissues Organs,* **177,** 189-98.

Manthorpe, M., Cornefert-Jensen, F., Hartikka, J., Felgner, J., Rundell, A., Margalith, M. & Dwarki, V. (1993) Gene therapy by intramuscular injection of plasmid DNA: studies on firefly luciferase gene expression in mice. *Human Gene Therapy,* **4,** 419-31.

Martanto, W., Davis, S. P., Holiday, N. R., Wang, J., Gill, H. S. & Prausnitz, M. R. (2004) Transdermal delivery of insulin using microneedles *in vivo*. *Pharmaceutical Research,* **21,** 947-52.

Martanto, W., Moore, J., Kashlan, O., Kamath, R., Wang, P., O'neal, J. & Prausnitz, M. (2006) Microinfusion using hollow microneedles. *Pharmaceutical Research,* **23,** 104-113.

Matriano, J. A., Cormier, M., Johnson, J., Young, W. A., Buttery, M., Nyam, K. & Daddona, P. E. (2002) Macroflux microprojection array patch technology: a new and efficient approach for intracutaneous immunization. *Pharmaceutical Research,* **19,** 63-70.

Mcallister, D. V., Cros, F., Davis, S. P., Matta, L. M., Prausnitz, M. R. & Allen, M. G. Three-dimensional hollow microneedle and microtube arrays. Transducers 99, International conference on solid state sensors and actuators; June 7-10 1999; Sendai. 1999, 1098-1101.

Mcallister, D. V., Wang, P. M., Davis, S. P., Park, J. H., Canatella, P. J., Allen, M. G. & Prausnitz, M. R. (2003) Microfabricated needles for transdermal delivery of macromolecules and nanoparticles: fabrication methods and transport studies. *Proceedings of the National Academy of Science, USA,* **100,** 13755-60.

Mccluskie, M. J., Brazolot Millan, C. L., Gramzinski, R. A., Robinson, H. L., Santoro, J. C., Fuller, J. T., Widera, G., Haynes, J. R., Purcell, R. H. & Davis, H. L. (1999) Route and method of delivery of DNA vaccine influence immune responses in mice and non-human primates. *Molecular Medicine,* **5,** 287-300.

Mcgrew, R. E. & Mcgrew, M. (1985) *Encyclopedia of Medical History,* New York, McGraw-Hill.

Medi, B. M. & Singh, J. (2003) Electronically facilitated transdermal delivery of human parathyroid hormone (1-34). *International Journal of Pharmaceutics,* **263,** 25-33.

Meidan, V. M., Bonner, M. C. & Michniak, B. B. (2005) Transfollicular drug delivery--Is it a reality? *International Journal of Pharmaceutics,* **306,** 1-14.

Meng, X., Sawamura, D., Baba, T., Ina, S., Ita, K., Tamai, K., Hanada, K. & Hashimoto, I. (1999) Transgenic TNF-alpha causes apoptosis in epidermal keratinocytes after subcutaneous injection of TNF-alpha DNA plasmid. *Journal of Investigative Dermatology,* **113,** 856-7.

Meng, X., Sawamura, D., Ina, S., Tamai, K., Hanada, K. & Hashimoto, I. (2002) Keratinocyte gene therapy: cytokine gene expression in local keratinocytes and in circulation by introducing cytokine genes into skin. *Experimental Dermatology,* **11,** 456-61.

Menon, G. K. & Elias, P. M. Chapter 1: The epidermal barrier and strategies for surmounting it: An overview. In: HENGGE, U. R. & VOLC-PLATZER, B., editors. The Skin and Gene Therapy. Berlin: Springer, 2001, 3.

Menon, G. K. (2002) New insights into skin structure: scratching the surface. *Advanced Drug Delivery Reviews,* **54,** S3-S17.

Merdan, T., Kopecek, J. & Kissel, T. (2002) Prospects for cationic polymers in gene and oligonucleotide therapy against cancer. *Advanced Drug Delivery Reviews,* **54,** 715-758.

Meykadeh, N., Mirmohammadsadegh, A., Wang, Z., Basner-Tschakarjan, E. & Hengge, U. (2005) Topical application of plasmid DNA to mouse and human skin. *Journal of Molecular Medicine,* **83,** 897-903.

Messager, S., Hann, A. C., Goddard, P. A., Dettmar, P. W. & Maillard, J. Y. (2003) Assessment of skin viability: is it necessary to use different methodologies? *Skin Research and Technology,* **9,** 321-30.

Meuli, M., Liu, Y., Liggitt, D., Kashani-Sabet, M., Knauer, S., Meuli-Simmen, C., Harrison, M. R., Adzick, N. S., Heath, T. D. & Debs, R. J. (2001) Efficient gene expression in skin wound sites following local plasmid injection. *Journal of Investigative Dermatology,* **116,** 131-135.

Mikszta, J. A., Alarcon, J. B., Brittingham, J. M., Sutter, D. E., Pettis, R. J. & Harvey, N. G. (2002) Improved genetic immunization via micromechanical disruption of skin-barrier function and targeted epidermal delivery. *Nature Medicine,* **8,** 415-419.

Mikszta, J. A., Sullivan, V. J., Dean, C., Waterston, A. M., Alarcon, J. B., Dekker, J. P., Brittingham, J. M., Huang, J., Hwang, C. R., Ferriter, M., Jiang, G., Mar, K., Saikh, K. U., Stiles, B. G., Roy, C. J., Ulrich, R. G. & Harvey, N. G. (2005) Protective immunization against inhalational anthrax: a comparison of minimally invasive delivery platforms. *The Journal of Infectious Diseases,* **191,** 278-88.

Mirmohammadsadegh, A., Maschke, J., Basner-Tschakarjan, E., Bar, A. & Hengge, U. R. (2002) Reaction of keratinocytes to exogenous DNA. *Cells Tissues Organs,* **172,** 86-95.

Mitragotri, S. (2004) Breaking the skin barrier. *Advanced Drug Delivery Reviews,* **56,** 555-6.

Miyano, T., Tobinaga, Y., Kanno, T., Matsuzaki, Y., Takeda, H., Wakui, M. & Hanada, K. (2005) Sugar Micro Needles as Transdermic Drug Delivery System. *Biomedical Microdevices,* **7,** 185-188.

Modamio, P., Lastra, C. F. & Marino, E. L. (2000) A comparative *in vitro* study of percutaneous penetration of beta-blockers in human skin. *International Journal of Pharmaceutics,* **194,** 249-59.

Moll, I., Houdek, P., Schmidt, H. & Moll, R. (1998) Characterization of epidermal wound healing in a human skin organ culture model: acceleration by transplanted keratinocytes. *Journal of Investigative Dermatology,* **111,** 251-8.

Moll, I. (2003) Human skin organ culture. *Methods in Molecular Medicine,* **78,** 305-10.

Montagna, W. & Parakkal, P. F. The structure and function of skin. In: MONTAGNA, W. & PARAKKAL, P. F., editors. The structure and function of skin. 3rd ed. New York: Academic Press Inc, 1974.

Morel, P. A., Falkner, D., Plowey, J., Larregina, A. T. & Falo, L. D. (2004) DNA immunisation: altering the cellular localisation of expressed protein and the immunisation route allows manipulation of the immune response. *Vaccine,* **22,** 447-56.

Morgan, R. A. & Anderson, W. F. (1993) Human Gene Therapy. *Annual Review of Biochemistry,* **62,** 191-217.

Mukerjee, E. V., Collins, S. D., Isseroff, R. R. & Smith, R. L. (2004) Microneedle array for transdermal biological fluid extraction and *in situ* analysis. *Sensors and Actuators A,* **114,** 267-275.

Mumper, R. J. & Cui, Z. (2003) Genetic immunization by jet injection of targeted pDNA-coated nanoparticles. *Methods,* **31,** 255-62.

Munkonge, F. M., Dean, D. A., Hillery, E., Griesenbach, U. & Alron, E. W. F. W. (2003) Emerging significance of plasmid DNA nuclear import in gene therapy. *Advanced Drug Delivery Reviews,* **55,** 749-760.

Nelson, J. S., Mccullough, J. L., Glenn, T. C., Wright, W. H., Liaw, L.-H. L. & Jacques, S. L. (1991) Mid-Infrared laser ablation of stratum corneum enhances *in vitro* percutaneous transport of drugs. *Journal of Investigative Dermatology,* **97,** 874-879.

Newton, A. M., Lal, A. & Chen, X. (2003) Ultrasonically driven microneedle arrays. *Advanced Drug Delivery Reviews,* **2003,** 77-88.

Nishikawa, M. & Huang, L. (2001) Nonviral vectors in the new millennium: delivery barriers in gene transfer. *Human Gene Therapy,* **12,** 861-70.

O'hagan, D. T. & Rappuoli, R. (2004) Novel approaches to vaccine delivery. *Pharmaceutical Research,* **21,** 1519-1530.

Odland, G. (1960) A submicroscopic granular component in human skin. *Journal of Investigative Dermatology,* **34,** 11-15.

Ohyama, M. & Vogel, J. C. (2003) Gene delivery to the hair follicle. *Jounrnal of Investigative Dermatology Symposium Proceedings,* **8,** 204-6.

Oota, S. (1999) Some new aspects of Langerhans Cells in the Human Epidermis: Light and Electron Microscopic Observations on the Swelling Sites Seen in the Process Terminals of the Dendritic Cells Described by Langerhans in 1868. *Yonago Acta medica,* **42,** 153-161.

Osorio, J. E., Zuleger, C. L., Burger, M., Chu, Q., Payne, L. G. & Chen, D. (2003) Immune responses to hepatitis B surface antigen following epidermal powder immunization. *Immunology and Cell Biology,* **81,** 52-8.

Panchagnula, R., Stemmer, K. & Ritschel, W. A. (1997) Animal models for transdermal drug delivery. *Methods and Findings in Experimental and Clinical Pharmacology,* **19,** 335-341.

Pardoll, D. M. & Beckerleg, A. M. (1995) Exposing the immunology of naked DNA vaccines. *Immunity,* **3,** 165-169.

Park, J. H., Allen, M. G. & Prausnitz, M. R. (2005) Biodegradable polymer microneedles: Fabrication, mechanics and transdermal drug delivery. *Journal of Controlled Release,* **104,** 51-66.

Park, Y. J., Liang, J. F., Ko, K. S., Kim, S. W. & Yang, V. C. (2003) Low molecular weight protamine as an efficient and nontoxic gene carrier: *in vitro* study. *The Journal of Gene Medicine,* **5,** 700-711.

Partidos, C. D., Beignon, A. S., Brown, F., Kramer, E., Briand, J. P. & Muller, S. (2002) Applying peptide antigens onto bare skin: induction of humoral and cellular immune responses and potential for vaccination. *Journal of Controlled Release,* **85,** 27-34.

Partidos, C. D. (2003) Delivering vaccines into the skin without needles and syringes. *Expert Review of Vaccines,* **2,** 753-61.

Partidos, C. D., Beignon, A. S., Mawas, F., Belliard, G., Briand, J. P. & Muller, S. (2003) Immunity under the skin: potential application for topical delivery of vaccines. *Vaccine,* **21,** 776-80.

Partidos, C. D. & Muller, S. (2005) Decision-making at the surface of the intact or barrier disrupted skin: potential applications for vaccination or therapy. *Cellular and Molecular Life Sciences,* **62,** 1418-1424.

Paulsen, D. F. (2000) *Part I: Fundamental concepts: Methods of Study,* New York, McGraw-Hill.

Pedroso De Lima, M. C., Simoes, S., Pires, P., Faneca, H. & Duzgunes, N. (2001) Cationic lipid-DNA complexes in gene delivery: from biophysics to biological applications. *Advanced Drug Delivery Reviews,* **47,** 277-94.

Peng, Z. (2005) Current Status of Gendicine in China: Recombinant Human Ad-p53 Agent for Treatment of Cancers. *Human Gene Therapy,* **16,** 1016-1027.

Perkin, F. S. (1950) Jet injection of insulin in treatment of diabetes mellitus. *Proceedings of the American Diabetes Association,* **10,** 185-199.

Pertmer, T. M., Eisenbraun, M. D., Mccabe, D., Prayaga, S. K., Fuller, D. H. & Haynes, J. R. (1995) Gene gun-based nucleic acid immunization: elicitation of humoral and cytotoxic T lymphocyte responses following epidermal delivery of nanogram quantities of DNA. *Vaccine,* **13,** 1427-30.

Piskin, E., Dincer, S. & Turk, M. (2004) Gene delivery: intelligent but just at the beginning. *Journal of Biomaterials Science Polymer Edition* **15,** 1181-202.

Potten, C. S. & Booth, C. (2002) Keratinocyte stem cells: a commentary. *Journal of Investigative Dermatology,* **119,** 888-99.

Potts, R. O. & Francoeur, M. L. (1991) The influence of stratum corneum morphology on water permeability. *Journal of Investigative Dermatology,* **96,** 495-499.

Prausnitz, M. R. (2001) Overcoming skin's barrier: the search for effective and user-friendly drug delivery. *Diabetes Technology & Therapeutics,* **3,** 233-236.

Prausnitz, M. R., Ackley, D. E. & Gyory, J. R. (2003) *Microfabricated microneedles for transdermal drug delivery,* New York, Marcel Dekker.

Prausnitz, M. R., Mitragotri, S. & Langer, R. (2004) Current status and future potential of transdermal drug delivery. *Nature Reviews: Drug Discovery,* **3,** 115-24.

Raghavachari, N. & Fahl, W. E. (2002) Targeted gene delivery to skin cells in vivo: a comparative study of liposomes and polymers as delivery vehicles. *Journal of Pharmaceutical Science,* **91,** 615-22.

Raju, P. A., Truong, N. K. & Kendall, M. A. F. (In Press) Assessment of epidermal cell viability by near infrared multi-photon microscopy following ballistic delivery of gold micro-particles. *Vaccine,* **Corrected Proof.**

Rakhmilevich, A. L., Turner, J., Ford, M. J., Mccabe, D., Sun, W. H., Sondel, P. M., Grota, K. & Yang, N.-S. (1996) Gene gun-mediated skin transfection with interleukin 12 gene results in regression of established primary and metastatic murine tumors. *Proceedings of the National Academy of Science, USA,* **93,** 6291-6296.

Rama Rao, P., Reddy, M. N., Ramakrishna, S. & Diwan, P. V. (2003) Comparative in vivo evaluation of propranolol hydrochloride after oral and transdermal administration in rabbits. *European Journal of Pharmaceutics and Biopharmaceutics,* **56,** 81-85.

Raper, S. E., Chirmule, N., Lee, F. S., Wivel, N. A., Bagg, A., Gao, G.-P., Wilson, J. M. & Batshaw, M. L. (2003) Fatal systemic inflammatory response syndrome in a ornithine transcarbamylase deficient patient following adenoviral gene transfer. *Molecular Genetics and Metabolism,* **80,** 148-158.

Raz, E., Carson, D. A., Parker, S. E., Parr, T. B., Abai, A. M., Aichinger, G., Gromkowski, S. H., Singh, M., Lew, D., Yankauckas, M. A. & Et Al. (1994) Intradermal gene immunization: the possible role of DNA uptake in the induction of cellular immunity to viruses. *Proceedings of the National Academy of Science, USA,* **91,** 9519-23.

Reece, J. C., Handley, A. J., Anstee, E. J., Morrison, W. A., Crowe, S. M. & Cameron, P. U. (1998) HIV-1 selection by epidermal dendritic cells during transmission across human skin. *Journal of Experimental Medicine,* **187,** 1623-31.

Reed, M. L., Wu, C., Kneller, J., Watkins, S., Vorp, D. A., Nadeem, A., Weiss, L. E., Rebello, K., Mescher, M., Smith, A. J. C., Rosenblum, W. & Feldman, M. D. (1998) Micromechanical devices for intravascular drug delivery. *Journal of Pharmaceutical Sciences,* **87,** 1387-1394.

Restifo, N. P., Ying, H., Hwang, L. & Leitner, W. W. (2000) The promise of nucleic acid vaccines. *Gene Therapy,* **7,** 89-92.

Rijnkels, J. M., Whiteley, L. O. & Beijersbergen Van Henegouwen, G. M. (2001) Time and dose-related ultraviolet B damage in viable pig skin explants held in a newly developed organ culture system. *Photochemistry and Photobiology,* **73,** 499-504.

Roberts, L. K., Barr, L. J., Fuller, D. H., Mcmahon, C. W., Leese, P. T. & Jones, S. (2005) Clinical safety and efficacy of a powdered hepatitis B nucleic acid vaccine delivered to the epidermis by a commercial prototype device. *Vaccine,* **23,** 4867-4878.

Roberts, M. S. & Walters, K. A. Chapter 1: The Relationship Between Structure and Barrier Function of Skin. In: ROBERTS, M. S. & WALTERS, K. A., editors. Dermal Absorption and Toxicity Assessment. New York: Marcel Dekker, 1998, 1-43.

Romani, N., Holzmann, S., Tripp, C. H., Koch, F. & Stoitzner, P. (2003) Langerhans cells - dendritic cells of the epidermis. *APMIS,* **111,** 725-740.

Rosenberg, S. A., Aebersold, P., Cornetta, K., Kasid, A., Morgan, R. A., Moen, R., Karson, E. M., Lotze, M. T., Yang, J. C. & Topalian, S. L. (1990) Gene transfer into humans - immunotherapy of patients with advanced melanoma, using tumour-infiltrating lymphocytes modified by retroviral gene transduction. *New England Journal of Medicine,* **323,** 570-578.

Roy, I., Mitra, S., Maitra, A. & Mozumdar, S. (2003) Calcium phosphate nanoparticles as novel non-viral vectors for targeted gene delivery. *International Journal of Pharmaceutics,* **250,** 25-33.

Ruponen, M., Honkakoski, P., Ronkko, S., Pelkonen, J., Tammi, M. & Urtti, A. (2003) Extracellular and intracellular barriers in non-viral gene delivery. *Journal of Controlled Release,* **93,** 213-7.

Sawamura, D., Meng, X., Ina, S., Sato, M., Tamai, K., Hanada, K. & Hashimoto, I. (1998) Induction of keratinocyte proliferation and lymphocytic infiltration by in vivo introduction of the IL-6 gene into keratinocytes and possibility of keratinocyte gene

therapy for inflammatory skin diseases using IL-6 mutant genes. *Journal of Immunology,* **161,** 5633-9.

Sawamura, D., Ina, S., Itai, K., Meng, X., Kon, A., Tamai, K., Hanada, K. & Hashimoto, I. (1999) *In vivo* gene introduction into keratinocytes using jet injection. *Gene Therapy,* **6,** 1785-7.

Sawamura, D., Akiyama, M. & Shimizu, H. (2002a) Direct injection of naked DNA and cytokine transgene expression: implications for keratinocyte gene therapy. *Clinical and Experimental Dermatology,* **27,** 480-4.

Sawamura, D., Yasukawa, K., Kodama, K., Yokota, K., Sato-Matsumura, K. C., Tosihiro, T. & Shimizu, H. (2002b) The majority of keratinocytes inocorporate intradermally injected plasmid DNA regardless of size, but only a small proportion of cells can express the gene product. *The Journal of Investigative Dermatology,* **118,** 967-971.

Sawamura, D., Abe, R., Goto, M., Akiyama, M., Hemmi, H., Akira, S. & Shimizu, H. (2005) Direct injection of plasmid DNA into the skin induces dermatitis by activation of monocytes through toll-like receptor 9. *Journal of Gene Medicine,* **7,** 664-71.

Scharton-Kersten T, G. G. M., Vassell R, Yu J, Walwender D, Alving C.R (1999) Principles of transcutaneous immunization using cholera toxin as an adjuvant. *Vaccine,* **17,** S37-S43.

Scheulplein, R. L. & Blank, I. H. (1971) Permeability of the Skin. *Physiology Reviews,* **51,** 702-747.

Schramm-Baxter, J. & Mitragotri, S. (2004) Needle-free jet injections: dependence of jet penetration and dispersion in the skin on jet power. *Journal of Controlled Release,* **97,** 527-35.

Schuetz, Y. B., Naik, A., Guy, R. H. & Kalia, Y. N. (2005) Emerging strategies for the transdermal delivery of peptide and protein drugs. *Expert Opinion in Drug Delivery,* **2,** 533-48.

Schuler, G. & Steinman, R. M. (1985) Murine epidermal Langerhans cells mature into potent immunostimulatory dendritic cells *in vitro*. *Journal of experimental medicine,* **161,** 526-46.

Sebestyen, M. G., Ludtke, J. J., Bassik, M. C., Zhang, G., Budker, V., Lukhtanov, E. A., Hagstrom, J. E. & Wolff, J. A. (1998) DNA vector chemistry: the covalent attachment of signal peptides to plasmid DNA. *Nature Biotechnology,* **16,** 80-85.

Sekkat, N. K., Y. N.; Guy, R. H. (2002) Biophysical study of porcine ear skin *in vitro* and its comparison to human skin *in vivo*. *Journal of Pharmaceutical Science,* **91,** 2376-2381.

Shedlock, D. J. & Weiner, D. B. (2000) DNA vaccination: antigen presentation and the induction of immunity. *Journal of Leukocyte Biology,* **68,** 793-806.

Shi, Z., Curiel, D. T. & Tang, D. (1999) DNA-based non-invasive vaccination onto the skin. *Vaccine,* **17,** 2136-2141.

Shirkhanzadeh, M. (2005) Microneedles coated with porous calcium phosphate ceramics: Effective vehicles for transdermal delivery of solid trehalose. *Journal of Materials Science: Materials in Medicine,* **16,** 37-45.

Singh, S. & Swerlick, R. A. Chapter 10: Structure and function of the cutaneous vasculature. In: FREINKEL, R. K. & WOODLEY, D. T., editors. The Biology of the Skin. 1st ed. New York: The Parthenon Publishing Group, 2001.

Sintov, A. C., Krymberk, I., Daniel, D., Hannan, T., Sohn, Z. & Levin, G. (2003) Radiofrequency-driven skin microchanneling as a new way for electrically assisted transdermal delivery of hydrophilic drugs. *Journal of Controlled Release,* **89,** 311-320.

Sivamani, R. K., Stoeber, B., Wu, G. C., Zhai, H., Liepmann, D. & Maibach, H. (2005) Clinical microneedle injection of methyl nicotinate: stratum corneum penetration. *Skin Research and Technology,* **11,** 152-156.

Smart, W. H. & Subramanian, K. (2000) The use of silicon microfabrication technology in painless blood glucose monitoring. *Diabetes Technology & Therapeutics,* **2,** 549-559.

Smith, P. K., Krohn, R. I., Hermanson, G. T., Mallia, A. K., Gartner, F. H., Provenzano, M. D., Fujimoto, E. K., Goeke, N. M., Olson, B. J. & Klenk, D. C. (1985) Measurement of protein using bicinchoninic acid. *Analytical Biochemistry,* **150,** 76-85.

Sondell, B., Thornell, L. E. & Egelrud, T. (1995) Evidence that stratum corneum chymotryptic enzyme is transported to the stratum corneum extracellular space via lamellar bodies. *Journal of Investigative Dermatology,* **104,** 819-823.

Sotomayor, M. G., Yu, H., Antonia, S., Sotomayor, E. M. & Pardoll, D. M. (2002) Advances in gene therapy for malignant melanoma. *Cancer Control,* **9,** 39-48.

Spradling, A., Drummond-Barbosa, D. & Kai, T. (2001) Stem cells find their niche. *Nature,* **414,** 98-104.

Sterne, G. D., Titley, O. G. & Christie, J. L. (2000) A qualitative histological assessment of various storage conditions on short term preservation of human split skin grafts. *British Journal of Plastic Surgery,* **53,** 331-6.

Stoitzner, P., Pfaller, K., Stossel, H. & Romani, N. (2002) A close-up view of migrating Langerhans cells in the skin. *Journal of Investigative Dermatology,* **118,** 117-25.

Stott, P. W., Williams, A. C. & Barry, B. W. (2001) Mechanistic study into the enhanced transdermal permeation of a model [beta]-blocker, propranolol, by fatty acids: a melting point depression effect. *International Journal of Pharmaceutics,* **219,** 161-176.

Tacket, C. O., Roy, M. J., Widera, G., Swain, W. F., Broome, S. & Edelman, R. (1999) Phase 1 safety and immune response studies of a DNA vaccine encoding hepatitis B surface antigen delivered by a gene delivery device. *Vaccine,* **17,** 2826-2829.

Tammi, R., Jansen, C. T. & Santti, R. (1979) Histometric analysis of human skin in organ culture. *Journal of Investigative Dermatology,* **73,** 138-140.

Tammi, R. & Maibach, H. (1987) Skin organ culture: why? *International Journal of Dermatology,* **26,** 150-60.

Tang, D., Shi, Z. & Curiel, D. T. (1997) Vaccination onto bare skin. *Nature,* **388,** 730-731.

Tang, D. C., Devit, M. & Johnston, S. A. (1992) Genetic immunization is a simple method for eliciting an immune response. *Nature,* **356,** 152-154.

Teo, M. A. L., Shearwood, C., Ng, K. C., Lu, J. & Moochhala, S. (2005) *In vitro* and *in vivo* characterization of MEMS microneedles. *Biomedical Microdevices,* **7,** 47-52.

Tezel, A., Paliwal, S., Shen, Z. & Mitragotri, S. (2005) Low-frequency ultrasound as a transcutaneous immunization adjuvant. *Vaccine,* **23,** 3800-7.

Ting, W. W., Vest, C. D. & Sontheimer, R. D. (2004) Review of traditional and novel modalities that enhance the permeability of local therapeutics across the stratum corneum. *International Journal of Dermatology,* **43,** 538-47.

Tomita, Y., Nihira, M., Ohno, Y. & Sato, S. (2004) Ultrastructural changes during in situ early postmortem autolysis in kidney, pancreas, liver, heart and skeletal muscle of rats. *Legal Medicine (Tokyo),* **6,** 25-31.

Trebotich, D., Zahn, J. D., Prabhakarpandian, B. & Liepmann, D. (2003) Modelling of microfabricated microneedles for minimally invasive drug delivery, sampling and analysis. *Biomedical Microdevices,* **5,** 245-251.

Trowell, O. A. (1954) A modified technique for organ culture *in vitro*. *Experimental Cell Research,* **6,** 246-248.

Trowell, O. A. (1959) The culture of mature organs in a synthetic medium. *Experimental Cell Research,* **16,** 118-147.

Uherek, C. & Wels, W. (2000) DNA-carrier proteins for targeted gene delivery. *Advanced Drug Delivery Reviews,* **44,** 153-166.

Uitto, J. & Pulkkinen, L. (2000) The genodermatoses: candidate diseases for gene therapy. *Human Gene Therapy,* **11,** 2267-75.

Udvardi, A., Kufferath, I., Grutsch, H., Zatloukal, K. & Volc-Platzer, B. (1999) Uptake of exogenous DNA via the skin. *Journal of Molecular Medicine,* **77,** 744-50.

Vaalasti, A., Tainio, H., Johansson, O. & Rechardt, L. (1988) Light and electron microscopic immunocytochemical demonstration of intraepidermal CGRP-containing nerves in human skin. *Skin Pharmacology,* **1,** 225-229.

Van Kampen, K. R., Shi, Z., Gao, P., Zhang, J., Foster, K. W., Chen, D. T., Marks, D., Elmets, C. A. & Tang, D. C. (2005) Safety and immunogenicity of adenovirus-vectored nasal and epicutaneous influenza vaccines in humans. *Vaccine,* **23,** 1029-36.

Van Roessel, P. & Brand, A. H. (2002) Imaging into the future: visualising gene expression and protein interactions with fluorescent proteins. *Nature Cell Biology,* **4,** E15-E20.

Van Ruissen, F., Jansen, B. J., De Jongh, G. J., Zeeuwen, P. L. & Schalkwijk, J. (2002) A partial transcriptome of human epidermis. *Genomics,* **79,** 671-8.

Varani, J. (1998) Preservation of human skin structure and function in organ culture. *Histology and histopathology,* **13,** 775-83.

Vyas, S. P., Singh, R. P., Jain, S., Mishra, V., Mahor, S., Singh, P., Gupta, P. N., Rawat, A. & Dubey, P. (2005) Non-ionic surfactant based vesicles (niosomes) for non-invasive topical genetic immunization against hepatitis B. *International Journal of Pharmaceutics,* **296,** 80-6.

Walther, W., Stein, U., Voss, C., Schmidt, T., Schleef, M. & Schlag, P. M. (2003) Stability analysis for long-term storage of naked DNA: impact on nonviral in vivo gene transfer. *Anal Biochem,* **318,** 230-5.

Wang, S., Joshi, S. & Lu, S. (2004) Delivery of DNA to skin by particle bombardment. *Methods in Molecular Biology,* **245,** 185-96.

Wang, P. M., Cornwell, M. G. & Prausnitz, M. R. (2002) Effects of Microneedle Tip Geometry on Injection and Extraction in the Skin. Joint EMBS BMES Conference 2nd; Houston, USA. 2002.

Wang, P. M., Cornwell, M. & Prausnitz, M. R. (2005) Minimally invasive extraction of dermal interstitial fluid for glucose monitoring using microneedles. *Diabetes Technology & Therapeutics,* **7,** 131-141.

Wang, P. M., Cornwell, M., Hill, J. & Prausnitz, M. R. (2006) Precise microinjection into skin using hollow microneedles. *Journal of Investigative Dermatology,* 1080-1087.

Watabe, S., Xin, K. Q., Ihata, A., Liu, L. J., Honsho, A., Aoki, I., Hamajima, K., Wahren, B. & Okuda, K. (2001) Protection against influenza virus challenge by topical application of influenza DNA vaccine. *Vaccine,* **19,** 4434-44.

Watkins, C., Hopkins, J. & Harkiss, G. (2005) Reporter gene expression in dendritic cells after gene gun administration of plasmid DNA. *Vaccine,* **23,** 4247-4256.

Wattiaux, R., Laurent, N., Wattiaux-De Coninck, S. & Jadot, M. (2000) Endosomes, lysosomes: their implication in gene transfer. *Advanced Drug Delivery Reviews,* **41,** 201-208.

Webster, P. (1999) The production of cryosections through fixed and cryoprotected biological material and their use in immunocytochemistry. *Methods in Molecular Biology,* **117,** 49-76.

Weiss, D. J., Liggitt, D. & Clark, J. G. (1997) In situ histochemical detection of beta-galactosidase activity in lung: assessment of X-Gal reagent in distinguishing lacZ gene expression and endogenous beta-galactosidase activity. *Human Gene Therapy,* **8,** 1545-54.

Weiss, D. J., Liggitt, D. & Clark, J. G. (1999) Histochemical discrimination of endogenous mammalian beta-galactosidase activity from that resulting from lac-Z gene expression. *Histochemical Journal,* **31,** 231-6.

Wertz, P. W. & Van Den Bergh (1998) Review. The physical, chemical and functional properties of lipids in the skin and other biological barriers. *Chemistry and Physics of Lipids,* **91,** 85-96.

Wester, R. C. & Noonan, P. K. (1980) Relevance of animal models for percutaneous absorption. *International Journal of Pharmaceutics,* **7,** 99-110.

Wet, J. R. D., Wood, K. V., Helinski, D. R. & Deluca, M. (1985) Cloning of firefly luciferase cDNA and the expression of active luciferase in Escherichia coli. *Proceedings of the National Academy of Science, USA,* **82,** 7870-7873.

Widera, G., Johnson, J., Kim, L., Libiran, L., Nyam, K., Daddona, P. E. & Cormier, M. (2006) Effect of delivery parameters on immunization to ovalbumin following intracutaneous administration by a coated microneedle array patch system. *Vaccine,* **24,** 1653-1664.

Wiethoff, C. M. & Middaugh, C. R. (2003) Barriers to nonviral gene delivery. *Journal of Pharmaceutical Science,* **92,** 203-217.

Wilke, N., Hibert, C., O'brien, J. & Morrissey, A. (2005a) Silicon microneedle electrode array with temperature monitoring for electroporation. *Sensors and Actuators A: Physical,* **123-124,** 319-325.

Wilke, N., Mulcahy, A., Ye, S.-R. & Morrissey, A. (2005b) Process optimization and characterization of silicon microneedles fabricated by wet etch technology. *Microelectronics Journal,* **36,** 650-656.

Williams, A. C. Chapter 1: Structure and function of human skin. In: WILLIAMS, A. C., editor. Transdermal and Topical Drug Delivery. London: Pharmaceutical Press, 2003, 1-25.

Williams, R. S., Johnston, S. A., Riedy, M., Devit, M. J., Mcelligott, S. G. & Sanford, J. C. (1991) Introduction of foreign genes into tissues of living mice by DNA-coated microprojectiles. *Proceedings of the National Academy of Science, USA,* **88,** 2726-30.

Williams, I. R. & Kupper, T. S. (1996) Minireview: Immunity at the surface: Homeostatic mechanisms of the skin immune system. *Life Sciences,* **58,** 1485-1507.

Wilson, J. M. (2005) Gendicine: The First Commercial Gene Therapy Product; Chinese Translation of Editorial. *Human Gene Therapy,* **16,** 1014-1015.

Woan-Ruoh, L., Shing-Chuan, S., Kuo-Hsien, W., Chung-Hong, H. & Jia-You, F. (2002) The effect of laser treatment on skin to enhance and control transdermal delivery of 5-fluorouracil. *Journal of Pharmaceutical Sciences,* **91,** 1613-1626.

Wolff, K. The fascinating story that began in 1868. In: SCHULER, G., editor. Epidermal Langerhans Cells. Boca Raton, FL: CRC Press Inc, 1991, 1-21.

Wolff, J. A. & Budker, V. The mechanism of naked DNA uptake and expression. Advances in Genetics: Academic Press, 2005, 1-20.

Woodley, D. T., Keene, D. R., Atha, T., Huang, Y., Ram, R., Kasahara, N. & Chen, M. (2004) Intradermal injection of lentiviral vectors corrects regenerated human dystrophic epidermolysis bullosa skin tissue in vivo. *Molecular Therapy,* **10,** 318-26.

Wu, J., Chappelow, J., Yang, J. & Weimann, L. (1998) Defects generated in human stratum corneum specimens by ultrasound. *Ultrasound in Medicine & Biology,* **24,** 705-710.

Xiao-Wen, H., Shu-Han, S., Zhen-Lin, H., Jun, L., Lei, J., Feng-Juan, Z., Ya-Nan, Z. & Ying-Jun, G. (2005) Augmented humoral and cellular immune responses of a hepatitis B DNA vaccine encoding HBsAg by protein boosting. *Vaccine,* **23,** 1649-56.

Xie, Y., Xu, B. & Gao, Y. (2005) Controlled transdermal delivery of model drug compounds by MEMS microneedle array. *Nanomedicine: Nanotechnology, Biology and Medicine,* **1,** 184-190.

Yang, J.-P. & Huang, L. (1997) Overcoming the inhibitory effect of serum on lipofection by increasing the charge ratio of cationic liposome to DNA. *Gene Therapy,* **4,** 950-961.

Yang, M. & Zahn, J. D. (2004) Microneedle insertion force reduction using vibratory actuation. *Biomedical Microdevices,* **6,** 177-82.

Yang, N. S., Burkholder, J., Roberts, B., Martinell, B. & Mccabe, D. (1990) *In vivo* and *in vitro* gene transfer to mammalian somatic cells by particle bombardment. *Proceedings of the National Academy of Science, USA,* **87,** 9568-72.

Yao, F. & Eriksson, E. (2000) Gene therapy in wound repair and regeneration. *Wound Repair and Regeneration,* **8,** 443-51.

Yu, R. C., Abrams, D. C., Alaibac, M. & Chu, A. C. (1994) Morphological and quantitative analyses of normal epidermal Langerhans cells using confocal scanning laser microscopy. *British Journal of Dermatology,* **131,** 848-848.

Yu, W. H., Kashani-Sabet, M., Liggitt, D., Moore, D., Heath, T. & Debs, R. J. (1999) Topical Gene Delivery to Murine Skin. *The Journal of Investigative Dermatology,* **112,** 370-375.

Zahn, J. D., Deshmukh, A. A., Pisano, A. P. & Liepmann, D. Continuous on-chip micropumping through a microneedle. 4th IEEE International Conference on Micro Electro Mechanical Systems; Interlaken, Switzerland. 2001, 503-506.

Zahn, J. D., Deshmukh, A., Pisano, A. P. & Liepmann, D. (2004) Continuous on-chip micropumping for microneedle enhanced drug delivery. *Biomedical Microdevices,* **6,** 183-90.

Zhang, J. S., Li, S. & Huang, L. (2003) Cationic liposome-protamine-DNA complexes for gene delivery. *Methods in Enzymology,* **373,** 332-42.

Zhang, G., Gao, X., Song, Y. K., Vollmer, R., Stolz, D. B., Gasiorowski, J. Z., Dean, D. A. & Liu, D. (2004) Hydroporation as the mechanism of hydrodynamic delivery. *Gene Therapy,* **11,** 675-82.

Zieger, M. A. J., Tredget, E. E. & Mcgann, L. E. (1993) A simple effective system for assessing viability in split-thickness skin with the use of oxygen consumption. *Journal of Burn Care and Rehabilitation,* **14,** 310-318.

Zuidam, N. J. & Barenholz, Y. (1998) Electrostatic and structural properties of complexes involving plasmid DNA and cationic lipids commonly used for gene delivery. *Biochimica et Biophysica Acta,* **1368,** 115-128.

# APPENDIX I

# (Microneedle Catalogue)

## 1. Cardiff School of Engineering (CSE)

Illustrated below are the dry-etch silicon microneedle arrays created by Cardiff Schoool of Engineering (CSE), Cardiff University, under the direction of Professor David Barrow.

**ARRAY A**

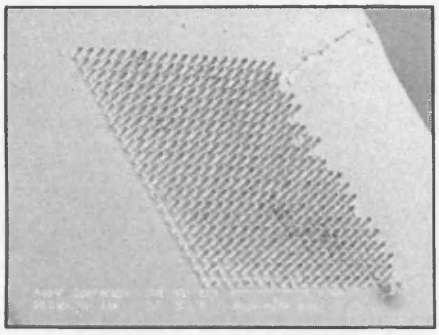

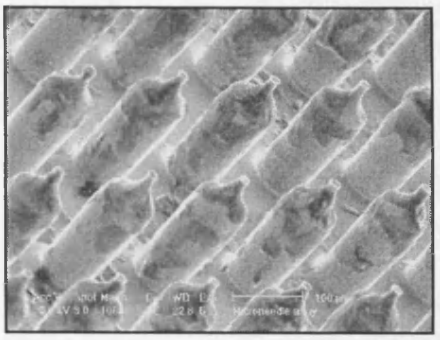

**ARRAY B**

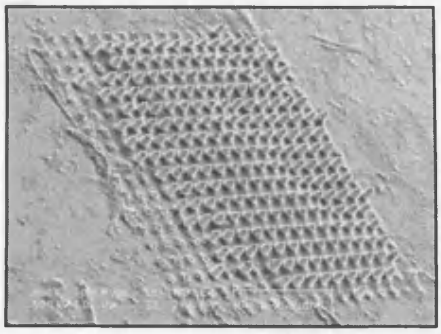

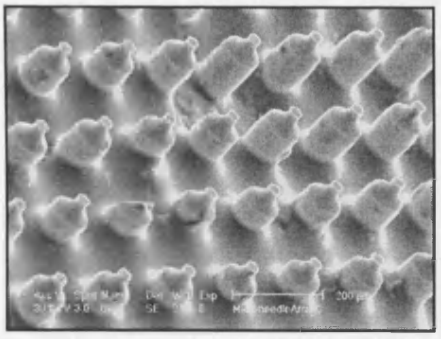

**ARRAY C**

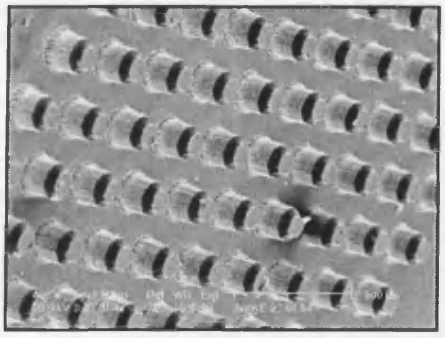

**ARRAY D**

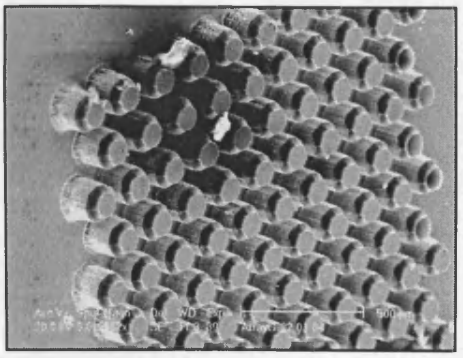

**ARRAY E**

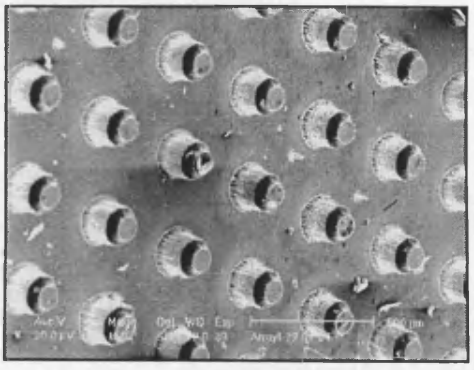

**ARRAY F**

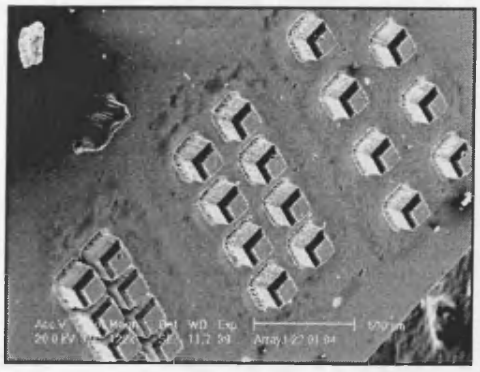

## 2. Tyndall National Institute (TNI)

Illustrated below are the dry-etch silicon microneedle arrays created by Tyndall national institute (TNI), Cork, under the direction of Dr Anthony Morrissey.

**ARRAY 1**

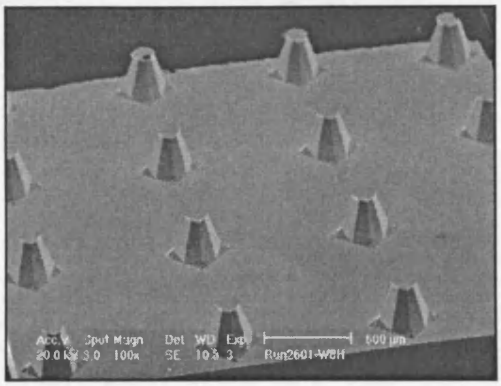

**ARRAY 2**

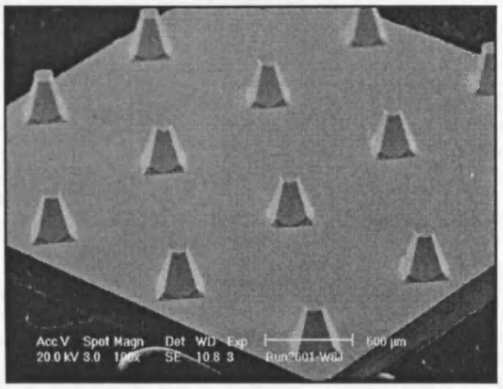

**ARRAY 3**

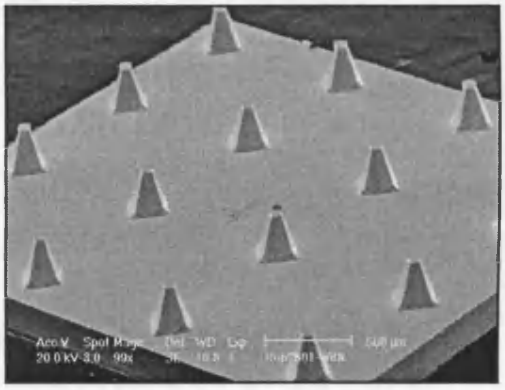

**ARRAY 4**

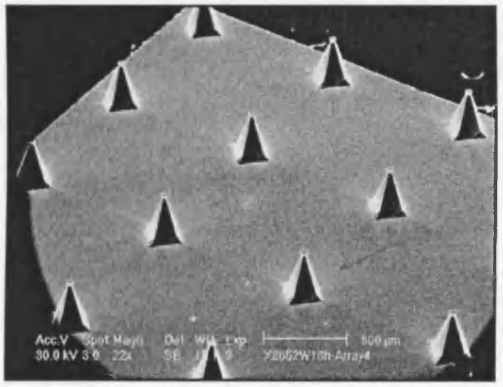

**ARRAY 5**

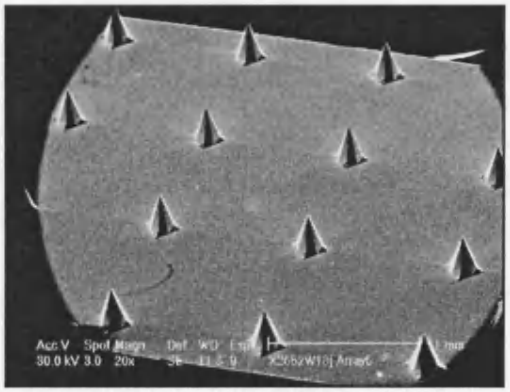

**ARRAY 6**

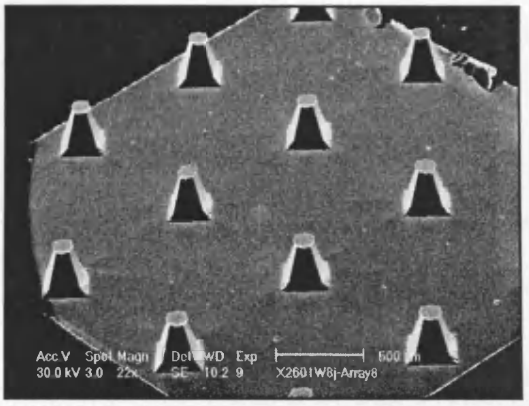

**ARRAY 7**

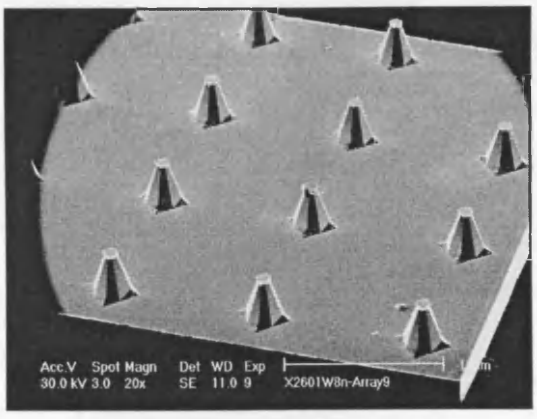


**ARRAY 8**

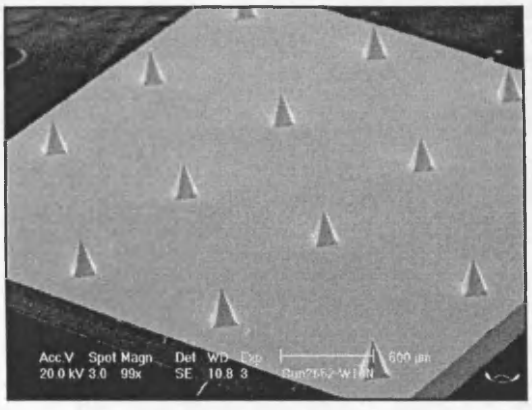


**ARRAY 9**

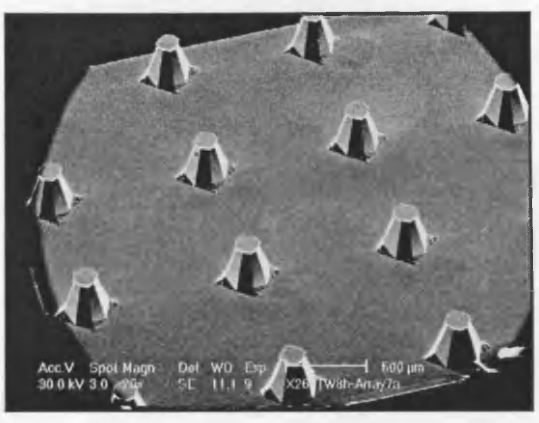


**ARRAY 10**

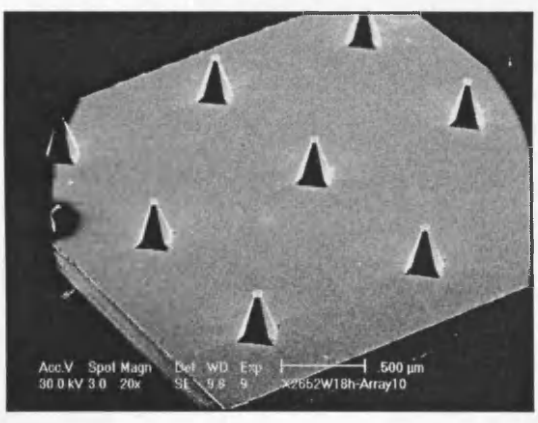


**ARRAY 11**

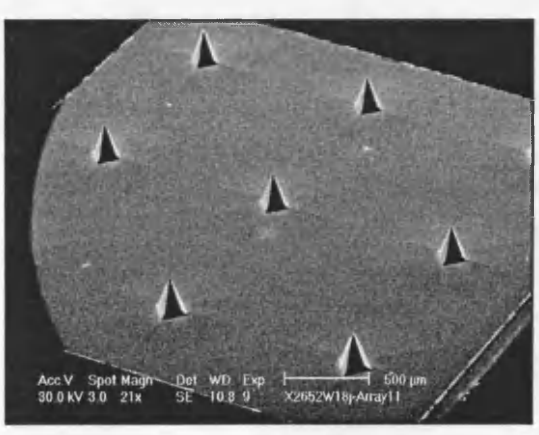


**ARRAY 12**

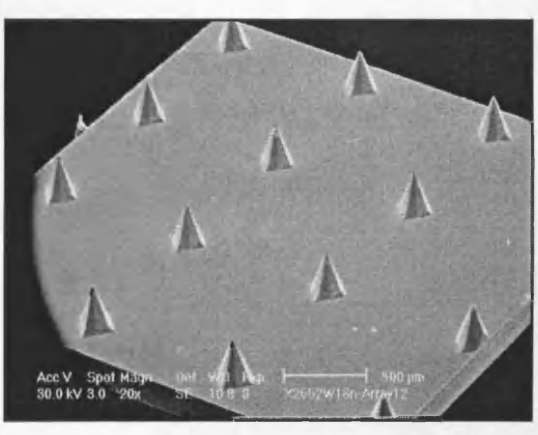

## ARRAY 13

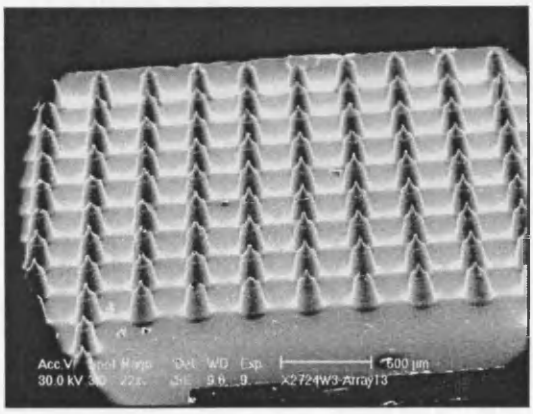


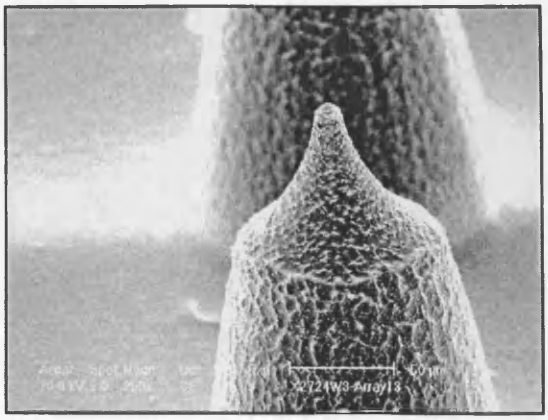


## ARRAY 15

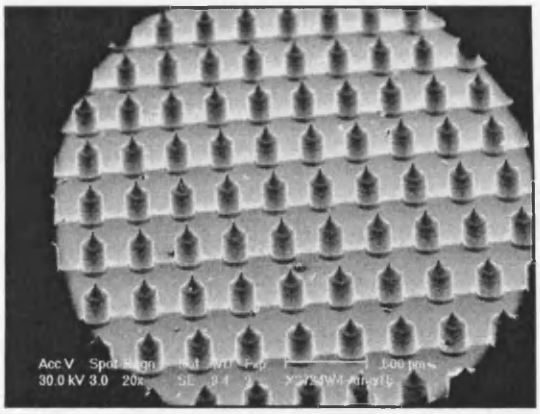


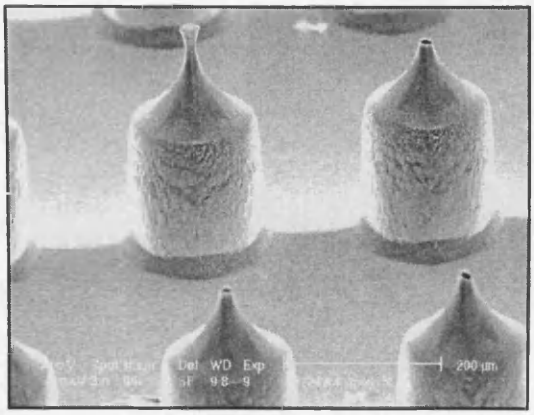

# APPENDIX II

# (Experimental data)

*1. Excitation and Emission Spectra for fluorescent nanospheres*

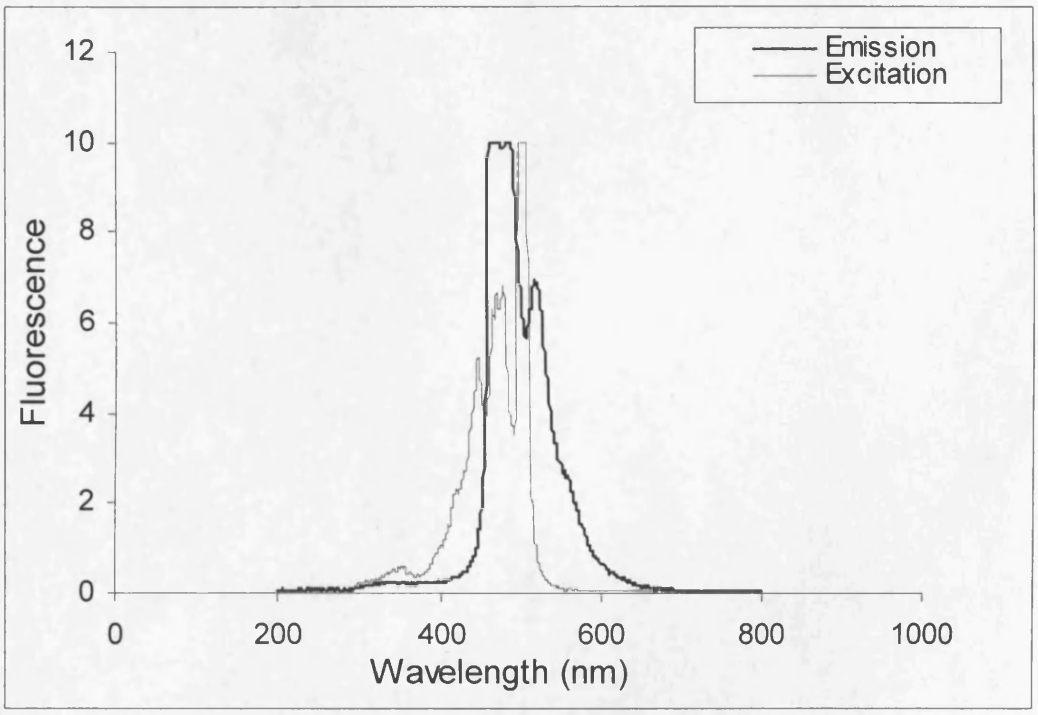


**2. Excitation and Emission Spectra for LCNs**

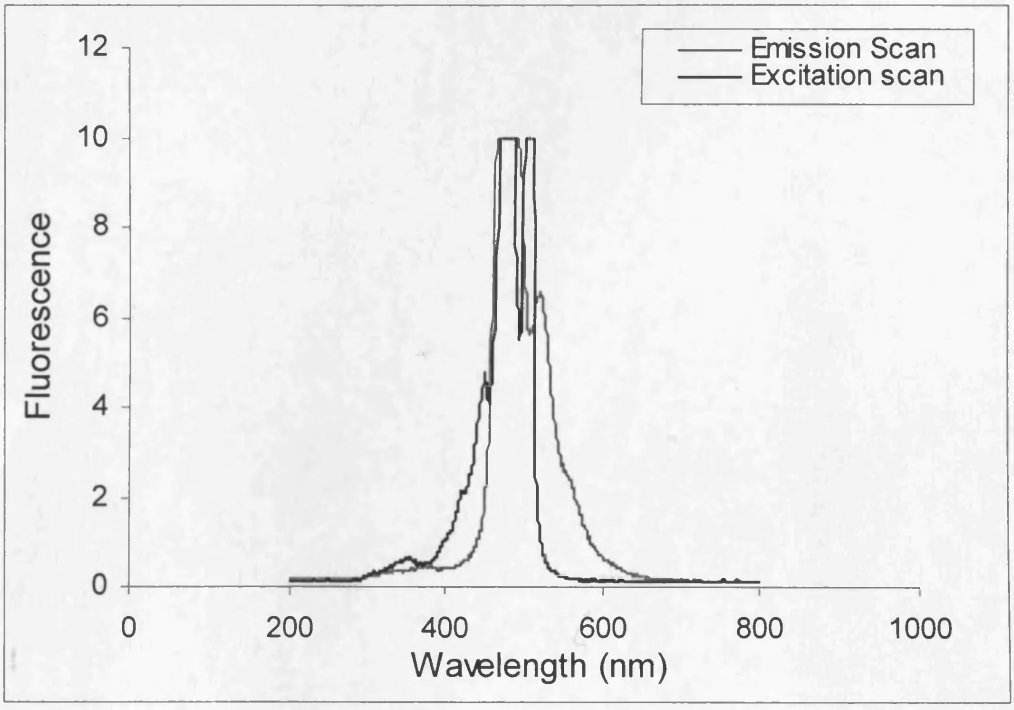

### 3. A summary of pCMVβ Intradermal Injection Experiments

Table A1 – A summary of the results achieved over a six-month period from experiments investigating the intradermal injection of pCMVβ into viable human skin. The total number of skin samples injected for each donor tissue is detailed. Positive identification of transfection is indicated by the asterix * and if more than one dose of a formulation has been used, its identity is listed and its N number stated.

| Donor | (N) | Trans-fection (N) | Formulation (N)<br>* indicates transfected samples | ID |
|---|---|---|---|---|
| - | 7 | 1 | 1mg/ml - 30µl*(4) / 3.67mg/ml - 20µl(3) | C58 |
| 51 | 10 | 6 | 1mg/ml - 20µl(5)****, 10µl**(5) | C66 |
| 87 | 4 | 0 | 1mg/ml - 10µl(4) | C71 |
| 66 | 4 | 0 | 1mg/ml - 10µl(4) | C71 |
| 67 | 8 | 2 | 1mg/ml - 20µl**(8) | C76 |
| 63 | 5 | 0 | 1mg/ml - 10µl(5) | C81 |
| 58 | 16 | 1 | 1mg/ml - 10µl*(16) | C93 |
| 58 | 8 | 1 | 1mg/ml - 20µl*(8) | C97 |
| 77 | 8 | 2 | 1mg/ml - 10µl(4) / 2.93mg/ml - 10µl**(4) | C102 |
| 61 | 16 | 0 | 1mg/ml - 20µl(8) / 2.93mg/ml - 20µl(8) | C105 |
| 78 | 4 | 4 | 2.87mg/ml - 10µl****(4) | C111 |
| 41 | 8 | 0 | 2.87mg/ml - 10µl(8) | C114 |
| 67 | 4 | 0 | 2.87mg/ml - 10µl(4) | C118 |
| 78 | 12 | 0 | 2.87mg/ml - 10µl(12) | C122 |
| **TOTAL** | **114** | **17** | **1mg/ml plasmid (11 from 71)**<br>**Concentrated plasmid (6 from 43)** | |

# APPENDIX III

# (Publications)

## Scientific papers

During my postgraduate studies the following scientific papers have been published (and are attached):-

1. Birchall, J.C. Coulman, S.A. Anstey, A. Gateley, C. Sweetland, H. Gershonowitz, A. Neville, L. Levin, G. (2006) Cutaneous gene expression of plasmid DNA in excised human skin following delivery via microchannels created by radio frequency ablation. *International Journal of Pharmaceutics*, **312** (1-2), 15-23.

2. Coulman, S.A. *et al* (2006) Minimally invasive cutaneous delivery of macromolecules and plasmid DNA *via* microneedles. *Current Drug Delivery*, **3** (1), 65-75.

3. Birchall, J.C. Coulman, S.A. Pearton, M. Allender, C. Brain, K. Anstey, A. Gateley, C. Wilke, N. Morrissey, A. (2005) Cutaneous DNA delivery and gene expression in *ex vivo* human skin explants via wet-etch microfabricated microneedles. *Journal of Drug Targeting*, **13** (7), 415-421.

## Published abstracts

During my postgraduate studies the following scientific abstracts have been published:-

1. Coulman, S.A. *et al* (2006) Microneedle arrays facilitate cutaneous gene delivery and expression. *Perspectives in Percutaneous Penetration.* Vol 10A, p 118.

2. Wilke, N. Allender, C, Birchall, J.C. Coulman, S.A. Pearton, M. Morrissey, A (2006) Assessment of penetration efficiency of microneedle arrays applied to human skin. *Perspectives in Percutaneous Penetration.* Vol 10A, p 123.

3. Morrissey, A. Wilke, N. Coulman, S.A. Pearton, S.A. Anstey, A. Gateley, C. Allender, C. Brain, K. Birchall, J. (2005) Determination of Mechanical Properties of Silicon and Polymer Microneedles, 3rd European Medical & Biological Engineering Conference, EMBEC'05, Prague.

4. Coulman, S.A. *et al* (2005) Microneedle facilitated gene delivery to human skin, *British Journal of Dermatology,* **152,** 846.

5. Coulman, S.A. *et al* (2004) Microneedle facilitated cutaneous delivery of a non-viral gene complex to the viable epidermis, *Journal of Pharmacy and Pharmacology*, **56** (supp), S10.

6. Coulman, S.A. *et al* (2004) Non-viral gene delivery to epidermal keratinocytes. *Perspectives in Percutaneous Penetration.* Vol 9A, p 33.

## Conferences and meetings

During my postgraduate studies I have also presented at the following conferences: -

*Oral communications:-*

September 2004: British Pharmaceutical Conference (BPC), GMEX Centre, Manchester.

April 2004: Perspectives in Percutaneous Penetration (PPP) 2004, La Grande Motte, Montpellier.

*Poster presentations :-*

April 2006: Dermochannel Symposium at Perspectives in Percutaneous Penetration (PPP) 2006, La Grande Motte, Montpellier.

June 2005: The Skin Forum, Winchester.

April 2005: British Society of Investigative Dermatology (BSID) annual meeting, Cambridge.

January 2005: USW Network meeting, University Hospital of Wales, Cardiff.

November 2004: The Annual European Society of Gene Therapy (ESGT) meeting, Tampere, Finland.

September 2004: British Pharmaceutical Conference (BPC), GMEX Centre, Manchester.

July 2004: The Skin Forum, Portsmouth University, Portsmouth.

April 2004: Genes as Medicines conference, RPSGB headquarters, London.

March 2004: Welsh School of Pharmacy Postgraduate Day, Cardiff University, Cardiff.

October 2003: SET for Britain, House of Commons, London.

July 2003: The Skin Forum, Newcastle.

March 2003: Analytical and regulatory challenges of Gene Therapy, RPSGB headquarters, London.

*Journal of Drug Targeting*, August 2005; 13(7): 415–421

Taylor & Francis
Taylor & Francis Group

# Cutaneous DNA delivery and gene expression in *ex vivo* human skin explants via wet-etch microfabricated microneedles

JAMES BIRCHALL[1], SION COULMAN[1], MARC PEARTON[1], CHRIS ALLENDER[1], KEITH BRAIN[1], ALEXANDER ANSTEY[2], CHRIS GATELEY[2], NICOLLE WILKE[3], & ANTHONY MORRISSEY[3]

[1]*Gene Delivery Research Group, Welsh School of Pharmacy, Cardiff University, Cardiff CF10 3XF, UK,* [2]*Gwent Healthcare NHS Trust, Royal Gwent Hospital, Cardiff Road, Newport, South Wales NP20 2UB, UK, and* [3]*Biomedical Microsystems Team, Tyndall National Institute, Prospect Row, Cork, Ireland*

*(Received 9 September 2005; revised 22 September 2005; accepted 22 September 2005)*

**Abstract**

Microneedle arrays increase skin permeability by forming channels through the outer physical barrier, without stimulating pain receptors populating the underlying dermis. It was postulated that microneedle arrays could facilitate transfer of DNA to human skin epidermis for cutaneous gene therapy applications. Platinum-coated "wet-etch" silicon microneedles were shown to be of appropriate dimensions to create microconduits, approximately 50 μm in diameter, extending through the stratum corneum (SC) and viable epidermis. Following optimisation of skin explant culturing techniques and confirmation of tissue viability, the ability of the microneedles to mediate gene expression was demonstrated using the β-galactosidase reporter gene. Preliminary studies confirmed localised delivery, cellular internalisation and subsequent gene expression of pDNA following microneedle disruption of skin. A combination of this innovative gene delivery platform and the *ex vivo* skin culture model will be further exploited to optimise cutaneous DNA delivery and address fundamental questions regarding gene expression in skin.

**Keywords:** *Microneedles, human skin, DNA, skin organ culture,* ex vivo, *gene expression*

## Introduction

Microfabricated microneedle arrays offer a minimally invasive method for breaching the external barrier that prevents delivery of macromolecular therapeutics to the viable region of skin (Henry et al. 1998). Microneedles designed to increase skin permeability are generally $< 400\,\mu m$ long, being of sufficient length to penetrate the stratum corneum (SC), the rate limiting barrier to diffusion, without stimulating the pain receptors that populate the underlying dermis. Their application is therefore free from pain or discomfort (Kaushik et al. 2001). Microneedle treatment results in the formation of transient micro-pores in the SC (Chabri et al. 2004) thereby facilitating the transfer of macromolecular nucleic acids, such as siRNA, anti-sense oligonucleotides and plasmid DNA (pDNA), to the viable epidermis or dermis. This in turn provides the opportunity for cutaneous gene therapy applications including the treatment of cutaneous malignancies (Hart and Vile 1994), hyperproliferative skin disorders (Menter 1998), alopecia (Li and Hoffman 1995, Ahamed et al. 1998), genodermatoses (Uitto and Pulkkinen 2000) and possible exploitation of the skin as a bioreactor for the production of pharmacologically relevant molecules (Lin et al. 2000). Genetic vaccination provides a method of immunizing patients by introducing DNA into cells, leading to expression of foreign antigen and the subsequent induction of an immune response (Fynan et al. 1993, Raz et al. 1994, Shi et al. 1999). Intra-cutaneous DNA vaccines take advantage of the excellent antigen-presenting capabilities of epidermal Langerhans

Correspondence: J. Birchall, Gene Delivery Research Group, Welsh School of Pharmacy, Cardiff University, Cardiff CF10 3XF, UK. Tel: 44 29 2087 5815. Fax: 44 29 2087 4149. E-mail: birchalljc@cardiff.ac.uk

ISSN 1061-186X print/ISSN 1029-2330 online © 2005 Taylor & Francis
DOI: 10.1080/10611860500383705

cells in eliciting a T-cell mediated immune reaction, leading to a more efficient and lower cost vaccination compared with the use of recombinant proteins (Lin et al. 2000).

It has been reported that microfabricated microneedle arrays, prepared from a range of substrate materials, including silicon (Henry et al. 1998, Chabri et al. 2004), various metals (McAllister et al. 2003), glass (McAllister et al. 2003) and polymers (McAllister et al. 2003, Park et al. 2005) can be used to enhance the transdermal penetration of a range of therapeutically active and representative model medicaments such as calcein (Henry et al. 1998), methylene blue (Chabri et al. 2004), trypan blue (McAllister et al. 2003), methyl nicotinate (Sivamani et al. 2005), insulin (Martanto et al. 2004), desmopressin (Cormier et al. 2004), protein antigens (Matriano et al. 2002) and 100 nm nanoparticles (Chabri et al. 2004). In addition, it has been demonstrated that microprojection structures can facilitate the delivery and functional expression of DNA vaccine in animal models (Mikszta et al. 2002). To date, however, the microneedle-assisted delivery of DNA to human skin resulting in gene expression in the viable epidermal layer has not been reported. Given that anatomical and biological differences between human skin and animal skin are well documented (Panchagnula et al. 1997), it is essential that microneedle arrays are designed appropriately for the delivery of pDNA to the appropriate cellular populations in human skin as well as the more commonly used animal models. In the present study, microneedles were used to facilitate localised delivery, cellular internalisation and subsequent gene expression of pDNA topically applied to *ex vivo* human skin. This will allow for future *ex vivo* investigations developing the optimum microneedle device composition and morphology, gene delivery vector and type of formulation to bring about optimal skin penetration, epidermal targeting and gene expression efficiency.

The microneedle arrays used in this study were prepared with high accuracy and excellent reproducibility from standard silicon wafers using a potassium hydroxide (KOH) "wet etching" approach. Wet etching is a commonly employed micromachining technique with advantages over dry-etch procedures, routinely used to make microneedles, including low processing and development costs (Wilke et al. in press). Wet etching of silicon to form microneedles can be a complex process but in our studies control of microneedle morphology was achieved by exploiting the crystal structure of silicon and its resulting etch characteristics in KOH.

## Materials and methods

### *Materials*

The plasmid pCMVβ (7.2 kb), containing the β-galactosidase reporter gene (Clontech, Palo Alto, USA), was propagated using a transformed DH5α strain of *Eschericia coli*, colonised onto an ampicillin selective Luria Bertani agar plate and cultured overnight at 37°C. The plasmid DNA was harvested and purified using a Qiagen Plasmid Mega Kit (Qiagen, Crawley, UK). All culture plastics were obtained from Corning-Costar (High Wycombe, UK). Dulbecco's Modified Eagle's Medium (DMEM), 25 mM HEPES, foetal bovine serum, penicillin–streptomycin solution and the β-galactosidase specific primers were from Invitrogen Corporation (Paisley, UK). Materials required for histological studies were from RA Lamb Limited (Eastbourne, UK). TRI reagent® and individual components of the X-gal staining solution were from Sigma-Aldrich Chemical Company (Poole, UK). The DNA-free™ kit was from Ambion (Cambridgeshire, UK) and the one step RT-PCR kit from Qiagen Ltd. (Crawley, UK). Other materials used during the course of these studies were of analytical grade and from Fisher Scientific UK (Loughborough, UK).

### *Microneedle fabrication*

A wet etch process using KOH was used to fabricate arrays of silicon microneedles. A standard silicon wafer with crystal alignment marks is the starting material. The first process step is the deposition of 1000 Å of silicon nitride on a 350 Å silicon oxide layer using low pressure chemical vapour deposition (LPCVD). The oxide improves the adhesion of the nitride to the silicon. This double layer will act as an etching mask protecting designed/patterned areas of the silicon from the KOH solution during the etching step. To generate microneedles in the crystalline material, square shape patterns are transferred into the masking double layer by standard photolithography, where a positive photoresist on the wafer is exposed to UV light to achieve the required pattern in the resist layer. The resist pattern is transferred into the nitride layer using a plasma etch process. The resist is stripped off and the oxide layer is then removed in the open areas by a wet etch process in HF (hydrofluoric acid). After lithography, the wafer undergoes a wet etch fabrication process. The patterned silicon wafer is etched using a 29% w/v aqueous KOH solution at a temperature of 79°C. The needle formation is based on convex-corner undercut. This means that crystal planes will form on every side of the square. Silicon has anisotropic etch behaviour in KOH; the etched structures are therefore formed along the crystal planes. Every crystal plane group has a specific etch rate. Very fast etching crystal planes start etching on the corners of the squares. When etching around 1 μm into the silicon wafer, the lateral etch rate of these planes is twice as fast. Two planes on every corner move towards the square centre. The plane angle to the surface, which is almost 90°, decreases to 72° when the eight planes meet each other, forming the needle tip. Viewed from overhead, the etch process evolves (Figure 1) until one can see a very uniform octagon—the eight high index crystal planes which form the needle (Figure 2).

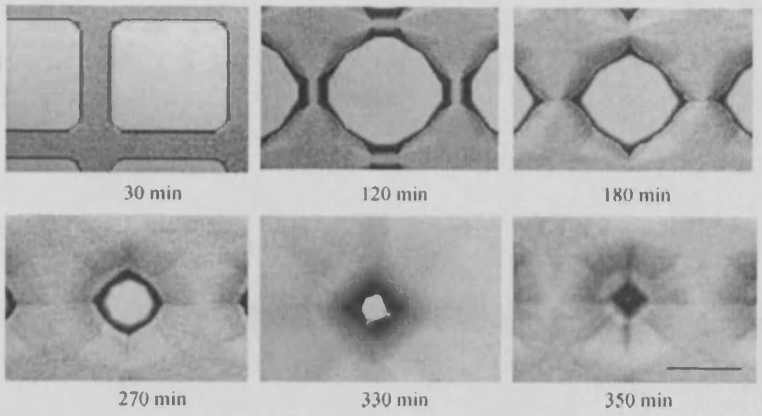


Figure 1. Top–down micrographs showing the evolution of microneedle formation through convex corner undercutting of a square mask. Needle shape is gradually formed when the eight high index crystal planes intersect on top of the frustum in a single point, generating a sharp needle tip. Bar = 500 μm.

*Examination of morphological effects of microneedle treatment of human epidermal membranes*

Skin from a 67-year-old female donor was immersed in heated deionised water (60°C) for 60 s to enable removal of the epidermal membrane from the underlying dermal tissue using forceps. The cooled epidermis was collected on aluminium foil and then placed on to the dermal layer before application of a microneedle array at a pressure of approximately 2 kg/cm$^2$ for 10 s. Following treatment the microneedle arrays and the epidermal membrane were air dried, mounted on an aluminium stub and gold sputter coated (EM Scope, Kent, UK) prior to being examined by scanning electron microscopy (SEM). In addition, epidermal membrane was also fixed in 2.5% glutaraldehyde and dehydrated in an increasing ethanol gradient (70, 90, 100%). A critical point dryer (Samdri 780, Maryland, USA) was used to completely dehydrate the specimen, which was mounted and gold sputter coated prior to SEM. Bar = 200 μm.

Figure 2. SEM image of an overhead view of a single octagonal wet-etch microneedle. Bar = 100 μm.

*Preparation and maintenance of an* ex vivo *human skin organ model*

Human breast skin from a 58-year-old female donor was collected immediately after excision, transported in media (DMEM 25 mM HEPES supplemented with 5% fetal bovine serum and 1% penicillin/streptomycin) on ice, and used within 2 h of surgical removal. Subcutaneous fat was removed using blunt dissection. The skin was separated using a scalpel blade to isolate the SC, viable epidermis and upper layers of the dermis (split-thickness skin).

*Isolation and identification of β-galactosidase mRNA*

Following disruption of the SC and application of 15 μg of pCMVβ plasmid DNA to the disrupted skin surface, approximately 1 cm$^2$ sections of skin were placed on lens tissue supported by metal gauze in a 6-well cell culture plate containing 3 ml media (DMEM 25 mM HEPES supplemented with 5% fetal bovine serum and 1% penicillin/streptomycin) per well (Figure 5A). The organ culture was maintained at an air–liquid interface for 24 h at 37°C. Subsequent to treatment, skin sections were snap frozen in liquid nitrogen and ground to a fine powder in a pre-cooled pestle and mortar. Total RNA was isolated from the *ex vivo* human skin and *E. coli* (control) using TRI Reagent® with contaminating genomic DNA removed using DNA-free™ kit. Two micrograms of isolated RNA was amplified using one step RT-PCR reaction containing primers specific for a 400 bp fragment of the β-gal transcript (5′-TTC ACT GGC CGT CGT TTT ACA ACG TCG TGA-3′ and 5′-ATG TGA GCG AGT AAC CCG TCG GAT TCT-3′). RT-PCR products were run on a 1% agarose gel, containing ethidium bromide, at 100 V for 1 h and visualized via a UV gel doc.

*Determination of β-galactosidase expression in the* ex vivo *human skin model*

Gene expression studies were carried out on human breast skin obtained from surgical procedures with full ethical approval and informed patient consent. Split-thickness skin was surface treated with 50 μl of pCMVβ plasmid DNA solution (2.5 mg/ml) prior to application of silicon microneedles. The skin, divided into approximate 1 $cm^2$ segments, was incubated for 24 h using the described organ culture conditions. Following one wash in PBS/$MgCl_2$ (30 min) the tissue was fixed for 2 h in 2% glutaraldehyde/$MgCl_2$ on ice. Subsequently, the tissue was rinsed in a series of PBS/$MgCl_2$ solutions for a total of 6 h. The tissue was stained for β-galactosidase expression using X-Gal staining solution. Selected tissue samples were counterstained with nuclear fast red (NFR); 5% solution applied topically to the treated area and removed after 30 min. Samples were then mounted between two microscope slides and visualised *en face* using a Zeiss Stemi 2000C Stereomicroscope with a 2,0X attachment and a Schott KL1500 electronic light source. For sectioning, tissue samples were embedded immediately (without NFR staining) in OCT and sectioned using a Leica CM3050S Cryostat. Tissue sections (12 μm) were collected onto Superfrost Plus® microscope slides and allowed to dry overnight before analysis using the Olympus BX50 microscope. Selected slides were stained with Harris' Haematoxylin and Gurr's Eosin and examined.

## Results and discussion

The morphology of the wet-etched microneedles were initially characterised by SEM. The same technique was used to visualise the microchannels produced when the microneedle arrays were applied to human skin. Figure 3 shows the array pattern and structural dimensions of the two types of wet-etch microneedles used in this study. In the example presented, the microneedle arrays comprised 16 microprojections of silicon in a 4 × 4 array across a total array size of 3 $mm^2$. The array size, however, is totally at the discretion of the user, thus smaller or larger arrays can be produced as required. Larger arrays would provide the benefit of increased treatable tissue area; however, arrays with greater surface areas may cause handling problems due to the inherent brittleness of thin microstructures. The pyramidal structures were approximately 280 μm in height with a width of 200 μm at the base and were prepared with either a sharp tip (Figure 3A and B) or a flattened tip, termed a frustrum (Figure 3C and D). Process variables, most notably etch time (but also mask pad size) determine the etched depth, and hence the needle height reported here. Needle heights up to 300 μm may be achieved given that the starting wafer thickness is approximately 525 μm, and sufficient material must remain non-etched to allow handling and process completion. We now have extremely accurate and reproducible process control over every step in the microneedle etching sequence. Traditionally, wet etching of microneedles has been viewed as being overly difficult to control and this is one of the primary reasons why dry etching techniques have replaced KOH etching for such micro-structures in silicon. But with the process control now achievable, benefits can be accrued from the lower costs and greater robustness of the needle arrays produced.

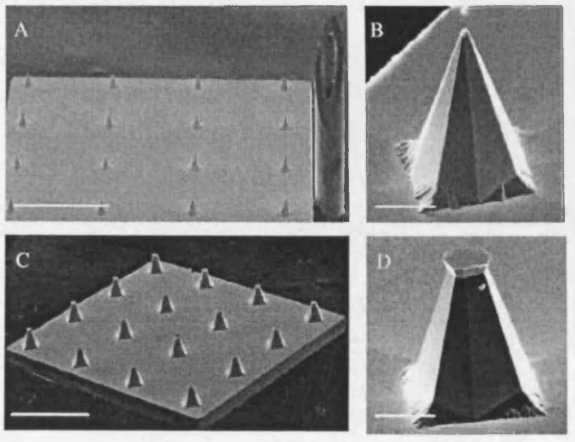


Figure 3. SEM images of wet-etch platinum coated microneedle arrays. (A) Sharp tipped microneedles; the tip of a 30 G hypodermic syringe providing a visual scale reference. Bar = 1 mm; (B) sharp tipped microneedles. Bar = 100 μm; (C, D) Frustum tipped microneedles. Bar = 1 mm (C) and 100 μm (D).

In order to assess microneedle skin penetration, full thickness human skin was heat separated to recover the epidermal membranes (SC and viable epidermis), replaced onto the dermal layer and treated with the microneedles prior to examination by SEM. Figure 4A depicts an electron micrograph showing an inverted view of the human epidermal sheet with the microneedle array still in position. The microneedle array pattern was transferred to the membrane creating an ordered arrangement of microconduits that extended through the SC and viable epidermis. At this magnification a number of microneedle tips can be observed penetrating through the sheet (see arrow). A critical point drying method was used to provide more detailed visualisation of the upper surface of heat-separated membrane. In this micrograph, the dermatoglyphics of microneedle treated human skin are clearly defined (Figure 4B). Using the described SEM processing conditions the epidermal microchannels were apparent as 50 μm fissures piercing the skin corneocytes and underlying upper skin layers. Following topical skin application it was noted that the needle array remained intact, indicating good mechanical robustness.

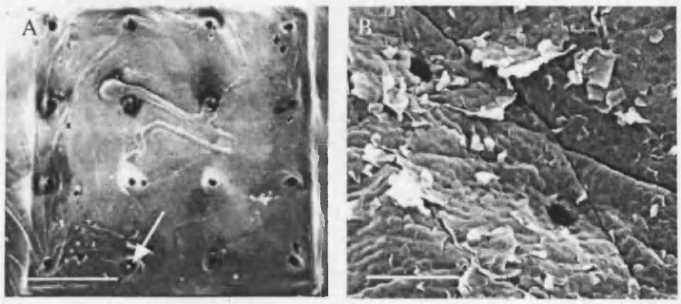


Figure 4. SEM images of heat separated epidermal membrane treated with the microneedle array. (A) Microneedles inserted into epidermal membrane (arrow denotes a microneedle penetrating through the epidermal sheet). Bar = 1 mm; (B) microneedle-treated epidermal membrane. Bar = 200 μm.

In order to maximise the cellular viability of the excised tissue, samples were immediately transferred from the patient into defined organ culture media at 0°C, transported to the laboratory and maintained at air–liquid-interface in growth media. Tissue viability was confirmed over a 24-hour-period through the continued production of endogenous epidermal mRNA and the transcription of β-galactosidase mRNA (Figure 5B) following intra-dermal application of the pCMVβ reporter plasmid.

Following confirmation of the presence of mRNA in the excised skin, the ability of the microneedles to facilitate gene expression was demonstrated using the β-galactosidase (pCMVβ) reporter gene. Figure 6 shows representative results of a skin transfection experiment. *En face* imaging, following topical application of reporter gene and microneedle puncturing, showed detectable reporter gene expression (Figure 6A and B). In control experiments, where pDNA was applied to skin, which had not been treated with microneedles, expression was not observed. Figure 6A shows the blue staining, arising from the reporter gene product, proximal to two microchannels created via application of the microneedle array, also shown in the figure for comparison. Figure 6B highlights the created microchannels by counterstaining with a low molecular weight red dye. As in Figure 6A, it is apparent that a minority of microchannels created in the skin stained positive for gene expression, despite the counterstain confirming that microconduits had been formed by each individual microneedle. The possible reasons for the variability in gene expression efficiency include limited access of the pDNA into the created microchannel, inefficient uptake of the pDNA into the cells located at the periphery of the microchannel, cell damage or death caused by the infiltrating microneedles, or simply unreliable detection of gene expression due to restricted access of the staining solution to the transfected cells. We are currently addressing these issues through the use of alternative microneedle materials and morphologies, different reporter pDNA constructs, improved detection methods and optimised pDNA delivery formulations. Clearly, for certain gene therapy applications, such as the correction or replacement of aberrant genes in genetic skin disorders and the treatment of cutaneous malignancies, such variable levels of expression would need to be addressed, although larger microneedle arrays could be utilised to increase surface coverage. In the case of genetic vaccination however, a sufficient number of cells may still be able to uptake and express the antigen gene to produce an appropriate quantity of antigen to stimulate an immune response. Indeed, in DNA vaccination, it may be more important to target appropriate loci within the skin rather than skin surface area in order to enhance antigen presentation to the immune responsive Langerhans cells. The depth and intensity of reporter gene expression in the underlying

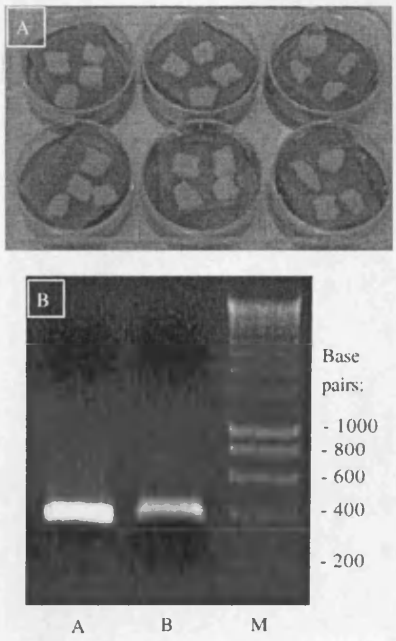


Figure 5. (A) The human skin organ culture procedure; (B) agarose gel showing presence of β-galactosidase mRNA isolated from viable human skin following 24 h incubation in organ culture [Lane A: β-galactosidase expression in *E. coli*; Lane B: β-galactosidase expression in *ex vivo* human skin; M: Molecular marker].

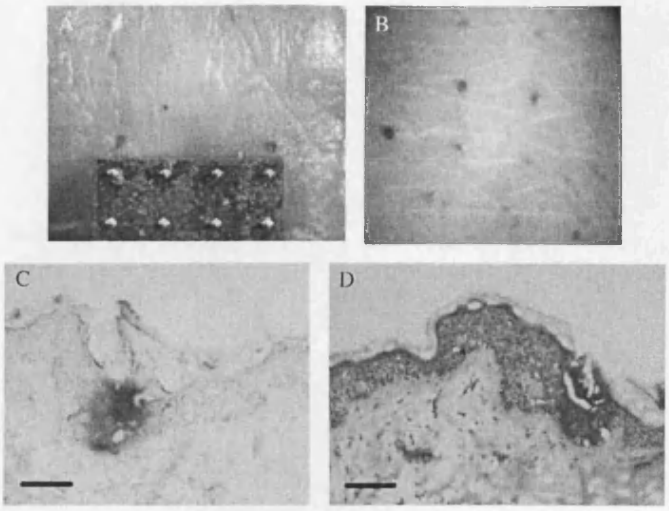


Figure 6. (A) *En face* image of β-galactosidase stained microchannels; the microneedle array providing a visual reference; (B) *En face* image of β-galactosidase stained microchannels with NFR counterstaining; (C) Unstained cryosection of β-galactosidase stained microchannel. Bar = 100 μm; (D) H&E stained cryosection of β-galactosidase stained microchannel. Bar = 100 μm.

skin strata was established by transversely sectioning the positively stained microchannels. Photomicrographs of 12 μm cryosections are presented in Figure 6C and D. Microchannels created in skin following application of the pyramidal microneedles appeared as 150 μm depth interruptions of the SC and epidermis. Figure 6C shows the intense level of reporter gene expression in cells proximal to the base of the microneedle channel. Haematoxylin and eosin staining of the sections revealed that the gene expression was restricted to the viable epidermal cells (Figure 6D).

During our studies, we observed that the extent of gene expression was unpredictable and somewhat difficult to control. However, we also observed that gene expression was more prevalent using microneedles with flattened as opposed to sharp points. We have tentatively attributed this to the likelihood that cells are more likely to suffer some limited damage to their cell membrane when perturbed by the insertion of the flattened microneedles, when compared to sharper microneedles. We suggest that such minor membrane damage may increase pDNA uptake and subsequently lead to enhanced gene expression efficiency. We are currently investigating this hypothesis in our laboratory.

## Conclusions

The advantages of using microneedles as opposed to alternative physical trans-cutanoeus drug delivery methodologies including biolistic particle bombardment (Kendall et al. 2004), jet injection (Sawamura et al. 1999), microscission (Herndon et al. 2004), tape stripping (Tregear and Dirnhuber 1962) and laser ablation (Lee et al. 2002) include: (i) direct and controlled delivery of the medicament; (ii) rapid exposure of large surface areas of skin to the delivery agents (microneedle arrays can be fabricated to contain over 1000 microneedles); (iii) effortless, convenient and painless delivery for the patient; (iv) ability to manipulate the therapeutic formulation, e.g. solution, suspension, emulsion, dry powder, gel; (v) enhancement of concomitant delivery methods such as transdermal patches and (vi) minimally invasive methodology not requiring complex machinery at time of application suited to patient self-administration without the need for medical supervision. We have confirmed the ability of solid silicon pyramidal microneedles, prepared using a low cost wet-etch microfabrication process, to penetrate the SC and create microchannels within human skin to facilitate the intra-epidermal delivery of pDNA. Further, in testing these devices we have developed an *ex vivo* human skin model with retained cellular viability.

The perceived importance of gene-based therapies in medicine is driving the development of novel and radical methods for delivering macromolecular drugs such as DNA. A combination of this innovative gene delivery system and the skin organ culture model can be further exploited to optimise cutaneous DNA delivery for clinical applications and importantly, can be used to answer more fundamental questions concerning the expression of genes in viable skin layers.

## References

Ahmad W, Faiyaz ul Haque M, Brancolini V, Tsou HC, ul Haque S, Lam H, Aita VM, Owen J, deBlaquiere M, Frank J, et al. 1998. Alopecia universalis associated with a mutation in the human hairless gene. Science 279:720–724.

Chabri F, Bouris K, Jones T, Barrow D, Hann A, Allender C, Brain K, Birchall J. 2004. Microfabricated silicon microneedles for nonviral cutaneous gene delivery. Br J Dermatol 150:869–877.

Cormier M, Johnson B, Ameri M, Nyam K, Libiran L, Zhang DD, Daddona P. 2004. Transdermal delivery of desmopressin using a coated microneedle array patch system. J Control Release 97:503–511.

Fynan EF, Webster RG, Fuller DH, Haynes JR, Santoro JC, Robinson HL. 1993. DNA vaccines: Protective immunization by parenteral, mucosal and gene innoculation. Proc Nat Acad Sci USA 90:11478–11482.

Hart IR, Vile RG. 1994. Targeted therapy for malignant melanoma. Curr Opin Oncol 6:221–225.

Henry S, McAllister DV, Allen MG, Prausnitz MR. 1998. Microfabricated microneedles: A novel approach to transdermal drug delivery. J Pharm Sci 87:922–925.

Herndon TO, Gonzalez S, Gowrishankar TR, Rox Anderson R, Weaver JC. 2004. Transdermal microconduits by microscission for drug delivery and sample acquisition. BMC Med 2:12.

Kaushik S, Hord AH, Denson DD, McAllister DV, Smitra S, Allen MG, Prausnitz MR. 2001. Lack of pain associated with microfabricated microneedles. Anesth Analg 92:502–504.

Kendall M, Mitchell T, Wrighton-Smith P. 2004. Intradermal ballistic delivery of micro-particles into excised human skin for pharmaceutical applications. J Biomech 37:1733–1741.

Lee WR, Shen SC, Wang KH, Hu CH, Fang JY. 2002. The effect of laser treatment on skin to enhance and control transdermal delivery of 5-fluoruracil. J Pharm Sci 91:1613–1626.

Li L, Hoffman RM. 1995. The feasibility of targeted selective gene therapy of the hair follicle. Nat Med 1:705–706.

Lin MTS, Pulkkinen L, Uitto J. 2000. Cutaneous gene therapy: Principles and prospects. Dermatol Clin 18:177–188.

Martanto W, Davis SP, Holiday NR, Wang J, Gill HS, Prausnitz MR. 2004. Transdermal delivery of insulin using microneedles *in vivo*. Pharm Res 21:947–952.

Matriano JA, Cormier M, Johnson J, Young WA, Buttery M, Nyam K, Daddona PE. 2002. Macroflux® microprojection array patch technology: A new and efficient approach for intracutaneous immunization. Pharm Res 19:63–70.

McAllister DV, Wang PM, Davis SP, Park JH, Canatella PJ, Allen MG, Prausnitz MR. 2003. Microfabricated needles for transdermal delivery of macromolecules and nanoparticles: Fabrication methods and transport studies. Proc Nat Acad Sci USA 100:13755–13760.

Menter A. 1998. Pathogenesis and genetics of psoriasis. Cutis 61:8–10.

Mikszta JA, Alarcon JB, Brittingham JM, Sutter DE, Pettis RJ, Harvey NG. 2002. Improved genetic immunization via micromechanical disruption of skin-barrier function and targeted epidermal delivery. Nat Med 8:415–419.

Panchagnula R, Stemmer K, Ritschel WA. 1997. Animal models for transdermal drug delivery. Methods Find Exp Clin Pharmacol 19:335–341.

Park JH, Allen MG, Prausnitz MR. 2005. Biodegradable polymer microneedles: Fabrication, mechanics and transdermal drug delivery. J Control Release 104:51–66.

Raz E, Carson DA, Parker SE, Parr TB, Abai AM, Aichinger G, Gromkowski SH, Singh M, Lew D, Yankauckas MA, et al. 1994. Intradermal gene immunization: The possible role of DNA uptake in the induction of cellular immunity to viruses. Proc Nat Acad Sci USA 91:9519–9523.

Sawamura D, Ina S, Itai K, Meng X, Kon A, Tamai K, Hanada K, Hashimoto I. 1999. *In vivo* gene introduction into keratinocytes using jet injection. Gene Ther 6:1785–1787.

Shi Z, Curiel DT, Tang DC. 1999. DNA-based non-invasive vaccination onto the skin. Vaccine 17:2136–2141.

Sivamani RK, Stoeber B, Wu GC, Zhai H, Liepmann D, Maibach H. 2005. Clinical microneedle injection of methyl nicotinate: Stratum corneum penetration. Skin Res Technol 11:152–156.

Tregear RT, Dirnhuber P. 1962. The mass of keratin removed from the stratum corneum by stripping with adhesive tape. J Investig Dermatol 38:375–381.

Uitto J, Pulkkinen L. 2000. The genodermatoses: Candidate diseases for gene therapy. Hum gene ther 11:2267–2275.

Wilke N, Mulcahy A, Ye SR, Morrissey A, Process optimization and characterization of silicon microneedles fabricated by wet etch technology. Microelectronics J (in press).

# Minimally Invasive Cutaneous Delivery of Macromolecules and Plasmid DNA *Via* Microneedles

Sion A. Coulman[1], David Barrow[2], Alexander Anstey[3], Chris Gateley[3], Anthony Morrissey[4], Nicolle Wilke[4], Chris Allender[1], Keith Brain[1] and James C. Birchall[1,*]

[1]*Gene Delivery Research Group, Welsh School of Pharmacy, Cardiff University, Cardiff, CF10 3XF, UK.;* [2]*Cardiff School of Engineering, Cardiff University, Cardiff, CF24 3TF, UK.;* [3]*Gwent Healthcare NHS Trust, Royal Gwent Hospital, Cardiff Road, Newport, South Wales, NP20 2UB, UK.;* [4]*Biomedical Microsystems Team, Tyndall National Institute, Prospect Row, Cork, Ireland*

**Abstract:** The stratum corneum (SC) represents a significant barrier to the delivery of gene therapy formulations. In order to realise the potential of therapeutic cutaneous gene transfer, delivery strategies are required to overcome this exclusion effect. This study investigates the ability of microfabricated silicon microneedle arrays to create micron-sized channels through the SC of *ex vivo* human skin and the resulting ability of the conduits to facilitate localised delivery of charged macromolecules and plasmid DNA (pDNA). Microscopic studies of microneedle-treated human epidermal membrane revealed the presence of microconduits (10-20μm diameter). The delivery of a macromolecule, β-galactosidase, and of a 'non-viral gene vector mimicking' charged fluorescent nanoparticle to the viable epidermis of microneedle-treated tissue was demonstrated using light and fluorescent microscopy.

Track etched permeation profiles, generated using 'Franz-type' diffusion cell methodology and a model synthetic membrane showed that >50% of a colloidal particle suspension permeated through membrane pores in ~2 hours. On the basis of these results, it is probable that microneedle treatment of the skin surface would facilitate the cutaneous delivery of lipid:polycation:pDNA (LPD) gene vectors, and other related vectors, to the viable epidermis.

Preliminary gene expression studies confirmed that naked pDNA can be expressed in excised human skin following microneedle disruption of the SC barrier. The presence of a limited number of microchannels, positive for gene expression, indicates that further studies to optimise the microneedle device morphology, its method of application and the pDNA formulation are warranted to facilitate more reproducible cutaneous gene delivery.

**Keywords:** Microneedles, human skin, DNA, microfabrication, gene delivery, non-viral, transfection.

## 1. INTRODUCTION

Localised delivery and expression of gene therapeutics within the skin may provide novel treatment strategies for a number of pathological conditions, including the correction of genetic skin disorders i.e. 'genodermatoses' [1-3] and the non-surgical management of malignancy [4,5]. The specific and efficient immune processing properties of skin has also resulted in significant interest in the development of genetic vaccines [6-8] that can capitalise on the innate ability of Langerhans cells, powerful antigen presenting cells (APCs) residing within the viable epidermis, to proficiently present antigen to stimulate an antigen-specific T cell immune response.

The cutaneous delivery of macromolecules to skin is significantly restricted however by the inherent barrier function of the tissue, attributable primarily to the outermost skin layer, the stratum corneum (SC). The SC, comprising a 10-15μm layer of flattened non-viable cells, has restricted effective transdermal delivery to a small number of low molecular weight, weakly lipophilic, potent therapeutic molecules. Increasing emphasis on the administration of biotechnology-derived macromolecular and DNA-based medicines has stimulated a number of novel delivery strategies and devices that circumnavigate the SC barrier to promote delivery of a wide range of therapeutics to the underlying epidermis and dermis.

Current non-chemical delivery strategies are generally divided into electrical and physical delivery methods. Electrical techniques such as iontophoresis [9], electroporation [10-12], sonophoresis [13] and laser ablation [14] have demonstrated increased permeability of the SC to certain macromolecules. However, the expensive and complex equipment employed is likely to limit widespread application of such technologies. Physical delivery methods, including particle bombardment [15-18], jet injection [19,20], radiofrequency ablation [21], microscission [22] and microseeding [23] have, to varying extents, enhanced permeation of macromolecules through the SC barrier. Such methods aim to transiently disrupt the integrity of the SC to facilitate therapeutic delivery without lasting skin damage.

*Address correspondence to this author at the Gene Delivery Research Group, Welsh School of Pharmacy, Cardiff University, Cardiff, CF10 3XF, UK.; Tel: 02920875815; Fax: 02920874149;
E-mail: birchalljc@cardiff.ac.uk

1567-2018/06 $50.00+.00 

In recent years a particularly exciting alternative method for enhancing cutaneous permeation of molecules across a very wide molecular weight range has been developed. Microneedle technology uses micro-fabrication techniques to create arrays of micron-sized needles onto the surface of a solid support backing. Commonly this support is silicon and in these cases needle fabrication can be achieved using well defined etching techniques [24]. Although the practical application of this technique was only demonstrated for the first time within the last ten years, the original concept for these delivery systems was described nearly thirty years ago [25]. Microneedles are designed to pierce the SC, thus providing a direct and controlled route of access to the underlying tissue layers. When inserted into the skin, individual microneedles create channels through the SC and into the viable epidermis. The length of the microneedle is controlled so that when they are applied they do not reach the nerve fibres and blood vessels that reside in the underlying dermis. The micron-sized channels can therefore potentially facilitate the localised delivery of both small and large molecular weight therapeutics without causing pain or bleeding at the site of application [26].

To date, the majority of studies investigating localised gene expression in skin have utilised local intradermal injection or biolistic devices to deliver DNA formulations to the target cells of the epidermis [27-29]. Alternatively another approach uses microstructures to laterally disrupt the SC [30]. The transfer of cutaneous gene therapy to the clinic requires the development of drug delivery technologies that can painlessly overcome the SC barrier and reproducibly deliver the gene to the appropriate depth. This study characterises microneedle induced trans-SC channels and assesses their potential to facilitate macromolecular localisation in the viable epidermis by studying micro-channel geometry and macromolecular permeability. Further, the gene delivery results, obtained using freshly excised human tissue, demonstrate the potential of this strategy for the delivery of both macromolecules and gene medicines to target cells located within the viable epidermis of human skin.

## 2. MATERIALS AND METHODS

### 2.1 Materials

The 7.2 kb pCMVβ plasmid construct containing the β-galactosidase reporter gene and the pEGFP-N1 (4.7kb) plasmid containing the green fluorescent protein reporter gene were propagated and purified as detailed previously [31]. 1,2-Dioleoyl-3-triammonium-tropane (DOTAP) was purchased as the methyl sulphate salt from Avanti Polar Lipids (Alabaster, AL, USA). 2-(12-(7nitrobenz-2-oxa-1,3-diazol-4-yl)amino)dodecanoyl-1-hexadecanoyl-sn-glycero-3-phosphocholine ($NBDC_{12}$-HPC) was purchased from Molecular Probes (Leiden, Netherlands). β-galactosidase enzyme was obtained within an X-gal staining kit from Promega Corporation (Madison, WI).

Protamine sulphate, Bovine serum albumin, fluorescent yellow/green polystyrene nanospheres (L-1280), fluorescent red polystyrene nanospheres (L-9279) and components of the X-gal staining solution were obtained from Sigma-Aldrich Chemical Company (Poole, UK).

Cell culture plastics were obtained from Corning-Costar (High Wycombe, UK). MEM (EAGLES) 25mM HEPES, Dulbecco's Modified Eagle's Medium (DMEM 25mM HEPES), fetal bovine serum and penicillin-streptomycin solution were obtained from Invitrogen Corporation (Paisley, UK). All histology materials were obtained from RA Lamb Limited (Eastbourne, UK). All other materials were of analytical grade and purchased from Fisher Scientific UK (Loughborough, UK).

### 2.2 Microneedle Fabrication and Characterisation

Microneedle fabrication was conducted using a modified form of the BOSCH deep reactive ion etch (DRIE) process as detailed previously [32]. Briefly, 4" silicon wafers were spin-coated with a layer of positive photoresist, selectively exposed to UV light through a high-resolution, chromium-plated photolithographic mask and developed to result in a uniform dot array pattern. The photoresist dots provide a mask against subsequent etch processes using fluorinated plasmas in an Inductively Coupled Plasma (ICP) etcher (Surface Technology Systems, Newport, UK). The symmetrical concave needle tips were formed by exposing the patterned wafers to an isotropic etch such that the photoresist dots were undercut almost to the centre of each dot. This was followed by a deep anisotropic etch producing needle shanks with near parallel sidewalls. Finally, the resist mask was removed and the silicon wafers were divided in to individual array chips using a wafer saw at Cardiff School of Engineering (Cardiff, UK). Microneedle array chips were mounted on aluminium stubs and morphology examined using a Philips XL-200 (Philips, Eindhoven, Netherlands) scanning electron microscope (SEM).

### 2.3 Scanning Electron Microscopy of Human Epidermis

Human breast skin was obtained from mastectomy or breast reduction procedures with full ethical committee approval and informed patient consent.

Tissue from a 66-year-old female donor stored at -20°C for 6 weeks was allowed to reach room temperature over a period of 1 hr. Immersion in heated deionised water (60°C) for 60 sec enabled removal of the epidermal membrane from the underlying dermal tissue using forceps. Transfer of the epidermis to cool deionised water allowed the outstretched membrane to orientate, with the hydrophobic stratum corneum facing upward. The epidermis was collected on aluminium foil and replaced on the dermal layer before application of a microneedle array to the skin surface at a pressure of approximately $2g/cm^2$ for 10 secs. Following removal of the microneedles the membrane was fixed (2.5% glutaraldehyde) and subsequently dehydrated in an increasing ethanol gradient (70%, 90%, 100%). A critical point dryer (Samdri 780, Maryland, USA) was used to complete dehydration of the specimen, which was mounted on an aluminium stub and gold sputter coated (EM Scope, Kent, UK) prior to SEM .

### 2.4 Confirmation of Channel Creation in Microneedle Treated Skin

Tissue from a female donor, age 30 years, was removed from storage at -20°C, sub-cutaneous fat was removed by blunt dissection and the tissue was allowed to equilibrate at

room temperature for 1 hour. The microneedle device was applied to tissue (~0.5cm$^2$), which was subsequently covered with a small volume of methylene blue staining solution. After 5 min excess staining solution was washed from the skin surface by submersion in 10ml phosphate buffered saline (PBS) followed by surface application of an ethanol (70%) swab. The skin was fixed in 2.5% glutaraldehyde on ice for 1hr. Finally, the tissue was rinsed in PBS for 5 min and visualised *en face* using an Olympus BX-50 microscope (Olympus UK Limited, Southall, UK) and Schott KLI500 fibre optic light source (Schott UK Limited, Stafford, UK). The tissue was subsequently embedded in OCT medium on solid carbon dioxide and stored at -86°C prior to cryosectioning using a Leica CM3050S cryomicrotome (Leica Microsystems (UK) Limited, Milton Keynes, UK).

### 2.5 Microneedle Mediated Delivery of β-galactosidase Enzyme

Human skin from a 43-year-old female donor was prepared and treated with microneedles as previously described (Section 2.4). 40µl of β-galactosidase (0.2units/ml in a bicene buffer [50mM] containing 100µg/ml of Bovine Serum Albumin (BSA)) was applied to the treated skin surface. The process was repeated on the same donor tissue applying PBS as a negative control. Each sample was placed in the chamber of a 6-well cell culture plate, and maintained at the air-liquid interface in organ culture (DMEM containing 10% Fetal Bovine Serum, 2% penicillin-streptomycin at 37°C and 95%:5% $O_2$:$CO_2$) over 26 hrs. The tissue was then briefly placed in a rinsing solution (PBS containing Magnesium Chloride [0.04M]) and fixed in 2.5% glutaraldehyde on ice for 1 hr before an overnight rinse in PBS to remove all trace of fixative. Incubation of the tissue sample for a further 20 hrs at 37°C in an X-Gal staining solution [33,34] (X-Gal [5%v/v of a 40mg/ml solution in dimethylformamide], Potassium ferricyanide [0.84%v/v of a 0.6M solution], Potassium ferrocyanide [0.84%v/v of a 0.6M solution], Magnesium chloride [0.2%v/v of a 1M solution], Tris-hydrochloride buffer pH8.5 [50%v/v of a 0.2M solution], deionised water to 100%) was used to detect the presence of the β-galactosidase enzyme. Samples were visualised *en face* and embedded in OCT medium for sectioning as previously described (Section 2.4).

### 2.6 Microneedle Mediated Delivery of Fluorescent Latex Nanospheres

Human skin was prepared as described previously (Section 2.4). Prior to microneedle treatment, an area of skin was treated with 50µl of fluorescent red amine-modified 100nm latex nanospheres. This suspension was also applied to untreated skin areas to demonstrate the integrity of the skin sample and the barrier properties of the intact SC (negative control). Following treatment, the human skin was maintained in organ culture for 16 hrs, fixed in 2.5% glutaraldehyde and subsequently embedded within OCT medium as previously described (Section 2.4).

### 2.7 Histology of Microneedle Treated Tissue

All tissue embedded in OCT medium was stored at -86°C overnight and cryosectioned. Sections were cut at 10-12µm, transferred to microscope slides and fixed in cold acetone. Selected slides were also stained with Harris' Haematoxylin and Gurr's Eosin. All tissue sections were viewed under light or blue fluorescence illumination at a range of magnifications. Image scale was calculated using a microscope slide graticule.

### 2.8 Preparation of Lipid:Polycation:DNA (LPD) Vectors and Lipid Coated Nanospheres (LCN) and Determination of Particle Diameter and Zeta Potential

The LCN particulates were prepared by a film hydration method whereby the cationic lipid, DOTAP, was dissolved in a small volume of chloroform (~10ml), which was subsequently removed under vacuum by rotary evaporation to produce a thin lipid film. The lipid film was hydrated with a known concentration of fluorescent yellow/green latex nanospheres (5µl/ml) (Ex. 470nm; Em. 505nm), vortexed briefly, incubated at 37°C for 1 hr and finally sonicated (Ultrawave, Cardiff, UK) to disperse any aggregates. LPD complexes were produced at 3:2:1 w/w/w ratio, using the pCMVβ plasmid (1mg/ml in Tris-EDTA buffer), protamine (1mg/ml in sterile deionised water) and unilamellar DOTAP liposomes approximately 100nm in diameter (1mg/ml in sterile deionised water), by a simple electrostatically mediated interaction as described previously [35,36].

Unimodal diameters of both colloidal formulations were measured at a light scattering angle of 90° using a Coulter N4 Plus photon correlation spectroscopy instrument (Coulter Electronics, Luton, UK). The zeta potential was determined by microelectrophoresis over a pH range of 3-11 using a Malvern 2000 Zetasizer and pH titrator (Malvern Instruments, Malvern, UK). All samples were prepared in degassed, deionised water with pH adjustment by addition of either sodium hydroxide or hydrochloric acid [0.25M].

### 2.9 Transmission Electron Microscopy (TEM)

Fifteen µl of the LPD or LCN sample was applied to the surface of a pioloform-coated 200-mesh nickel grid. After 3 min excess sample was wicked from the grid, and the grid placed on a freshly filtered drop of 2% aqueous uranyl acetate for 30 secs. The grid was rinsed in deionised water stages and allowed to dry before visualisation using a Philips 208 transmission electron microscope.

### 2.10 Franz Cell Diffusion Studies

Isopore® polycarbonate track etched membranes possessing three different pore diameters, 0.1µm, 1.2µm and 10µm, were mounted within static Franz-type diffusion cells. The receptor compartment of each cell was filled with deionised water (adjusted to approximately pH 7.4 with 1M HCl or 1M NaOH) and the sample arm sealed with a foil cap. The magnetically agitated receptor compartments were maintained at 37°C, resulting in a membrane surface temperature of 32°C. 0.5ml of formulation was introduced into the donor compartment which was subsequently occluded. The receptor compartment was sampled at 30, 60 120, 240, 360 and 720 min.

The fluorescent LPD formulation used in diffusion studies comprised 0.4mg pEGFP-N1 (1mg/ml) to which was added 7.6ml of deionised water, 0.8mg of protamine

(1mg/ml) and, after a ten minute incubation period, 1.2mg of DOTAP liposomes labelled by the inclusion of a fluorescent lipid, $NBDC_{12}$-HPC (Ex. 460nm; Em. 534nm), at a mass ratio of 1:20. The LCN formulation (Section 2.8) was used at a nanoparticle concentration of 5µl/ml and these membranes were removed from the diffusion apparatus at the end of the incubation period and visualised using SEM.

Quantitative analysis of LPD and LCN was achieved by fluorescence spectroscopy using a Fluostar® fluorometer (BMG Labtechnologies Inc., Durham, USA). Reproducible calibration curves were completed for both formulations and were used to determine colloidal concentration.

### 2.11 Gene Expression in Excised Human Skin

For gene expression studies, human skin from both 48 and 52 year old female donors was surgically separated to remove the majority of the dermis. Split-thickness skin was surface treated with 50µl of pCMVβ plasmid DNA solution (2.5mg/ml) prior to application of dry-etch silicon microneedles. Control samples were treated with an alternative reporter plasmid (pEGFP-N1). The skin was then placed on lens tissue supported by metal gauze in a 6 well cell culture plate containing 7.5ml media (DMEM 25mM HEPES supplemented with 5% fetal bovine serum and 1% penicillin/streptomycin) per well. This organ culture maintained the skin at an air-liquid interface for 24 hrs at 37°C. Following one wash in PBS/$MgCl_2$ (30 min) the tissue was fixed for 2 hrs in 2% glutaraldehyde/$MgCl_2$ on ice. Subsequently the tissue was rinsed in a series of PBS/$MgCl_2$ solutions for a total of 6 hrs. The tissue was stained for β-galactosidase expression using X-Gal staining solution (see Section 2.5).

For *en face* imaging, selected tissue samples were then counterstained with Nuclear Fast Red (NFR), a low molecular weight dye normally used for histological examination, in order to confirm the presence of microchannels created by the device. A 5% solution of Nuclear Fast Red was applied topically to the treated area and removed after 30 mins. The sample was then mounted between two microscope slides and visualised *en face* using both a Zeiss Stemi 2000C Stereomicroscope with a 2,0X attachment and an Olympus BX50 microscope, both with a Schott KL1500 electronic light source.

For sectioning, tissue samples were embedded immediately (without NFR staining) in OCT and sectioned using a Leica CM3050S Cryostat. Tissue sections (12µm) were collected onto Superfrost Plus® microscope slides and allowed to dry overnight before analysis using the Olympus BX50 microscope.

## 3. RESULTS

### 3.1 Microneedle Characterisation

Microscopic analysis of the 20x20 silicon microneedle arrays confirms that the microneedles were approximately 200µm in length and 80µm in diameter at their base with interspacing of approximately 100µm (Fig. **1**). The blend of BOSCH and isotropic etch process conditions produces needles with a sharp angle of curvature to facilitate SC penetration. Previous work within our laboratory [32] suggested that the integrity of the device was maintained after a limited number of applications. Continued use of the device resulted in defects in the array attributed to fragility of the silicon needles and contamination of the device by biological debris. A surface coating of biological material on the microneedle tips (Fig. **1C**) reduces the capabilities of individual needles to penetrate the skin. However, a simple cleaning protocol (overnight soaking in acetone) was shown to remove such contaminants and to restore penetration efficiency. In contrast, the fragility of a silicon microneedle can result in irreparable damage to the device, as demonstrated by broken microneedles on the perimeter of the array (Fig. **1A**).

### 3.2 Microscopic Analysis of Microneedle Treated Human Skin

Scanning electron microscopy demonstrated the capability of the microneedle device to create an array of microconduits through the SC (Fig. **2**). The epidermis was removed from full thickness human breast skin, before application of the array. This provides a more accurate indication of the microchannel dimensions in contrast to that reported in a previous study [32] where microneedle treatment of the skin was followed by epidermal removal. It is likely that this former approach resulted in over-estimation of channel diameter due to epidermal membrane expansion during separation. A more representative image of the skin surface was obtained using critical point drying for sample preparation. In (Fig. **2A**) the arrows show the location of an array of microchannels. The channels are 30-50µm in diameter and although biological debris on the skin surface obscures some channels, a uniform array of microconduits is evident.

### 3.3 Microneedle Array Penetration Efficiency

The distribution and extent of channels within microneedle-treated full thickness human skin was confirmed by post-application staining with methylene blue. Rapid diffusion of the hydrophilic low molecular weight dye across the compromised SC barrier and its subsequent retention within the resulting SC / viable epidermis micro-channels provided a simple yet clear demonstration of the utility of the microneedles in facilitating cutaneous delivery (Fig. **3A,B**). This approach demonstrated that a large proportion of the microneedle array appeared to have penetrated the skin.

*En face* images (Fig. **3A,B**) suggest that the microneedle-created pores are approximately 50-100µm in diameter. However, cryosections (Fig. **3C,D**) of the tissue reveal lateral diffusion of the dye into the tissue surrounding the microchannel which may exaggerate this estimation. The diameter of the microchannel, measured in (Fig. **3C,D**), is in agreement with SEM images at approximately 20-30µm with a channel depth of approximately 100-120µm. An eosin stained section (Fig. **3D**) shows the conduit being limited to the viable epidermis however, it should be noted that within other areas of the tissue, it was observed that these ~100µm channels penetrated the upper layers of the dermis (the papillary layer).

### 3.4 Microneedle-Mediated Delivery of Macromolecules

β-galactosidase (β-gal), the enzyme product of a reporter gene to be used in subsequent qualitative gene delivery

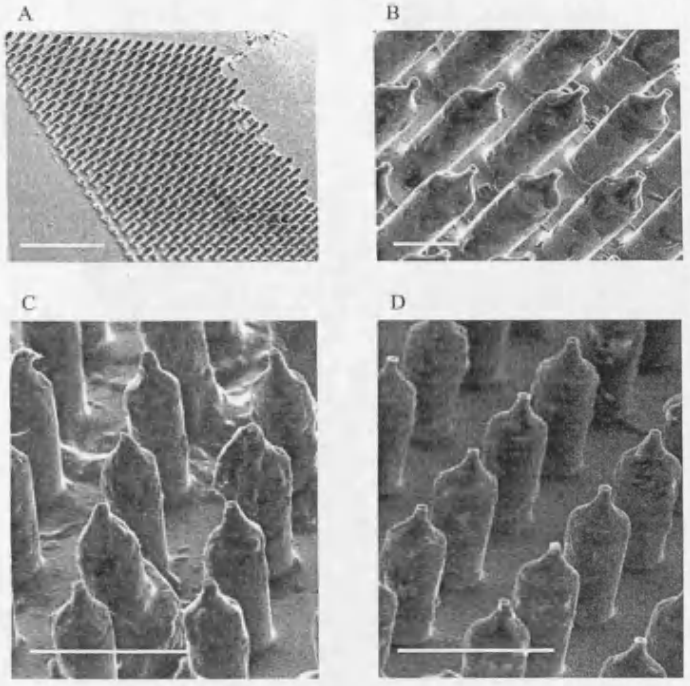


**Fig. (1).** Scanning electron microscopy of silicon microneedle arrays. A) Microneedles prior to skin application, Bar = 1mm; B) Microneedles prior to skin application, Bar = 100μm; C) Repeated application results in contamination of microneedles by biological debris, Bar = 200μm; D) Decontamination of the device restores microneedle functionality, Bar = 200μm.

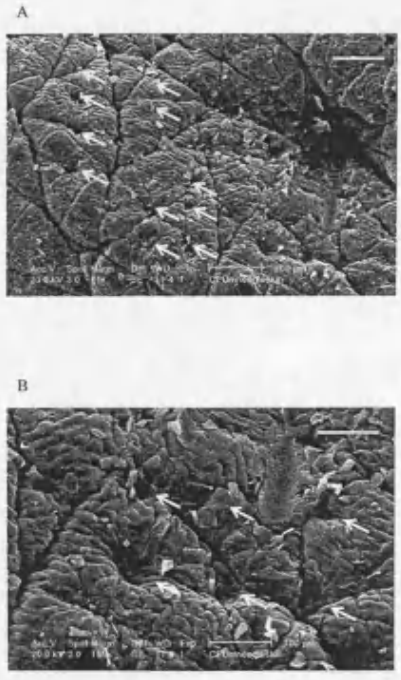


**Fig. (2).** Scanning electron microscopy of heat separated human skin. Heat separated epidermal sheet treated with a microneedle array and prepared for SEM analysis using a critical point drying procedure reveals a uniform pattern of surface abrasions within the SC (see arrows). A) Bar = 200μm; B) Bar = 100μm.

studies, can be detected by conversion of an indoyl galactosidase substrate to a visible blue product. This enzyme was selected as a model protein to demonstrate, through histochemical staining, the potential of the microneedle device to deliver biologically active macromolecules through the SC barrier. Detection of the blue reaction product, within the upper skin layers (Fig. **4A**) confirms the ability of a microneedle device to disrupt the SC barrier and to provide a localised route of delivery for the β-galactosidase enzyme: a molecule that is orders of magnitude larger than those molecules delivered by traditional transdermal delivery strategies. A negative control served to confirm the absence of any endogenous β-galactosidase activity. Haematoxylin and Eosin (H&E) staining revealed the layered structure of the skin and the presence of the β-galactosidase enzyme up to 80μm below the skin surface (Fig. **4B**). Localised delivery to the viable epidermis, a highly nucleated area consisting primarily of keratinocyte cells, is evident. However, there is no evidence of macromolecular delivery to the dermis suggesting that the micro-channels did not usually extend into the dermal tissue layers.

### 3.5 Microneedle Mediated Delivery of Nanoparticles

Investigations within our laboratory aim to exploit microneedle arrays for the delivery of a range of gene therapy formulations to the cells of the viable epidermis. These studies will compare the expression efficiency of non-viral gene therapy vectors such as LPD, comprising cationic lipid (DOTAP), polycation (protamine sulphate) and plasmid DNA against naked plasmid DNA. The LPD complex is a

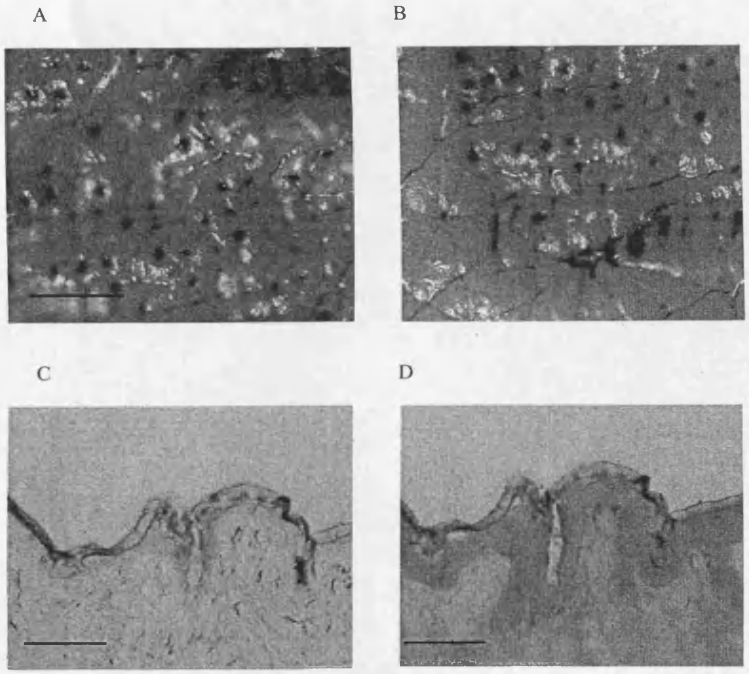


**Fig. (3).** Methylene blue staining of microneedle-treated human skin. Disruptions within the SC indicate microneedle penetration efficiency. A-B) *En face* images of microneedle treated human skin, Bar = 600 μm; C) Unstained 10μm cryosection of microneedle treated human skin, Bar = 80μm; D) Eosin stained 10μm cryosection of microneedle treated human skin, Bar = 80μm.

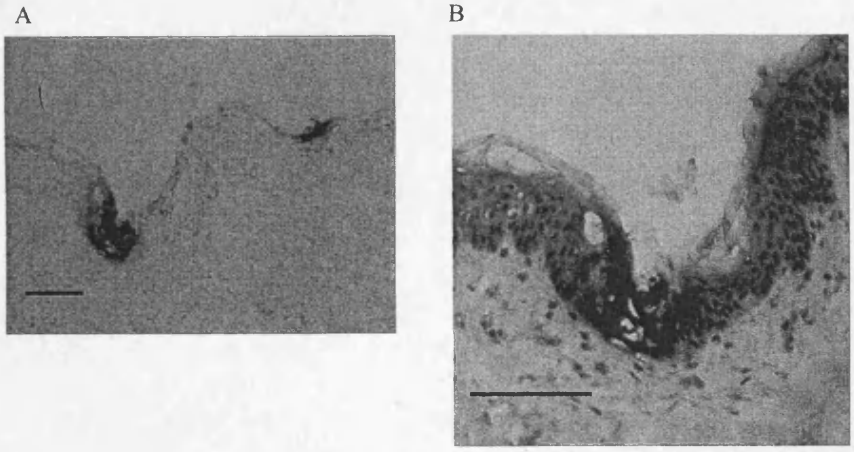


**Fig. (4).** Photomicrographs of cryosections from microneedle treated human skin stained for β-galactosidase. A) Unstained 12μm cryosection; B) H&E stained 12μm cryosection, Bar = 100μm.

colloidal suspension of charged nanoparticles, approximately 100nm in diameter [30]. Therefore, to evaluate the potential of microneedle-mediated delivery of LPD complexes, latex fluorescent nanospheres, of a comparable diameter, were used as a representative model. Topical application of the nanospheres followed by treatment with the microneedle array resulted in the migration of the charged fluorescent particles into the microchannels, and to the cells of the viable epidermis (observed as red or co-localised yellow against the autofluorescent green background) (Fig. **5A,B**). The lower magnification micrograph (Fig. **5C**) demonstrates the inability of nanoparticles to traverse the SC in non-treated areas and confirms the integrity of the tissue sample that was used in the study.

### 3.6 Predicting Microneedle Mediated Delivery of Nanoparticles

Microneedle treated SC can be likened to a simple porous membrane with pore diameter ~20μm. A synthetic model membrane was employed to investigate the permeation of colloidal particles through membrane pores. The primary

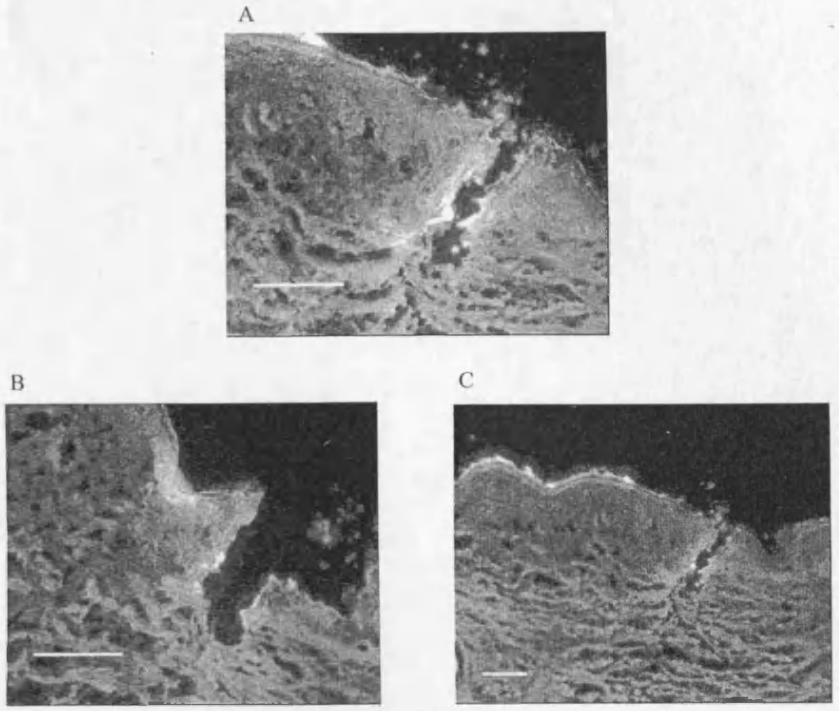


**Fig. (5).** Fluorescent photomicrographs of cryosections (12μm) showing localisation of fluorescent nanoparticles in microneedle treated human skin, Bar = 100μm.

reason for this was to reduce inter-experiment variability due to the biological variability of skin tissue and also to negate the effect of variation in microneedle penetration efficiency. The purpose of these experiments was to study the process of migration of nanometer dimensioned particles through micrometer sized pores. Although the use of microneedle treated epidermal membrane would have better predicted the overall process of delivery, the effects of physicochemical variables on nanoparticulate mass-transport would have been less obvious. Therefore Franz type cell diffusion studies, using a model synthetic membrane and a size-representative model formulation, were conducted to quantitatively assess the diffusion rates of nanoparticulate formulations through membrane pores. A colloidal model for the LPD non-viral gene vector was prepared and characterised (Table **1**). Polycarbonate track-etched membranes of thickness 10μm and possessing uniform circular pores of 100nm, 1.2μm and 10μm diameter were selected as a simple diffusion model for microneedle-treated human skin membrane. The 10μm pore membrane provides an approximate representation for the conduits produced in microneedle treated human epidermal membrane [24]. Membranes with reduced pore size were also studied to investigate the effect of microchannel dimensions on the passive diffusion of nanoparticles.

The comparable size, lamellar surface morphology (Fig. **6**) and zeta potential of the LCN and LPD particles resulted in comparable diffusion profiles (Fig. **7**). For the three membranes studied, the LCNs appear to mimic the permeability of the LPD gene therapy formulation. The diffusion profiles show the importance of microchannel dimensions on the permeability of charged colloidal particles. As was predicted, when pore diameter was approximately the same as the particle diameter, i.e. 100nm, permeability approached zero. Although a small degree of fluorescence was observed in the receptor phase for the LPD particles, and may possibly reflect a degree of deformation of the tri-component LPD vector permitting diffusion through the 100nm pores, it is more likely that this fluorescence is attributed to the presence of uncomplexed fluorescently-labelled lipid. Increasing the diameter of the microchannel to 1.2μm in diameter

**Table 1. Mean Diameter and Zeta Potential of the LPD and LCN Particles. Mean±SD, n = 6**

| | Mean Diameter (nm) | Zeta Potential (mV) pH ~5.5 | Zeta Potential (mV) pH ~7.4 |
|---|---|---|---|
| LCN | 141.4 ±46.9 | 52.2 ±1.4 | 49.5 ±1.0 |
| LPD | 101±17.4 | 32.5 ±0.5 | 33.9 ±3.2 |

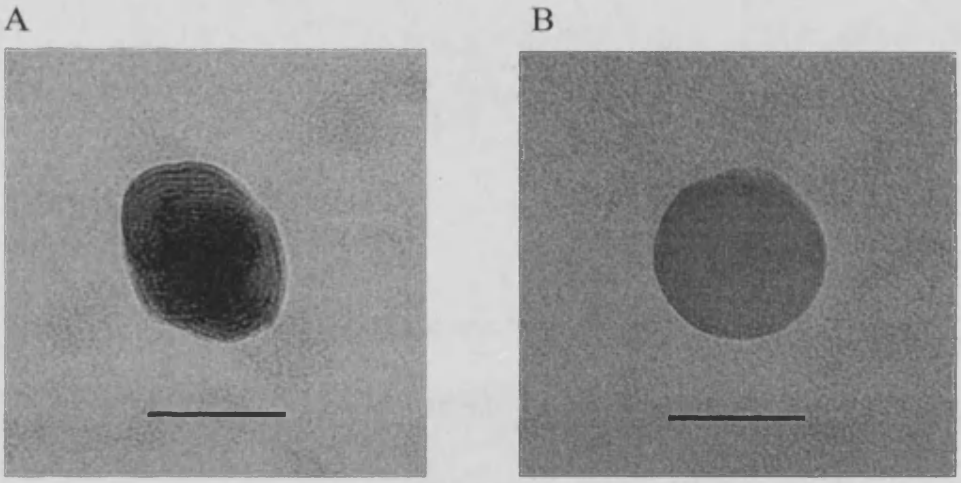


**Fig. (6).** Negative stain transmission electron microscopy of nanoparticles. A) Lipid:polycation:pDNA (LPD) vector; B) Lipid-coated nanoparticle (LCN), Bar = 100nm.

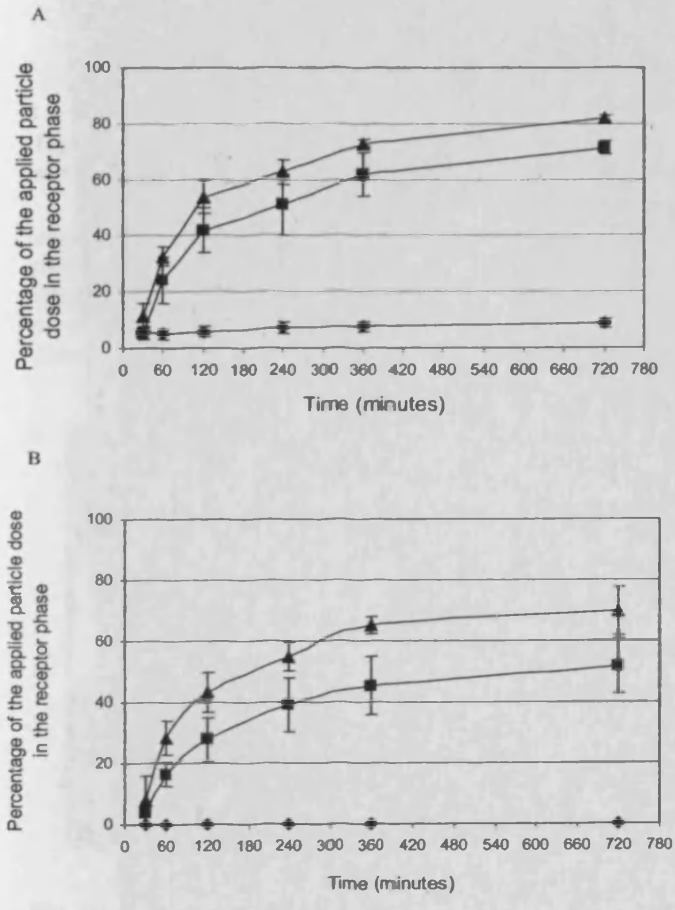


**Fig. (7).** Cumulative diffusion profiles of nanoparticles through synthetic membranes. LPD (A) and LCN (B) diffusion at pH 7.3 through Isopore® polycarbonate track-etched membranes possessing pore dimensions of increasing orders of magnitude. ◆ = 100nm pore membrane, ■ = 1.2μm pore membrane, ▲ = 10μm pore membrane. Mean±SD, n = 3-5.

(approximately 10X the diameter of the particles) resulted in the migration of approximately 50% of the applied LPD dose into the donor compartment within 4 hrs (Fig. **7A**). This increased to over 60% when the channel diameter was increased to 10μm. After 12 hrs, over 80% of the LPD formulation was detected in the receptor phase for the 10μm pore size membranes and the profile was observed to tail due to a combination of dose depletion and back diffusion. Permeability of LCN particles was ~10% below that of LPD particles at nearly all time points.

Fig. **8** rationalises the diffusion results through direct comparison of the diameter of the LCN model and relative dimensions of the membrane pores. Fig. **8C** clearly shows the nanoparticles residing in the cavities of the 100nm pore size membrane.

### 3.7 Microneedle-Mediated Gene Expression in Excised Human Skin

Our stated aim is to utilise microfabricated microneedles to study the effect of formulatory components, e.g. non-viral gene vectors, on mediating the uptake and expression of pDNA in human skin. In preparation for this work our preliminary studies aimed to corroborate whether the delivery of 'naked' pDNA via microneedle-facilitated microchannels mediated measurable levels of reporter gene expression in excised human skin. For these studies a new batch of microneedles was prepared using the dry etch microfabrication technique (Biomedical Microsystems Team, Tyndall National Institute, Cork). Fig. **9** shows that these microprojections are approximately the same height as those used for penetration and diffusion studies, however needle-shaft diameter is approximately double (~160μm at base) which should allow for improved *en face* visualisation of positively transfected microchannels.

Fig. **10** shows a typical result of a transfection experiment. *En face* imaging, following delivery of pCMVβ reporter gene, staining with X-Gal and microchannel counterstaining with NFR, shows that a small proportion of the microchannels have mediated detectable reporter gene expres-

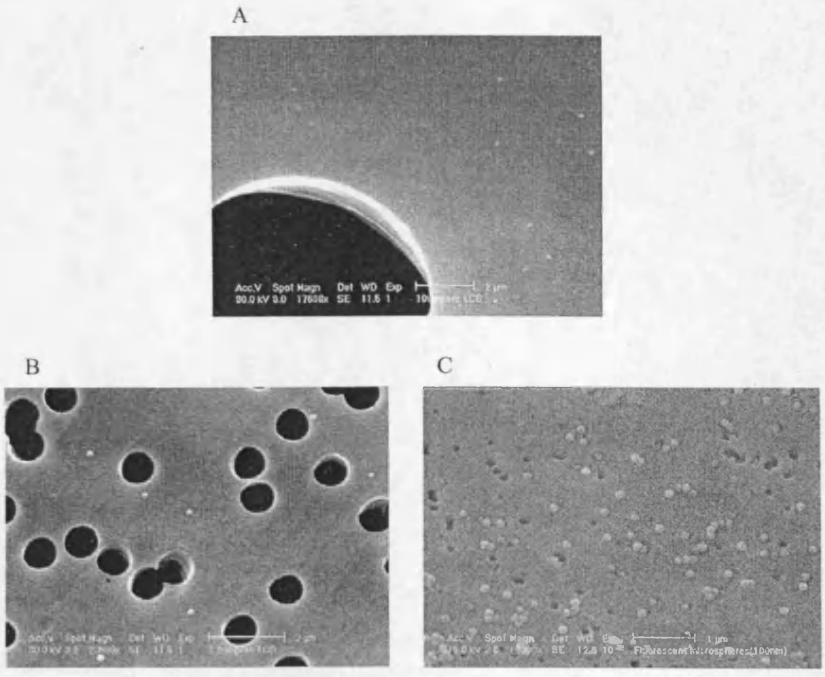


**Fig. (8).** Scanning electron microscopy of polycarbonate track etched membranes following diffusion studies with the lipid coated nanoparticle (LCN). A) 10μm pore diameter; B) 1.2μm pore diameter; C) 100nm pore diameter.

sion (Fig. **10A,B**). A gallery of pictures showing 6 consecutive 12μm cryosections is presented in Fig. **10C-H**. This figure clearly illustrates the high level of reporter gene expression in viable epidermal cells proximal to a microneedle channel.

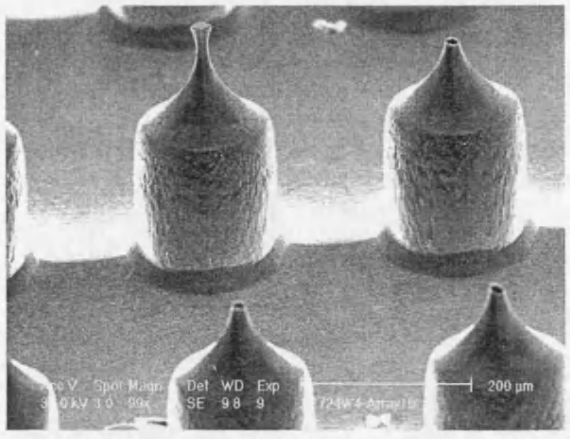


**Fig. (9).** Scanning electron microscopy of silicon microneedle arrays used for gene expression studies, Bar = 200μm.

## 4. DISCUSSION

Innovative techniques are required to overcome the SC barrier to exploit the potential of macromolecule and gene therapeutics within skin. Microneedle arrays have been shown to create transient micron sized conduits through the SC thereby providing a route though which therapeutic agents can access the underlying tissue layers. The microfabricated microneedles developed for use within our laboratory are approximately 200μm in length and possess sharp tips. A uniform pattern of pore like structures on the surface of microneedle-treated human epidermis (Fig. **2**) and retention of a small molecule dye, methylene blue, within the created channel (Fig. **3**) confirm successful penetration of the SC. However, inconsistencies in the pattern of channels on the skin surface highlight a degree of variability in penetration attributable to the dermatoglyphics of the skin surface or fragility or biological contamination of the individual silicon needles. These inconsistencies are possibly reflected in subsequent gene expression studies (Fig. **10**). Despite the fact that silicon is generally an inert material, microneedle fracturing and biological contamination would restrict the likely clinical exploitation of such devices to single application. Advances in microfabrication technologies have led to the development of arrays with a range of geometries made from alternative materials, such as glass, metal and plastic [37,38]. Such developments will ultimately provide increasingly robust and reliable delivery systems.

Detection of topically applied β-galactosidase enzyme within the viable epidermis initially confirmed the ability of the microneedle array to facilitate delivery of large hydrophilic molecules to skin. The epidermis is not a uniform tissue layer, possessing projections that interdigitate with the underlying dermal papillae layer. This results in an epidermal thickness that is highly variable both within and between donor tissues. Therefore, in some areas of the tissue microneedles will deliver to the epidermis only whereas in oth-

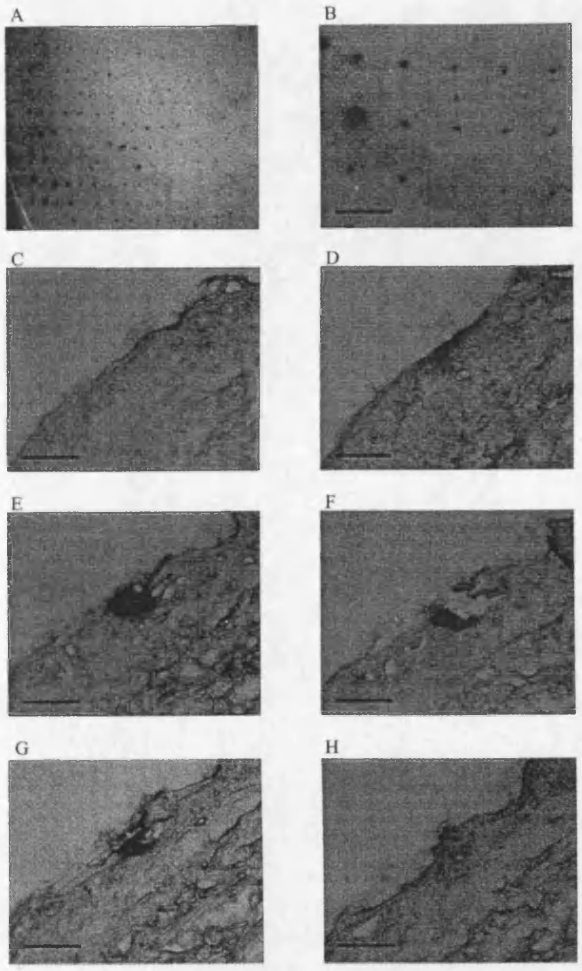


**Fig. (10).** Photomicrographs of microneedle treated human skin stained for β-galactosidase expression. A) *En face* stereomicroscopy; B) *En face* microscopy, Bar = 0.5mm; C-H) Consecutive unstained cryosections, original magnification = X200, Bar = 100μm.

ers, we might expect disruption of the basement membrane zone and the creation of a conduit to the upper layers of the dermis. This was apparent in studies examining microneedle-facilitated delivery of fluorescent nanoparticles to human skin, where the charged particles were delivered to both the epidermis and upper dermis. The dimensions of a microchannel are governed by factors such as the needle height and morphology and therefore modification of the device will enable control over the depth of delivery and access to cellular targets.

Cutaneous delivery of nanoparticulate formulations will rely upon novel delivery techniques to disrupt the otherwise impervious SC barrier [39]. We have shown that microneedle devices are able to breach the SC barrier and allow cutaneous delivery of a fluorescent polymeric nanoparticle. For the application of cutaneous gene therapy however, rapid passage of the plasmid or gene vector from the skin surface to the target cells is vital to avoid physicochemical interaction of the DNA with the surrounding tissue components or its degradation by deoxyribonucleases within the extracellular matrix [40]. The diffusion experiments confirm that increasing the diameter of a microchannel will facilitate a more rapid delivery of the colloidal formulation. However, the physicochemical characteristics of the delivered particles must also be considered. Electrostatic interaction with the tissue surface or exposure to components within the channel may impede the delivery of charged particles to those target cells within the epidermis. Therefore increasing the diameter of a microchannel, by adapting the structure of the microneedle, will reduce contact between the nanoparticle and the tissue. Permeation of approximately 50% of a fluorescent LPD formulation within a 2 hr period through a 10μm pore diameter synthetic membrane indicates that the microchannels created within human skin during this study, approximately 30μm in diameter, should facilitate rapid delivery of the gene therapy formulation to the viable epidermis.

Our initial gene expression studies have shown that naked pDNA can be expressed in excised human skin only in areas where microneedles have disrupted the SC barrier. Although a minority of microchannels were shown to be positive for gene expression these studies have served to validate our organ culture conditions in maintaining the cellular viability of excised human skin and provide a realistic assessment of the current efficiency of the microneedle technique for facilitating gene transfer. Further studies are currently utilising alternative optimised microneedle devices to facilitate more reproducible cutaneous gene delivery and explore those formulatory components that influence gene expression in epidermal cells.

## 5. CONCLUSIONS

The increasing application of macromolecular and gene-based therapies in medicine is driving the development of novel methods for cutaneous delivery. This investigation has systematically confirmed the ability of a solid silicon microneedle array to penetrate the SC and create microchannels within human skin that can facilitate the intra-epidermal delivery of biologically active macromolecules, charged 100nm diameter nanoparticles and plasmid DNA. This technology can be exploited to deliver large molecules including gene medicines to the viable cells of the epidermis in a controlled and pain-free manner.

## ACKNOWLEDGEMENTS

The authors wish to thank the Rutherford Appleton Laboratory for use of microfabrication facilities and the technical support of Professor Ron Lawes, Dr Robert Stevens, Mr. Derek Jenkins and Mr. Kostas Bouris. The authors also acknowledge the assistance of Dr Anthony Hann and Mr Mike Turner with microscopy studies and the financial support of The Royal Pharmaceutical Society of Great Britain.

## REFERENCES

[1] Ortiz-Urda, S.; Thyagarajan, B.; Keene, D.R.; Lin, Q.; Fang, M.; Calos, M.P.; Khavari, P.A. *Nat. Med.* **2002**, *8*, 1166 – 1170.

[2] Ortiz-Urda, S.; Lin, Q.; Yant, S.R.; Keene, D.R.; Kay, M.A.; Khavari, P.A. *Gene Ther.* **2003**, *10*, 1099-1104.

[3] Woodley, D.T.; Keene, D.R.; Atha, T.; Huang, Y.; Ram, R.; Kashara, N.; Chen, M. *Mol. Ther.* **2004**, *10*, 318-326.
[4] Hart, I.R.; Vile R.G. *Curr. Opin. Oncol.* **1994**, *6*, 221-225.
[5] Rakhmilevich, A.L.; Turner, J.; Ford, M.; McCabe, D.; Sun, W.H.; Sondel, P.M.; Grota, K.; Yang, N.S. *Proc. Natl. Acad. Sci. USA* **1996**, *93*, 6291-6296.
[6] Larregina, A.T.; Falo, L.D. *Hum. Gene Ther.* **2000**, *11*, 2301-2305.
[7] Peachman, K.K.; Rao, M.; Alving, C.R. *Methods* **2003**, *31*, 232-242.
[8] Partidos, C.D.; Beignon, A.-S.; Mawas, F.; Belliard, G.; Briand, J.-P.; Muller, S. *Vaccine* **2003**, *21*, 776-780.
[9] Badkar, A.V.; Banga, A.K. *J. Pharm. Pharmacol.* **2002**, *54*, 907-912.
[10] Zhang, L.; Nolan, E.; Kreischitz, S.; Rabussay, D.P. *Biochim. Biophys. Acta* **2002**, *1572*, 1-9.
[11] Zhang, L.; Widera, G.; Rabussay, D. *Bioelectochem.* **2004**, *63*, 369-373.
[12] Dujardin, N.; Preat, V. *Methods Mol. Biol.* **2004**, *245*, 755-763.
[13] Smith, N.B.; Lee, S.; Maione, E.; Roy, R.B.; McElligott, S.; Shung, K.K. *Ultrasound Med. Biol.* **2003**, *29*, 311-317.
[14] Nelson, J.S.; McCullough, J.L.; Glenn, T.C.; Wright, W.H.; Liaw, L.H.; Jacques, S.L. *J. Invest. Dermatol.* **1991**, *97*, 874-879.
[15] Dean, H.J.; Fuller, D.; Osorio, J.E. *Comp. Immunol. Microbiol. Infect. Dis.* **2003**, *26*, 373-383.
[16] Lin, M.T.S.; Wang, F.; Uitto, J.; Yoon, K. *Br. J. Dermatol.* **2001**, *144*, 34-39.
[17] Wang, S.; Joshi, S.; Lu, S. *Methods Mol. Biol.* **2004**, *245*, 185-196.
[18] Kitagawa, T.; Iwazawa, T.; Robbins, P.D.; Lotze, M.T.; Tahara, H. *J. Gene Med.* **2003**, *5*, 958-965.
[19] Schramm Baxter, J.; Mitragotri, S. *J. Control. Release* **2004**, *97*, 527-535.
[20] Sawamura, D.; Ina, S.; Itai, K.; Meng, X.; Kon, A.; Tamai, K.; Hanada, K.; Hashimoto, I. *Gene Ther.* **1999**, *6*, 1785-1787.
[21] Sintov, A.C.; Krymberk, I.; Daniel, D.; Hannan, T.; Sohn, Z.; Levin, G. *J. Cont. Release* **2003**, *89*, 311-320.
[22] Herndon, T.O.; Gonzalez, S.; Gowrishankar, T.R.; Rox Anderson, R.; Weaver, J.C. *BMC Med.* **2004**, *2*, 12.
[23] Eriksson, E.; Yao, F.; Svensjo, T.; Winkler, T.; Slama, J.; Macklin, M.D.; Andree, C.; McGregor, M.; Hinshaw, V.; Swain, W.F. *J. Surg. Res.* **1998**, *78*, 85-91.
[24] Henry, S.; McAllister, D.V.; Allen, M.G.; Prausnitz, M.R. *J. Pharm. Sci.* **1998**, *87*, 922-925.
[25] Gerstel, M.S.; Place, V.A. Drug Delivery Device, *US Patent 3,964,482*, **1976**.
[26] Kaushik, S.; Hord, A.H.; Denson, D.D.; Mcallister, D.V.; Smitra, S.; Allen, M.G.; Prausnitz, M.R. *Anesth. Analg.* **2001**, *92*, 502-504.
[27] Hengge, U.R.; Walker, P.S.; Vogel, J.C. *J. Clin. Invest.* **1996**, *97*, 2911-2916.
[28] Condon, C.; Watkins, S.C.; Celluzzi, C.M.; Thompson, K.; Falo, L.D. *Nat. Med.* **1996**, *2*, 1122-1127.
[29] Sawamura, D.; Yasukawa, K.; Kodama, K.; Yokota, K.; Sato-Matsumura, K.C.; Toshihiro, T.; Shimizu, H. *J. Invest. Dermatol.* **2002**, *118*, 967-971.
[30] Mikszta, J.A.; Alarcon, J.B.; Brittingham, J.M.; Sutter, D.E.; Pettis, R.J.; Harvey, N.G. *Nat. Med.* **2002**, *8*, 415-419.
[31] Birchall, J.C.; Kellaway, I.W.; Gumbleton, M. *Int. J. Pharm.*, **2000**, *197*, 221-231.
[32] Chabri, F.; Bouris, K.; Jones, T.; Barrow, D.; Hann, A.; Allender, C.; Brain, K.; Birchall, J. *Br. J. Dermatol.* **2004**, *150*, 869-877.
[33] Weiss, D.J Liggitt, D.; Clark, J.G. *Hum. Gene Ther.* **1997**, *8*, 1545-1554.
[34] Weiss, D.J.; Liggitt, D.; Clark, J.G. *Histochem. J.* **1999**, *31*, 231-236.
[35] Gao, X.; Huang, L. *Biochem.* **1996**, *35*, 1027-1036.
[36] Li, S.; Huang, L. *Gene Ther.* **1997**, *4*, 891-900.
[37] McAllister, D.V.; Wang, P.M.; Davis, S.P.; Park, J-H.; Canatella, P.J.; Allen, M.G.; Prausnitz, M.R. *Proc. Natl. Acad. Sci. USA* **2003**, *100*, 13755-13760.
[38] Prausnitz, M.R. *Adv. Drug Del. Rev.* **2004**, *56*, 581-587.
[39] Alvarez-Roman, R.; Naik, A.; Kalia, Y.M.; Guy, R.H.; Fessi, H. *J. Cont. Release* **2004**, *99*, 53-62.
[40] Barry, M.E.; Pinto-Gonzalez, D.; Orson, F.M.; Mckenzie, G.J.; Petry, G.R.; Barry, M.A. *Hum. Gene Ther.* **1999**, *10*, 2461-2480.

Received: February 14, 2005 Revised: May 09, 2005 Accepted: May 30, 2005

Available online at www.sciencedirect.com
SCIENCE DIRECT
ELSEVIER
International Journal of Pharmaceutics 312 (2006) 15–23
INTERNATIONAL JOURNAL OF PHARMACEUTICS
www.elsevier.com/locate/ijpharm

# Cutaneous gene expression of plasmid DNA in excised human skin following delivery via microchannels created by radio frequency ablation

James Birchall [a,*], Sion Coulman [a], Alexander Anstey [b], Chris Gateley [b], Helen Sweetland [c], Amikam Gershonowitz [d], Lewis Neville [d], Galit Levin [d]

[a] *Gene Delivery Research Group, Welsh School of Pharmacy, Cardiff University, Cardiff CF10 3XF, UK*
[b] *Gwent Healthcare NHS Trust, Royal Gwent Hospital, Cardiff Road, Newport, South Wales NP20 2UB, UK*
[c] *School of Medicine, Cardiff University & University Hospital of Wales, Heath Park, Cardiff CF14 4XN, UK*
[d] *TransPharma Medical Ltd., 2 Yodfat Street, Northern Industrial Zone, Lod 71291, Israel*

Received 8 September 2005; received in revised form 5 December 2005; accepted 5 December 2005
Available online 15 February 2006

**Abstract**

The skin is a valuable organ for the development and exploitation of gene medicines. Delivering genes to skin is restricted however by the physico-chemical properties of DNA and the stratum corneum (SC) barrier. In this study, we demonstrate the utility of an innovative technology that creates transient microconduits in human skin, allowing DNA delivery and resultant gene expression within the epidermis and dermis layers. The radio frequency (RF)-generated microchannels were of sufficient morphology and depth to permit the epidermal delivery of 100 nm diameter nanoparticles. Model fluorescent nanoparticles were used to confirm the capacity of the channels for augmenting diffusion of macromolecules through the SC. An ex vivo human organ culture model was used to establish the gene expression efficiency of a β-galactosidase reporter plasmid DNA applied to ViaDerm™ treated skin. Skin treated with ViaDerm™ using 50 μm electrode arrays promoted intense levels of gene expression in the viable epidermis. The intensity and extent of gene expression was superior when ViaDerm™ was used following a prior surface application of the DNA formulation. In conclusion, the RF-microchannel generator (ViaDerm™) creates microchannels amenable for delivery of nanoparticles and gene therapy vectors to the viable region of skin.


*Keywords:* Radiofrequency-microchannels; Radiofrequency ablation; Plasmid DNA; Skin; Gene therapy

## 1. Introduction

The ability to target genes directly to the skin provides a strategy for the treatment of certain localised heritable genetic skin diseases (Greenhalgh et al., 1994; Ehrlich et al., 1995), various forms of malignancies (Hart and Vile, 1994) and cutaneous wounds (Byrnes et al., 2004; Lee et al., 2004). Furthermore, 'genetic immunisation' via the skin provides a method of vaccinating patients by introducing DNA into cells, leading to expression of foreign antigen and the subsequent induction of an immune response (Fynan et al., 1993; Raz et al., 1994; Shi et al., 1999). Intra-cutaneous DNA vaccines utilise the highly competent antigen-presenting capabilities of epidermal Langerhans cells in eliciting a systemic immune response, leading to more proficient and cost-efficient vaccination compared with conventional vaccines (Lin et al., 2000). As the immune response is induced by a single gene rather than an entire organism, this approach is also considered to be safer than using live attenuated vaccines (Durrant, 1997).

The challenge of delivering genes to the viable region of skin is a product of the physico-chemical properties of the large hydrophilic DNA molecule, with or without an additional carrier vehicle, and the significant barrier properties of cutaneous tissue. Superficially the skin is regarded as a valuable organ for the development and clinical administration of gene medicines as it is readily accessed, well characterized and easily monitored (Hengge et al., 1996). However, if cutaneous gene therapy is to translate from the laboratory to clinical practice then approaches

* Corresponding author. Tel.: +44 29 20875815; fax: +44 29 20874149.
*E-mail addresses:* birchalljc@cardiff.ac.uk, birchalljc@cf.ac.uk (J. Birchall).

0378-5173/$ – see front matter © 2006 Elsevier B.V. All rights reserved.
doi:10.1016/j.ijpharm.2005.12.036

must be developed to efficiently and reproducibly transport the delivered transgene to the target cell population. The primary role of the skin however, is to serve as a physical barrier to the invasion of foreign material. In humans, the epidermis, which constitutes the uppermost layer of the skin, is approximately 50–150 μm thick with the non-viable SC layer, approximately 15–20 μm in thickness, representing the principal barrier to penetration and permeation of substances through the skin (Birchall, 2004). Therefore, in order to deliver therapeutic compounds to the epidermis, the underlying dermis or the systemic circulation, delivery strategies must overcome the physical barrier created by the nature of the tightly packed dead cells of the SC. Traditional transdermal formulation strategies aim to enhance the delivery of small therapeutic molecules, less than 500 molecular weight, across the SC by paracellular, transcellular or intracellular routes. However, in order to deliver DNA and proteins, more innovative and radical methods of drug delivery are required. To date, the physico-chemical methods employed to promote therapeutic drug or gene transfer to the skin include the use of direct DNA injection (Hengge et al., 1995, 1996; Chesnoy and Huang, 2002) chemical enhancers (Barry, 1987; Pillai and Panchagnula, 2003), iontophoresis (Green, 1996; Préat and Dujardin, 2001), biolistic particle bombardment (Cheng et al., 1993; Heiser, 1994; Udvardi et al., 1999), electroporation (Prausnitz et al., 1993; Dujardin et al., 2001; Zhang et al., 2002), sonophoresis (Lavon and Kost, 2004), laser ablation (Nelson et al., 1991), microseeding (Eriksson et al., 1998), skin tattooing (Bins et al., 2005) and the recent use of microfabricated microneedles (Henry et al., 1998; McAllister et al., 2000, 2003; Chabri et al., 2004).

Recently, we have developed an innovative technology, coined ViaDerm™, which creates transient microchannels across the SC thereby enabling a more direct and controlled passage of molecules to the underlying viable epidermis and dermis. ViaDerm™ has an intimately spaced array of microelectrodes which are placed against the surface of skin to individually conduct an applied alternating electrical current at radio frequency (RF). Application of this rf electrical current (100–500 kHz) to the tissue elicits a vibration in motion of ions with localized frictional heating of tissue resulting in a rapid obliteration of cells close to the energy source. The intimate and orderly spacing of the microelectrodes therefore drives the orderly generation of functional microchannels. The passage of the electric current through cells in the upper skin strata generates localised ionic vibrations, heating, evaporation and cell ablation to create microchannels.

Previously, we have reported that RF-generated microchannels reside in the epidermis and dermis and are amenable to the effective transdermal delivery of small molecules (Sintov et al., 2003) and proteins (Levin et al., 2005) into the systemic circulation. Furthermore, the microchannels did not impinge on underlying blood vessels and nerve endings thus minimizing skin trauma, bleeding and neural sensations (Sintov et al., 2003). Clearly, the use of electricity for augmenting transcutaneous drug delivery also applies to some of the other aforementioned physical delivery methods, e.g. iontophoresis, electroporation. Unlike these examples however, the technology described in this study leads to the creation of an orderly array of defined microchannels by cell ablation at specific locations (Levin et al., 2005).

The purpose of the present study using the ViaDerm™ technology was two-fold. Firstly, to extensively characterize ViaDerm™-generated microchannels within ex vivo human skin. Secondly, to assess the feasibility of ViaDerm™ in supporting the transdermal delivery of a mammalian expression plasmid with subsequent reporter expression within the target region of the skin.

## 2. Materials and methods

### 2.1. Materials

The 7.2 kb pCMVβ plasmid construct containing the β-galactosidase reporter gene and the pEGFP-N1 (4.7 kb) plasmid containing the green fluorescent protein reporter gene were propagated and purified as detailed previously (Birchall et al., 1999). Fluorescein isothiocyante (FITC)-labelled polystyrene nanospheres (L-1280) were obtained from Sigma Chemicals (Poole, UK). OCT embedding medium and Histobond® microscope slides were from RA Lamb Ltd. (Eastbourne, UK). One percent aqueous eosin solution and Harris' haematoxylin solution were from BDH Laboratory Supplies (Dorset, UK). One percent aqueous toludine blue solution was from TAAB Laboratories Equipment Ltd. (Berkshire, UK). Cell culture plastics were obtained from Corning-Costar (High Wycombe, UK). MEM (EAGLES) 25 mM HEPES, Dulbecco's Modified Eagle's Medium (DMEM 25 mM HEPES), foetal bovine serum, penicillin-streptomycin solution and trypsin-EDTA solution 1× were obtained from In-Vitrogen Corporation, Paisley, UK. All other reagents were of analytical grade and purchased from Fisher Scientific UK (Loughborough, UK).

### 2.2. ViaDerm™ treatment of human skin

Full-thickness human breast skin was obtained from mastectomy or breast reduction with ethical committee approval and informed patient consent. Skin was collected from a variety of donors ranging from 45 to 65 years of age. Matched samples were used for each individual experiment. To maintain structural and cellular viability the skin tissue was transported on ice in MEM (EAGLES) 25 mM HEPES growth media and used within 3 h of excision. All excess adipose tissue was removed by blunt dissection.

The components and operating conditions of the RF-microchannel generator (ViaDerm™, TransPharma Medical, Israel) have been described previously (Sintov et al., 2003). Briefly the ViaDerm™ device comprises an electronic controller unit and a disposable array of stainless steel electrodes (100 or 50 μm in length) at a density of 100 electrodes/cm$^2$ in a total area of 1.4 cm$^2$. Thus, application of an RF-activated array (1.2 cm × 1.2 cm) resulted in the generation of 144 microchannels over the 1.4 cm$^2$ area. Studies were performed using the electrodes at device parameter settings resulting in one, two or five bursts of 700 μs burst length at an applied voltage of 290 or 330 V and an RF frequency of 100 kHz. Control experiments

involved equivalent pressure application of the ViaDerm™ device to human skin in the absence of the RF-generating power source.

### 2.3. Electron microscopy of full thickness skin

ViaDerm™ treated (100 μm electrode, density of 200 microchannels/cm$^2$) full thickness human skin samples were fixed with 2.5% glutaraldehyde in 0.1 M sodium cacodylate buffer (pH 7.4) for 60 min at room temperature and washed for 10 min (2 × 5 min) in the same buffer. The samples were post-fixed in 1% osmium tetroxide in 0.1 M cacodylate buffer for 1 h at 4 °C and then dehydrated with a graded series of ethanol concentrations as follows (70% for 10 min at 4 °C, 100% for 10 min at 4 °C, 100% for 10 min at 4 °C, 100% for 10 min at 4 °C). The samples were subsequently transferred to a critical point drier (Samdri 780, Maryland, USA) for 12 h. The samples were mounted on metal stubs and gold sputter coated, using an Edward sputter coater, prior to examination in a Philips XL-20 scanning electron microscope.

### 2.4. Electron microscopy of epidermal sheets

Following ViaDerm™ treatment (100 μm electrode) of full thickness human skin, epidermal sheets were isolated by a heat separation technique (Christophers and Kligman, 1963). The resulting epidermal sheets were placed in cold distilled water and then gently lifted from the water onto a metal stub. The mounted epidermal sheet was allowed to dry, gold sputter coated and the samples were examined using a scanning electron microscope (Philips Xl-200 SEM) (Electron Microscopy Unit, Cardiff School of Biosciences, Cardiff University, Cardiff, UK).

### 2.5. Visualisation of microchannels en face

ViaDerm™ treated (100 μm electrode) skin was incubated in media (MEM (EAGLES), 25 mM HEPES) for 24 h at 37 °C. Following two washes in phosphate buffered saline (PBS) the skin was fixed in 0.5% gluataraldehyde for 2 h on ice. Methylene blue staining involved a 5 min surface application of five drops of methylene blue solution on the ViaDerm™ treated skin followed by removal of excessive stain with a brief PBS rinse and an ethanol surface swab. Tissue stained with methylene blue was visualised using an Olympus BX50 microscope and a Schott KL1500 electronic light source.

### 2.6. Histology of ViaDerm™ treated tissue

Skin was treated with ViaDerm™ using either 50 or 100 μm electrode arrays. Following treatment the skin was washed with PBS and fixed for 4 h in 0.5% glutaraldehyde on ice. Fixed tissue was embedded in OCT and sectioned using a Leica CM3050S Cryostat. Sections were collected on Histobond® microscope slides and stained with either—(i) eosin: 1% aqueous eosin solution for 5 s, (ii) haematoxylin and eosin (H&E): Harris' haematoxylin solution for 5 min followed by 1% aqueous eosin solution for 5 s or (iii) toludine blue: 1% aqueous toludine blue solution for 5 min.

### 2.7. Diffusion of fluorescent nanoparticles through RF-microchannels™

Non-treated and ViaDerm™ treated (50 and 100 μm electrodes) full thickness human skin was heat separated in order to isolate the epidermal membranes which were subsequently mounted between the donor and receptor compartments of static Franz-type glass diffusion cells. The receptor phase of each cell was filled with phosphate buffered saline (PBS; pH 7.4). The receptor arm was sealed with a foil cap and the donor chamber occluded with NESCO® film to prevent sample evaporation. The cells were placed on a stirring plate in a water-bath maintained at 37 °C, to provide continuous agitation and a skin surface temperature of 32 °C. Prior to addition of the test formulations to the donor chamber, cells were allowed to equilibrate for at least 30 min and the integrity of epidermal membranes was visually inspected.

Fluorescently (FITC) labelled polystyrene nanospheres (100 nm diameter) were used as a size-representative model for the delivery of non-viral gene therapy vectors (Chabri et al., 2004). A volume of 500 μl of a 50 μl/ml dilution of the fluorescent nanosphere stock suspension, concentration $4.57^{10}$ μl$^{-1}$, was applied to the surface of ViaDerm™ treated epidermal membranes. Control cells consisted of untreated epidermal membrane with either the nanosphere suspension or PBS applied to the donor phase. At each timepoint 200 μl samples were removed from the receptor arm at regular intervals and replaced with PBS. On completion of the experiment, samples were analysed using a fluorescence spectrophotometer (BMG Fluostar, Aylesbury, UK) with excitation and emission wavelengths set at 485 and 520 nm, respectively. A calibration curve was performed using standard dilutions of the suspension of fluorescent nanoparticles.

### 2.8. Localised delivery of fluorescent nanoparticles in ViaDerm™ treated human skin

ViaDerm™ treated (100 μm electrode) skin was placed in a six-well cell culture plate and maintained in 1.5 ml MEM (EAGLES) 25 mM HEPES. Fifty microliters of a concentrated ($4.57^{10}$ μl$^{-1}$) stock of fluorescent red polystyrene nanospheres was applied to the treated skin surface and the sample incubated for 6 h at 37 °C. At 6 h a further 2 ml of media was added the submerged skin was incubated for a further 18 h. Following two washes in PBS the skin was fixed in 0.5% gluataraldehyde for 1 h on ice and embedded in OCT medium prior to tissue sectioning using a Leica CM3050S Cryostat. Sections were either visualised unstained under blue fluorescence or stained with haematoxylin and eosin (H&E) (Olympus BX50 microscope).

### 2.9. Gene expression in ViaDerm™ treated human skin

Human skin was pre-treated with the ViaDerm™ device, 50 μm electrode arrays, prior to the topical application of 50 μl

of pCMVβ plasmid DNA solution (1 mg/ml) to the skin surface. This area of skin was thereafter post-treated with the ViaDerm™ device at the identical skin location as the first ViaDerm™ application. The treated human skin was placed on lens tissue supported by metal gauze in a six-well cell culture plate containing 7.5 ml media (DMEM 25 mM HEPES supplemented with 5% foetal bovine serum and 1% penicillin/streptomycin) per well. This organ culture maintained the skin at an air–liquid interface for 24 h at 37 °C. Following one wash in PBS/$MgCl_2$ (30 min) the tissue was fixed for 2 h in 2% glutaraldehyde/$MgCl_2$ at 4 °C. Subsequently the tissue was rinsed in a series of PBS/$MgCl_2$ solutions for 2, 3 h and 30 min. The tissue was stained for β-galactosidase expression over 20 h using X-Gal staining solution [X-Gal (5% (v/v) of a 40 mg/ml solution in dimethylformamide), potassium ferricyanide (0.84% (v/v) of a 0.6 M solution), potassium ferrocyanide (0.84% (v/v) of a 0.6 M solution), magnesium chloride (0.2% (v/v) of a 1 M solution), Tris–HCl buffer pH 8.5 (50% (v/v) of a 0.2 M solution), deionised water to 100%]. Tissue was visualised en face using either a Zeiss Stemi 2000C Stereomicroscope with a 2.0× attachment or an Olympus BX50 microscope, both with a Schott KL1500 electronic light source.

For sectioning, the samples were embedded in OCT and sectioned using a Leica CM3050S Cryostat. Tissue sections were collected onto Histobond® microscope slides and stained with H&E.

## 3. Results and discussion

The surface morphology of the microchannels created in full-thickness breast skin following application of ViaDerm™ was initially investigated using scanning electron microscopy (SEM). Fig. 1 shows a channel created using the 100 μm electrode appearing as a deep invagination into the surface of the skin tissue. Further SEM characterisation of the heat-separated epidermal membrane, comprising of SC and viable epidermis, treated with ViaDerm™ is shown in Fig. 2. These data show that the RF-microchannels either totally or partially penetrate the epidermal membrane. Although the depth of the microchannels was variable, possibly due to variation in thickness of the separated epidermal sheet (Eriksson et al., 1998), the diameter of the microchannels (~50 μm), was reproducible and consistent

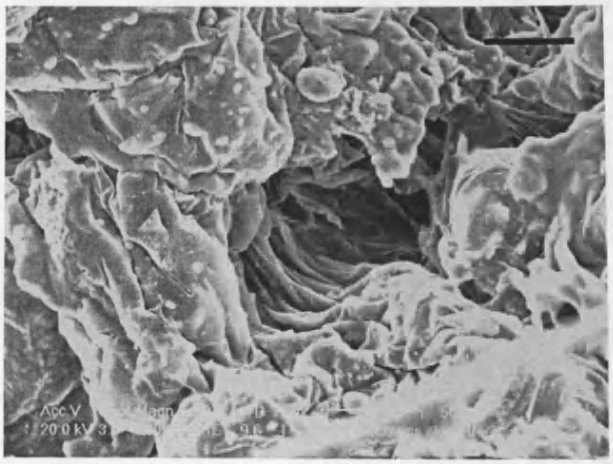

Fig. 1. Scanning electron microscopy of an RF-microchannel in intact human skin. Bar = 50 μm.

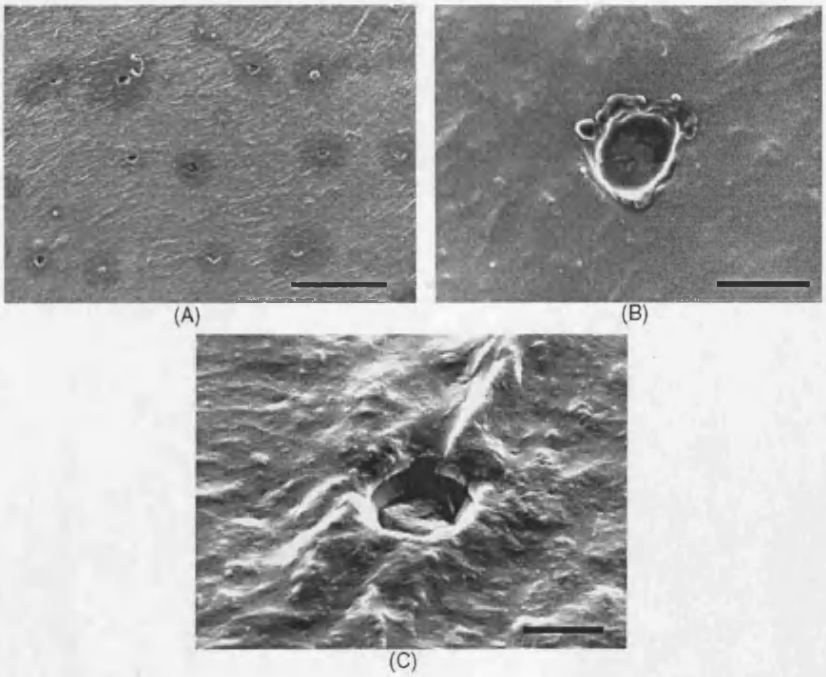


Fig. 2. Scanning electron microscopy of RF-microchannels in heat-separated epidermal membrane. (A) Low magnification showing distribution pattern of channels following two applications of ViaDerm™, bar = 1 mm; (B) high magnification showing dimensions of microchannels, bar = 100 μm; (C) visualisation of microchannel depth using an angled electron beam, bar = 50 μm.

with the microchannel dimensions observed in full-thickness skin (Fig. 1). More accurate determinations of the depth and structural morphology of the microchannels are provided in the histological tissue sections.

The quantity and distribution pattern of microchannels created in ViaDerm™ treated skin is shown in Fig. 3. The distribution pattern of the channels can be visualised through their ability to uptake and retain a low molecular weight marker, i.e. methylene blue (Fig. 3A). At higher magnification the dye appears to diffuse to the periphery of the microchannel (Fig. 3B). The application and considerable potential of this technology for the cutaneous delivery of low molecular weight medicaments has previously been reported (Sintov et al., 2003).

The structural dimension of microchannels created in human breast skin following application of ViaDerm™ was assessed using transverse sectioning. The photomicrographs are representative of the entire population of channels observed. Fig. 4 illustrates the dimensions of RF-microchannels that are created in human breast skin following application of ViaDerm™ with 50 μm electrode arrays at different parameter settings. In the majority of processed skin sections ($n > 100$), the channels are approximately 50 μm in length and 30–50 μm at their widest aperture, extending only to the viable epidermis.

In line with the data depicted in Fig. 4, doubling the electrode length to 100 μm resulted in further penetration through the human epidermis and impingement into the superficial dermal layer (Fig. 5). Representative sections ($n > 100$) show that microchannels were approximately 100 μm in length and 30–50 μm at their widest aperture. Consequently, using isolated human breast skin, the 100 μm electrode arrays can create a microchannel of sufficient length to permit specific cell targeting for localised cutaneous gene therapy applications (Greenhalgh et al., 1994; Sawamura et al., 2002) and genetic vaccination (Dean et al., 2003). Clearly, the exploitation of different electrode lengths for creating microchannels of varying depths underscores the flexibility of ViaDerm™ for permitting controlled delivery of therapeutics to different target cell populations.

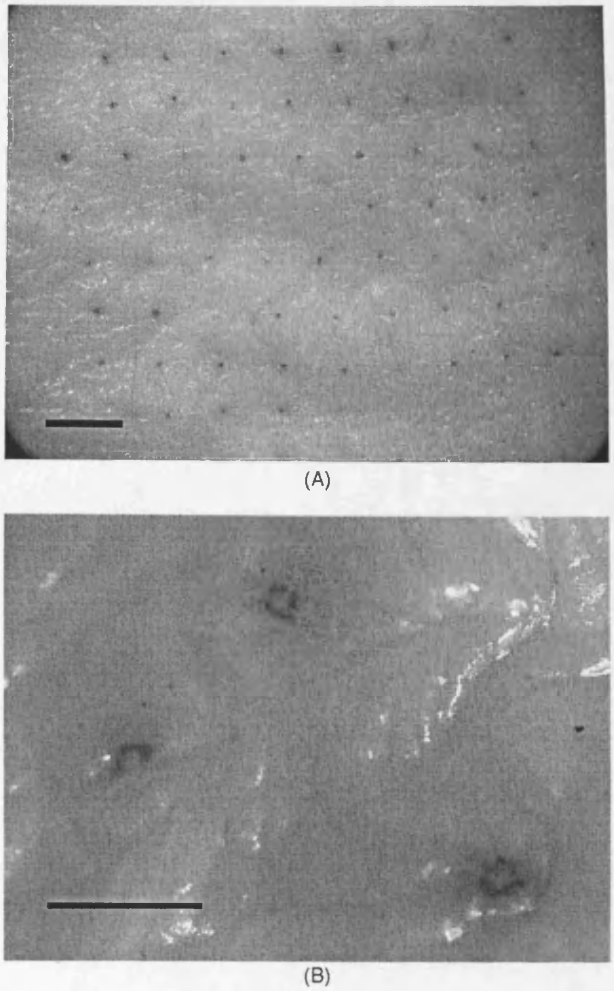


Fig. 3. Light microscopy of methylene blue stained skin following ViaDerm™ treatment. (A) Low magnification, bar = 1 mm; (B) high magnification, original magnification = 40×, bar = 500 μm.

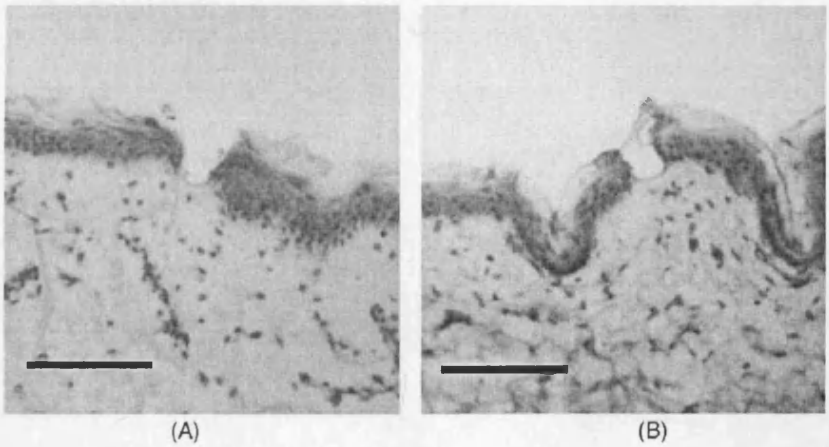


Fig. 4. Light microscopy of human breast skin treated with ViaDerm™ 50 μm electrode arrays. (A) One burst of 700 μs burst length, toludine blue stained; (B) two bursts of 700 μs burst length, toludine blue stained. Original magnification = 200×, bar = 100 μm.

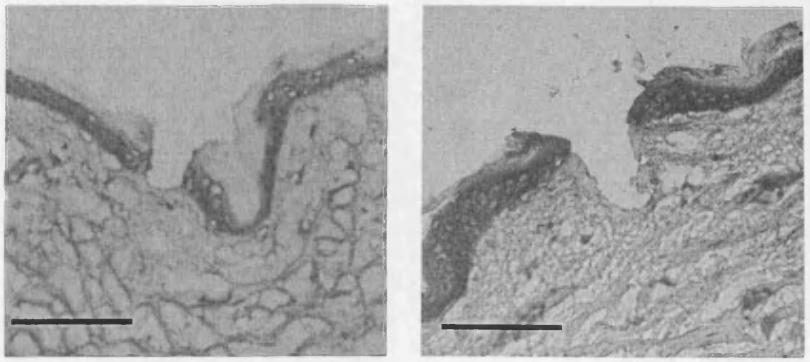


Fig. 5. Light microscopy of human breast skin treated with ViaDerm™ 100 μm electrode arrays. (A) One burst of 700 μs burst length, toludine blue stained; (B) three bursts of 700 μs burst length, toludine blue stained. Original magnification = 200×, bar = 100 μm.

Previously, from ex vivo studies employing a permeation methodology, we have demonstrated the total inability of the ViaDerm™ device to generate microchannels when disconnected from a power source as evidenced by both negative visualization and lack of drug permeation (Sintov et al., 2003). Such findings were totally substantiated in follow up in vivo studies whereby application of drugs at a ViaDerm™ treated skin site in the absence of a power supply resulted in no transdermal drug delivery as compared to robust drug deliveries with a functional power supply (Sintov et al., 2003; Levin et al., 2005). In our histological studies, and subsequent gene delivery experiments, we confirm the previously published ex vivo and in vivo observations (Sintov et al., 2003; Levin et al., 2005) of the total absence of microchannels on the surface skin following the placement of the ViaDerm™ device disconnected from a functional power source.

Following confirmation of the ability of ViaDerm™ to create microchannels in human skin, further experiments were

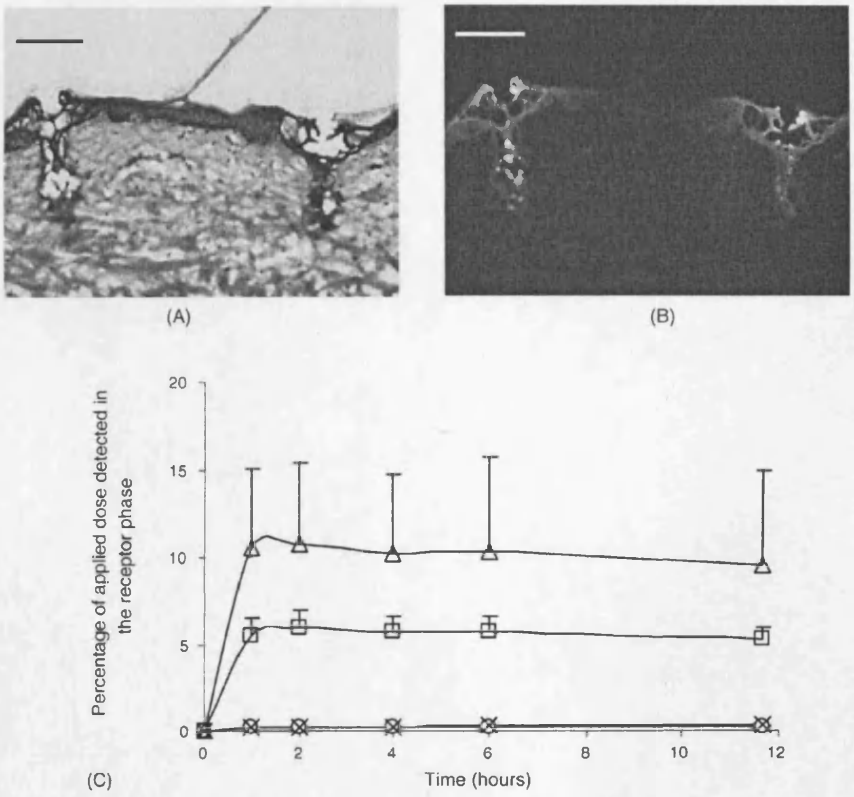


Fig. 6. Light (A) and fluorescent (B) photomicrographs of RF-microchannels containing fluorescent nanoparticles. Original magnification = 100×, bar = 100 μm; (C) diffusion of fluorescent nanoparticles through ViaDerm™ treated epidermal membranes. Data presented as percentage of topical nanoparticle dose detected in the receptor phase of Franz cells over a 12 h period. (○) Untreated skin—PBS donor phase, (×) Untreated skin—topical nanoparticles, (□) 50 μm array ViaDerm™ treated skin—topical nanoparticles, (△) 100 μm array ViaDerm™ treated skin—topical nanoparticles ($N = 3 \pm$ S.D.).

performed to demonstrate the capability of these microchannels to permit cutaneous delivery of macromolecules or nanoparticulates. To that end, 100 nm fluorescent nanoparticles were selected as an easily detectable and size-representative model nanoparticle delivery system. Indeed, we have previously reported their application as an experimental tool for lipid:polycation:pDNA (LPD) non-viral gene delivery particle studies (Chabri et al., 2004). Fig. 6 confirms that the RF-microchannels created in skin following application of ViaDerm™ are of sufficient dimensions to uptake, entrap and permit the diffusion of 100 nm fluorescent nanoparticles. The channels shown in Fig. 6A and B appear to be larger than those observed in Fig. 5, possibly due to changes in the tissue sample over the incubation period (24 h compared with 0 h). These micrographs imply that the RF-microchannels generated can be considered to be of appropriate dimensions for the cutaneous delivery of macromolecules and non-viral gene therapy vectors.

Fig. 6C shows the data from a Franz-type diffusion experiment designed to determine the transit of the 100 nm nanoparticles through ViaDerm™ treated and control epidermal

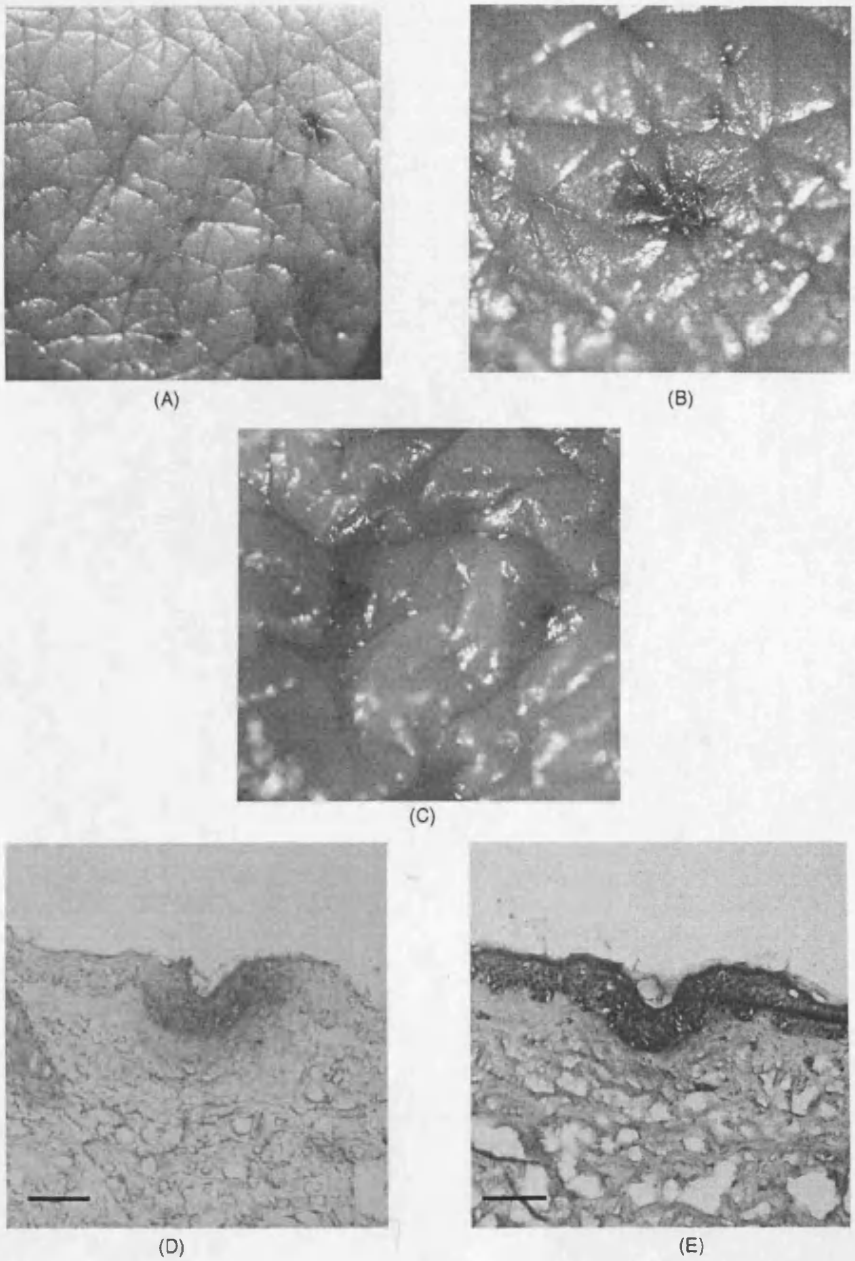


Fig. 7. Photomicrographs of ViaDerm™ treated human skin stained for β-galactosidase expression (50 μm arrays). (A) En face stereomicroscopy; (B) en face light microscopy, original magnification = 40×; (C) en face stereomicroscopy of ViaDerm™ treated human skin treated with the pEGFP-N1 plasmid; (D) unstained cryosection, original magnification = 100×; (E) H&E stained cryosection, original magnification = 100×, bar = 100 μm.

membranes. The non-treated epidermal membranes demonstrate the significant barrier function of this membrane to 100 nm nanoparticles, with undetectable penetration observed following 12 h incubation. Following ViaDerm™ treatment the epidermal membranes demonstrated a significantly enhanced ($p > 0.05$, one-way analysis of variance) permeability to the nanoparticles. Interestingly, whilst application of the 50 μm electrode arrays mediated reproducible permeation of the membrane to facilitate the diffusion of approximately 5% of the surface-applied nanoparticles, appliance of the 100 μm electrode arrays led to enhanced, though more variable, disruption of the membrane, as evidenced by an increase in mean penetration of the 100 nm nanoparticles. A possible mechanism for the more variable permeation of nanoparticles following ViaDerm™ treatment using the 100 μm electrodes is provided by the SEM images in Fig. 2. When the skin is treated with ViaDerm™ using the 50 μm electrodes and the epidermal membrane is subsequently removed by heat separation, it is not guaranteed that the entire membrane, i.e. stratum corneum and viable epidermis, will be punctured although disruption of the outer 15–30 μm will be sufficient to overcome the primary diffusive barrier, the stratum corneum. The observed increase in nanoparticle permeation therefore results from particle transit through the ablated SC channels and subsequent diffusion through the underlying epidermis. As shown in Fig. 2, skin treatment with ViaDerm™ using the 100 μm electrodes can occasionally effect complete penetration through the heat-separated epidermal sheet. Variability will therefore arise from the proportion of complete punctures, which in turn will depend on the thickness of the epidermal membrane following heat separation.

The delivery and expression of plasmid DNA in viable human skin via RF-microchannels has been initially demonstrated using the 50 μm electrode arrays. In these experiments the plasmid was used alone, i.e. without any non-viral carrier system, as numerous studies have shown the ability of naked DNA to undergo efficient expression in vivo (Hengge et al., 1995, 1996; Chesnoy and Huang, 2002). Fig. 7A and B clearly show the presence of intense blue staining, relating to substantial reporter gene expression with no expression evident in skin treated with ViaDerm™ and probed with the pEGFP-N1 plasmid (control; Fig. 7C). The expression is primarily localised in the viable epidermal cells surrounding the RF-microchannel (Fig. 7D and E). Interestingly, when a solution of DNA is applied topically to an area of ViaDerm™ treated skin the resulting epidermal gene expression is relatively low (data not shown). When the skin is treated with ViaDerm™ both prior to and following a topical application of the DNA solution the extent and level of gene expression is demonstrably greater. Consequently, it is reasonable to suggest that the ViaDerm™ might be used not only to create microchannels in the skin but also to enhance the intracellular uptake of the delivered DNA via a mechanism analogous to electroporation (Titomirov et al., 1991; Zhang et al., 2002).

In conclusion, we have demonstrated that the channels created in human breast skin following application of the RF-microchannel generator (ViaDerm™) are of appropriate dimensions, and enhance skin permeability to such a degree, as to permit the delivery of macromolecules and gene therapy vectors to the skin. The ViaDerm™ device represents a significant breakthrough in the challenge of delivering high molecular weight medicaments through the SC barrier. In particular, the ability to facilitate minimally invasive, targeted and controlled delivery of genes to the viable epidermis further supports the experimental and clinical evaluation of this novel transdermal drug delivery technology.

## Acknowledgement

The authors acknowledge the support of Dr. Antony Hann, Cardiff School of Biosciences for assistance with electron microscopy.

## References

Barry, B.W., 1987. Mode of action of penetration enhancers in human skin. J. Contr. Release 6, 85–97.

Bins, A.D., Jorritsma, A., Wolkers, M.C., Hung, C.F., Wu, T.C., Schumacher, T.N., Haanen, J.B., 2005. A rapid and potent DNA vaccination strategy defined by in vivo monitoring of antigen expression. Nat. Med. 11, 899–904.

Birchall, J.C., 2004. Cutaneous gene delivery. In: Amiji, M.M. (Ed.), Polymeric Gene Delivery: Principles and Applications. CRC Press, Florida, USA, pp. 573–588.

Birchall, J.C., Kellaway, I.W., Mills, S.N., 1999. Physico-chemical characterisation and transfection efficiency of cationic lipid–plasmid DNA gene delivery complexes. Int. J. Pharm. 183, 195–207.

Byrnes, C.K., Malone, R.W., Akhtar, N., Nass, P.H., Wetterwald, A., Cecchini, M.G., Duncan, M.D., Harmon, J.W., 2004. Electroporation enhances transfection efficiency in murine cutaneous wounds. Wound Rep. Reg. 12, 397–403.

Chabri, F., Bouris, K., Jones, T., Barrow, D., Hann, A., Allender, C., Brain, K., Birchall, J.C., 2004. Microfabricated silicon microneedles for nonviral cutaneous gene delivery. Br. J. Dermatol. 150, 869–878.

Cheng, L., Ziegelhoffer, P.R., Yang, N.-S., 1993. In vivo promoter activity and transgene expression in mammalian somatic tissues evaluated by using particle bombardment. Proc. Natl. Acad. Sci. U.S.A. 90, 4455–4459.

Chesnoy, S., Huang, L., 2002. Enhanced cutaneous gene delivery following intradermal injection of naked DNA in a high ionic strength solution. Mol. Ther. 5, 57–62.

Christophers, E., Kligman, A., 1963. Preparation of isolated sheets of human stratum corneum. Arch. Dermatol. 88, 702–704.

Dean, H.J., Fuller, D., Osorio, J.E., 2003. Powder and particle-mediated approacxhes for delivery of DNA and protein vaccines into the epidermis. Comp. Immun. Microbiol. Infect. Dis. 26, 373–388.

Dujardin, N., Van Def Smissen, P., Préat, V., 2001. Topical gene transfer into rat skin using electroporation. Pharm. Res. 18, 61–66.

Durrant, L., 1997. Cancer vaccines. Anticancer Drugs 8, 727–733.

Ehrlich, P., Sybert, V.P., Spencer, A., Stephens, K., 1995. A common keratin 5 gene mutation in Epidermolysis Bullosa Simplex–Weber–Cockayne. J. Invest. Dermatol. 104, 877–879.

Eriksson, E., Yao, F., Svensjö, T., Winkler, T., Slama, J., Macklin, M.D., Andree, C., McGregor, M., Hinshaw, V., Swain, W.F., 1998. In vivo gene transfer to skin and wound by microseeding. J. Surg. Res. 78, 85–91.

Fynan, E.F., Webster, R.G., Fuller, D.H., Haynes, J.R., Santoro, J.C., Robinson, H.L., 1993. DNA vaccines: protective immunization by parenteral, mucosal and gene innoculation. Proc. Natl. Acad. Sci. U.S.A. 90, 11478–11482.

Green, P.G., 1996. Iontophoretic delivery of peptide drugs. J. Contr. Release 41, 33–48.

Greenhalgh, D.A., Rothnagel, J.A., Roop, D.R., 1994. Epidermis: an attractive target tissue for gene therapy. J. Invest. Dermatol. 103, 63S–69S.

Hart, I.R., Vile, R.G., 1994. Targeted therapy for malignant melanoma. Curr. Opin. Oncol. 6, 221–225.

Heiser, W.C., 1994. Gene transfer into mammalian cells by particle bombardment. Anal. Biochem. 217, 185–196.

Hengge, U.R., Chan, E.F., Foster, R.A., Walker, P.S., Vogel, J.C., 1995. Cytokine gene expression in epidermis with biological effects following injection of naked DNA. Nat. Genet. 10, 161–166.

Hengge, U.R., Walker, P.S., Vogel, J.C., 1996. Expression of naked DNA in human, pig and mouse skin. J. Clin. Invest. 97, 2911–2916.

Henry, S., McAllister, D.V., Allen, M.G., Prausnitz, M.R., 1998. Microfabricated microneedles: a novel approach to transdermal drug delivery. J. Pharm. Sci. 87, 922–925.

Lavon, I., Kost, J., 2004. Ultrasound and transdermal drug delivery. Drug Discovery Today 9, 670–676.

Lee, P-Y., Chesnoy, S., Huang, L., 2004. Electroporatic delivery of TFG-β1 gene works synergistically with electric therapy to enhance diabetic wound healing in db/db mice. J. Invest. Dermatol. 123, 791–798.

Levin, G., Gershonowitz, A., Sacks, H., Stern, M., Sherman, A., Rudaev, S., Zivin, I., Phillip, M., 2005. Transdermal delivery of human growth hormone through RF-microchannels. Pharm. Res. 22, 550–555.

Lin, M.T.S., Pulkkinen, L., Uitto, J., 2000. Cutaneous gene therapy: principles and prospects. New Emerg. Therap. 18, 177–188.

McAllister, D.V., Allen, M.G., Prausnitz, M.R., 2000. Microfabricated microneedles for gene and drug delivery. Annu. Rev. Biomed. Eng. 2, 289–313.

McAllister, D.V., Wang, P.M., Davis, S.P., Park, J.H., Canatella, P.J., Allen, M.G., Prausnitz, M.R., 2003. Microfabricated needles for transdermal delivery of macromolecules and nanoparticles: fabrication methods and transport studies. Proc. Natl. Acad. Sci. U.S.A. 100, 13755–13760.

Nelson, J.S., McCullough, J.L., Glenn, T.C., Wright, W.H., Liaw, L.H., Jacques, S.L., 1991. Mid-infrared laser ablation of stratum corneum enhances in vitro percutaneous transport of drugs. J. Invest. Dermatol. 97, 874–879.

Pillai, O., Panchagnula, R., 2003. Transdermal delivery of insulin from poloxamer gel: ex vivo and in vivo skin permeation studies in rat using iontophoresis and chemical enhancers. J. Contr. Release 89, 127–140.

Prausnitz, M.R., Bose, V.G., Langer, R.S., Weaver, J.C., 1993. Electroporation of mammalian skin: a mechanism to enhance transdermal drug delivery. Proc. Natl. Acad. Sci. U.S.A. 90, 10504–10508.

Préat, V., Dujardin, N., 2001. Topical delivery of nucleic acids in the skin. Pharmascience 11, 57–68.

Raz, E., Carson, D.A., Parker, S.E., Parr, T.B., Abai, A.M., Aichinger, G., Gromkowski, S.H., Singh, M., Lew, D., Yankauckas, M.A., Baird, S.M., Rhodes, G.H., 1994. Intradermal gene immunization: The possible role of DNA uptake in the induction of cellular immunity to viruses. Proc. Natl. Acad. Sci. U.S.A. 91, 9519–9523.

Sawamura, D., Yasukawa, K., Kodama, K., Yokota, K., Sato-Matsumura, K.C., Toshihiro, T., Shimizu, H., 2002. The majority of keratinocytes incorporate intradermally injected plasmid DNA regardless of size but only a small proportion of cells can express the gene product. J. Invest. Dermatol. 118, 967–971.

Shi, Z., Curiel, D.T., Tang, D.C., 1999. DNA-based non-invasive vaccination onto the skin. Vaccine 17, 2136–2141.

Sintov, A.C., Krymberk, I., Daniel, D., Hannan, T., Sohn, Z., Levin, G., 2003. Radiofrequency-driven skin microchanneling as a new way for electrically assisted transdermal delivery of hydrophilic drugs. J. Contr. Release 89, 311–320.

Titomirov, A.V., Sukharev, S., Kistanova, E., 1991. In vivo electroporation and stable transformation of skin cells of newborn mice by plasmid DNA. Biochim. Biophys. Acta 1088, 131–134.

Udvardi, A., Kufferath, I., Grutsch, H., Zatloukal, K., Volc-Platzer, B., 1999. Uptake of exogenous DNA via the skin. J. Mol. Med. 77, 744–750.

Zhang, L., Nolan, E., Kreitschitz, S., Rabussay, D.P., 2002. Enhanced delivery of naked DNA to the skin by non-invasive in vivo electroporation. Biochim. Biophys. Acta 1572, 1–9.